

TECHNICAL REPORT

A-3808 AND A-3809 9-85

ANALYSIS OF HYDROGEN PRODUCTION DURING  
A BWR6 CORE HEATUP TRANSIENT

J. W. YANG AND W. T. PRATT

ACCIDENT ANALYSIS GROUP

DEPARTMENT OF NUCLEAR ENERGY, BROOKHAVEN NATIONAL LABORATORY  
UPTON, NEW YORK 11973



Prepared for the U.S. Nuclear Regulatory Commission  
Office of Nuclear Reactor Regulation  
Contract No. DE-AC02-76CH00016

8512230385 851217  
PDR TOPRP EXIBNL  
C PDR

TECHNICAL REPORT  
A-3808 and A-3809, 9-85

ANALYSIS OF HYDROGEN PRODUCTION DURING A BWR6 CORE HEATUP TRANSIENT

J. W. Yang and W. T. Pratt

Accident Analysis Group  
Department of Nuclear Energy  
Brookhaven National Laboratory  
Upton, New York 11973

Prepared for

U. S. Nuclear Regulatory Commission  
Washington, D. C. 20555  
Under Contract No. DE-AC02-76CH00016  
FIN Nos. A-3808 and A-3809

ABSTRACT

Hydrogen production during the heatup of a BWR6 core during a postulated degraded core accident has been analyzed using the MARCH2 (Version 151) computer code. The study includes both un-mitigated and mitigated cases with initial heatup conditions comparable to that used in HCOG analyses. Detailed comparisons with HCOG analyses have been made. Similar analysis with initial heatup conditions determined by following the emergency procedure guidelines were performed. Separate effects of the mitigated case have been investigated. Various sources which contribute to hydrogen production have been identified.

#### ACKNOWLEDGEMENTS

The work is being performed for the Division of Systems Integration (DSI) at the U.S. Nuclear Regulatory Commission (NRC). J. Rosenthal is the NRC section leader for this project.

We wish to acknowledge J. Rosenthal, W. Lyon and Wayne Hodges of NRC, H. Komoriya and P. Abramson of International Technical Services, Inc. for providing valuable discussions during the preparation of this report. B. Bornstein of BNL has updated the MARCH2 computer code used for the hydrogen analysis presented in this report.

We would also like to express our appreciation to Theresa Skelaney and Sheree Flippen for their excellent typing and assembling of this report.



CONTENTS

	<u>Page</u>
ABSTRACT.....	iii
ACKNOWLEDGEMENTS.....	iv
LIST OF FIGURES.....	vi
LIST OF TABLES.....	xi
1. INTRODUCTION.....	1
2. HYDROGEN GENERATION MODELS.....	2
3. HCOG SAMPLE PROBLEMS.....	8
4. MARCH ANALYSIS USING HCOG INITIAL CONDITIONS.....	14
5. MARCH ANALYSIS OF SEPARATE EFFECTS.....	43
6. MARCH ANALYSIS USING THE EMERGENCY PROCEDURE GUIDELINES.....	70
7. SCDAP/MARCH2 COMPARISON.....	93
8. ORNL MARCH-BWR/MARCH2 COMPARISON.....	107
9. APPLICATIONS TO GRAND GULF, CLINTON, PERRY, AND RIVER BEND PLANTS.....	123
10. SUMMARY.....	124
11. REFERENCES.....	125
APPENDIX A - HCOG Core Heatup Code Input Data.....	A-1
APPENDIX B - Representative MARCH2 (Version 151) Code Input Data.....	B-1
APPENDIX C - SCDAP Code Input Data.....	C-1
APPENDIX D - ORNL MARCH-BWR Code Input Data.....	D-1
APPENDIX E - Design Parameters of Grand Gulf, Clinton, Perry, and River Bend Plants.....	E-1

LIST OF TABLES

<u>Table</u>	<u>Title</u>	<u>Page</u>
2.1	Hydrogen Production Based on Fraction of Metal Reacted.....	7
2.2	Reaction Heat Based on Fraction of Metal Reacted.....	7
2.3	Hydrogen Generation Rate and Reaction Rate from Zr/steam Reaction.....	7
3.1	Comparison of Decay Heat Power.....	9
3.2	Summary of HCOG Results.....	9
4.1	Comparison of Initial Conditions.....	21
4.2	Comparison of Steam Production for Case 4.1 at 50.8 minutes.....	22
4.3	Comparison of Steam Production for Case 4.1 at 71.2 minutes.....	23
4.4	Comparison of Steam Production for Case 4.2 at 50.8 minutes.....	24
4.5	Comparison of Temperature and Water Level for Case 4.2.....	25
4.6	Comparison of Steam Production for Case 4.3.....	26
4.7	Summary of MARCH Results and Comparison with HCOG Results.....	27
5.1	Comparison of Effect of Steam Flow in Bypass Region.....	48
5.2	Summary of Results of Separate Effects.....	49
6.1	Summary of Results Based on Emergency Procedure Guidelines.....	73
7.1	SCDAP and MARCH Initial Axial Temperature Distributions.....	96
8.1	Comparison of ORNL Case 1 with MARCH Prediction.....	109
8.2	Comparison of ORNL Case 2 with MARCH Prediction.....	110

LIST OF FIGURES

<u>Figure</u>	<u>Title</u>	<u>Page</u>
3.1	HCOG predicted Zr melt fraction for case 2.....	10
3.2	HCOG predicted H <sub>2</sub> generation rate for case 2.....	11
3.3	HCOG predicted Zr melt fraction for case 3.....	12
3.4	HCOG predicted H <sub>2</sub> generation rate for case 3.....	13
4.1	Fuel axial power distribution used in MARCH and HCOG analyses....	28
4.2	Melt fraction and oxidation fraction for case 4.1.....	29
4.3	Comparison of H <sub>2</sub> generation for case 4.1.....	30
4.4	System pressure and core temperature for case 4.1.....	31
4.5	Reactor vessel water level for case 4.1.....	32
4.6	Reactor vessel water level for case 4.2.....	33
4.7	Core temperature for case 4.2.....	34
4.8	Melt fraction and oxidation fraction for case 4.2.....	35
4.9	Comparison of H <sub>2</sub> generation for case 4.2.....	36
4.10	Heat transfer to gas in core and decay heat for case 4.2.....	37
4.11	Reactor vessel water level for case 4.2.....	38
4.12	Core temperature for case 4.3.....	39
4.13	Melt fraction and oxidation fraction for case 4.3.....	40
4.14	Comparison of H <sub>2</sub> generation for case 4.3.....	41
4.15	System pressure and temperature for case 4.3.....	42
5.1	Reactor vessel water level and core temperature for case 5.1.....	50
5.2	Melt fraction and oxidation fraction for case 5.1.....	51
5.3	Hydrogen generation for case 5.1.....	52
5.4	Hydrogen generation for case 5.2.....	53
5.5	Reactor vessel water level and boiling rate for case 5.2.....	54

LIST OF FIGURES (Cont.)

<u>Figure</u>	<u>Title</u>	<u>Page</u>
5.6	Melt fraction and oxidation fraction for case 5.2.....	55
5.7	Reactor vessel water level and core temperature for case 5.3.....	56
5.8	Melt fraction and oxidation fraction for case 5.3.....	57
5.9	Hydrogen generation for case 5.3.....	58
5.10	Reactor vessel water level and core temperature for case 5.4.....	59
5.11	Melt fraction and oxidation fraction for case 5.4.....	60
5.12	Hydrogen generation for case 5.4.....	61
5.13	Comparison of hydrogen generation rate for cases 5.5, 4.2 and BWR013A.....	62
5.14	Comparison of total hydrogen production for cases 5.5, 4.2 and BWR013A.....	63
5.15	Comparison of core temperature for cases 5.5 and 4.2.....	64
5.16	Comparison of melt fraction for cases 5.5 and 4.2.....	65
5.17	Comparison of oxidation for cases 5.5 and 4.2.....	66
5.18	Reactor vessel water level and core temperature for case 5.6.....	67
5.19	Melt fraction and oxidation fraction for case 5.6.....	68
5.20	Hydrogen generaion for case 5.6.....	69
6.1	System pressure and temperature for case 6.1.....	74
6.2	Reactor vessel water level for case 6.1.....	75
6.3	Core temperature for case 6.1.....	76
6.4	Hydrogen generation for case 6.1.....	77
6.5	Core temperature above water level for case 6.1.....	78
6.6	Melt fraction and oxidation fraction for case 6.1.....	79
6.7	Comparison of H <sub>2</sub> generation rate for cases 6.1 and 4.1.....	80
6.8	System pressure and temperature for case 6.2.....	81

LIST OF FIGURES (Cont.)

<u>Figure</u>	<u>Title</u>	<u>Page</u>
6.9	Reactor vessel water level for case 6.2.....	82
6.10	Hydrogen generation for case 6.2.....	83
6.11	Core temperature for case 6.2.....	84
6.12	Melt fraction and oxidation fraction for case 6.2.....	85
6.13	Comparison of hydrogen generation rate for case 6.2.....	86
6.14	System pressure and temperature for case 6.3.....	87
6.15	Reactor vessel water level for case 6.3.....	88
6.16	Core temperature for case 6.3.....	89
6.17	Hydrogen generation for case 6.3.....	90
6.18	Melt fraction and oxidation fraction for case 6.3.....	91
6.19	Comparison of hydrogen generation for case 6.3.....	92
7.1	SCDAP bundle inlet mass flow rate history.....	97
7.2	SCDAP power history of a fuel bundle.....	98
7.3	SCDAP/MARCH2 comparison: primary system pressure.....	99
7.4	SCDAP/MARCH2 comparison: steam/water mixture level.....	100
7.5	MARCH2 prediction: coolant injection rate for 800 bundles.....	101
7.6	MARCH2 prediction: fuel temperature.....	102
7.7	MARCH2 prediction: fraction of Zr reacted.....	103
7.8	MARCH2 prediction: fraction of channel box melted.....	104
7.9	MARCH2 prediction: hydrogen generation rate for 800 bundles.....	105
7.10	MARCH2 prediction: total hydrogen production from 800 bundles...	106
8.1	ORNL Case 1: Core temperature.....	111
8.2	ORNL Case 1: Swollen mixture level and primary system pressure..	112
8.3	ORNL Case 1: Clad oxidation.....	113

LIST OF FIGURES (Cont.)

<u>Figure</u>	<u>Title</u>	<u>Page</u>
8.4	ORNL Case 1: Channel box oxidation.....	114
8.5	ORNL Case 1: Control blade oxidation.....	115
8.6	ORNL Case 1: Hydrogen generation.....	116
8.7	ORNL Case 2: Core temperature.....	117
8.8	ORNL Case 2: Swollen mixture level and primary system pressure..	118
8.9	ORNL Case 2: Clad oxidation.....	119
8.10	ORNL Case 2: Channel box oxidation.....	120
8.11	ORNL Case 2: Control blade oxidation.....	121
8.12	ORNL Case 2: Hydrogen generation.....	122

## 1. INTRODUCTION

When a reactor core is substantially uncovered during a degraded core event and the internal temperatures exceed the oxidation temperatures of the different materials inside the core region, the stainless steel, zircaloy and possibly the neutron absorbing materials will react with steam to produce hydrogen. The hydrogen, if released to the containment in sufficient amounts, has the potential to deflagrate and detonate. As a result, certain LWR owners have been required to install systems to continuously ignite the hydrogen in order to maintain hydrogen concentrations below detonable limits. The system must be designed such that the accident sequence will not proceed to an unrecoverable state because of standing flames damaging vital equipment.

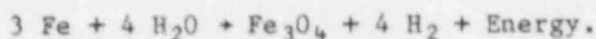
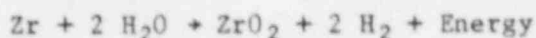
Uncertainties still remain as to the possible rates of production of hydrogen and the total amount of hydrogen produced while maintaining a quenchable core. The effect of zircaloy melting is primary among these uncertainties. Certain utilities that own LWR plants have formed an owners group to study the issue. A BWR core heatup code was developed by the Hydrogen Control Owners Group (HCOG). The heatup code was used to establish a test matrix for a facility in which hydrogen was injected and the adequacy of hydrogen ignition systems tested. At the review meeting of the BWR core heatup code in October 3rd and 4th of 1984, the HCOG staff presented their analysis of a sample problem.<sup>1,2</sup> The sample problem involves the predictions of hydrogen generation rate and total hydrogen production during a transient heating of a BWR6 reactor core with 300 gpm injected at 2530 seconds. The sample problem was extended to include the case of no core reflood and the case of 5000 gpm injected at 3400 seconds. The HCOG staff presented detailed computations of these cases at a meeting at BNL on June 4, 1985.

These sample problems become the base cases from which comparative studies using the MARCH2 (Version 151) code<sup>3</sup> were performed and presented in this report. Various parametric studies important for hydrogen generation are included in the study. This report is divided into ten sections. The introduction section is followed by the second section in which a brief discussion of the modeling of hydrogen generation in both the MARCH code and HCOG heatup code are presented. In the third section, the HCOG sample problems are described. The MARCH analysis using the HCOG initial conditions is given in Section 4. Parametric analyses of various separate effects determined by the MARCH code are discussed in Section 5. In Section 6, analyses were performed with reactor vessel depressurization determined by following the Emergency Procedure Guidelines.<sup>4</sup> The MARCH predictions are compared with that of the SCDAP code in Section 7, and with ORNL MARCH/BWR code in Section 8. The comparative studies are used to compare predictions made by the MARCH2 (Version 151) code. All analyses are based on the design data of the Grand Gulf power plant. The application of the present results to similar plants, such as Clinton, Perry, and River Bend are discussed in Section 9. The summary and conclusions based on this preliminary study were given in the final section. Appendix A, B, C, and D contain the input data used for the various codes. Detailed comparisons of design parameters of the four BWR power plants are given in Appendix E.



## 2. HYDROGEN GENERATION MODELS

The zirconium/steam reaction and steel/steam reaction are the two most important hydrogen sources during a degraded core accident. The two reactions became important when the zirconium and steel in the reactor core are heated to sufficiently high temperatures as the core is partially or completely uncovered. Typically, a zirconium temperature in excess of 1832°F (1000°C) is required to produce a high reaction rate. The oxidation rate of steel can become larger than that of zirconium when the melting point of steel is approached at 2500 ~ 2700°F (1370 ~ 1500°C). The reaction of zirconium and steel in a steam environment are given as



The  $\text{Fe}_3\text{O}_4$  is assumed to be the major product of the complex steel/steam reaction. The above two reactions show that two moles of hydrogen is produced for every mole of zirconium reacted, and four moles of hydrogen for every three moles of steel reacted. Thus, from the fractions of metal reacted in the core region, the total amount of hydrogen production could be predicted. A typical BWR6 core with 800 fuel assemblies and 193 control blades has, approximately

84000 pounds of zirconium in cladding,  
68500 pounds of zirconium in channel boxes,  
and 11580 pounds of steel in control blades.

The amount of hydrogen production approximated from the fraction of metal reacted are shown in Table 2.1.

Both the Zr/steam and Fe/steam reactions are exothermic. The energy released from the two reactions are 2762 Btu/lb-Zr and 457 Btu/lb-Fe.<sup>3</sup> Thus, the amount of energy released can be approximated from the fraction of metal reacted as shown in Table 2.2. During the heatup transient, the reaction heat is an important heat source and is directly related to the hydrogen generation rate as given in Table 2.3. It is seen that for moderate hydrogen generation rate (about 50 lb/min) the reaction heat is comparable to the decay heat at about one hour after the scram of power.

The metal/steam reaction rates are dependent on the temperature and amount of steam available at the reacting surface. In general, the reaction rate is limited by the gaseous diffusion of steam from the coolant through a hydrogen boundary layer near the oxidizing surface or the solid-state diffusion process through the oxidized layer to the reacting interface. The actual reaction rate would be the most limiting of these two processes. In the MARCH2 (Version 151) code,<sup>3</sup> the gaseous diffusion limitation for the zirconium/steam reaction is given by the Baker-Just correlation: (when the channel box option, IBWR=1, is used)

$$x = \frac{1.847 \times 10^{-7} R_p T_F^{0.68}}{(R_p - X_0/30.48)^2} \quad (1)$$



and the solid-state diffusion limitation by the Cathcart equation:

$$\dot{x} = \frac{A}{x_0} e^{-B/(T_R + 460)} \quad (2)$$

where

$\dot{x}$  = oxidation rate, cm/s

$R_p$  = rod radius, ft

$T_F$  = film temperature, °K

$x_0$  = thickness of oxidized layer, cm

$T_R$  = rod temperature, °F

$A$  = 0.0373, cm<sup>2</sup>/s

$B$  = 36181, °R

Similar rate equations are used for the stainless steel/steam reaction with modified constants in Equations (1) and (2). The MARCH2 code also has the option to use the Baker-Just correlation for the solid-state diffusion limitation. However, the Cathcart's correlation is used for this study.

In the HCOG core heatup code,<sup>1</sup> only the solid-state diffusion equations are used for the computation of metal/steam reaction rates. Three correlations are used for the zirconium/steam reaction at different temperature ranges:

Biederman correlation for  $T < 1102$  K

Cathcart correlation for  $1102 < T < 1850$  K

Baker-Just correlation for  $1850 \text{ K} < T < 2425$  K

A single correction is used for the steel/steam reaction. All correlations have the same functional form as Equation (2), but with the constants  $A$  and  $B$  assigned to different values. The Baker-Just solid-state diffusion correlation predicts a higher reaction rate at elevated temperatures.<sup>10</sup>

A number of assumptions are made in both the MARCH code and the HCOG code for the study of metal/steam reaction presented in this report. The common assumptions used in both codes are:

- (1) No hydrogen blanket effect;
- (2) No steam starvation due to local blockage;
- (3) Zircaloy oxidation is irreversibly stopped in each node that reaches the high temperature of 2400°K, defined as the cut-off temperature (TMWOFF in the MARCH code and TOXOFF in the HCOG code);

- (4) Core slump is not modeled for the entire transient, thus, the oxidation is not disrupted by the potential core slump.

The following assumptions differ in the two codes:

- (1) In the MARCH code, the cut-off temperature is abruptly applied at 2400°K. In the HCOG core heatup code, "the zircaloy oxidation cut-off is modeled as a progressive effect starting 50 K below TOXOFF and decreasing to zero at TOXOFF as a cosine function."<sup>2</sup> Thus, in the temperature range of 2350°K to 2400°K, the HCOG predicted oxidation rate is about 64% of the MARCH prediction. (The 64% is the average value of a cosine function.)
- (2) The HCOG code assumes an oxidation cut-off temperature for the stainless steel. The cut-off temperature is 150°K above the melting temperature. No stainless steel/steam oxidation cut-off temperature is assumed in the MARCH code.
- (3) The MARCH code has the option of assuming no metal/steam reaction when the temperature of any node reaches to its melting temperature. This assumption was exercised for the control blade in the analysis presented in this report. It is noted that the MARCH code permits refreezing of any molten node by the ECC water. Thus, refreezing of any melted node could potentially start the metal/steam reaction again if the steam flow can reach the node.
- (4) Different heat of reaction are used in the two codes.

	<u>Zr/steam</u>	<u>Fe/steam</u>
MARCH	2762 Btu/lb-Zr	457 Btu/lb-Fe
HCOG	2811-2827	582

The HCOG code uses a liner temperature-dependent equation for the evaluation of Zr/steam reaction heat between 1450 K and the zirconium melting temperature.

- (5) Different values of melting temperatures are assumed in the two codes.

	<u>HCOG</u>	<u>MARCH</u>
UO <sub>2</sub>	5161°F	(4130°F)
Clad	3451	(4130°F)
Channel Box	3451	3365
Control Blade Sheath	2821	2600

Note that in the MARCH code, the clad and fuel are lumped together and a single melt temperature is assumed. The lumped clad-fuel nodding assumes all zirconium/steam reaction energy

being deposited in the fuel. This assumption would underestimate clad temperature during oxidation.

In addition, to the physical modeling of the oxidation rate, the computation of water boil-off rate is another important factor determining the hydrogen production. In the MARCH2-151 computer code, steam is produced by heat transfer to water and by depressurization in the reactor vessel. There are several heat transfer sources in the water-covered core region. The important heat sources are the decay heat power, the downward thermal radiation from hot surfaces above the water level, the sensible heat associated with the structure materials within the water and the quenching of hot surfaces as the core is reflooded. In addition, the injection of coolant into the reactor vessel also represents another energy source (or sink) into the water. The depressurization in the reactor vessel causes the vessel water to remain at the saturation state. The saturation temperature and the associated saturation enthalpy vary according to the transient pressure. During the heatup transient, the pressure differential between the reactor vessel and containment is small. A variation of vessel pressure due to the transient boiloff rate, safety relief rate and containment back pressure is expected. The reflood of reactor vessel certainly affects the vessel pressure. A decrease of vessel pressure implies a decrease of water enthalpy and an evaporation of water. On the other hand, the water enthalpy increases with the increase of vessel pressure, which implies an absorption of heat from other heat sources and a reduction of net boiloff rate. The assumption of a constant vessel pressure maintained for the entire transient simplifies the dynamic situation in the reactor vessel and eliminates a potential steam source.

The steam production due to the various mechanisms can be expressed by the following approximation:

$$\dot{W}_2 = \frac{Q_{DK} + Q_{Rad} + Q_{NCH} + Q_{SLB} + Q_{ECC} - W_1(\Delta h/\Delta t)}{h_{fg}} \quad (1)$$

where  $Q_{ECC} = \dot{W}_{ECC} (h_{ECC} - h_2)$

$$\frac{\Delta h}{\Delta t} = \frac{h_2 - h_1}{t_2 - t_1} < 0 \text{ for depressurization, i.e., } P_2 < P_1$$

$$> 0 \text{ for pressurization, i.e., } P_2 > P_1$$

$\dot{W}_{ECC}$  = rate of coolant injection, lb/min

$h_{ECC}$  = enthalpy of coolant injection, Btu/lb

$h$  = liquid water saturation enthalpy, Btu/lb

$t$  = time, min

$Q_{DK}$  = decay power below water-steam mixture level, Btu/min

$Q_{Rad}$  = downward radiation from core to water, Btu/min

$Q_{NCH}$  = heat from quenching the core material, Btu/min

$Q_{SLB}$  = heat transfer from structures in water, Btu/min

$P$  = vessel pressure, psia

$\dot{W}$  = steam production rate, lb/min

Subscripts 1 and 2 refer to states 1 and 2.

The above equation is not and cannot be used directly to calculate the steam production rate ( $\dot{W}$ ) in the MARCH2 code because the new system pressure ( $P_2$ ) and the new saturation enthalpy ( $h_2$ ) are not known at timestep  $t_2$ . The calculation of  $P_2$  requires knowledge of steam generation rate ( $\dot{W}$ ), volumes of steam and water, and coolant injection rate at state 1. An iterative solution technique is required in general. In the MARCH code, the coupling effects of vessel pressure and steam production rate are solved in an approximate manner described in Section 3.2-3 of the MARCH manual.<sup>3</sup> However, the above expression, Eq. (1), can be used to show the relative importance of the various sources of steam production. For the three cases considered in this study, the important time for hydrogen generation is between 40 minutes to 70 minutes after scram.

In the HCOG BWR Core Heatup code,<sup>1</sup> the water boiloff rate is computed in the subroutine FLRATE for fuel bundles and in the subroutine SUPER for the bypass region. The steam production due to the decay power, quenching of the "hardware just above the free surface" and the channel boxes are included in the subroutine FLRATE. The quenching of control blades and shroud are in the subroutine SUPER. No mathematical expression for the quenching of the "hardware" is given in Reference [1]. The downward thermal radiation heat transfer in Eq. (1) is not considered in the HCOG heatup code. The mass and energy balances in the downcomer and lower plenum are performed in the subroutine LOPDC. The possibility of void formation (flashing) when the system pressure is dropping is included in this subroutine. The steam formed in the downcomer flows directly into the steam dome and is not involved in the oxidation process. Only the steam formed in the lower plenum is assumed to flow into the core. In computing the energy balance in the lower plenum, the sensible heat from structures in the lower plenum is not included. The HCOG heatup code contains a subroutine DPRESS which calculates energy transferred from (or to) the submerged core hardware caused by changes in the two-phase liquid level when the system pressure changes. The term  $dP/dt$  appears directly in the mathematical expressions of volumetric fluxes of liquid water and steam. However, in the HCOG analyses, a constant vessel pressure (i.e.,  $dP/dt=0$ ) is assumed for the three sample cases. Hence, no steam production due to the change of system pressure is included in the computation.

Table 2.1 Hydrogen Production (lb) Based on Fraction of Metal Reacted

% Reacted	Cladding	Channel Boxes	Control Blades
100	3680	3000	550
75	2790	2250	411
50	1840	1500	275
30	1104	900	165
25	920	750	137
20	736	600	110
15	552	450	83

Table 2.2 Reaction Heat (MW-hr) Based on Fraction of Metal Reacted

% Reacted	Cladding	Channel Boxes	Control Blades
100	68	55	1.6
75	51	42	1.2
50	34	28	0.8
30	20	17	0.5
25	17	14	0.4
20	14	11	0.3
15	10	8	0.2

Table 2.3 Hydrogen Generation Rate and Reaction Rate from the Zr/steam Reaction

H <sub>2</sub> Generation Rate (lb/min)	Reaction Heat Release Rate (MW)
150	166
100	111
75	83
50	55
40	44
30	33
20	22
10	11

### 3. HCOG SAMPLE PROBLEMS

At the review meeting of the BWR core heatup code in October 3rd and 4th of 1984, the HCOG staff (Hydrogen Control Owners Group) presented their analysis of a sample problem.<sup>2</sup> The sample problem describes the transient heating of a BWR6 reactor core from 2000 seconds to 4000 seconds. This heatup begins after an assumed automatic depressurization sequence (ADS) that has lowered system pressure to an assumed constant 2 atm (29.4 psia). The ADS also resulted in at least 3/4 of the core being uncovered at completion of the depressurization and start of the ensuing core heatup. There is no planned inflow of cooling water to the vessel until 2600 seconds after scram, with 300 gpm inflow (18.88 kg/sec).

The BWR fuel dimensions, core power peaking factors, initial and boundary conditions used in the HCOG sample problem are listed in Appendix A. The decay power used in the sample problem is in a tabular form. Comparisons of the HCOG decay power with the ANS 1979 standard decay power used in the MARCH2 code are given in Table 3.1. The HCOG decay power is about 9% lower in the time interval between 2000 to 9000 seconds. According to Reference (5), users many employ their own computer programs and nuclear data to compute decay heat power based on the standard model. The MARCH2 code used the computational procedure developed by the Sandia National Laboratory. A constant R defined as atoms of  $^{239}\text{U}$  produced per second per fission per second evaluated for the reactor composition at the time of shutdown is specified as 0.8. R. Jaung of BNL has evaluated the decay heat power based on a computational procedure developed at Oak Ridge National Laboratory using R as 0.6 and yield a result very close to that used in the HCOG core heatup code.<sup>6</sup>

On June 4, 1985, HCOG staff presented results of three additional runs, referred as

- BWR000 - 3/4 uncovered core with no reflood to 50% zirc melt;
- BWR013A - 3/4 uncovered core with 300 gpm at 2530 seconds with approximately 30% zirc melt;
- BWR560 - 3/4 uncovered core with 500 gpm at 3400 seconds with approximately 30% zirc melt.

The computed Zr melt fraction and hydrogen generation rate for Runs BWR013A and BWR560 are shown in Figures 3.1 to 3.4. The results of the three runs are summarized in Table 3.2. Comparisons with MARCH2 predictions will be presented in Section 4.



Table 3.1 Comparison of Decay Heat Power

Time (second)	BWR Core Heatup Code (Sample Problem)	1979 ANS Standard	Difference (%)
2000	0.01681	0.01831	-8.2
3000	0.01476	0.01616	-8.7
4000	0.01344	0.01478	-9.1
5000	0.01253	0.01379	-9.2
6000	0.01186	0.01306	-9.2
7000	0.01133	0.01248	-9.2
8000	0.01091	0.01202	-9.2
9000	0.01056	0.01163	-9.2

Table 2.2 Summary of HCOG Results

Run	BWR000	BWR013A	BWR560
Reflood gpm second	0 -	300 2530	5000 3400
Transient time, s (min)	4200 (70)	4300 (72)	3645 (61)
Total H <sub>2</sub> production, Kg (lb)	217 (478)	265 (585)	189 (416)
Peak H <sub>2</sub> production rate Kg/s (lb/min)	0.18 (24)	0.57 (76)	2.33 (308)
at time s (min)	3120 (52)	3150 (53)	3405 (57)
Maximum Zr melt, %	54.7	29	29
at time s (min)	4200 (70)	3525 (59)	3405 (57)
Equivalent core Zr reacted, %	13.5	16.5	11.8

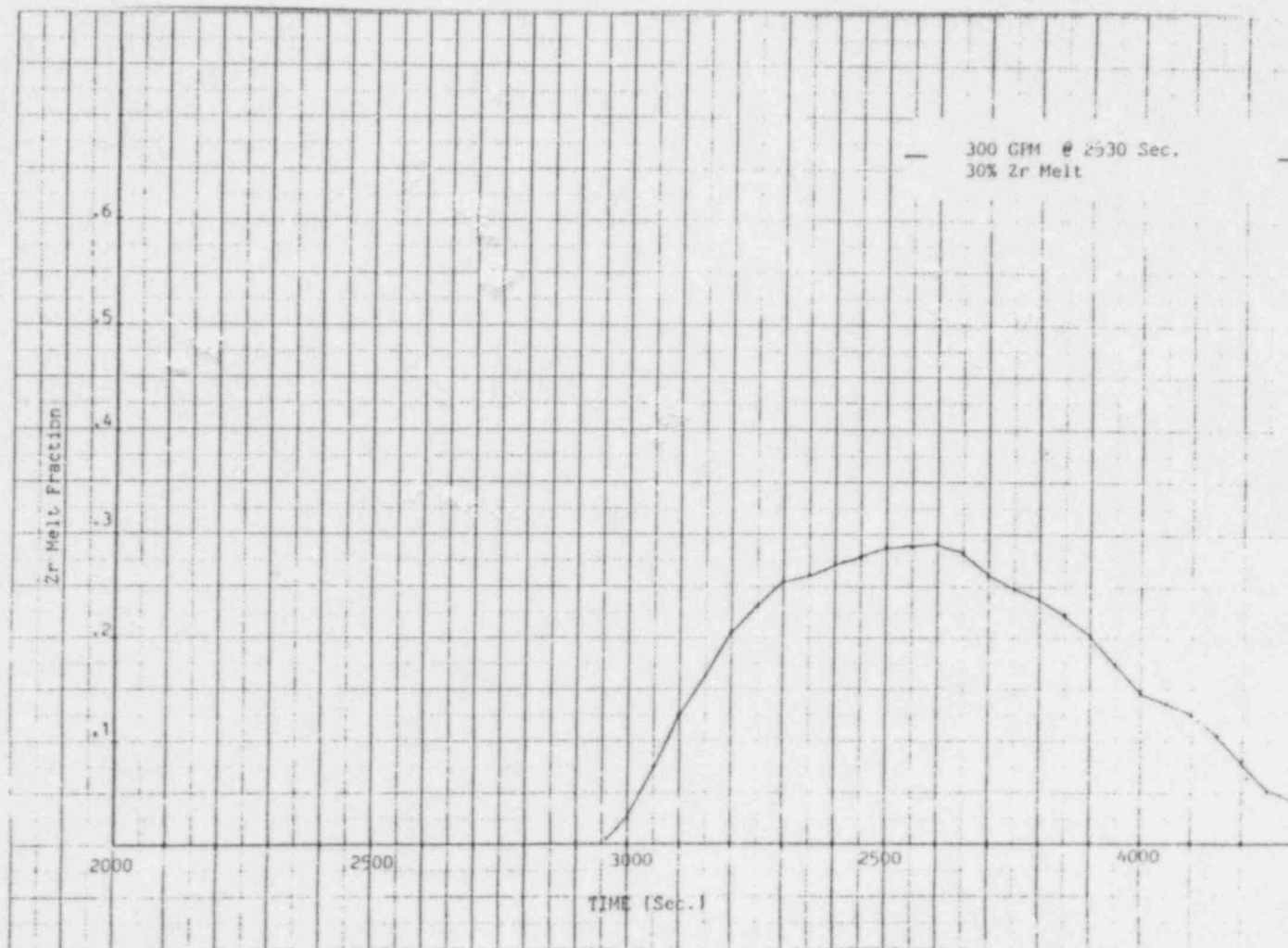


Figure 3.1 HCOG predicted Zr melt fraction for case 2  
(provided by G. Thomas of EPRI).



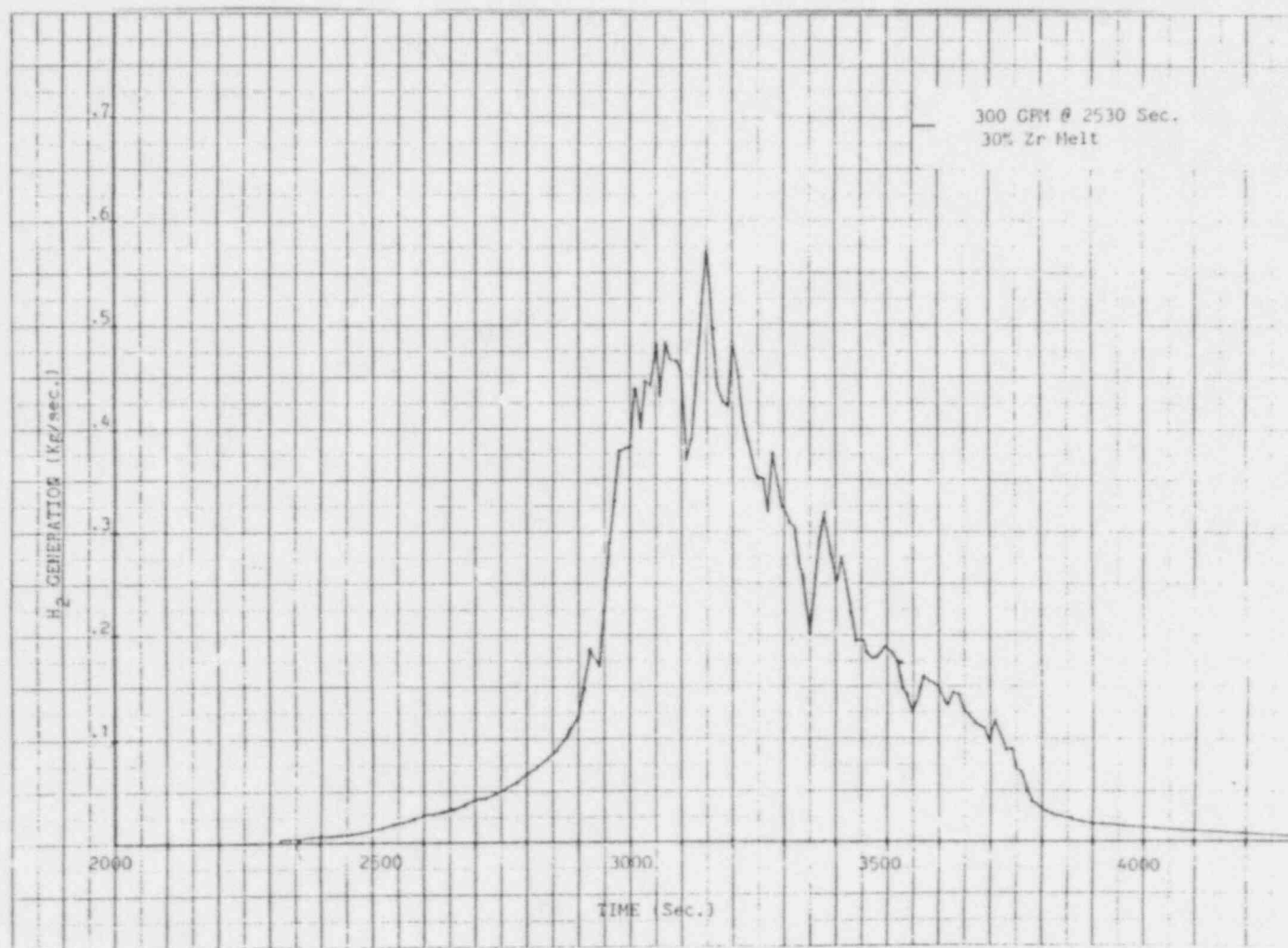


Figure 3.2 HCOG predicted H<sub>2</sub> generation rate for case 2  
(provided by G. Thomas of EPRI).

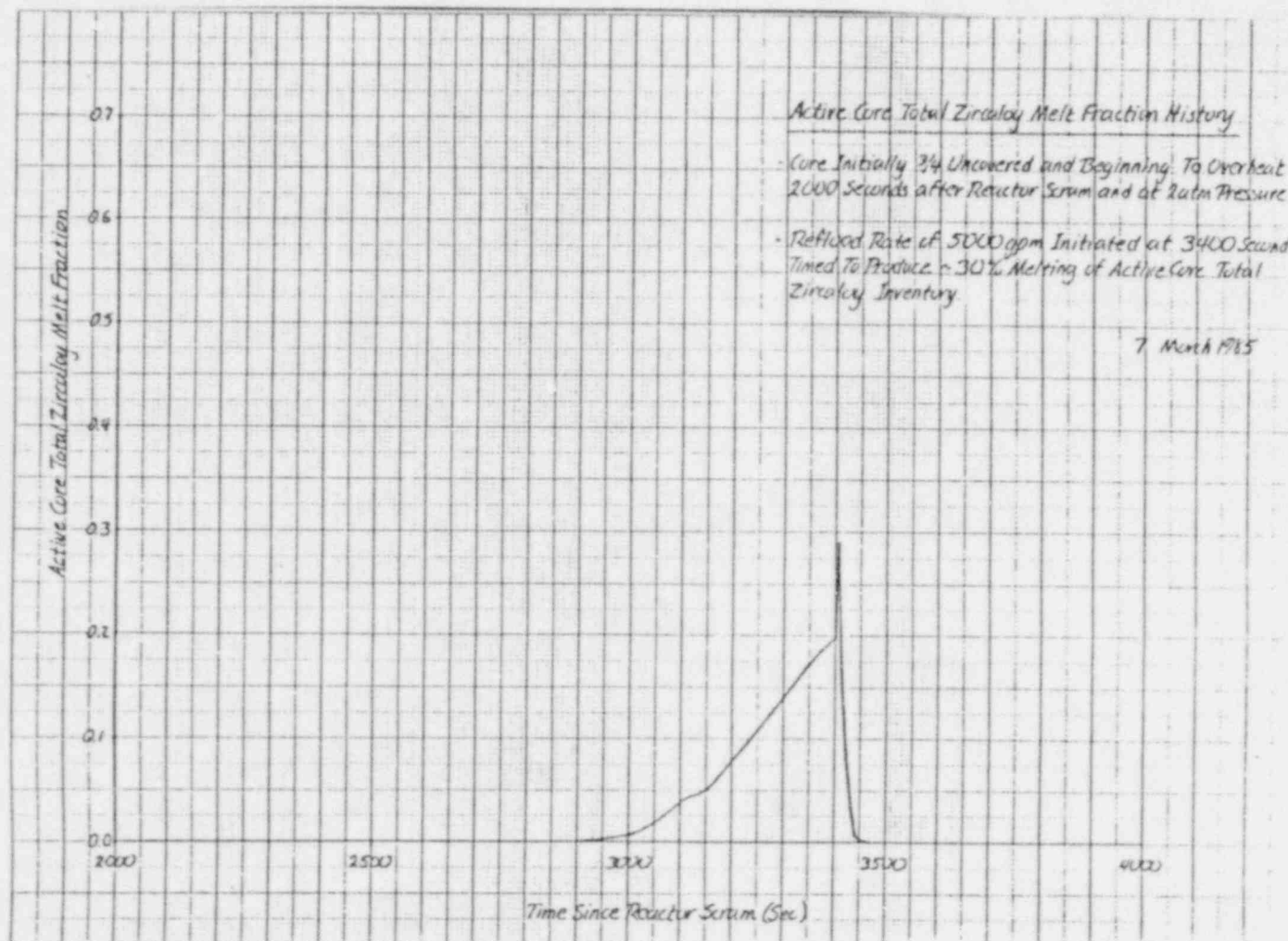


Figure 3.3 HCOG predicted Zr melt fraction for case 3 (provided by G. Thomas of EPRI).

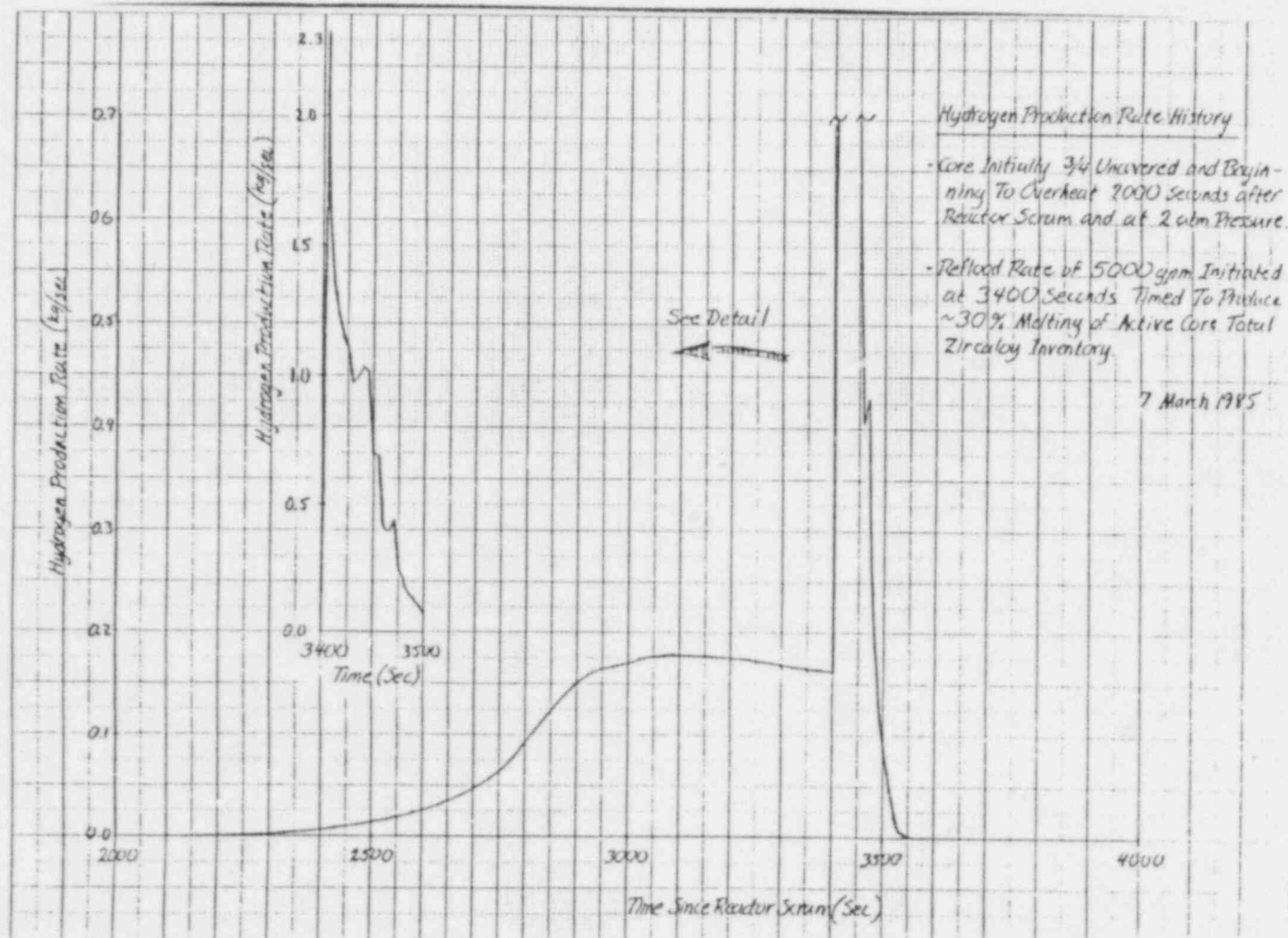


Figure 3.4 HCOG predicted  $H_2$  generation rate for case 3 (provided by G. Thomas of EPRI).

#### 4. MARCH ANALYSIS USING HCOG INITIAL CONDITIONS

##### 4.1 Introduction

This section describes a series of MARCH analyses of a transient involving loss-of-coolant make-up to the reactor core and successful insertion of control rods. The MARCH analyses were performed to closely simulate the HCOG analyses described in Section 3. It is recognized that the initial and boundary conditions were specified as input in the HCOG sample problems. These conditions were not directly used in the MARCH analysis. The initiation of core heatup was explicitly determined by the MARCH code assuming the actuation of the Automatic Depressurization System (ADS). Actuation of the ADS valves could yield an initial condition of the heatup transient comparable to that specified in the HCOG study. Three attempts were made to actuate the eight ADS valves at 5, 10, and 20 minutes after the start of the transient based on normal operation condition of a typical BWR6 3000 MW reactor. The predicted initial conditions of the three cases are summarized in Table 4.1, which includes the HCOG sample problem for comparison. Two sets of transient conditions are given in Table 4.1. Condition 1 gives the vessel pressure and core temperature when the water-steam mixture level reaches 2.7 feet. Condition 2 provides the mixture level and core temperature when the vessel pressure is reduced to 30 psia. It is seen that the vessel pressure and water-steam mixture level, which are two independent parameters, cannot be adjusted simultaneously to match the initial conditions assumed in the HCOG analysis. The MARCH predicted mixture level and vessel pressure in Case 1 are close to that of HCOG sample problems. However, this condition is reached much sooner in the MARCH calculation than the 33.3 minutes assumed in the HCOG analysis. All three cases indicate a high core temperature. During the period of core uncover, the core is heated by the decay power and cooled by the steam flow. The steam flow has a very small heat removal capability when compared with nucleate boiling heat transfer and it cannot maintain the uncovered core region at the saturation temperature as claimed in the HCOG analysis. The assumption of the entire vessel being at the saturation temperature (250°F) in the HCOG analysis is an over-simplified approximation of the transient heatup in the core region.

The MARCH2 initial and boundary conditions of Case 1 in Table 4.1 were used for all MARCH analyses discussed in this section. Note that the core heatup period determined by the MARCH code is an integral part of the entire transient which includes the initiation of the accident depressurization in the reactor vessel, uncover of the core region and reflood of the reactor core.

The basic assumptions involved with the MARCH2 analyses are listed below:

1. No fuel rod axial conduction (IAXC=0).
2. In-core radiation heat transfer model included (IRAD=2).
3. Dittus-Boelter and forced laminar flow correlations for convection model (ICONV=12).
4. Condensed steam not added to core (ICON=0).

5. Convective heat transfer continues in molten region (IHC=1).
6. Rod-to-steam radiation heat transfer included (IHR=1).
7. Zr/water reaction not stopped by node melting (IMWA=3, IMWBOX=3).
8. Cladding and channel box oxidation controlled by turn-off temperature (TMWOFF=2400K).
9. Control blade oxidation (Fe/steam reaction) is not restricted by any cut-off temperature but is stopped by node melting (IMWCB=1).
10. Zr-steam oxidation rate calculated using Cathcart solid-state oxidation rate and Baker-Just gaseous diffusion oxidation rate (MWORNL=3).
11. Melting temperatures for control blade, channel box, and fuel rod (Zr and  $UO_2$ ) are 2600 F, 3365 F, and 4130 F, respectively.

In addition to the basic assumptions described above, the Haling axial power profile reported in the Grand Gulf Power Station FSAR<sup>7</sup> is used in the MARCH calculation. The profile is different from the symmetrical profile used in the HCOG calculation as compared in Figure 4.1. (The effect of power profile will be discussed in Section 5.4.) Based on the design data of the Grand Gulf Power Station, the following masses were modeled in the MARCH2 code:

Mass of zircaloy cladding = 84033 lb.  
Mass of zircaloy channel boxes = 68523 lb.  
Mass of steel in control blades = 11582 lb.

The oxidation and melting of the above masses are major parameters of interest during the heatup analysis. Normal operating conditions are assumed prior to the initiation of the accident transient. For example, the reactor vessel pressure and the average fuel temperature are 1180 psia and 1100°F, respectively.

## 4.2 Discussion

### 1. Case 1 - No Reflood

This case (Base Case) was selected to have no coolant injection into the core during the transient. The core slump model in the MARCH2 code was not used for this analysis. It was intended to estimate the maximum melting and oxidation which could potentially be achieved without significant distortion of the core geometry. The base case was used only as a reference for the parametric study. Figure 4.2 shows that 93% of the control blades and 86% channel boxes could be melted at about 100 minutes. The melting of the core starts at about 80 minutes and reaches 29% at about 100 minutes. The oxidation of the cladding, channel box and control blade are 17%, 5%, and 1%, re-



limited by the assumption of the cut-off temperature and the availability of the steam in the core region. Since no cut-off temperature is assumed for the steel/steam reaction, the oxidation of the control blade is limited by steam flow in the bypass region. The total hydrogen production and peak hydrogen generation rate are 746 pounds and 28 lb/min, respectively. There is a large fluctuation in the predicted hydrogen generation rate. This is caused by the simple numerical scheme used in the code to compute the change of hydrogen production during a small time interval. The time-step used in the MARCH code for the core heatup period is on the order of 0.05 minutes and the change of hydrogen production is about 1% to 2%. The computed rate of hydrogen generation is very sensitive to the computing method. The computation could be improved if a more stable numerical differentiation method is used.

For the case of no core reflood, the termination of hydrogen generation is due to steam starvation. The comparison of hydrogen generation shown in Figure 4.3 indicates a reasonable agreement between the predictions of the two codes. The MARCH code predicts a higher steam production which results in higher hydrogen generation prior to peak hydrogen generation (which occurs at about 50 minutes). The various steam sources that contribute to hydrogen generation at time 50.8 minutes are given in Table 4.2. Item 5 of Table 4.2 shows that the total decay power in the MARCH analysis is about 9% higher than that predicted in the HCOG analysis. The difference is caused by the different computation method applied to the ANS standard model. But the portion of decay power below the two-phase mixture level which contributes to water boil-off is about 37% lower in the MARCH calculation (Item 6). This is caused by the MARCH predicted low two-phase water level (0.63 ft) in comparison with the HCOG prediction (1.39 ft). The HCOG assumed a water level of 2.7 ft and a system pressure of 30 psia as the initial condition for its analysis. This initial condition could not be achieved using the MARCH code as reported in Table 4.1. The MARCH code predicted a water level of 0.3 ft when the reactor vessel is depressurized to 30 psia. Thus, in the MARCH analysis, the water level is lower than that in the HCOG analysis during the heatup transient. In addition to the decay heat, the MARCH code includes radiation and structure sensible heat as heat sources for water boiloff. These two sources are relatively small as shown in Table 4.2. However, the MARCH results indicate that the system pressure decreases by about 0.4 psia within a time interval of 2.5 minutes. The variation of pressure causes a change of water enthalpy by 0.5 Btu/lb-min. This enthalpy change multiplied by the large amount of water in the system ( $1.55 \times 10^5$  pounds) yields a steam production of 81 lb/min (Item 13 of Table 4.2). The total steam estimated according to Eq. (1) of Section 2 is comparable between the two codes. Hence, the two codes predicted approximately the same amount of hydrogen generation at this transient time. It is noted that the estimated steam production based on Eq. (1) differs from the code predicted steam production (Items 14 and 15). The major difference is caused by the approximation of the  $\Delta h/\Delta t$  term from Eq. (1) based on MARCH results given at large time intervals (2.5 minutes). In the MARCH code, the water boiloff due to enthalpy change is computed by a different scheme using a much smaller time interval (0.1 minutes).

The various steam sources at 71.2 minutes is shown in Table 4.3. During the late stage of the transient, the water level is extremely low and the core temperature is high. The downward radiation heat transfer from the core becomes the dominant source of water boiloff as given by the MARCH results in Table 4.3. The sum of MARCH decay power and radiation heat transfer yield

total steam production comparable to that of HCOG analysis. At this transient time, the estimated water enthalpy change is negligible. The MARCH predicted system pressure, temperature and water level are shown in Figures 4.4 and 4.5.

## 2. Case 2 - 300 gpm CRDHS Flow Injected at 42 Minutes

The first case of calculation for the degraded core accident involves the injection of 300 gpm into the reactor vessel. The flowrate (300 gpm) represents the maximum flow available from the Control Rod Drive Hydraulic System (CRDHS). In the MARCH analysis the injection water is assumed at 100°F. The injection of 300 gpm saturated water into the reactor vessel is assumed in the HCOG sample problem. The cooling water injection starts at 42 minutes (2530 seconds) as assumed in the HCOG sample problem. The MARCH2 calculation shows that at the time of water injection, the water level in the reactor vessel is about 0.9 ft in the core region and the core is rapidly heating up as shown in Figures 4.6 and 4.7. With steam available due to the injection of cooling water and with the high core temperature, the oxidation process is enhanced. The oxidation and melting of the core, channel box and control blade are illustrated in Figure 4.8. No melting of the core is predicted in this case. The melting of channel boxes and control blades are 24% and 70%, respectively. This implies that an early injection of the CRDHS water could terminate the progression of core degradation. The fraction of zircaloy reacted is about 24% and 21% for cladding and the channel boxes, respectively.

Figure 4.9 shows a comparison of hydrogen generation predicted by the two codes. Both codes show peak hydrogen generation at about 53 minutes. However, the prediction of the MARCH code is higher than that of the HCOG code for the entire transient. An examination of the steam production computed by the two codes reveals that this is a case in which the oxidation is not limited by the steam availability. The steam produced during the transient is more than that consumed by the oxidation process. The various steam sources at time 50.8 minutes are given in Table 4.4. In the MARCH analysis, the quenching heat transfer is the largest contribution to water boiloff. The quenching heat transfer is not reported in the HCOG code output. Based on the difference between Items 12 and 15 of the HCOG results, the quenching heat transfer is estimated to be less than  $10^6$  Btu/min, about 38% of the MARCH prediction. According to MARCH modeling, the 300 gpm flow injected at 100°F absorbs about  $4 \times 10^5$  Btu/min of heat as it must be heated to the water saturation temperature. This energy loss from the vessel water reduces the net boiloff rate. The injection of coolant into the reactor vessel causes an increase of system pressure and an increase of water enthalpy, which requires heat transfer to the water as indicated in Eq. (1) of Section 2. This pressurization is a significant factor on the reduction of net boiloff of the vessel water as shown in Table 4.4. However, both codes predict a large amount of steam production which could not cause the limitation of hydrogen generation. The total steam predicted by the two codes are approximately three or four times more than that required for the predicted hydrogen generation (Items 4 and 15 of Table 4.4).

The large amount of steam produced in the core has a pronounced effect on fuel cooling. During the time period between 50 minutes to 70 minutes, the code predicted core exit steam flows are:

MARCH: 1500 - 2500 lb/min  
HCOG: 1000 - 2000 lb/min.

This amount of steam serves as a heat transfer medium in the core. The effect of steam cooling represented by heat transfer to gas (steam and hydrogen) in the core region given by the MARCH calculation is illustrated in Figure 4.10. The heat transfer is about  $1.4 \times 10^8$  Btu/hr (40 MW) comparable to the decay heat level which is included in Figure 4.10 for comparison. (The steam cooling predicted by the HCOG code is not available.) The cooling of fuel by steam flow is revealed by inspection of Table 4.5, in which the fuel average and maximum temperatures are listed. According to the MARCH calculation, the first fuel node reaches the Zr/steam reaction cut-off temperature (3860°F) at about 51 minutes. The cut-off of the oxidation process is irreversible. Hence, the reaction heat is eliminated and the decay power becomes the only heat source in that fuel node. With sufficient steam cooling the temperature of that node could be maintained near or below the cut-off temperature level. This is indicated by the maximum fuel temperature of the MARCH analysis shown in Table 4. (The location of the maximum temperature shown in Table 4 could vary with time.) The MARCH predicted fuel average temperature increases slowly during the transient (7-8 °F/min), which further reveals the effectiveness of steam cooling. The implication is that a larger portion of fuel nodes are at temperatures below the cut-off temperature and are available for the Zr/steam reaction. However, the HCOG code predicts a less effective steam cooling because of the smaller steam generation rate. According to the HCOG predictions, the first node reaches the cut-off temperature (3770°F) at about 49 minutes. In the HCOG core heatup code, "the zircaloy oxidation cut-off is modeled as a progressive effect starting 50K below the TOXOFF (2400K) and decreasing to zero at TOXOFF as a cosine function."<sup>1</sup> Comparisons given in Table 4 show that the HCOG predicted maximum temperature is much higher than that predicted by the MARCH code because of the less effective steam cooling. The HCOG predicted average temperature, which is not available, would be higher than that predicted by the MARCH code due to the smaller steam flow in the core region. Thus, it is reasonable to assume that a larger portion of fuel nodes are at or above the cut-off temperature level. These nodes are not available for hydrogen production in the HCOG analysis. Another interesting comparison included in Table 4.5 is the two-phase mixture level in the core region. It is noted that the MARCH predicted "average" level is about the same as the HCOG predicted "minimum level." If the maximum or average level predicted by the HCOG code are considerably higher than the minimum level, the surface area exposed in the steam covered region could be much less than that predicted by the MARCH code. Hence, the HCOG analysis could yield a further reduction of surface area available for oxidation.

In summary, for the case of core reflood by 300 gpm CRD flow, the MARCH code predicts a higher steam generation which, in turn, provides a more effective core cooling and a lower water level. The steam cooling would keep more fuel nodes below the assumed cut-off temperature and a lower water level would expose more surface area for oxidation. Therefore, the MARCH code predicts a higher hydrogen generation than the HCOG code does.

### 3. Case 3 - 5000 gpm ECC Flow Injected at 56.7 Minutes

This case involves a large increase in the coolant injection rate to 5000 gpm. The injection corresponds to the flow from one Low Pressure Core



Injection pump (LPCI). With the large cooling water injection flow at 56.7 minutes the core is rapidly reflooded and quenched as illustrated in Figures 4.11 and 4.12. The oxidation of the zircaloy and steel are low and the no core melt is predicted as shown in Figure 4.13. It is seen that injection of LPCI water prior to core melt would be sufficient to terminate core degradation without severe loss of the core geometry if shattering of oxidized metal is neglected.

Figure 4.14 shows the comparison of hydrogen generation predicted by the two codes. The hydrogen generation prior to the coolant injection is the same as that given in Figure 4.3 for the case of no core reflood. During this period, the MARCH code predicts a slightly higher generation of hydrogen due to the higher steam production. However, as the core is reflooded by the 5000 gpm flow, the HCOG code predicts an immediate rise of hydrogen generation and yields a peak rate of 308 lb/min at 3405 seconds (56.75 minutes). On the other hand, the MARCH code shows a lower peak rate of 151 lb/min at 57.6 minutes. The difference is again caused by the treatment of steam production as revealed in Table 4.6, in which the various steam sources at the time of peak hydrogen production are compared, i.e., 57.6 minutes (3458 seconds) for the MARCH code and 56.7 minutes (3405 seconds) for the HCOG code.

The MARCH code shows that within one minute after the injection of 5000 gpm flow into the core, the two-phase mixture level reaches 6.83 ft as shown in Table 4.6. A large portion of core is quenched by the rapid increase of water level and the quenching heat transfer becomes the largest heat source for water boiloff (Item 8 of Table 4.6). The injection of coolant also causes a rapid increase of vessel pressure and the water saturation temperature as illustrated in Figure 4.15. Consequently, heat is transferred from vessel water to structures in the water-covered region (Item 9) and to the subcooled ECC water injected at 100°F (Item 10). The loss of heat from vessel water would reduce the net boiloff rate. In addition, the increase of water enthalpy due to the pressurization in the reactor vessel requires a large amount of heat transfer from decay power, radiation and quenching. The heat absorbed by the increase of enthalpy is equivalent to a flashing rate of approximately 7700 lb/min (Item 13). The net steam production predicted by the MARCH code is 1820 lb/min (Item 15) of which 1359 lb/min of steam is consumed to produce 151 lb/min of hydrogen. This is the peak rate of hydrogen production when the middle of the core is recovered.

The HCOG predicted peak rate of hydrogen generation given in Table 4.6 occurs when the minimum two-phase mixture level in the fuel bundle is only 1.38 ft at 3405 seconds (Item 2 of Table 4.6), i.e., 5 seconds after the coolant injection has started. It is noted that the HCOG code models a gradual increase of the core inlet flow rate. The core inlet flow rate is about 2450 gpm at 3405 seconds and reaches 5000 gpm in about 20 seconds. The decay heat below the two-phase mixture level is about  $1.8 \times 10^5$  Btu/min (Item 6). This decay heat could only produce 189 lb/min of steam, which is much less than the 2772 lb/min of steam required for the generation of 308 lb/min of hydrogen predicted by the HCOG code (Items 3 and 4). The other heat source modeled in the HCOG code is the quenching heat transfer but is not reported in the code output. The quenching heat transfer is estimated to be in the order of  $5 \times 10^6$  Btu/min based on the total steam production rate of 5847 lb/min (Item 15) predicted by the HCOG code. It is not clear why a large amount of steam is produced when the water level is relatively low. It is also not clear why

peak hydrogen generation occurs so early in the transient when only 1.38 ft of the core is recovered. (The maximum and average water level in the fuel bundle are not available from the code output.) The high peak rate of hydrogen generation in the HCOG analysis is probably caused by the high steam production based on the constant pressure boundary condition. The assumption of constant vessel pressure in the HCOG analysis ignores the potential increase of water enthalpy by the pressurization in the reactor vessel as the large amount of coolant is injected in the core. The absorption of heat to increase the water enthalpy would reduce the net water boiloff rate which could, in turn, limit the hydrogen production.

#### 4. Summary

The final results of the three cases considered in this study are summarized in Table 4.7. The predictions of the two codes are comparable for the case of no reflood. For the case of 300 gpm flow injection, the MARCH code predicts a higher hydrogen generation, larger oxidation and less core damage. This is caused by the effective steam cooling due to a higher steam production predicted by the MARCH code. The effective steam cooling reduces the rate of core temperature rise toward the assumed oxidation cut-off temperature. For the case of 5000 gpm flow injection, the HCOG code yields a high peak of hydrogen generation. The peak occurs in a narrow time duration and has no significant effect on the total hydrogen generation. The study shows that the hydrogen generation is strongly affected by various steam sources such as decay power, radiation, quenching, and the enthalpy change caused by the depressurization and pressurization in the reactor vessel. All these factors must be critically examined for an accurate assessment of the hydrogen production.

In addition, the following conclusions are made based on MARCH analyses:

- 1) A degraded core accident could be terminated if the CRDHS water is injected during the early stage of the heatup period (Case 4.2).
- 2) A degraded core accident could also be terminated if the injection of cooling water is delayed but a high injection rate from the LPCI pump is used (Case 4.3).
- 3) The fraction of cladding reacted is no more than 34% if the Zr/steam reaction cut-off temperature is used. Oxidation of the cladding provides the major contribution to the total hydrogen production. The channel boxes and control blades contribute less to hydrogen production.
- 4) MARCH2 predicts severe damage of the control blades during the transient. About 70% of the control blades could melt when the accident is terminated by core reflood.

Table 4.1 Comparison of Initial Conditions

Case	HCOG	1	MARCH 2	3
No. of ADS Valves	-	8	8	8
Actuating time, min	-	5	10	20
Core uncover, min	-	11	15	23
(1) Y	2.7	2.7	2.7	2.7
P	30	43	56	122
T	250	612	585	591
t	33.3	15.4	17.4	24
(2) P	30	30	30	30
Y	2.7	0.3	-0.5	-2.4
T	250	803	812	858
t	33.3	18.4	21.1	29.6

<sup>1</sup>Conditions at a water/steam mixture level of 2.7 feet above the bottom of the core.

<sup>2</sup>Conditions after depressurization to 30 psia.

Y = water/steam mixture level above the bottom of core, ft

P = reactor vessel pressure, psia

T = average core temperature, °F

t = time, minutes

\*Case 5.2 is a high-pressure case described in Section 5.

Table 4.2 Comparison of Steam Production for Case 4.1 (No Reflood)  
at 50.8 Minutes

	MARCH	HCOG
1. Pressure, psia	21.44	29.4
2. Two-phase level, ft <sup>*1</sup>	0.63	1.39
3. H <sub>2</sub> generation rate, lb/min	25.3	23.3
4. Required steam rate, lb/min <sup>*2</sup>	228	210
5. Total decay power, Btu/min <sup>*3</sup>	3.51E6	3.20E6
6. Decay power below two-phase mixture level, Btu/min	1.15E5	1.83E5
7. Radiation heat transfer, Btu/min	7.53E2	0
8. Quenching heat transfer, Btu/min	0	0
9. Heat transfer from structures, Btu/min	1.25E3	0
10. Energy associated with coolant injection, Btu/min	0	0
11. Total energy (Items 6 to 11), Btu/min	1.17E5	1.83E5
12. Steam produced (from Item 11), lbm/min	112	193
13. Steam produced by flashing, lbm/min <sup>*4</sup>	81	0
14. Estimated total steam production (Items 12 + 13), lbm/min	203	193
15. Code predicted steam production, lb/min	280	237

\*<sup>1</sup>MARCH: average level, HCOG: minimum level

\*<sup>2</sup>Corresponding to Item 3 assuming complete reaction of available steam with metal.

\*<sup>3</sup>HCOG decay power model predicts about 9% less power

\*<sup>4</sup>Computed by Eq. (1). The term  $\Delta h/\Delta t$  is approximated from limited code output.

Table 4.3 Comparison of Steam Production for Case 4.1 (No Reflood)  
at 71.2 Minutes

	MARCH	HCOG
1. Pressure, psia	20.6	29.4
2. Two-phase level, ft <sup>*1</sup>	0.19	1.0
3. H <sub>2</sub> generation rate, lb/min	16.3	14.5
4. Required steam rate, lb/min <sup>*2</sup>	147	131
5. Total decay power, Btu/min <sup>*3</sup>	3.16E6	2.89E6
6. Decay power below two-phase mixture level, Btu/min	3.05E4	1.11E5
7. Radiation heat transfer, Btu/min	7.75E4	0
8. Quenching heat transfer, Btu/min	0	0
9. Heat transfer from structures, Btu/min	7.57E2	0
10. Energy associated with coolant injection, Btu/min	0	0
11. Total energy (Items 6 to 11), Btu/min	1.09E5	1.11E5
12. Steam produced (from Item 11), lbm/min	114	117
13. Steam produced by flashing, lbm/min <sup>*4</sup>	0	0
14. Estimated total steam production (Items 12 + 13), lbm/min	114	117
15. Code predicted steam production, lb/min	148	132

\*<sup>1</sup>MARCH: average level, HCOG: minimum level

\*<sup>2</sup>Corresponding to Item 3 assuming complete reaction of available steam with metal.

\*<sup>3</sup>HCOG decay power model predicts about 9% less power

\*<sup>4</sup>Computed by Eq. (1). The term  $\Delta h/\Delta t$  is approximated from limited code output.

Table 4.4 Comparison of Steam Production of Case 4.2  
(300 gpm at 42 min) at Time 50.8 Minutes

	MARCH	HCOG
1. Pressure, psia	35.9	29.4
2. Two-phase level, ft <sup>*1</sup>	4.63	3.26
3. H <sub>2</sub> generation rate, lb/min	90	64
4. Required steam rate, lb/min <sup>*2</sup>	810	576
5. Total decay power, Btu/min <sup>*3</sup>	3.51E6	3.20E6
6. Decay power below two-phase mixture level, Btu/min	1.38E6	6.17E5
7. Radiation heat transfer, Btu/min	1.10E4	0
8. Quenching heat transfer, Btu/min	2.35E6	( - ) <sup>*5</sup>
9. Heat transfer from structures, Btu/min	1.39E2	0
10. Energy associated with coolant injection, Btu/min	-3.95E5	0
11. Total energy (Items 6 to 11), Btu/min	3.35E6	6.17E5
12. Steam produced (from Item 11), lbm/min	3567	652
13. Steam produced by flashing, lbm/min <sup>*4</sup>	-622	0
14. Estimated total steam production (Items 12 + 13), lbm/min	2945	-
15. Code predicted steam production, lb/min	3155	1530

\*<sup>1</sup>MARCH: average level, HCOG: minimum level

\*<sup>2</sup>Corresponding to Item 3 assuming complete reaction of available steam with metal.

\*<sup>3</sup>HCOG decay power model predicts about 9% less power

\*<sup>4</sup>Computed by Eq. (1). The term  $\Delta h/\Delta t$  is approximated from limited code output.

\*<sup>5</sup>Not available.

Table 4.5 Comparisons of Temperature and Water Level of Case 2

Time (min)	MARCH			HCOG		
	Fuel Temperature		Average Two-Phase Mixture Level (ft)	Clad Temperature		Minimum Two-Phase Water Level (ft)
	Maximum (°F)	Average (°F)		Maximum (°F)	Average	
45.7	2485	1591	2.02	2479	-	2.45
48.3	3090	1713	3.17	3084	-	2.89
50.8	3855	1801	4.63	3828	-	3.26
53.4	3880	1859	4.39	3858	-	3.57
55.9	3703	1879	4.01	3916	-	3.85
58.5	3889	1904	3.90	3943	-	4.14
61.0	3636	1891	4.24	3961	-	4.38
63.5	3834	1883	4.23	3946	-	4.60
66.0	3487	1889	4.19	3925	-	4.79
68.7	3533	1925	4.47	3969	-	4.98
71.2	3791	1949	5.26	3770	-	5.17

NOTE: The first node reaches to cut-off temperature (3860°F) at 51 minutes by the MARCH code and 49 minutes by the HCOG code. In the HCOG analysis, oxidation cut-off starts at 3770°F.

Table 4.6 Comparison of Steam Production for Case 4.3  
(5000 gpm at 55.7 minutes)

	MARCH	HCOG
1. Pressure, psia	27.4	29.4
2. Two-phase level, ft <sup>*1</sup>	6.83	1.38
3. H <sub>2</sub> generation rate, lb/min	151	308
4. Required steam rate, lb/min <sup>*2</sup>	1359	2772
5. Total decay power, Btu/min <sup>*3</sup>	3.37E6	3.08E6
6. Decay power below two-phase mixture level, Btu/min	2.03E6	1.80E5
7. Radiation heat transfer, Btu/min	6.45E4	0
8. Quenching heat transfer, Btu/min	1.27E7	-
9. Heat transfer from structures, Btu/min	-4.58E4	0
10. Energy associated with coolant injection, Btu/min	-6.0E6	0
11. Total energy (Items 6 to 11), Btu/min	8.75E6	(1.80E5)
12. Steam produced (from Item 11), lbm/min	9222	(189)
13. Steam produced by flashing, lbm/min <sup>*4</sup>	(-7700)	-
14. Estimated total steam production (Items 12 + 13), lbm/min	(1522)	-
15. Code predicted steam production, lb/min	1820	5847

\*<sup>1</sup>MARCH: average level, HCOG: minimum level

\*<sup>2</sup>Corresponding to Item 3 assuming complete reaction of available steam with metal.

\*<sup>3</sup>HCOG decay power model predicts about 9% less power

\*<sup>4</sup>Computed by Eq. (1). The term  $\Delta h/\Delta t$  is approximated from limited code output.



Table 4.7 Summary of MARCH Results and Comparison with HCOG Results

Case	No Reflood		300 gpm at 42 min		5000 gpm at 56.7 min	
Code	MARCH	HCOG	MARCH	HCOG	MARCH	HCOG
Transient Time, m	70	70	72	72	61	61
Total H <sub>2</sub> Production, lb	524	478	1310	585	412	416
Peak H <sub>2</sub> Generation						
Rate, lb/min	28	23.6	100	76	151	308
Time, min	50	52	52	53	58	57
Oxidation, %						
Cladding *1	17	13.5	24	16.5	8.5	11.8
Channel Box	5		21		2.9	
Control Blade	1		12		3.1	
Melt %						
Core *2	29	54.7	0	29	0	29
Channel Box	16		24		0	
Control Blade	33		70		39	

\*1 - HCOG: Active zircaloy including both cladding and channel box.

\*2 - MARCH: Fuel rod with eutectic melting temperature given as 4130°F, zircaloy melting temperature 3365°.  
HCOG: Active zircaloy with melting temperature given as 3451°F.

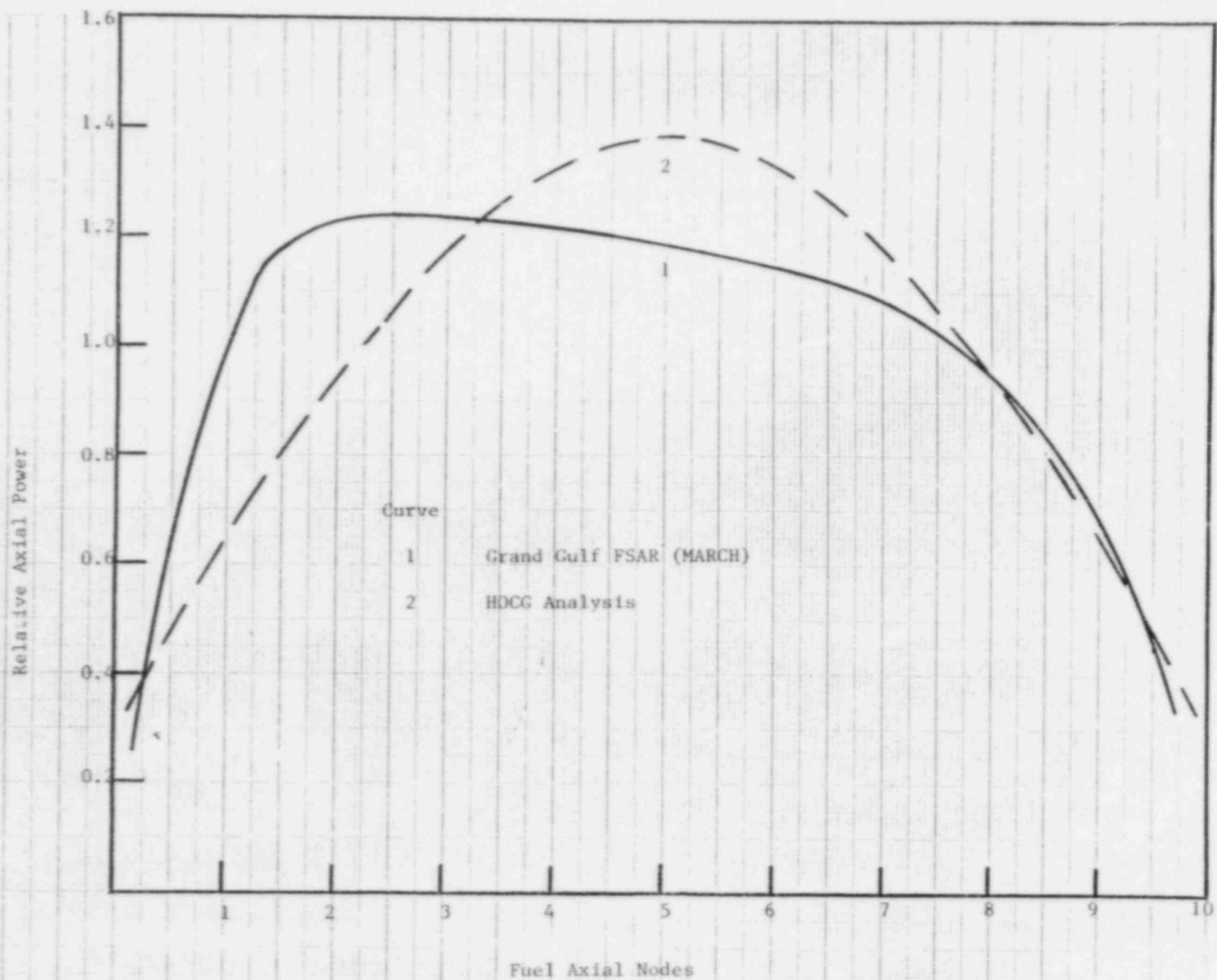


Figure 4.1 Fuel axial power distribution used in MARCH and HCOG analyses.

NO ECC GG POWER 10 NODES ADS(8) AT 5

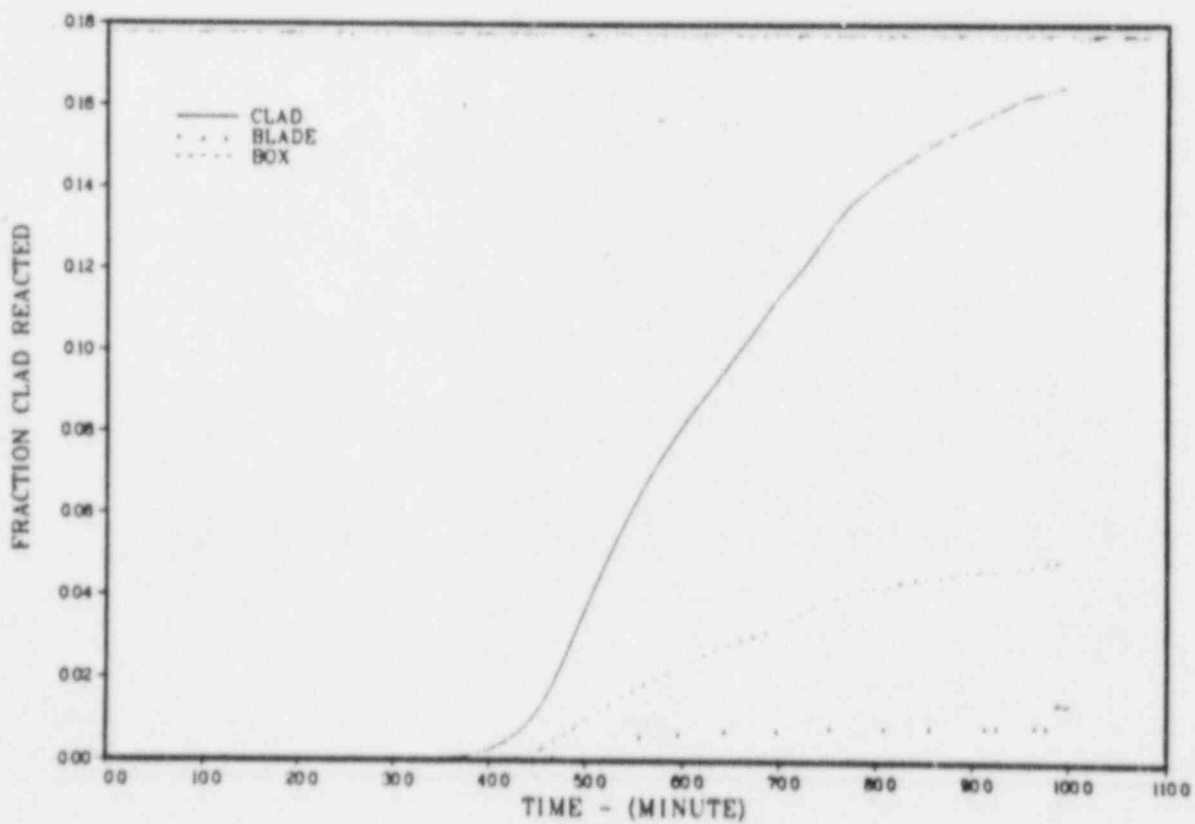
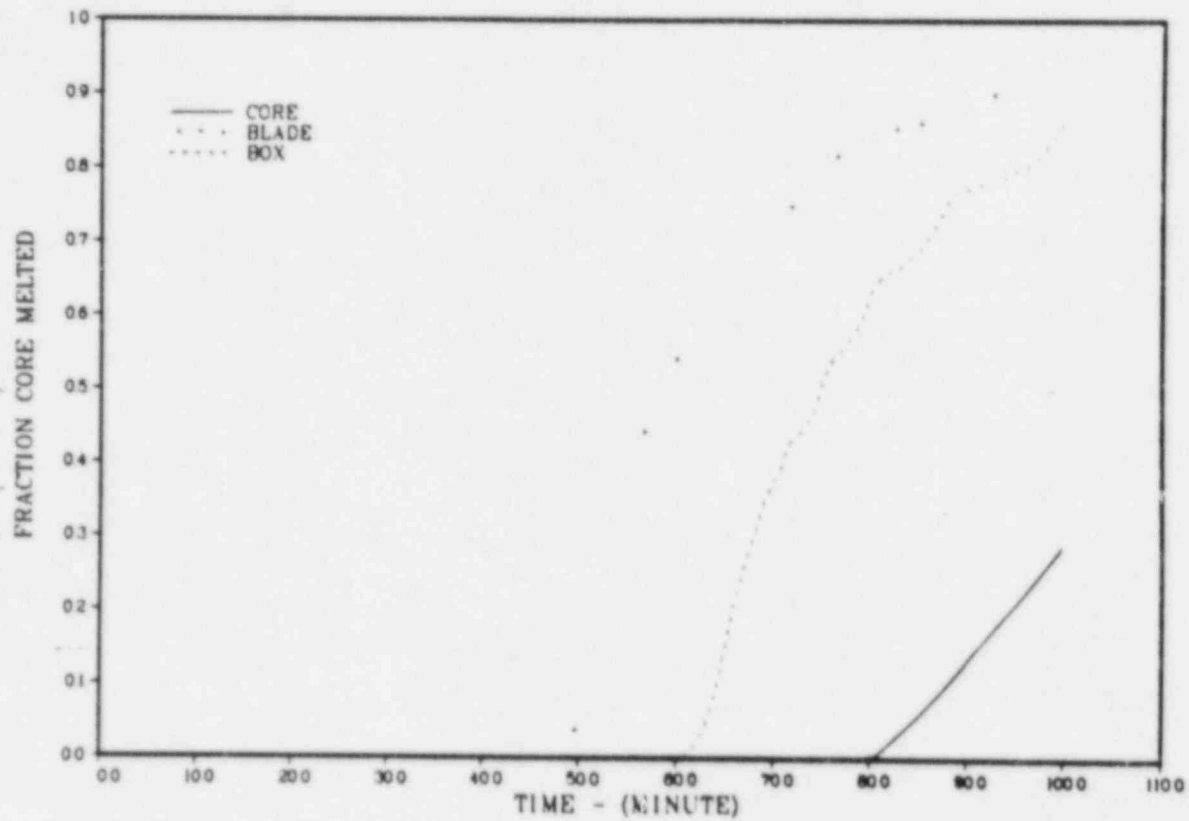


Figure 4.2 Melt fraction and oxidation fraction for case 4.1.

NO ECC GG POWER 10 NODES ADS(8) AT 5

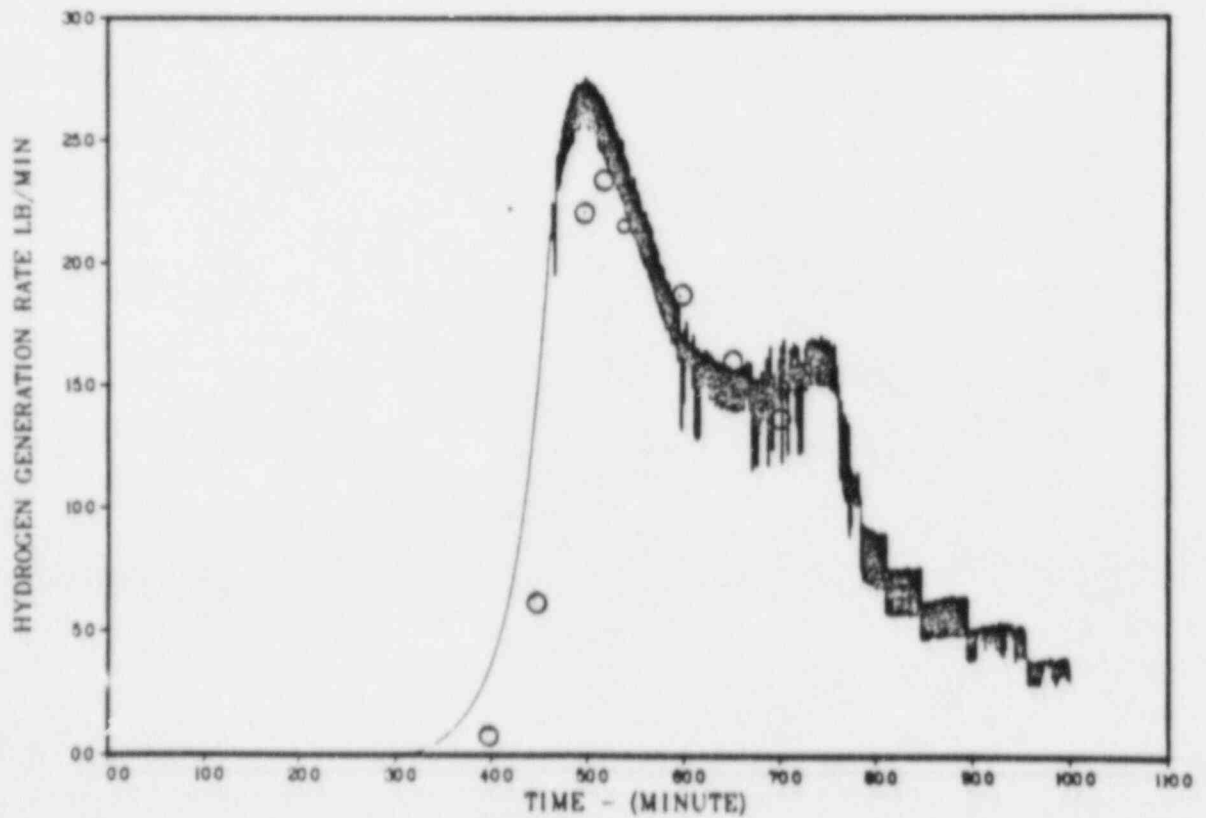
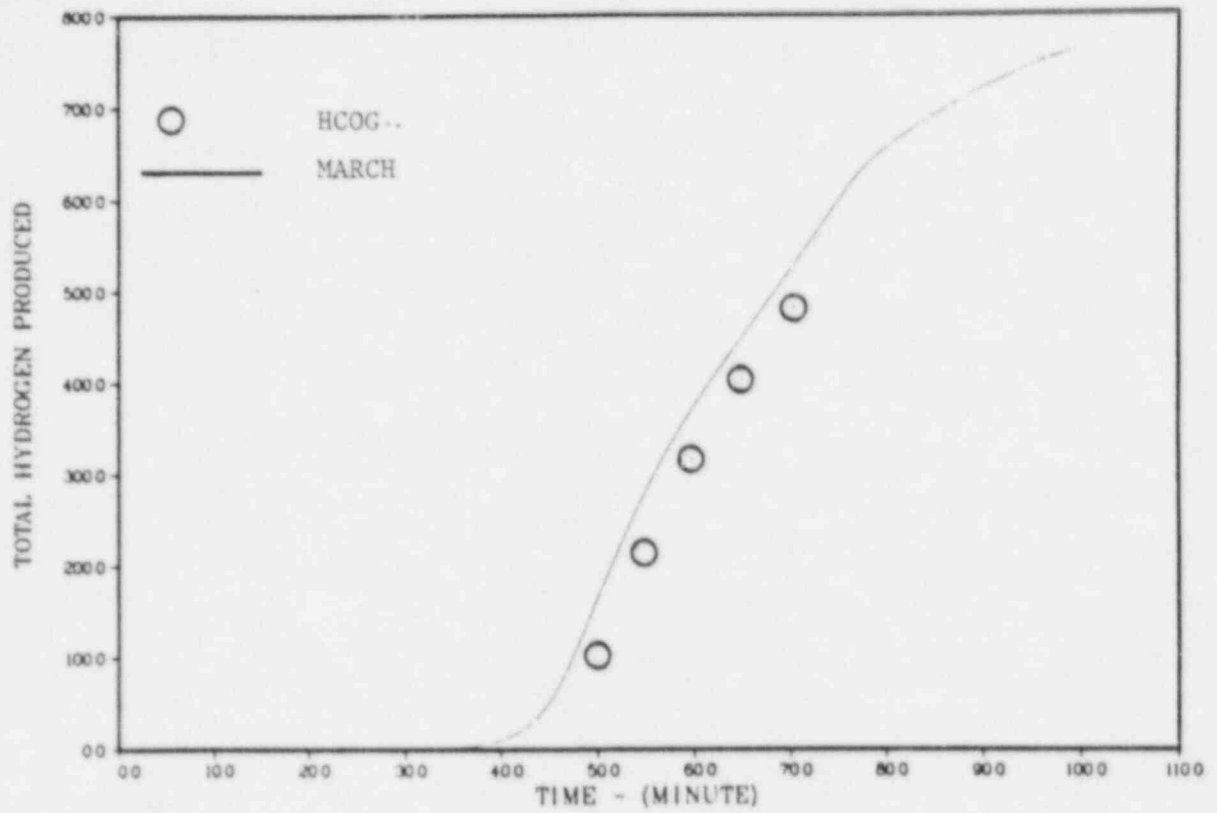


Figure 4.3 Comparison of  $H_2$  generation for case 4.1.

NO ECC GG POWER 10 NODES ADS(8) AT 5

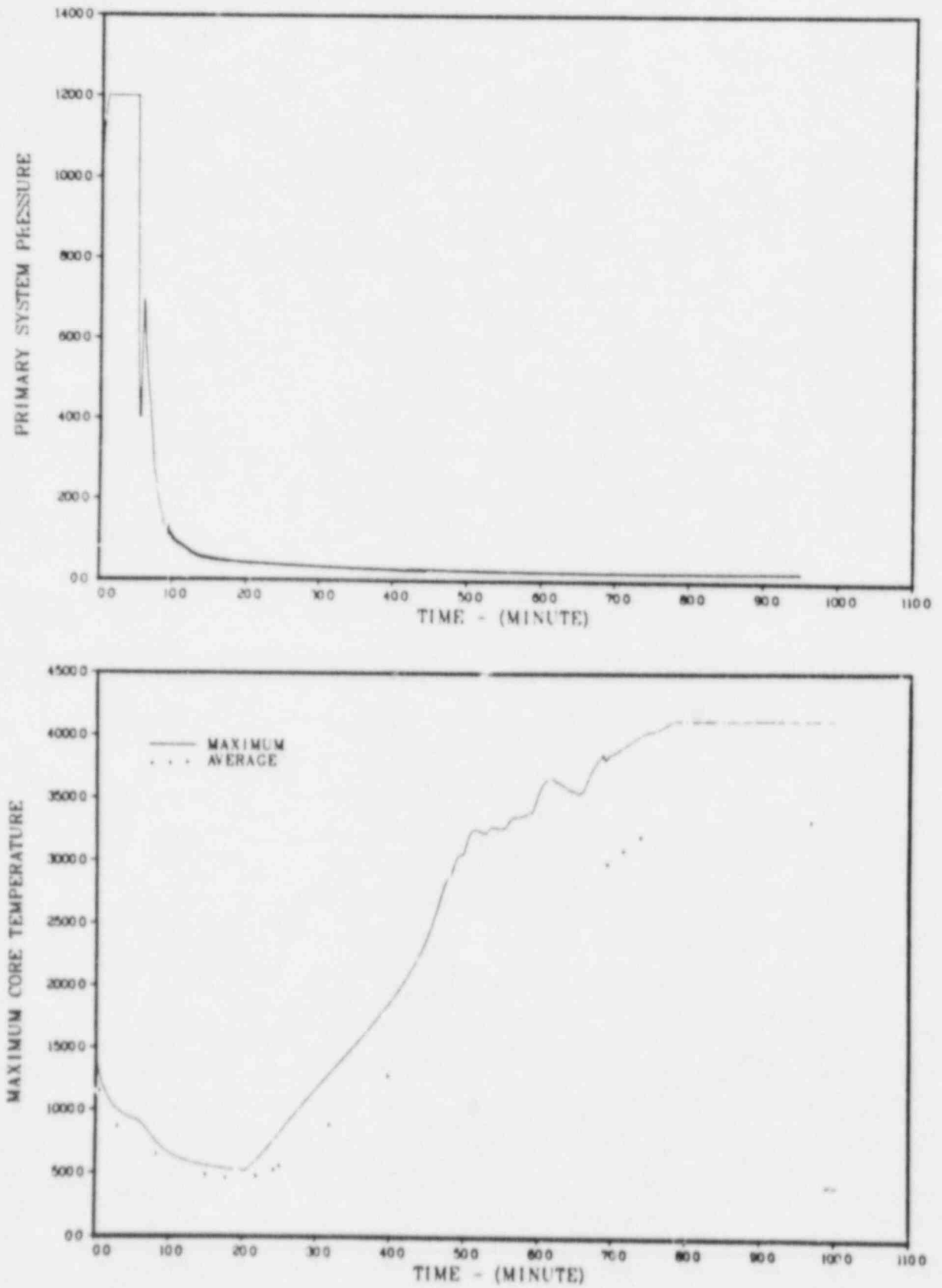


Figure 4.4 System pressure and core temperature for case 4.1.

NO ECC GG POWER 10 NODES ADS(8) AT 5

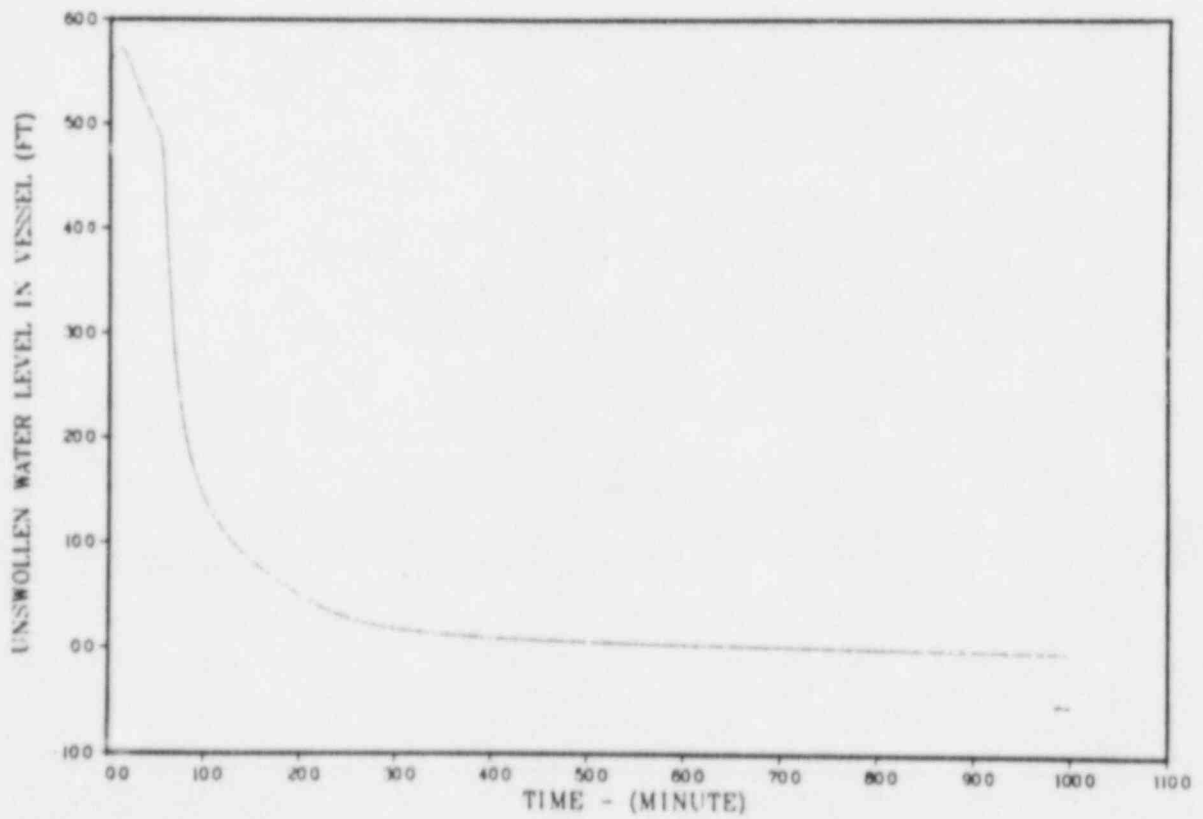
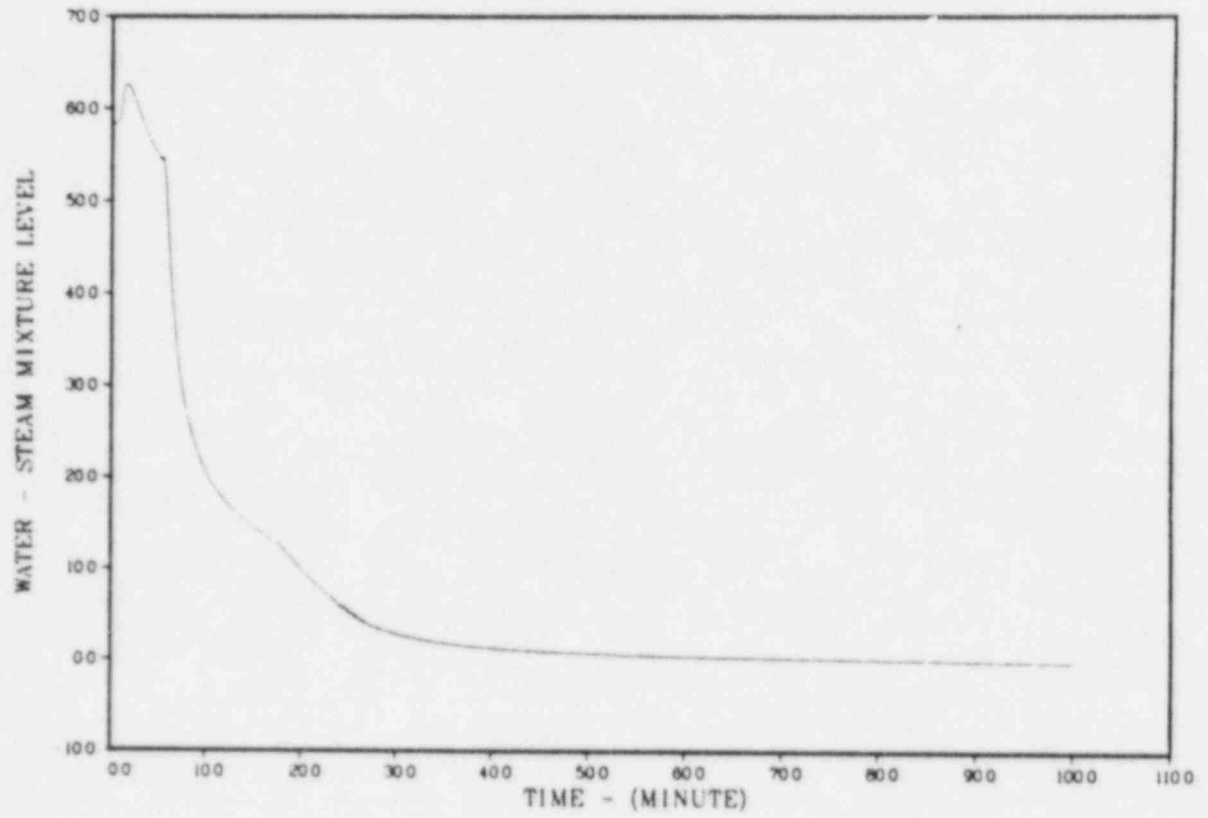


Figure 4.5 Reactor vessel water level for case 4.1.

300GPM AT 42 GG POWER 10 NODES ADS(8) AT 5

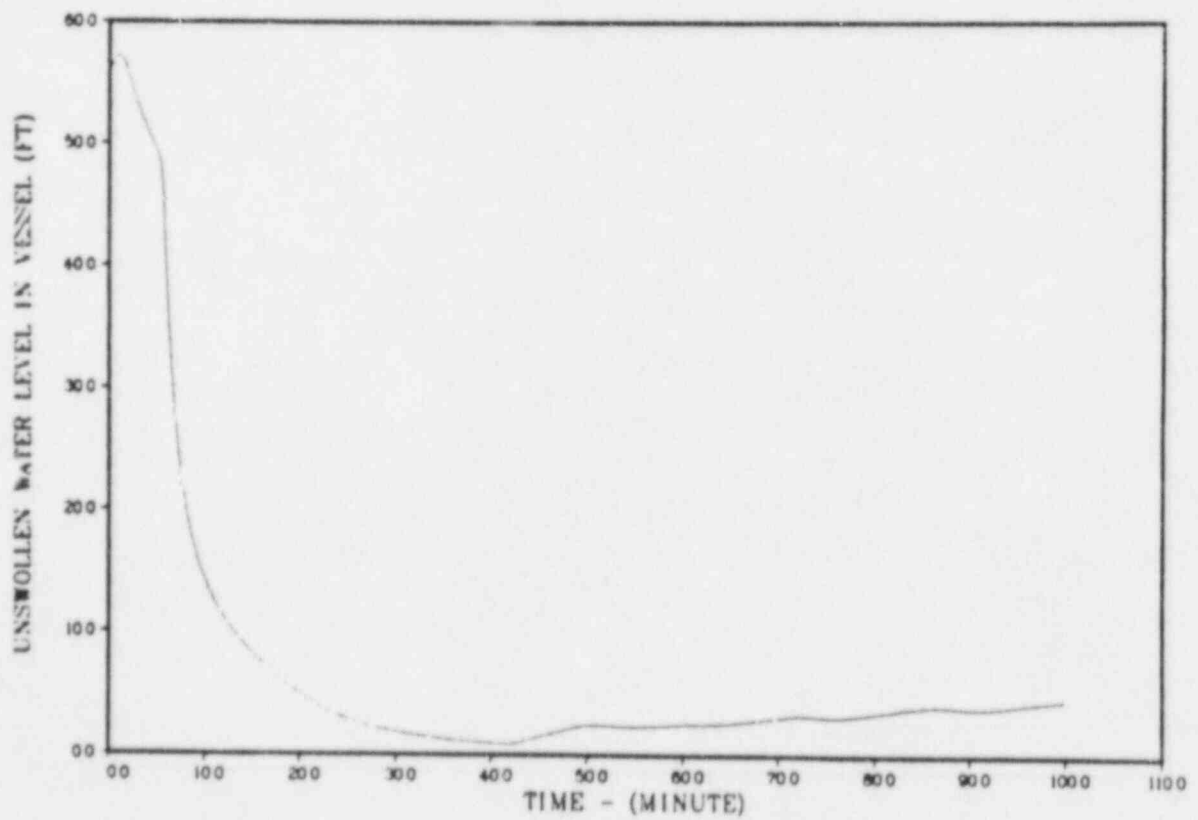
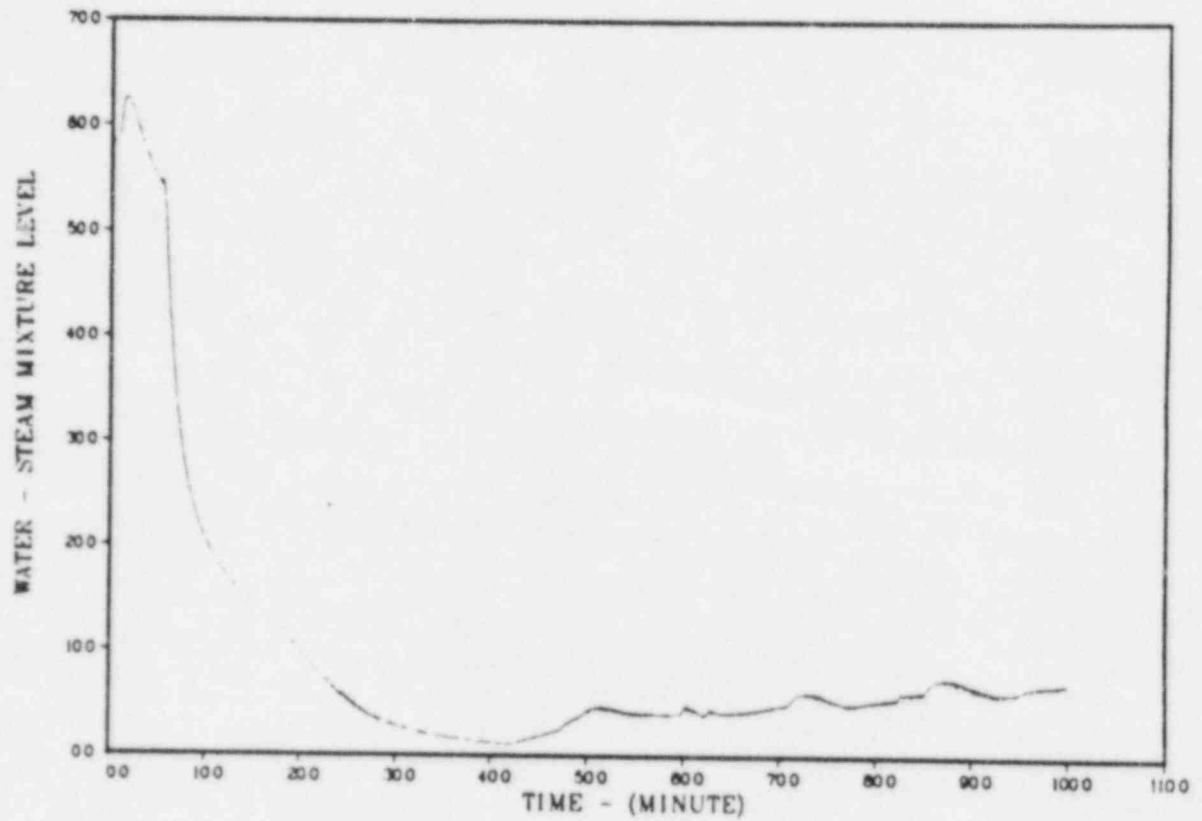


Figure 4.6 Reactor vessel water level for case 4.2.

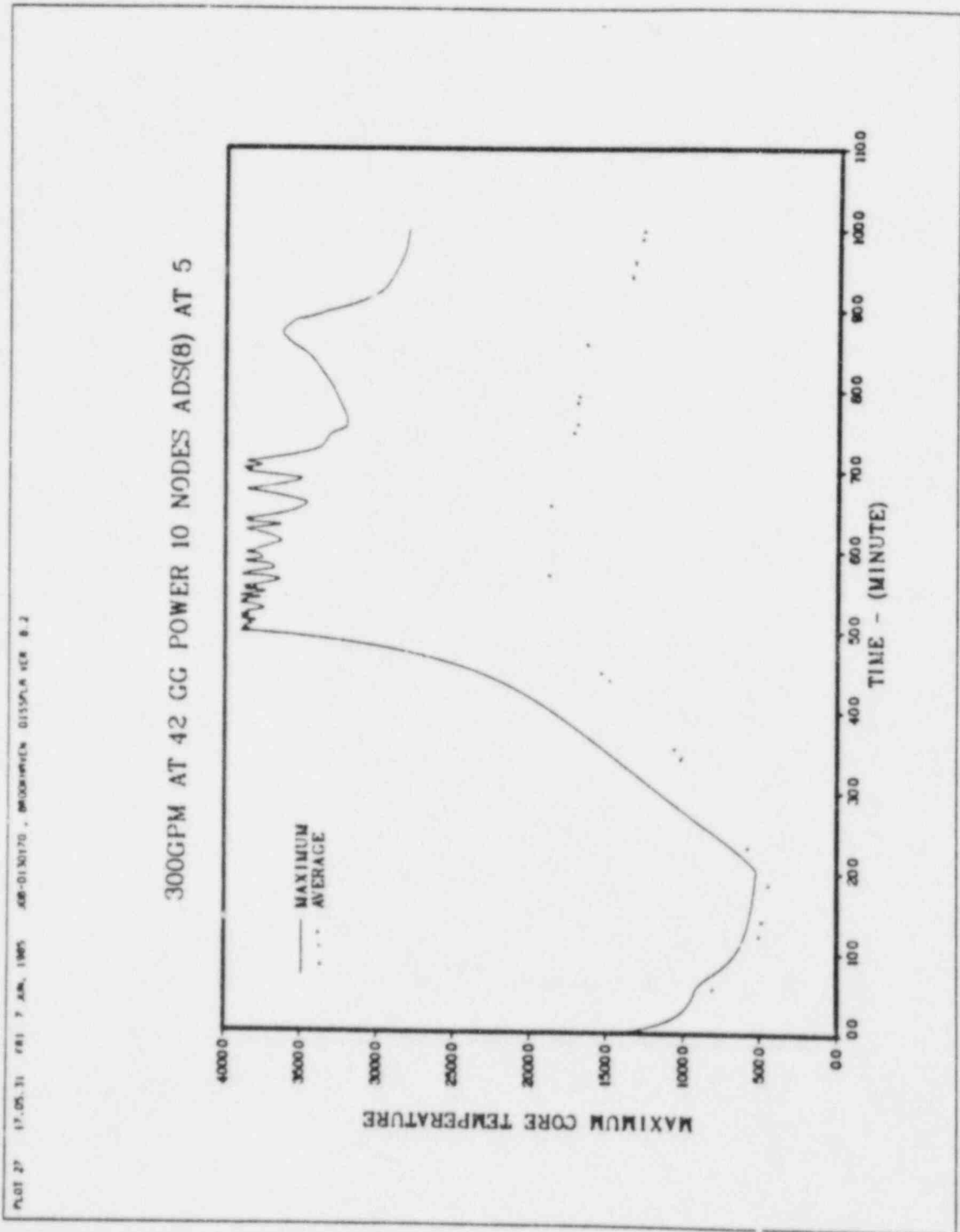


Figure 4.7 Core temperature for case 4.2.



300GPM AT 42 GG POWER 10 NODES ADS(8) AT 5

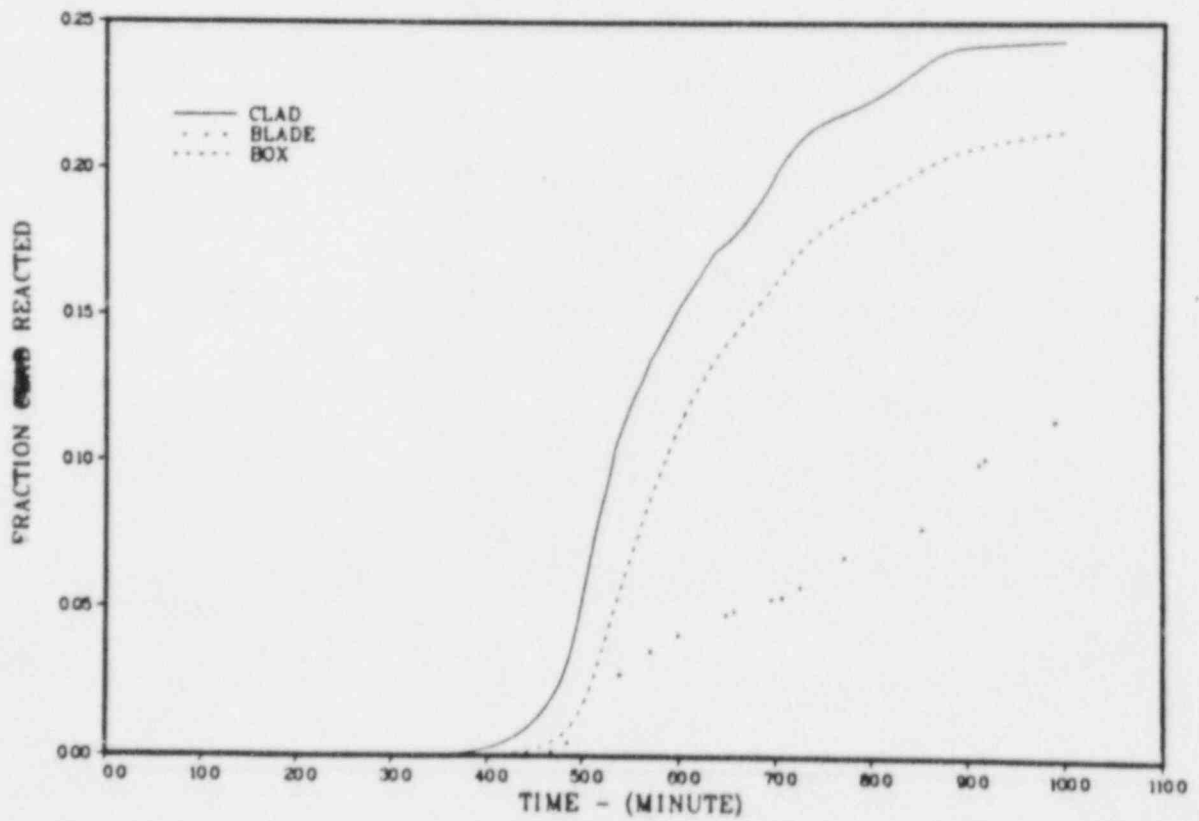
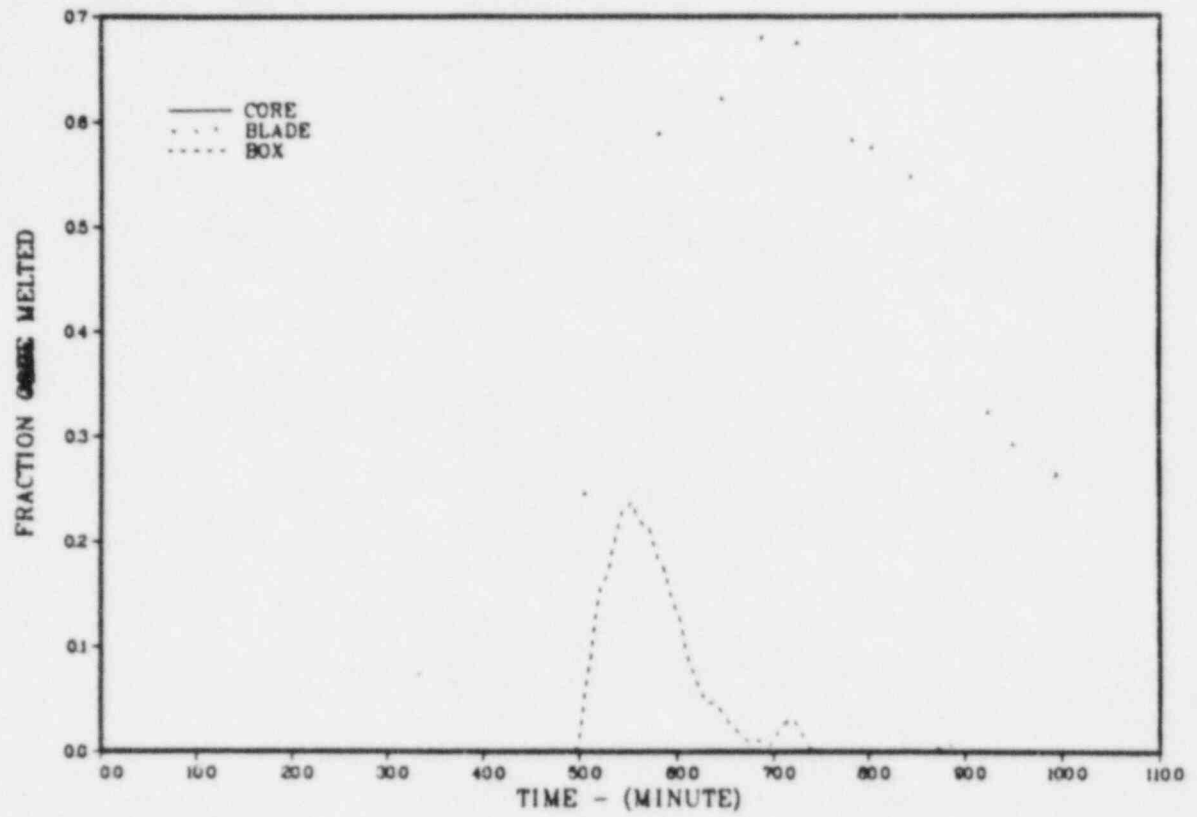


Figure 4.8 Melt fraction and oxidation fraction for case 4.2.

300GPM AT 42 GG POWER 10 NODES ADS(8) AT 5

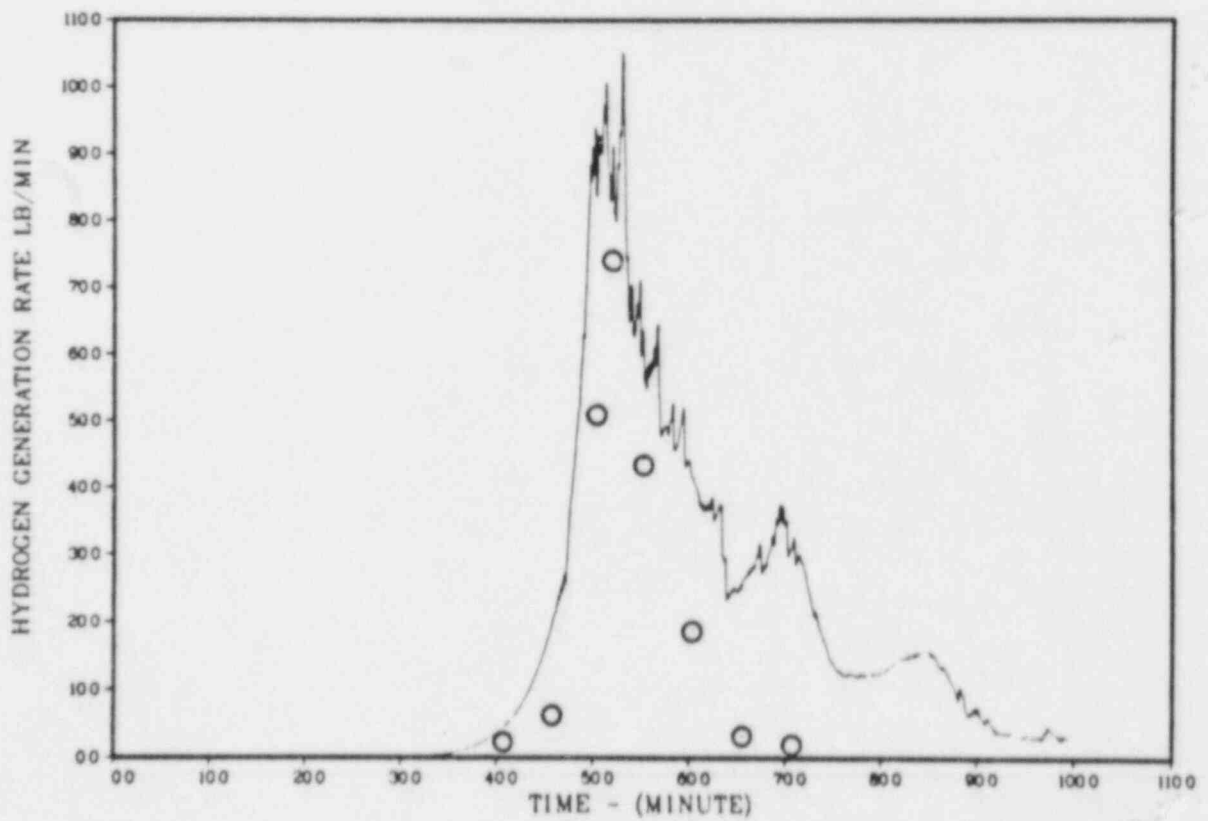
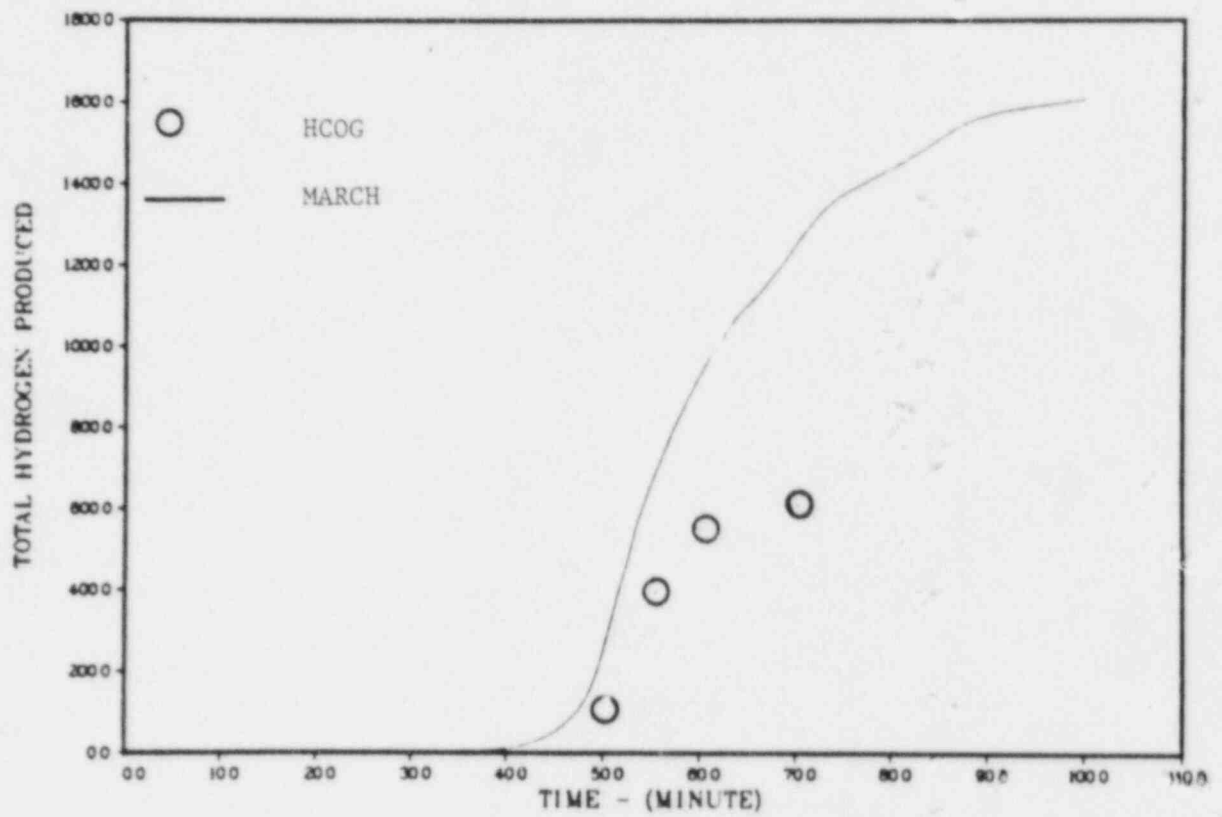


Figure 4.9 Comparison of  $H_2$  generation for case 2.

300GPM AT 42 GG POWER 10 NODES ADS(8) AT 5

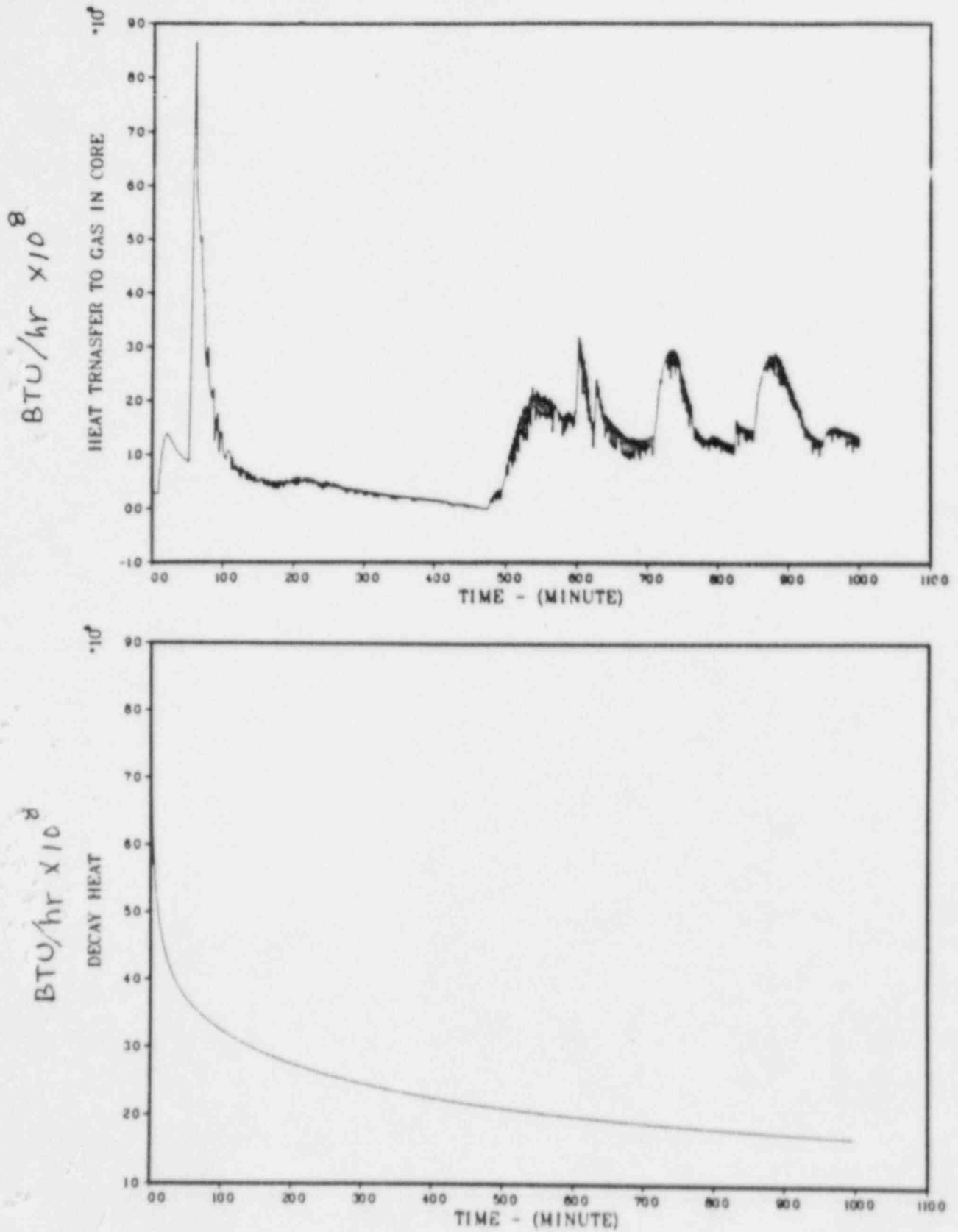


Figure 4.10 Heat transfer to gas in core and decay heat for case 2.

5000GPM AT 56.7 GG POWER 10 NODES ADS(8) AT 5

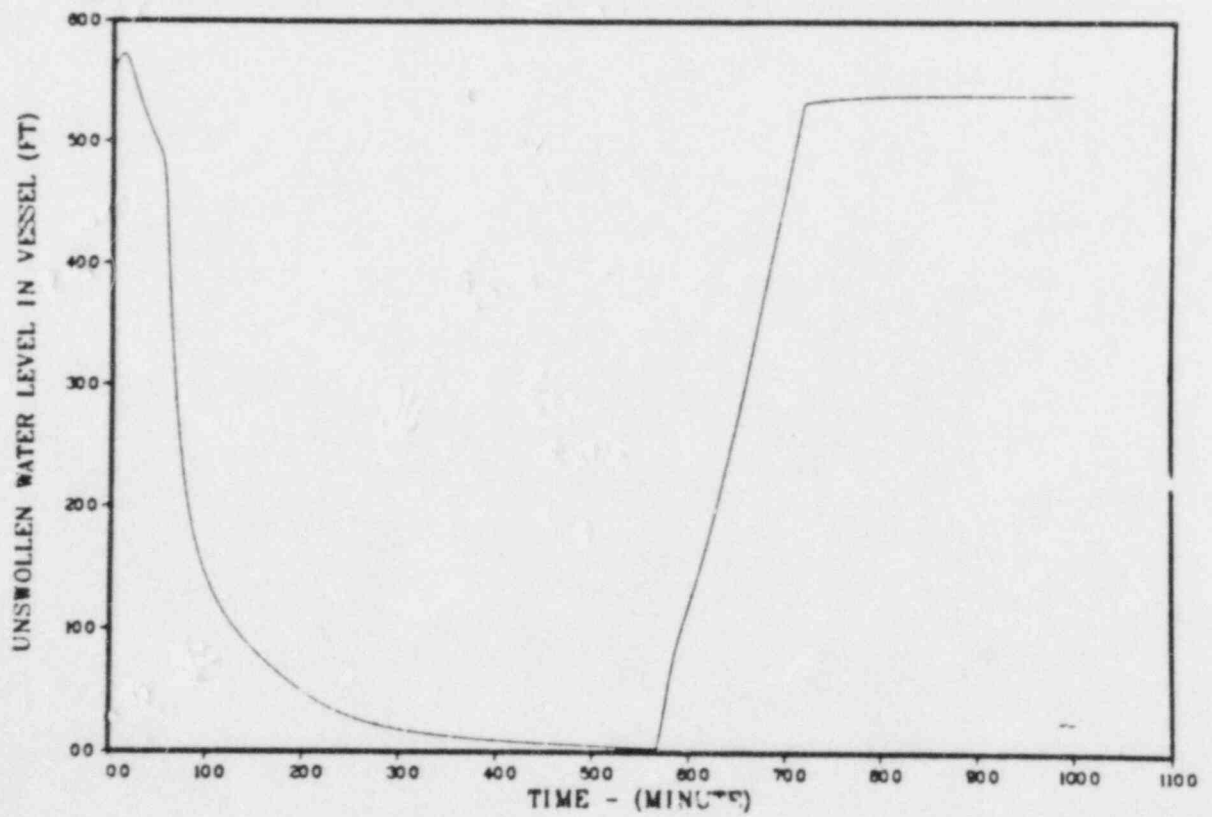
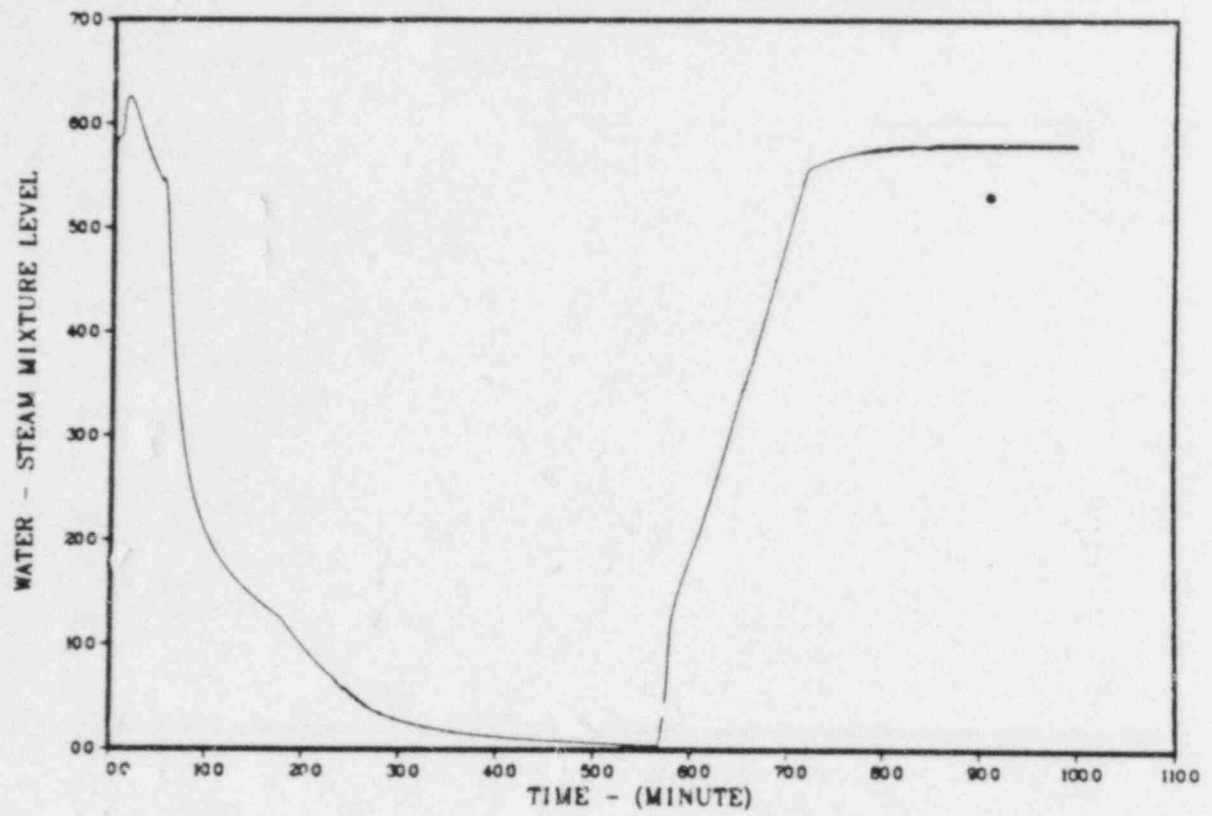


Figure 4.11 Reactor vessel water level for case 4.2.

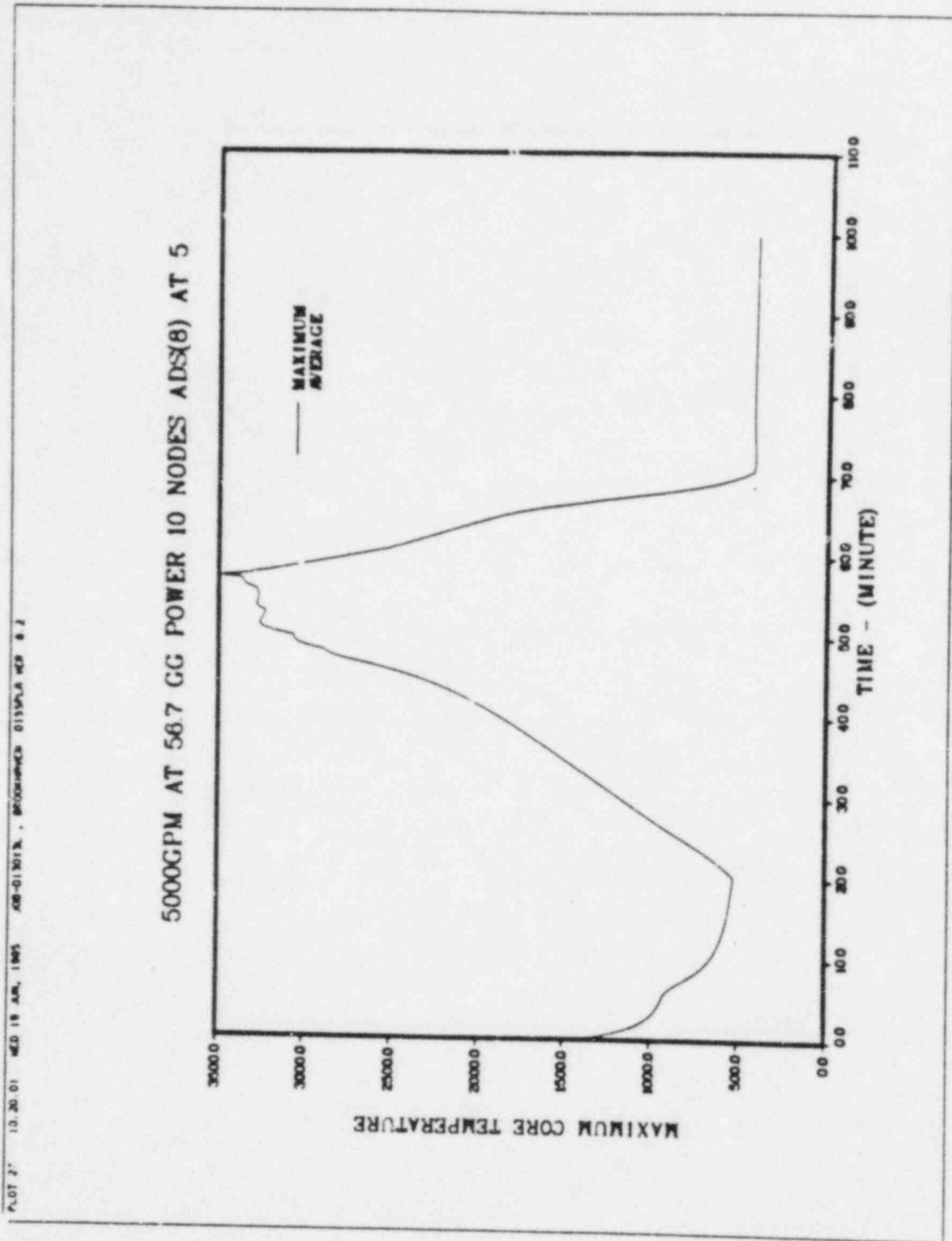


Figure 4.12 Core temperature for case 4.3.

5000GPM AT 56.7 GG POWER 10 NODES ADS(8) AT 5

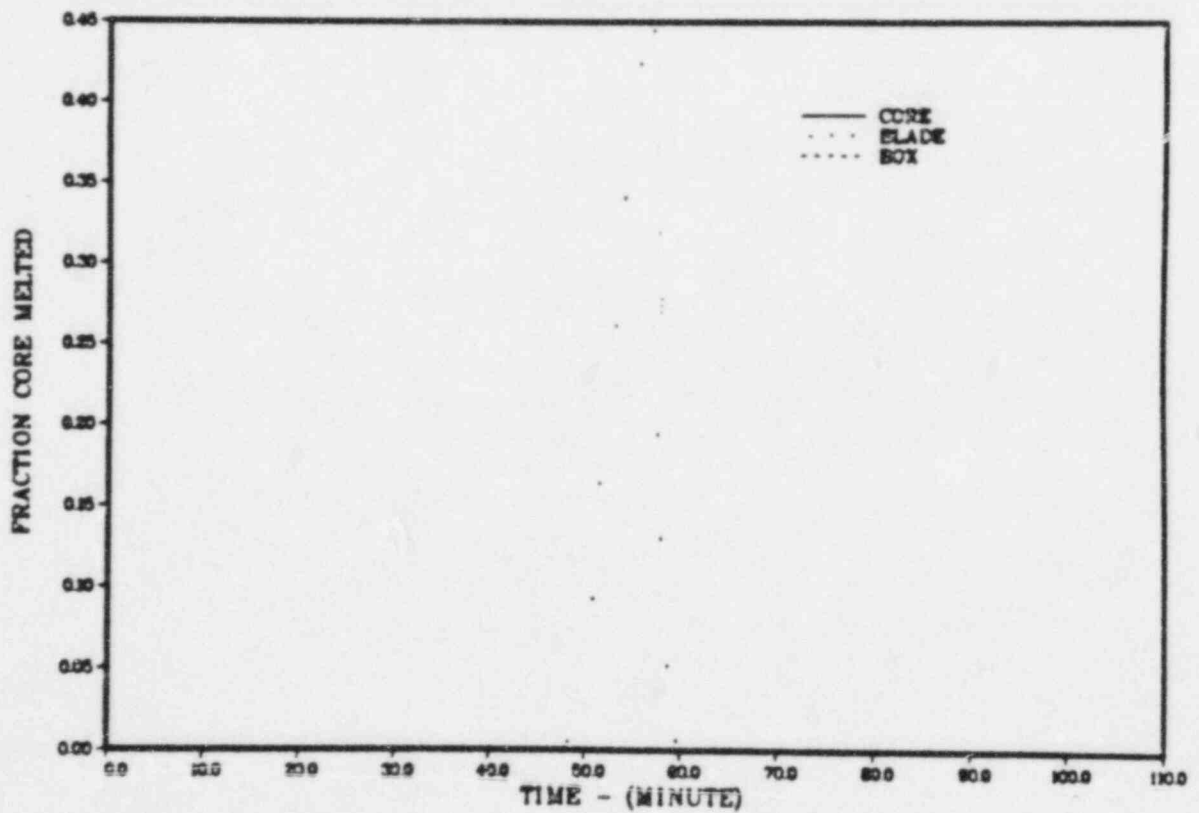
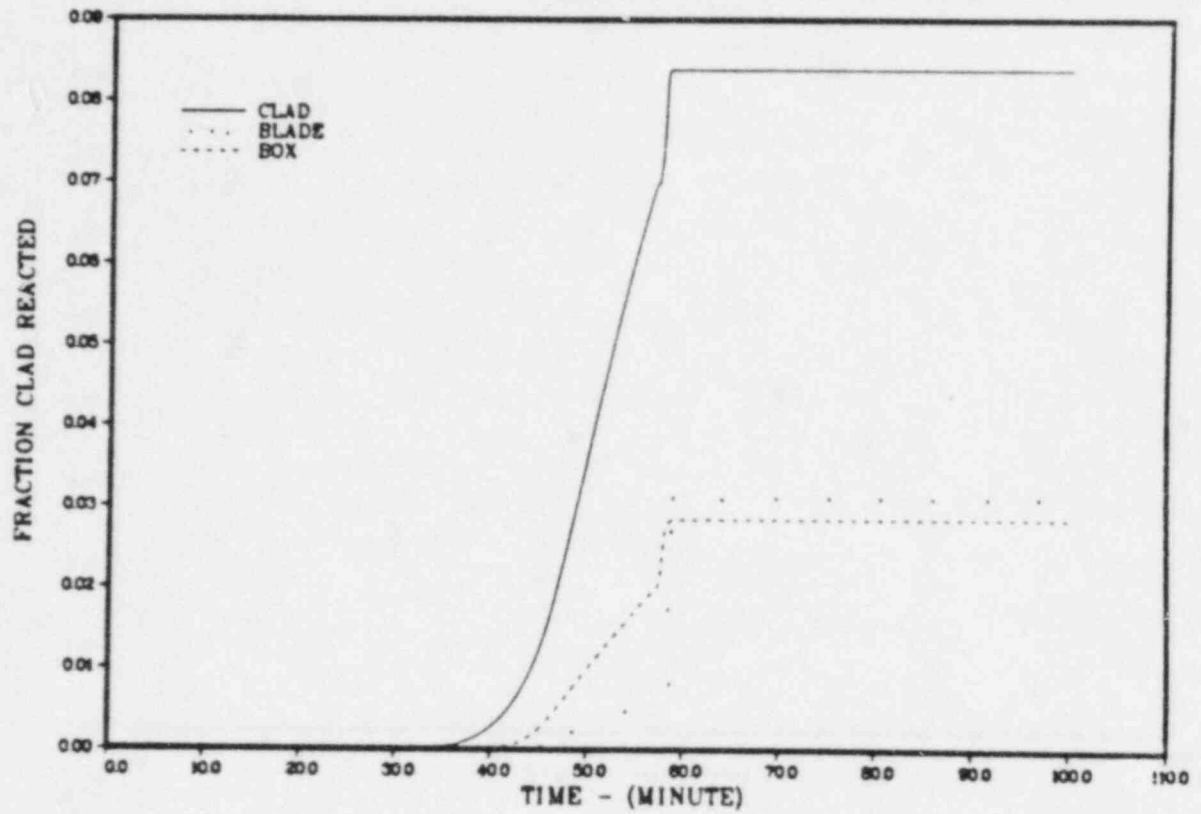


Figure 4.13 Melt fraction and oxidation fraction for case 4.3.

5000GPM AT 56.7 GG POWER 10 NODES ADS(8) AT 5

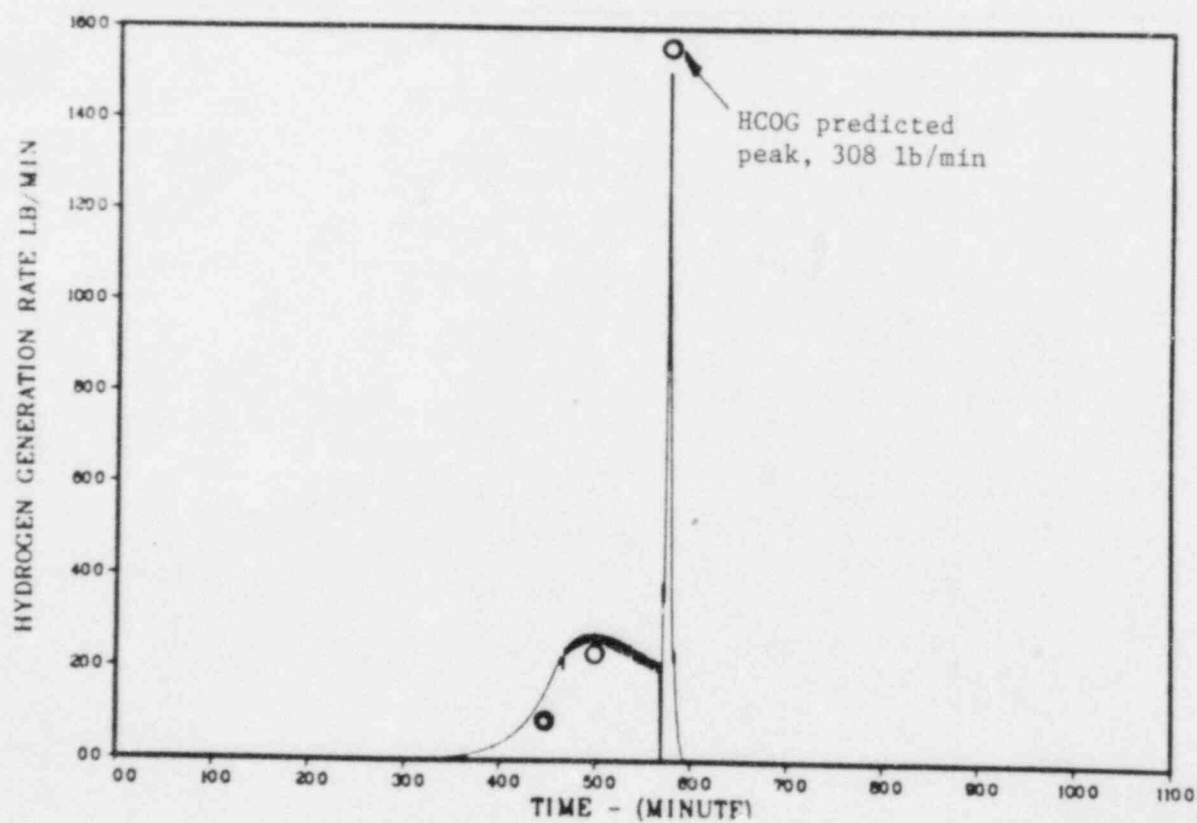
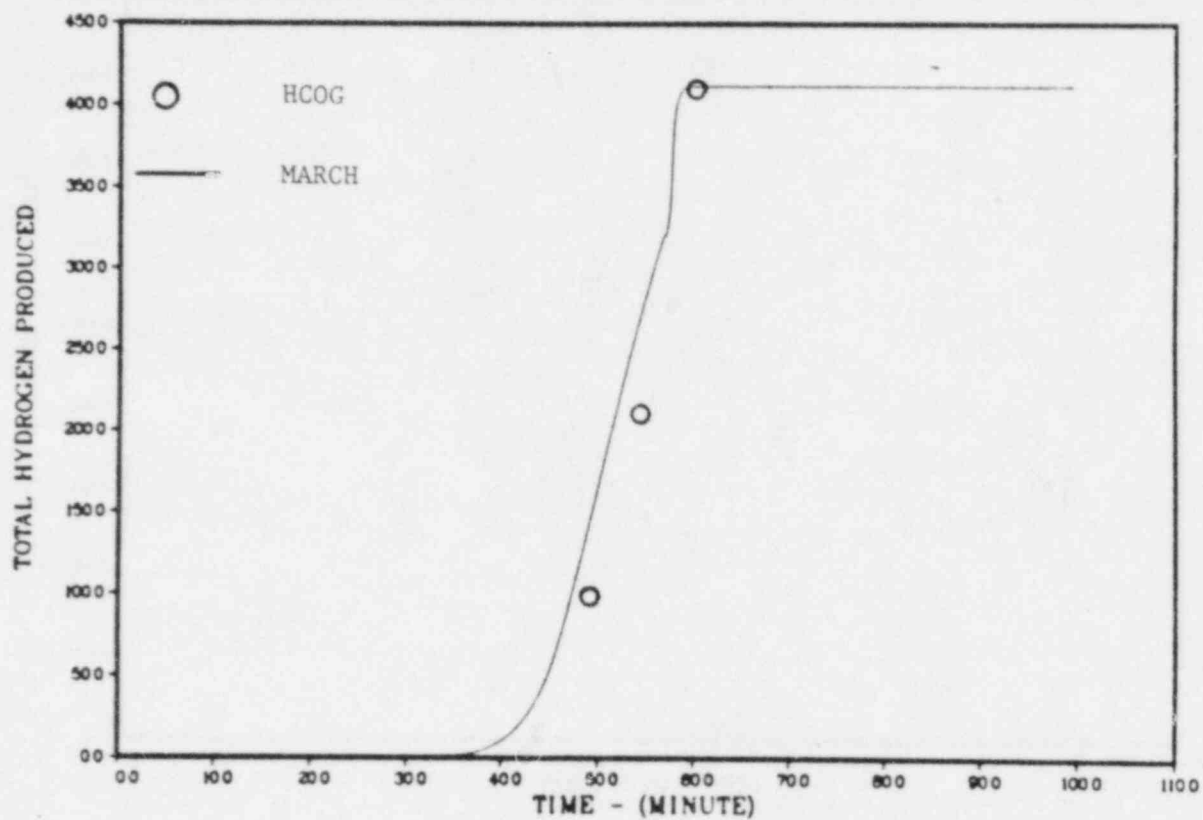


Figure 4.14 Comparison of  $H_2$  generation for case 4.3.

5000GPM AT 56.7 GG POWER 10 NODES ADS(8) AT 5

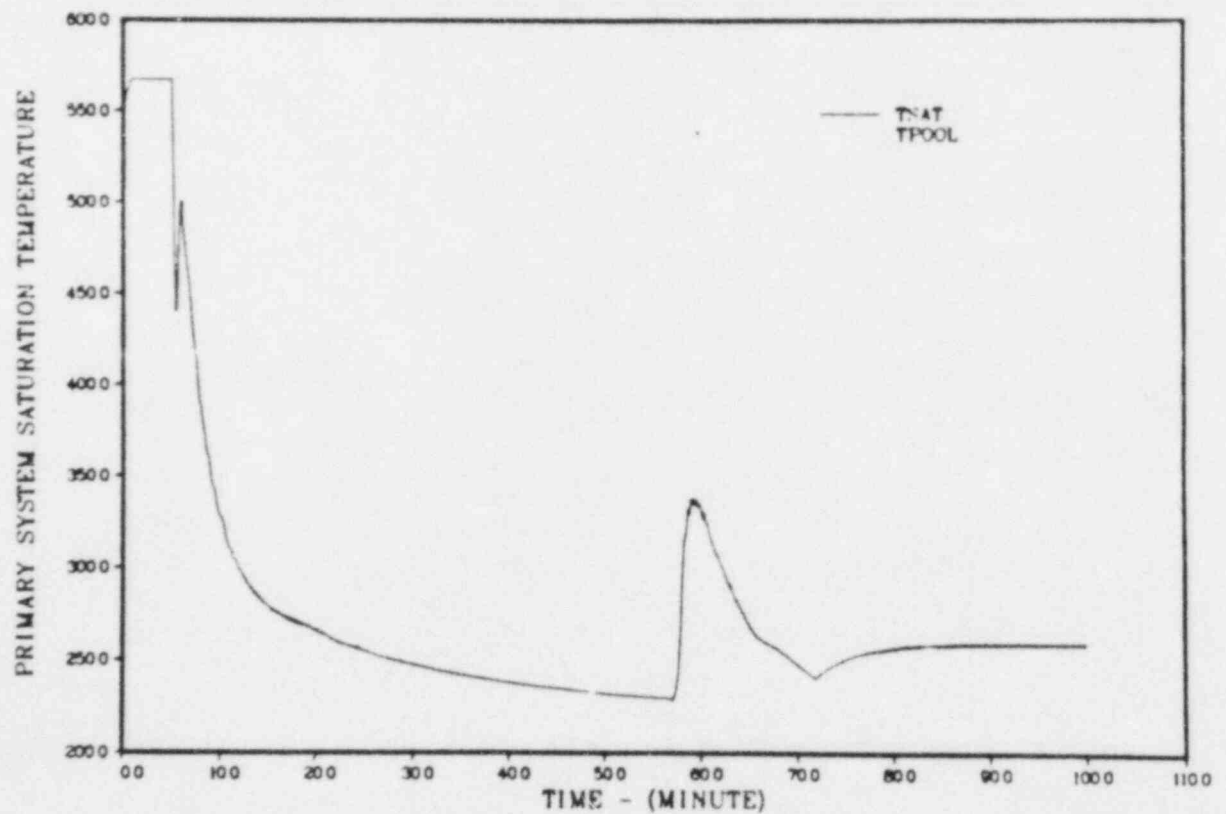
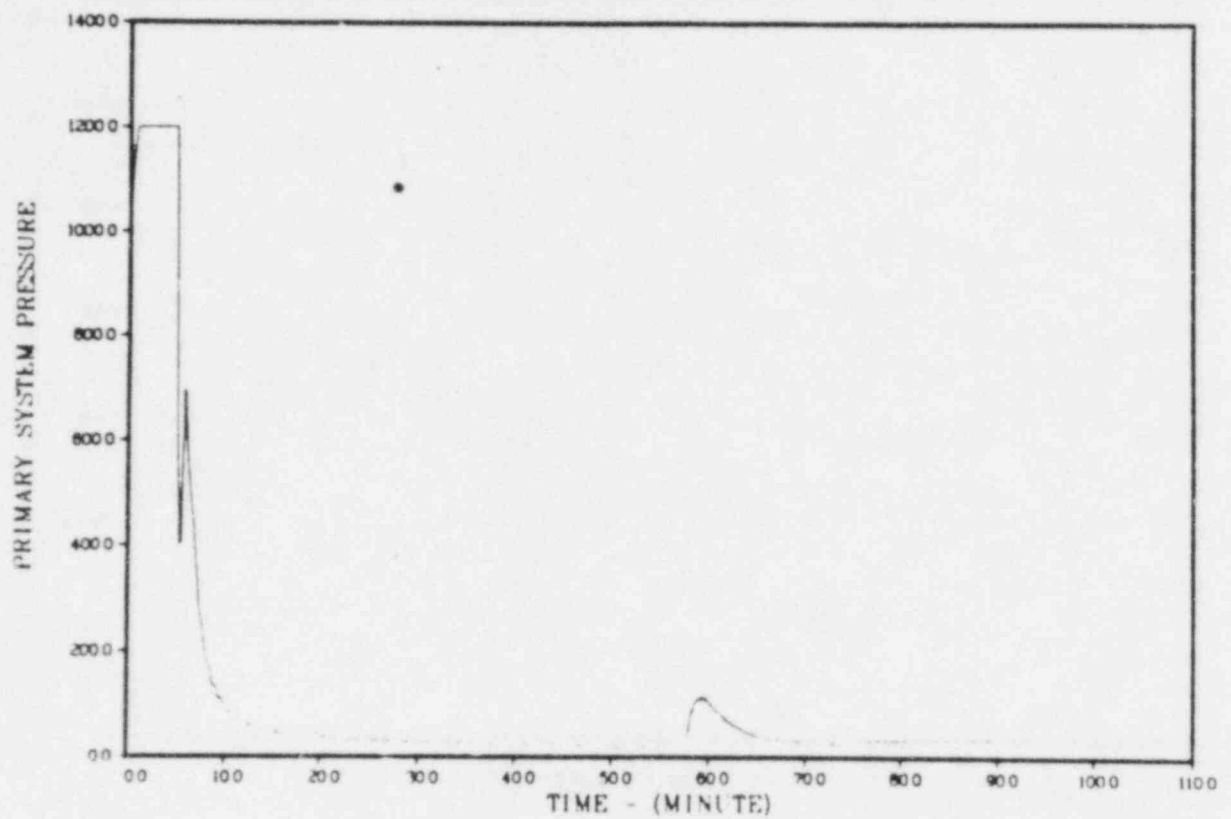


Figure 4.15 System pressure and temperature for case 4.3.



## 5. MARCH ANALYSIS OF SEPARATE EFFECTS

In performing the MARCH analysis discussed in Section 4, it is recognized that there are several important parameters related to core heat transfer and hydraulics. These parameters could potentially affect the predictions of hydrogen production. Hence, each of these parameters was examined separately and its impact on hydrogen production is presented in this section. Case 4.2 (300 gpm of CRDHS flow injected at 42 minutes) was selected as the base case for comparison. The following parameters used in the base case analysis were varied in the study of the separate effects:

- Coolant Injection Time = 42 minutes
- Coolant Injection Rate = 300 gpm
- Number of Fuel Axial Node = 10
- Axial Power Profile - Curve 1 of Figure 4.1
- Fraction of Steam Flow in Bypass Region = 10%
- Zircaloy Oxidation Cut-Off Temperature = 2400°K (3860°F)

### 5.1 Effect of Coolant Injection Time

The potential for terminating the degraded core accident by delayed injection of cooling water was considered in this case. The injection was delayed from 42 minutes (base case) to 52 minutes, at which time the swollen water level is about 0.6 ft in the core region. The maximum and average core temperatures are 3250°F and 2030°F, respectively as shown in Figure 5.1. The injection of water at 52 minutes when the core is at high temperature causes a rapid water boil-off and oxidation of zircaloy. At the end of 100 minutes transient time, the fractions of oxidation are 29%, 31% and 7% for cladding, channel boxes and control blades, respectively. A maximum of 45% and 87% of channel boxes and control blades are melted before the core is completely reflooded as shown in Figure 5.2. Comparison with the base case indicates that a delayed injection of cooling water could lead to severe core damage as indicated by the melting of a large amount of channel boxes and control blades.

The hydrogen production is shown in Figure 5.3. It is seen that the delayed injection of cooling water results in a very sharp peak hydrogen generation rate (243 lb/min) at 57 minutes. This is caused by the reflood of the core which is at temperatures much higher than that of the base case (Figure 4.7). Consequently, the total hydrogen production (2010 pounds) is about 25% more than that of the base case.

### 5.2 Effect of Coolant Injection Rate

As discussed in Section 4.2, the assumed 300 gpm flowrate of the CRDHS flow appears sufficient to suppress the progress of core melting and terminate the accident. The 300 gpm flow rate is based on the operation of two CRDHS pumps. The potential of failure of one CRDHS pump is examined in this section. The maximum flowrate with one operating CRDHS pump is about 175 gpm.<sup>8</sup> Using this reduced injection rate, the MARCH code predicted a different behavior of hydrogen generation as illustrated in Figure 5.4. There are four peaks of hydrogen generation rate. The first (i.e., the maximum) peak rate is about 155 lb/min and is followed by three successive peaks slightly less than 100 lb/min. Consequently, a total of 2450 pounds of hydrogen is generated in 100 minutes, an increase of about 53% in comparison with the base case (Figure

4.9). The repeated surge of hydrogen generation is caused by the repeated core reflood illustrated in Figure 5.5. Apparently, the reduced injection rate is not sufficient to rapidly recover the core region. The oscillation of water level in the core region indicates the injected coolant is unable to balance the water boil-off. The oscillation of water level illustrates a repeated core reflood which enhances hydrogen production. A large fraction of cladding and channel boxes are oxidized and the melting of channel boxes and control blades are increased as shown in Figure 5.6.

### 5.3 Effect of Fuel Axial Node

The core reflood and quenching of fuel rods play an important role on hydrogen production as discussed in Sections 4.2 and 4.3. The computation of core reflood and quenching are related to the axial noding modeled in the MARCH code. The base case assumed ten nodes in the fuel axial direction. In this section, the ten nodes were extended to 24 nodes and the potential effect on hydrogen generation is examined. The MARCH predicted core temperature, fractions of oxidation and melt, and hydrogen generation are shown in Figures 5.7 to 5.9, respectively. Comparisons with the base case show that the hydrogen production is reduced by about 11% using more axial nodes (i.e., smaller node size). The total hydrogen production and its peak generation rate are 1420 pounds and 88 lb/min, respectively. The core damage is reduced by about 9%.

### 5.4 Effect of Fuel Axial Power Profile

One of the differences between the analyses of the MARCH code and the HCOG Core Heatup Code is the assumed axial power profile in the fuel rods as given in Figure 4.1 of Section 4. A bottom-skewed (Haling) power distribution is used in the MARCH analysis and a symmetrical cosine-type distribution used in the HCOG analysis. For the case of the MARCH analysis, the bottom nodes with high peaking power factor are within the water covered region during the core heatup transient. The high decay heat in these nodes would generate more steam and enhance the oxidation process. Hence, more hydrogen production is expected by using the FSAR power profile. On the other hand, the cosine-type power profile assumed in the HCOG analysis has high peaking power factor in the central portion of the fuel rods. These nodes are expected to yield a high rate of hydrogen generation when they are quenched during core reflood. These effects were examined by performing a MARCH analysis using the cosine-type power profile assumed in the HCOG analysis (Curve 2 in Figure 4.2).

The MARCH predicted core temperature, fractions of oxidation and melt, and hydrogen generation are shown in Figures 5.10 to 5.12. It is seen that using the cosine-type symmetrical power distribution reduces the oxidation and total hydrogen production by about 11%. As one expects, a large peak of hydrogen generation is produced when the central portion of core is reflooded. The peak rate is 123 lb/min, a 23% increase in comparison with the base case.

### 5.5 Effect of Steam Flow in the Channel Box-Control Blade Bypass Region

It is recognized that the amount of steam flow in the bypass region of a BWR6 core has an important effect on the oxidation of control blades and outer surface of the channel boxes during a heatup transient. The flow split between the fuel region and the box-blade region is particularly important for

the case of injection of CRDHS flow. The CRDHS flow first enters the bypass region and then passes through a number of leakage paths into the bottom of the fuel assembly.

In the MARCH2 computer code, the coolant injection is assumed to enter the core from the bottom of the reactor vessel. The injection of coolant into the bypass region and the potential leakage into the fuel region are not modeled in the MARCH code. A detailed analysis of backflow leakage from the bypass region in a BWR core is presented in a General Electric Report.<sup>9</sup> According to the report, the total leakage flow from the bypass region to the fuel region would be larger than the 300 gpm CRDHS flow under a small pressure differential. (The exact flow values given in Reference (9) are not quoted in this memorandum because the information is GE Proprietary.) It appears that MARCH modeling of the CRDHS injection directly into the core is an adequate approximation, as the 300 gpm CRDHS flow could pass through the leakages in the bottom of the core into the fuel region. However, the MARCH assumption of a uniform water level across the entire core is not accurate. A water level differential is required for the leakage from the bypass region to the fuel region.

The steam flow split between the fuel region and bypass region is specified in the MARCH code by an input parameter FBP, which is defined as the fraction of steam flowing through the box-blade region. The code first performs an overall heat and mass balance computing the total steam generation. The fractions of steam in the fuel and bypass regions are determined according to the parameter FBP. The MARCH code default suggests that 10% of the steam flow should be directed to the bypass region (FBP=0.1) based on the area ratio of the fuel region and bypass region. In fact, the flow split would be determined by the total hydraulic resistance in each region, which is related to the flow area. During a core heatup transient, the reactor vessel is depressurized and partially uncovered. The fluid density difference and water boil-off rate in each region become important driving forces for flow entering the region. Thus, the assumption of 10% of steam flow in the bypass region may not be valid. To test the impact of flow in the bypass region, we considered a limiting case in which no steam flow in the bypass region was assumed (FBP=0). This is the condition used in the HCOG analyses. The results are shown in Table 1 and compared with the base case analysis (FBP=0.1) and the HCOG sample problem. Comparisons of hydrogen generation, fuel temperature, fraction of melt and oxidation are illustrated in Figures 5.13 to 5.17. The following conclusions are made from this study:

1. The peak hydrogen generation rate is reduced from 100 lbm/min to 77 lbm/min by assuming FBP=0; the total hydrogen production is also reduced from 1610 pounds to 1040 pounds for a transient time of 100 minutes as shown in Table 5.1 and Figure 5.13.
2. No oxidation of the control blade and outer surface of the channel box is predicted for FBP=0. Without the reaction heat from the outer surface as a heat source in the channel box wall, the wall temperature is lower and the oxidation of the inner surface is reduced in comparison with the FBP=0.1 case. Hence, the oxidation of the channel box is less than half of that for the case of FBP=0.1, in which both surfaces are oxidized.

3. The MARCH analysis with FBP=0 provides better agreement with the HCOG predictions for  $H_2$  generation shown in Figure 5.13. The agreement is reasonably good prior to the peak hydrogen generation. However, due to the different treatment of core reflood, the MARCH predicted hydrogen generation is higher as the core is gradually recovered after 55 minutes.
4. The temperature and oxidation of cladding are not affected by the fraction of steam flow in the bypass region. For the present case of 300 gpm CRDHS flow injection, termination of oxidation is due to the reflood of reactor vessel.
5. Reduction of steam flow in the box-blade region reduces the melt of channel boxes and control blades as shown in Table 5.1 and Figure 5.16. Hence, the total core damage is reduced.

#### 5.6 Effect of Zircaloy Oxidation Cut-Off Temperature

The Zr/steam reaction was assumed to be stopped at a cut-off temperature 2400°K (3860°F) in the base case. According to Reference 10, there is no physical bases for the existence of a temperature cut-off for the zircaloy oxidation. However, in performing the numerical analysis, both the MARCH code and the HCOG Core Heatup Code used the zircaloy oxidation cut-off temperature to address the phenomenological uncertainties associated with fuel relocation at high temperatures. Fuel relocation could cause the surface area for the Zr/steam reaction to be limited as observed in some experiments.<sup>10</sup> Nevertheless, a large uncertainty is involved in modeling the termination of zircaloy oxidation by using the cut-off temperature.

The impact of the cut-off temperature is investigated by performing a MARCH analysis, in which the Zr/steam reaction is allowed to continue above 3860°F. It is also assumed in the MARCH analysis that the reaction is not stopped by node melting. The fuel node is assumed to melt at 4130°F (the melting temperature of the Zr-UO<sub>2</sub> eutectic solution) and the channel box at 3365°F (melting temperature of zircaloy). Figure 5.18 shows that the maximum core temperature reaches 3860°F at 50.3 minutes. With continuous oxidation of the cladding and addition of reaction heat into the core, the core temperature rapidly increases to the melting temperature of 4130°F at 50.6 minutes. Within less than 10 minutes, a maximum of 21% core and 35% channel boxes are melted as shown in Figure 5.19. It is noted that this is the only case for which a core melting is predicted by the MARCH code. However, the core melting is suppressed by core reflood when about 1/3 of the core is recovered at about 60 minutes. Without the cut-off temperature, the oxidation of cladding is much higher (45%) than that in the base case (24%) as one expects. Consequently, a total of 2150 pounds of hydrogen is produced and the peak generation rate is as high as 168 lb/min as shown in Figure 5.20.

#### 5.7 Summary

The results of the study of separate effects are summarized in Table 5.2. An inspection of table 5.2 reveals that:

1. A delay of coolant injection time (Case 5.1) or a reduction of coolant injection rate (Case 5.2) would lead to severe core damage and large increase of hydrogen production.



2. Changing the fuel axial node (Case 5.3) and power profile (Case 5.4) do not have a significant effect on hydrogen production. However, using smaller axial node would reduce the total hydrogen production and its peak generation rate. A symmetrical cosine-type axial power profile shows an increase of peak hydrogen generation rate.
3. The 10% steam flow in the channel box- control blade region assumed in the base case overestimates the steam flow in that region. The limiting case (Case 5.5) in which no steam flow is assumed in the bypass region shows a large reduction of hydrogen production.
4. The assumption of no Zr/steam oxidation cut-off temperature (Case 5.6) would lead to large core damage and hydrogen production. The MARCH calculation shows that the progress of core melting cannot be suppressed if the Zr/steam oxidation is allowed to continue beyond the cut-off temperature 3860°F under the conditions of Case 5.6.

Table 5.1 Comparison of Effect of Steam Flow in Bypass Region

	MARCH	MARCH	HCOG
Fraction of Steam Flow in Bypass Region, FBP	0.1	0	0
Oxidation, %, at 100 min			
Clad	24	22	17
Channel Box	21	8	
Control Blade	12	0	
Melt, %			
Core	-	-	
Channel Box	24	13	29
Control Blade	70	62	
Peak H <sub>2</sub> Production Rate			
lb/min	100	77	76
time, min	52	53	53
Total H <sub>2</sub> Production			
lb, at 70 min	1260	879	585
at 100 min	1610	1040	



Table 5.2 Summary of Results of Separate Effects

CASE	4.2 (Base)	5.1	5.2	5.3	5.4	5.5	5.6
Coolant Injection							
Rate, gpm	300	300	175	300	300	300	300
Time, min	42	52	42	42	42	42	42
Fuel Axial Power Profile*	G	G	G	G	H	G	G
No. of Axial Node	10	10	10	24	10	10	10
Fraction of Steam Flow in Bypass Region, %	10	10	10	10	10	0	10
Zr/steam Oxidation Cut-off	YES	YES	YES	YES	YES	YES	NO
Oxidation, %							
Cladding	24	29	36	22	21	22	45
Channel Box	21	31	37	19	21	8	14
Control Blade	12	7	5	11	12	0	9
Melt, %							
Core	0	0	0	0	0	0	21
Channel Box	24	45	33	22	22	13	35
Control Blade	70	87	98	63	71	62	65
H <sub>2</sub> Production, lb.	1600	2010	2450	1420	1470	1040	2150
Peak rate, lb/min	100	243	155	88	123	77	168
Time, min	52	57	54	54	50	53	55

\*Fuel axial power profile, G = curve 1, H = curve 2 of Fig. 4.1.

300GPM AT 52 GG POWER 10 NODES ADS(8) AT 5

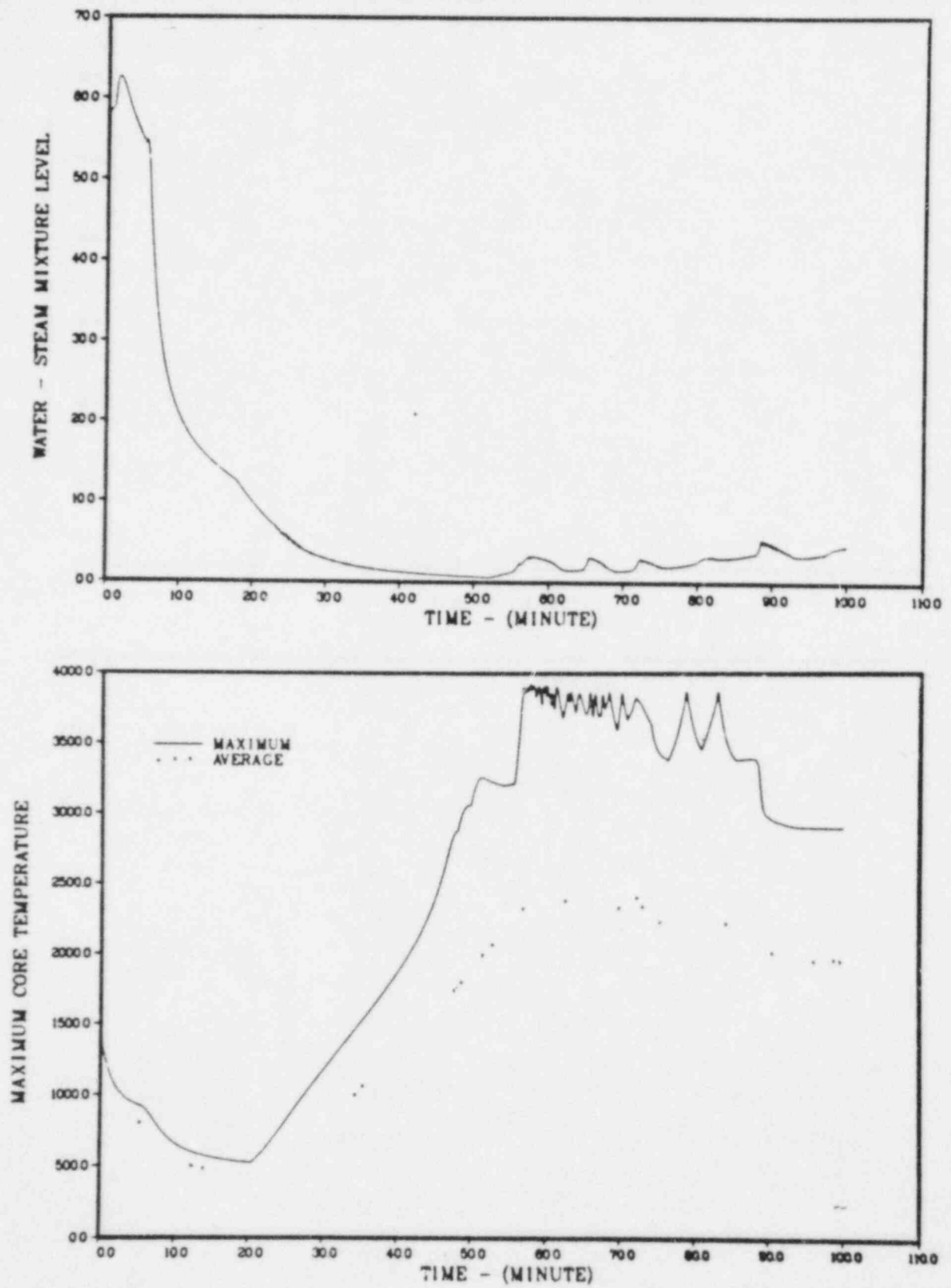


Figure 5.1 Reactor vessel water level and core temperature for case 5.1.

300GPM AT 52 GG POWER 10 NODES ADS(8) AT 5

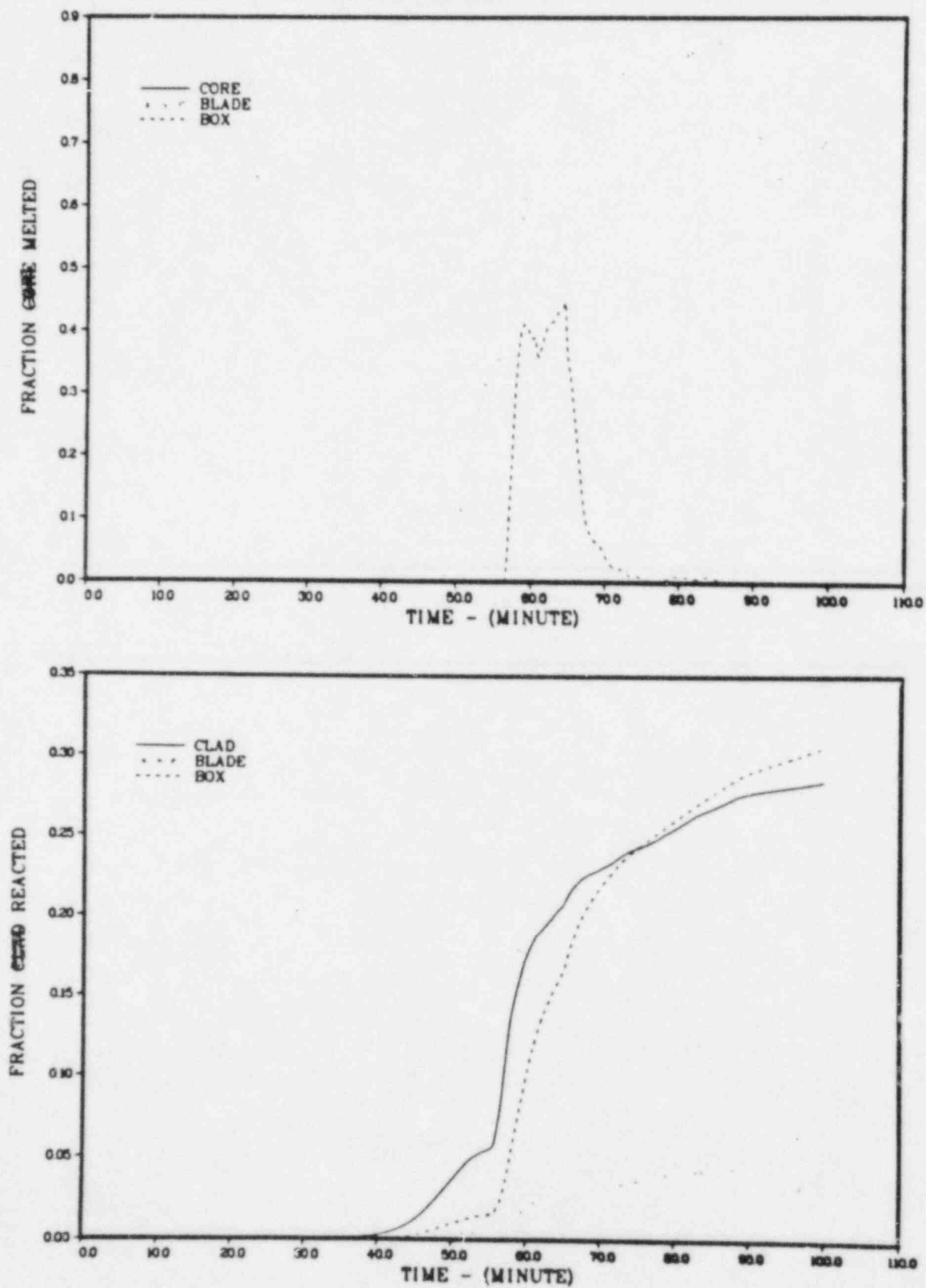


Figure 5.2 Melt fraction and oxidation fraction for case 5.1.

300GPM AT 52 GG POWER 10 NODES ADS(8) AT 5

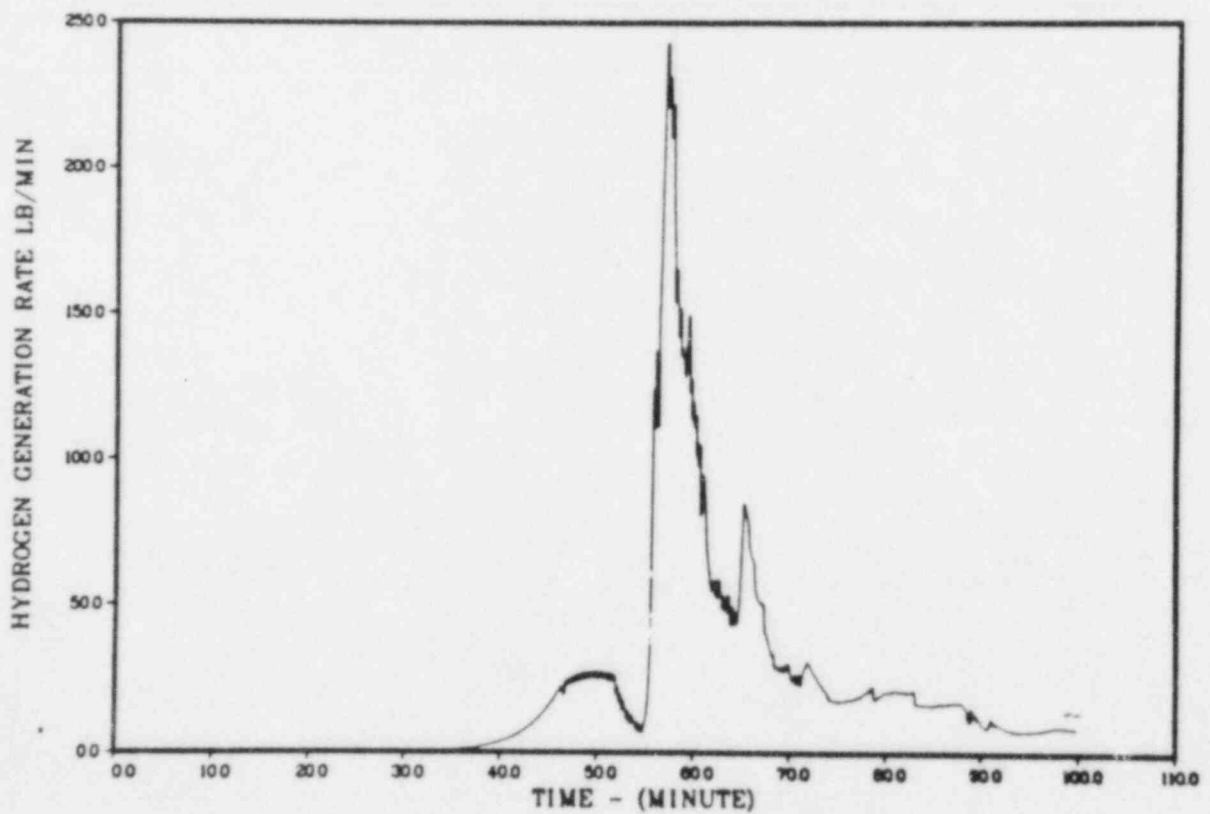
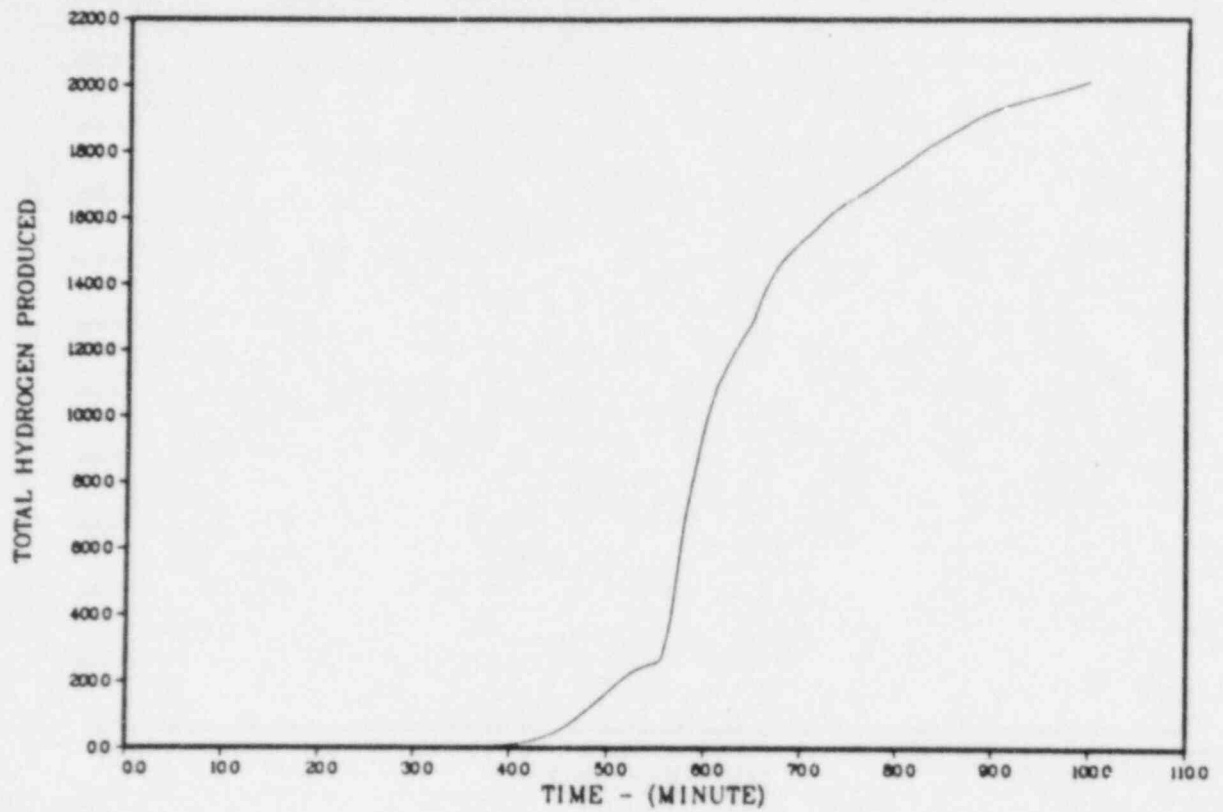


Figure 5.3 Hydrogen generation for case 5.1.

175GPM AT 42 GG POWER 10 NODES ADS(8) AT 5

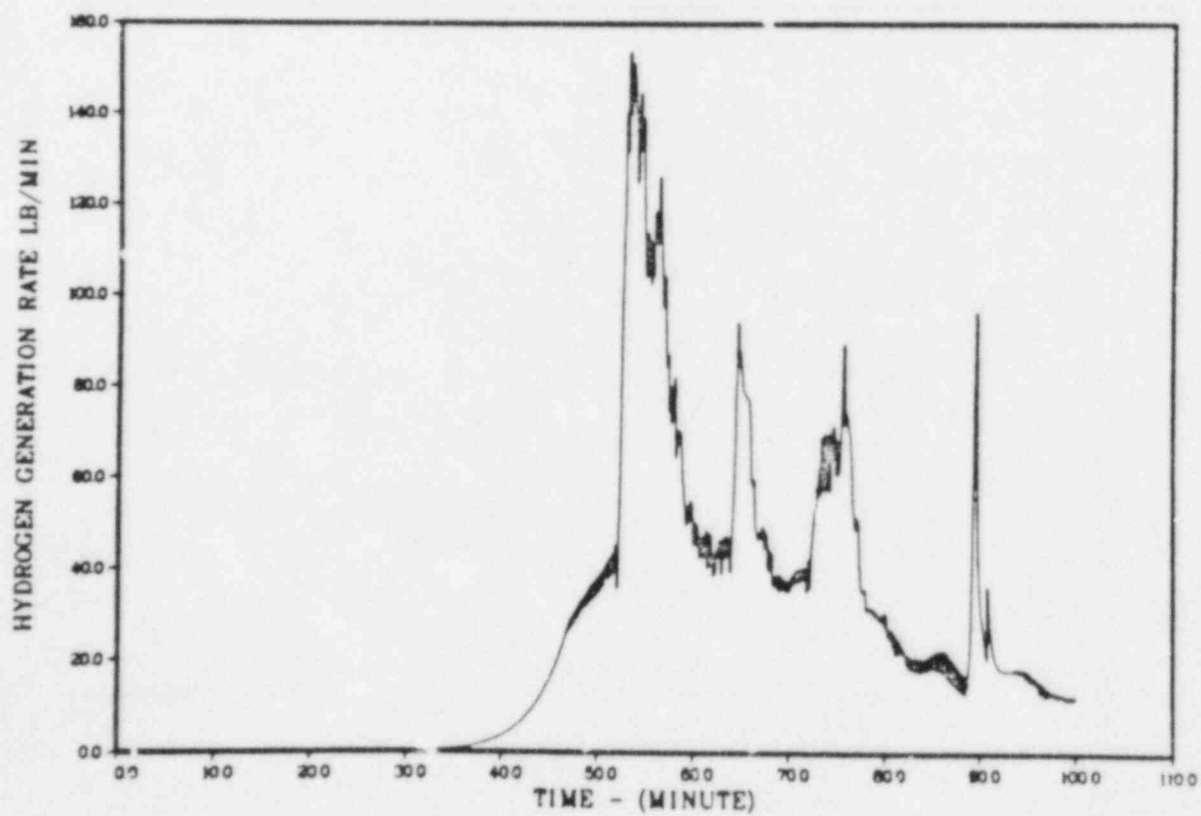
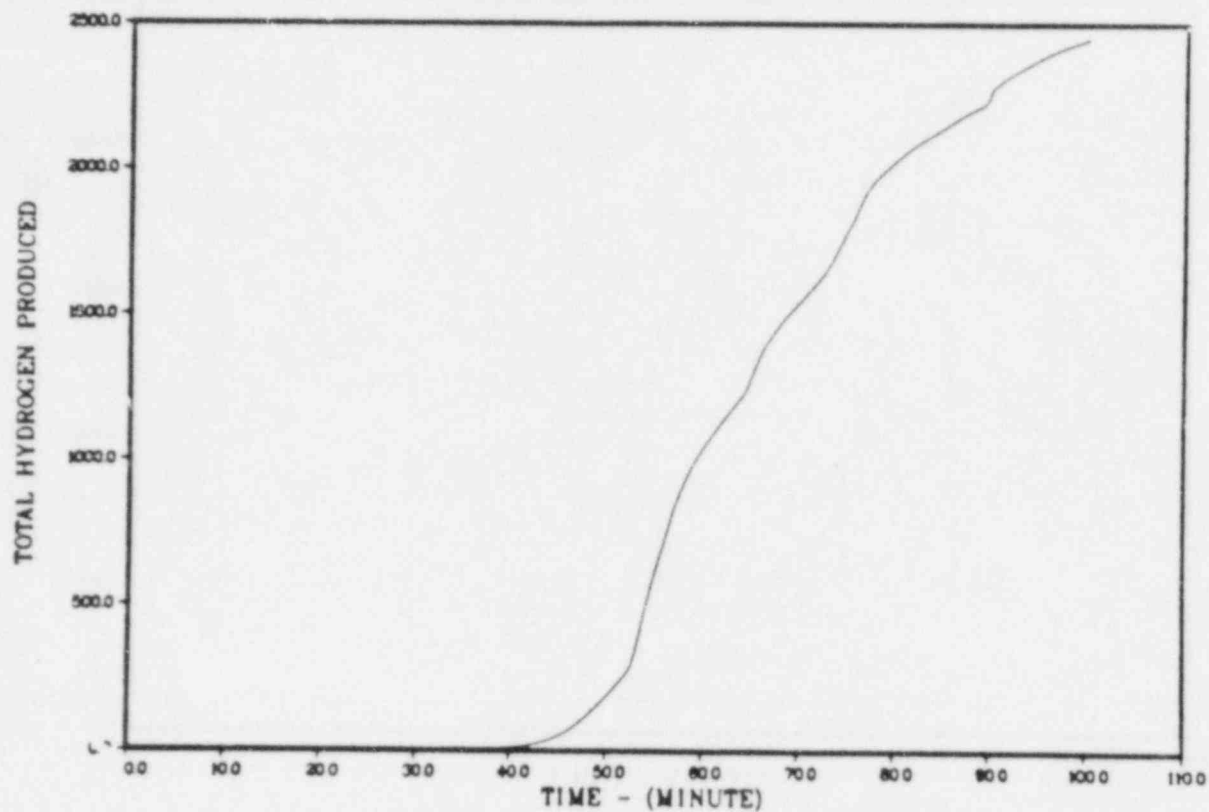


Figure 5.4 Hydrogen generation for case 5.2.

175GPM AT 42 GG POWER 10 NODES ADS(8) AT 5

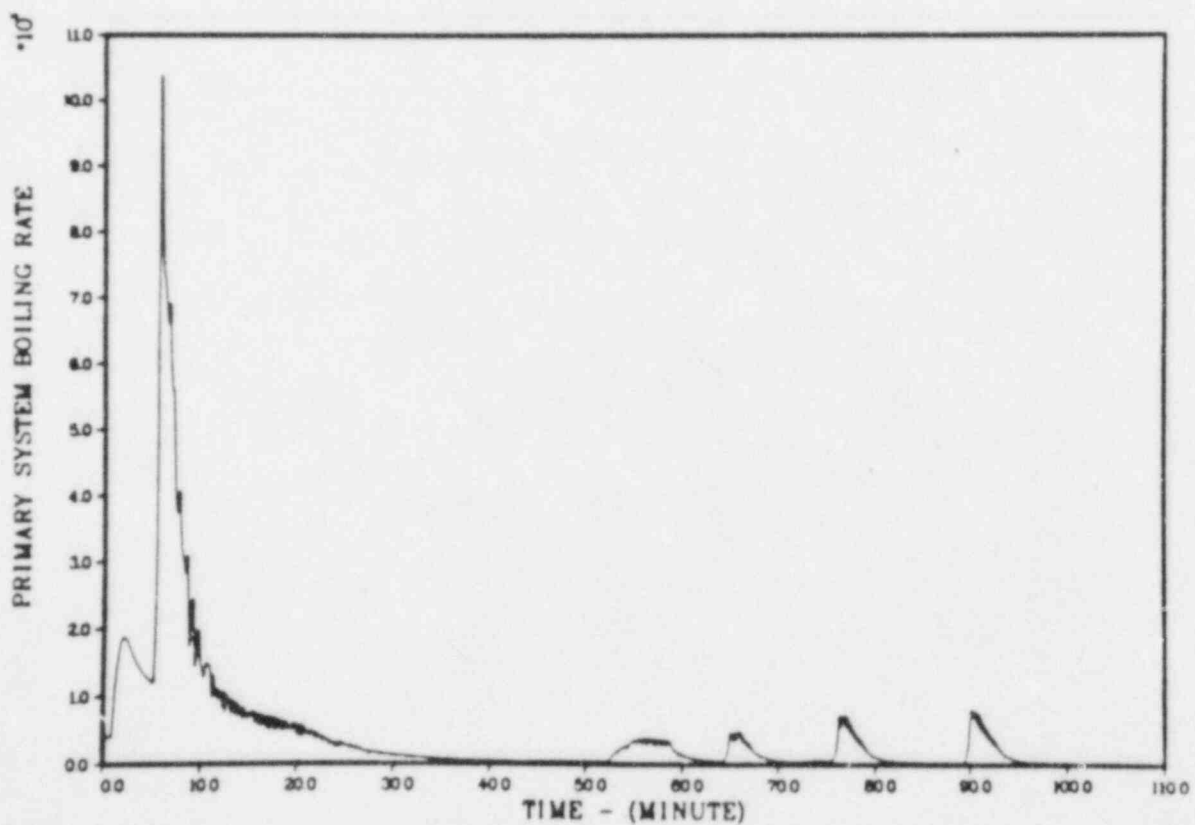
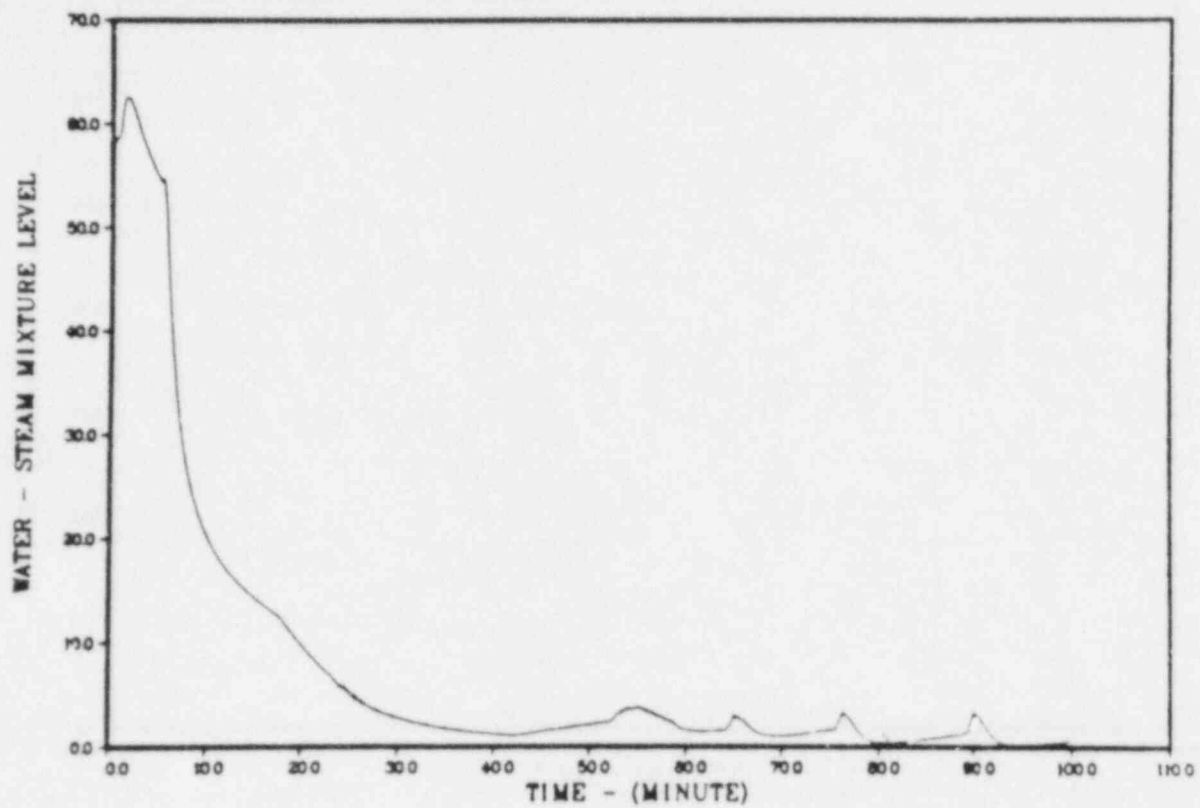


Figure 5.5 Reactor vessel water level and boiling rate for case 5.2.



175GPM AT 42 GG POWER 10 NODES ADS(8) AT 5

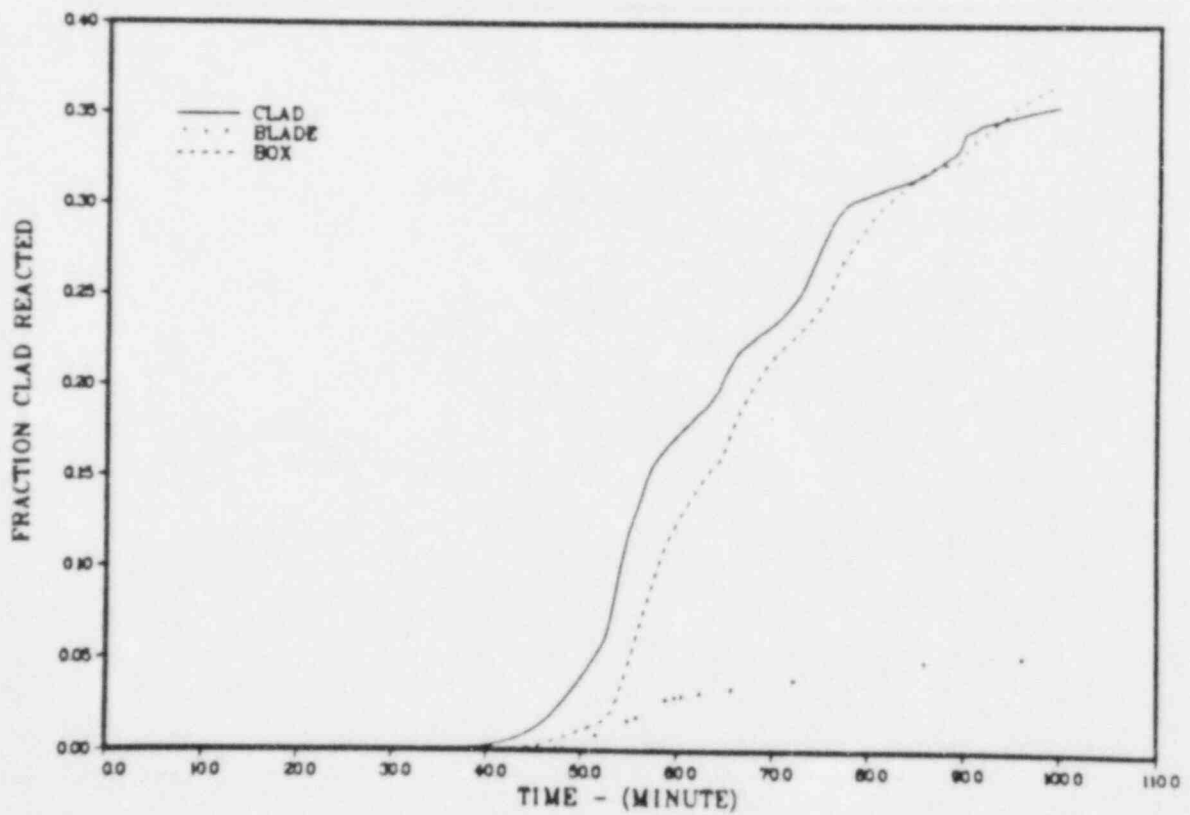
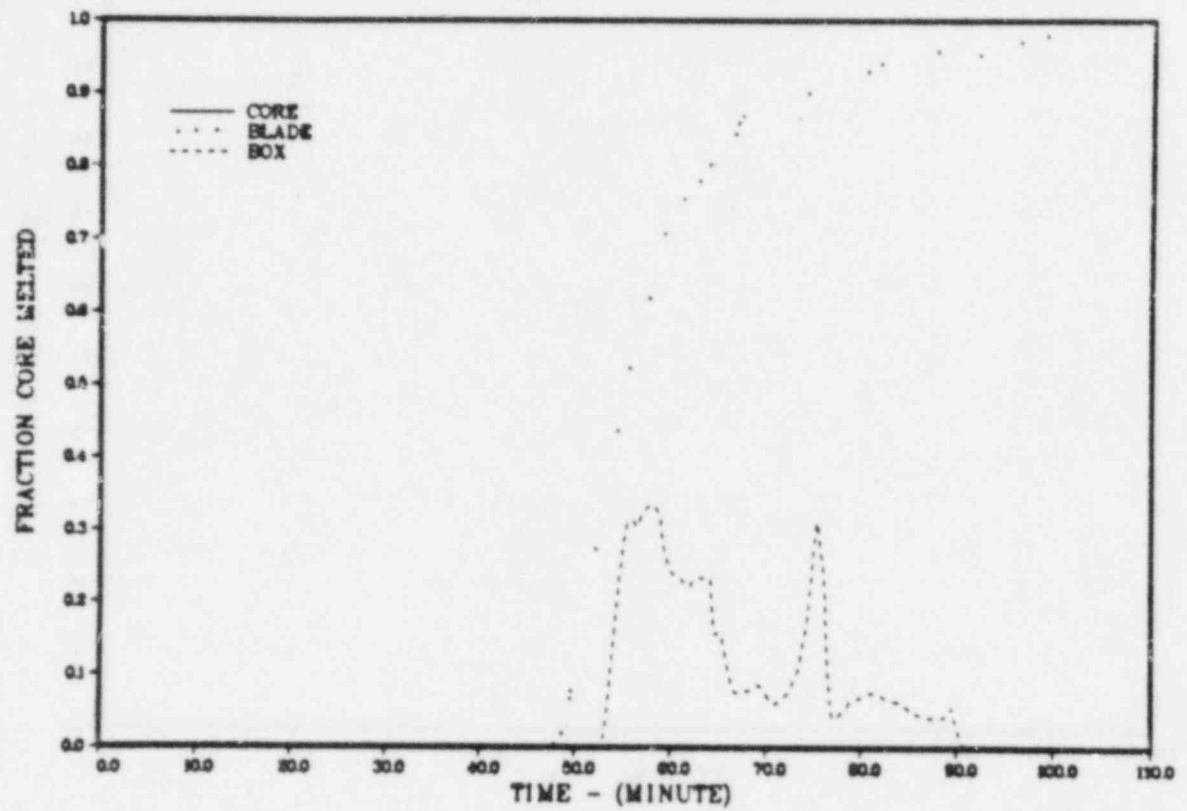


Figure 5.6 Melt fraction and oxidation fraction for case 5.2.

300GPM AT 42 GG POWER 24 NODES ADS(8) AT 5

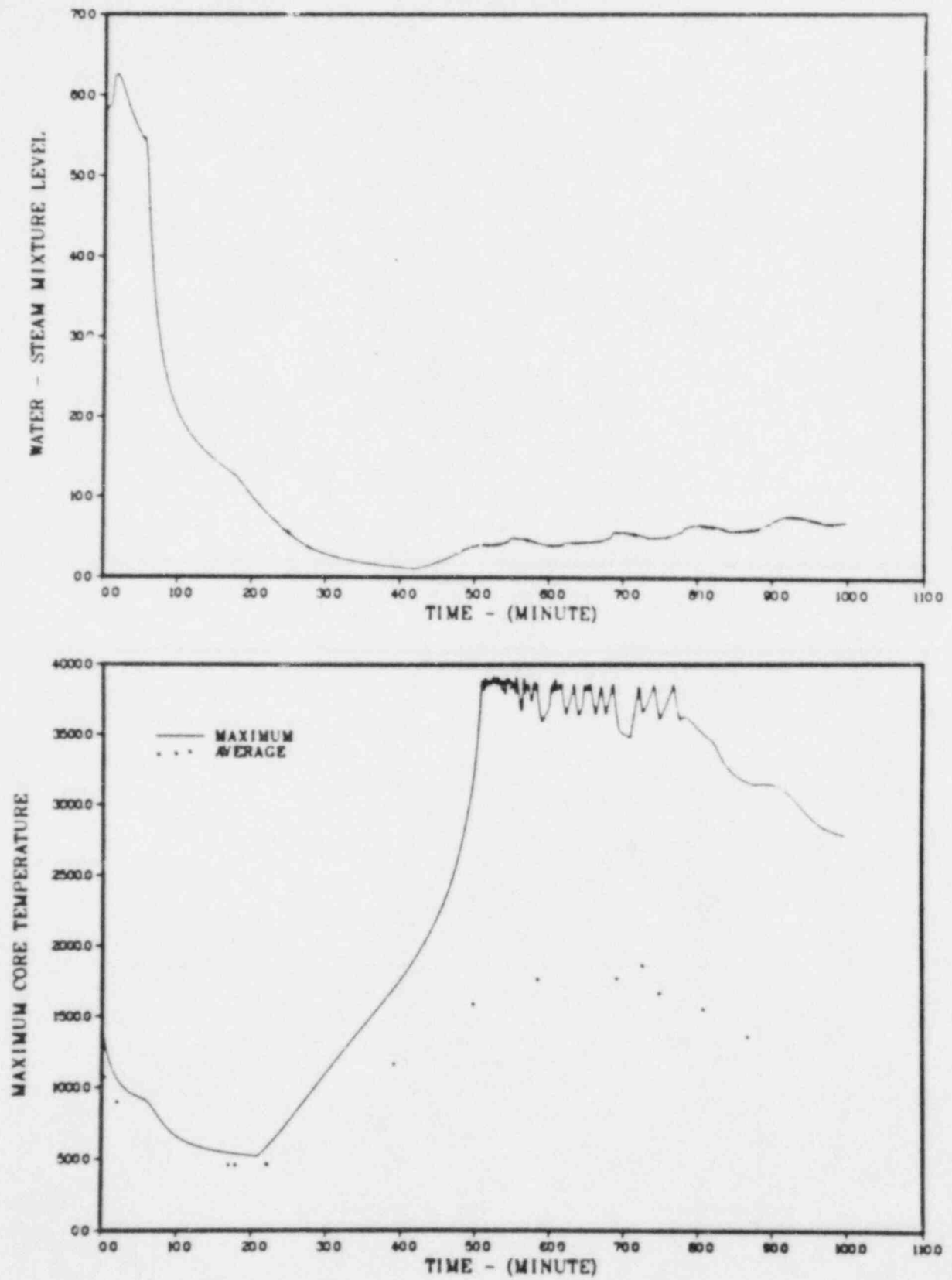


Figure 5.7 Reactor vessel water level and core temperature for case 5.3.

300GPM AT 42 GG POWER 24 NODES ADS(8) AT 5

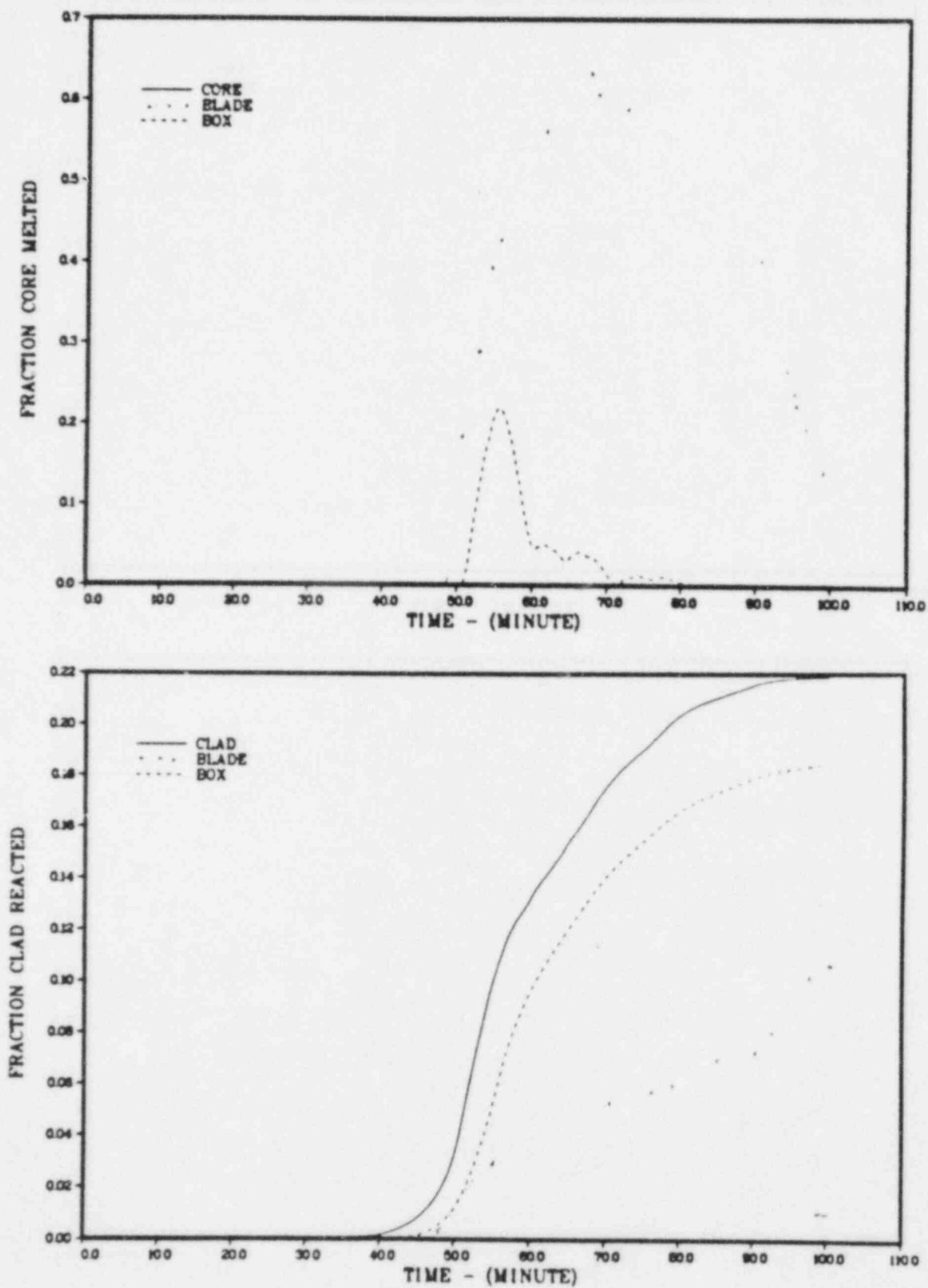


Figure 5.8 Melt fraction and oxidation fraction for case 5.3.

300GPM AT 42 GG POWER 24 NODES ADS(8) AT 5

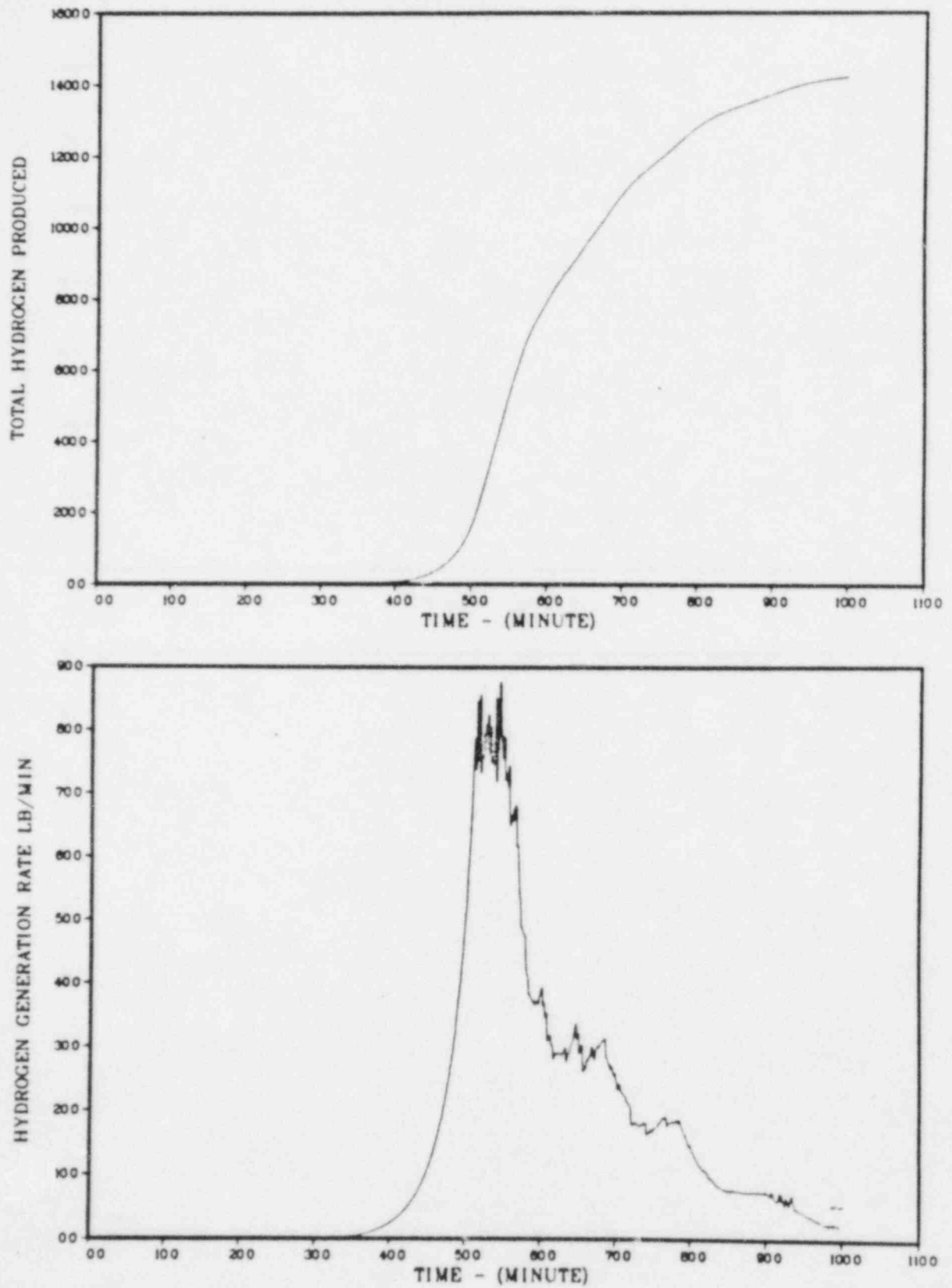


Figure 5.9 Hydrogen generation for case 5.3.

300GPM AT 42 HCOG POWER 10 NODES ADS(8) AT 5

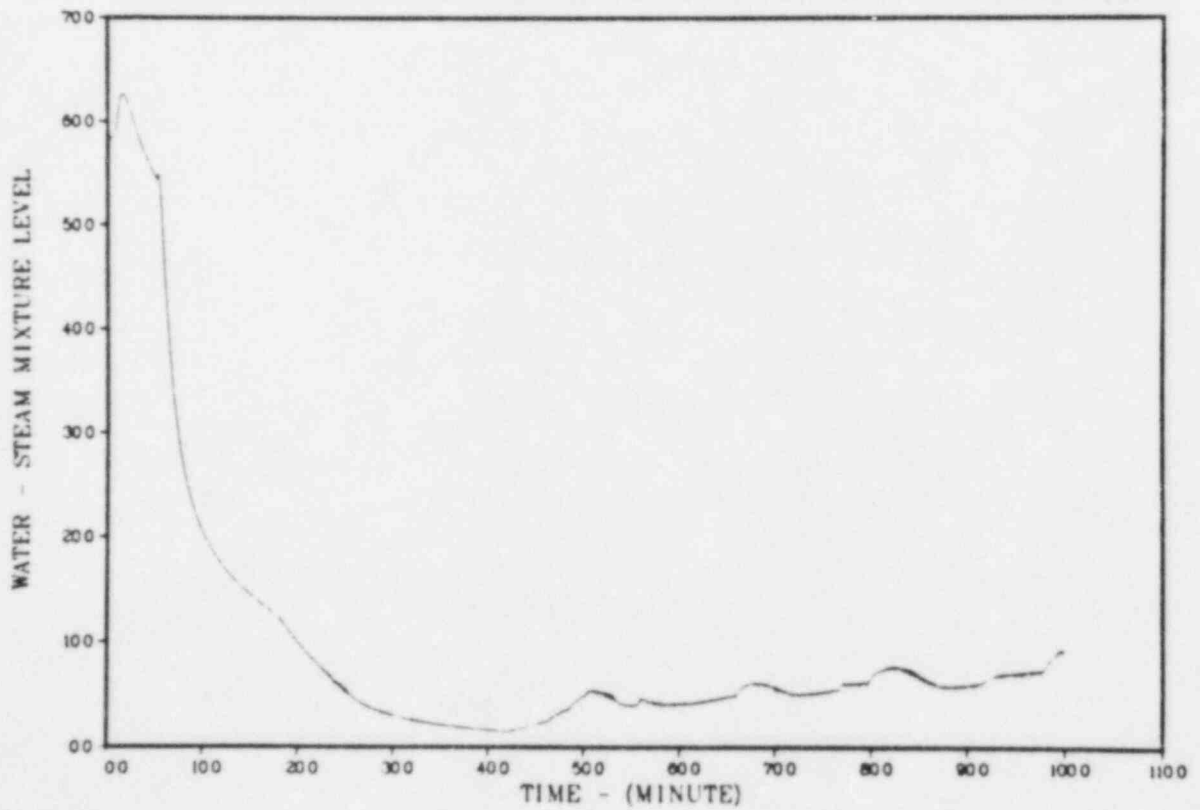
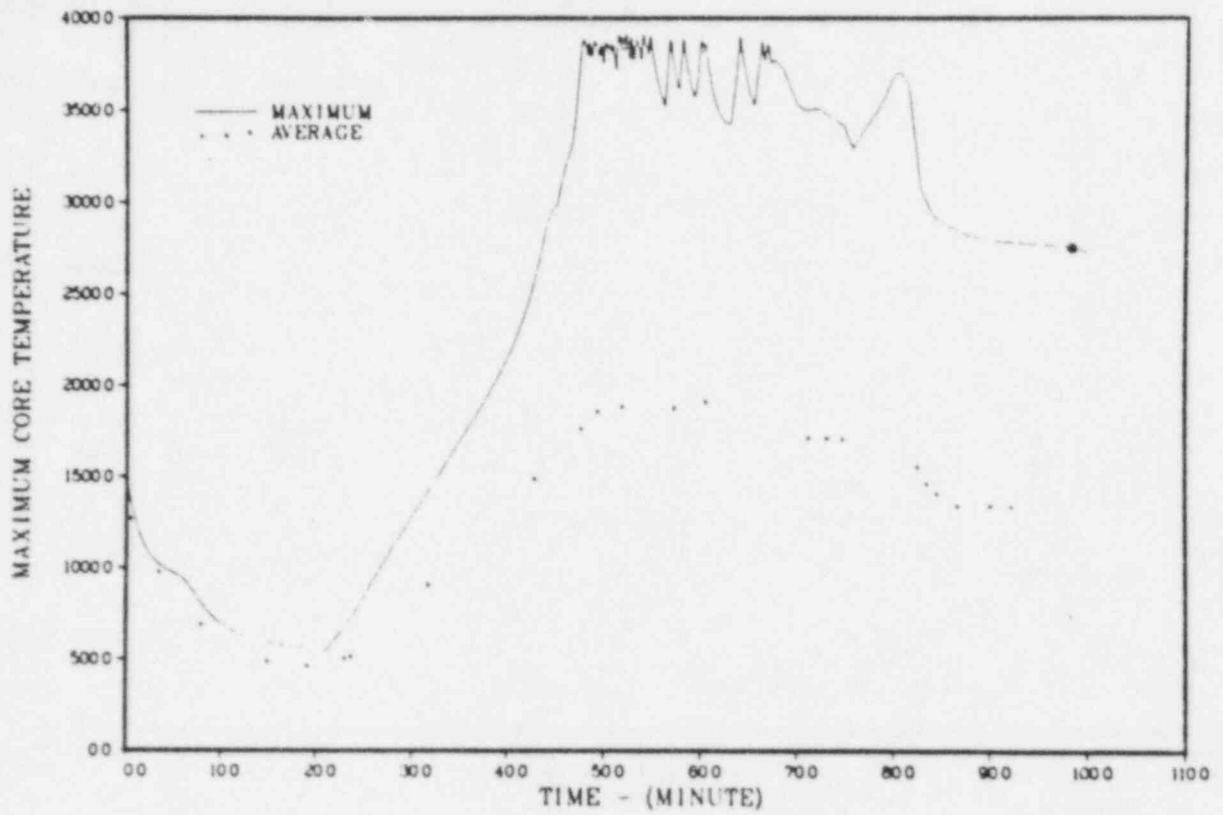


Figure 5.10 Reactor vessel water level and core temperature for case 5.4.

300GPM AT 42 HCOG POWER 10 NODES ADS(8) AT 5

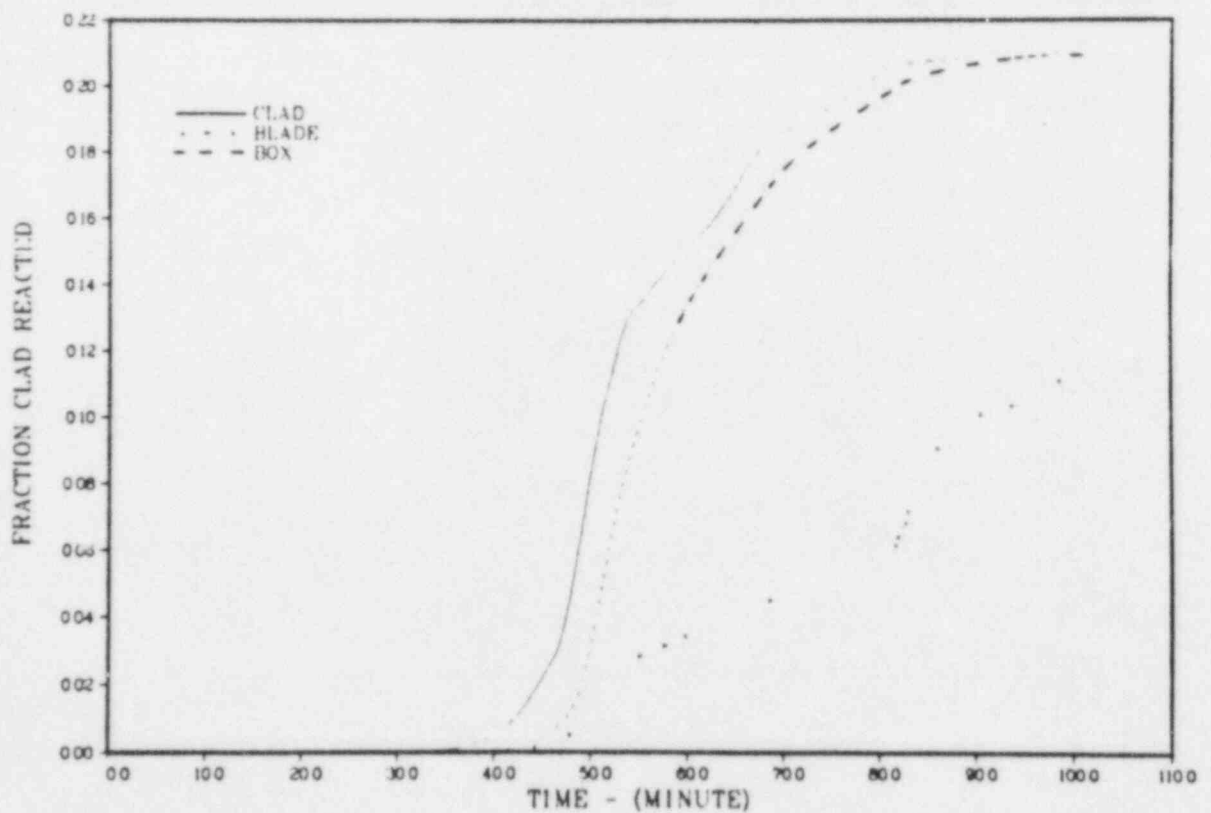
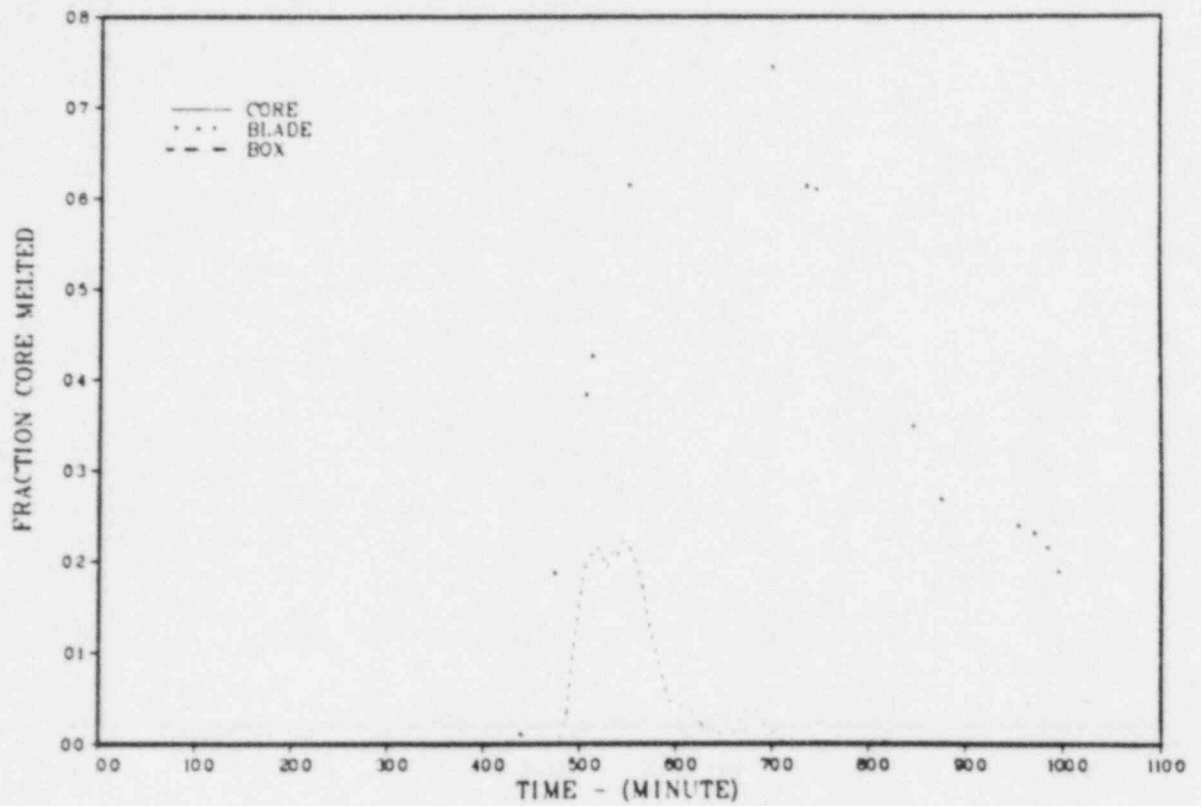


Figure 5.11 Melt fraction and oxidation fraction for case 5.4.

300GPM AT 42 HCOG POWER 10 NODES ADS(8) AT 5

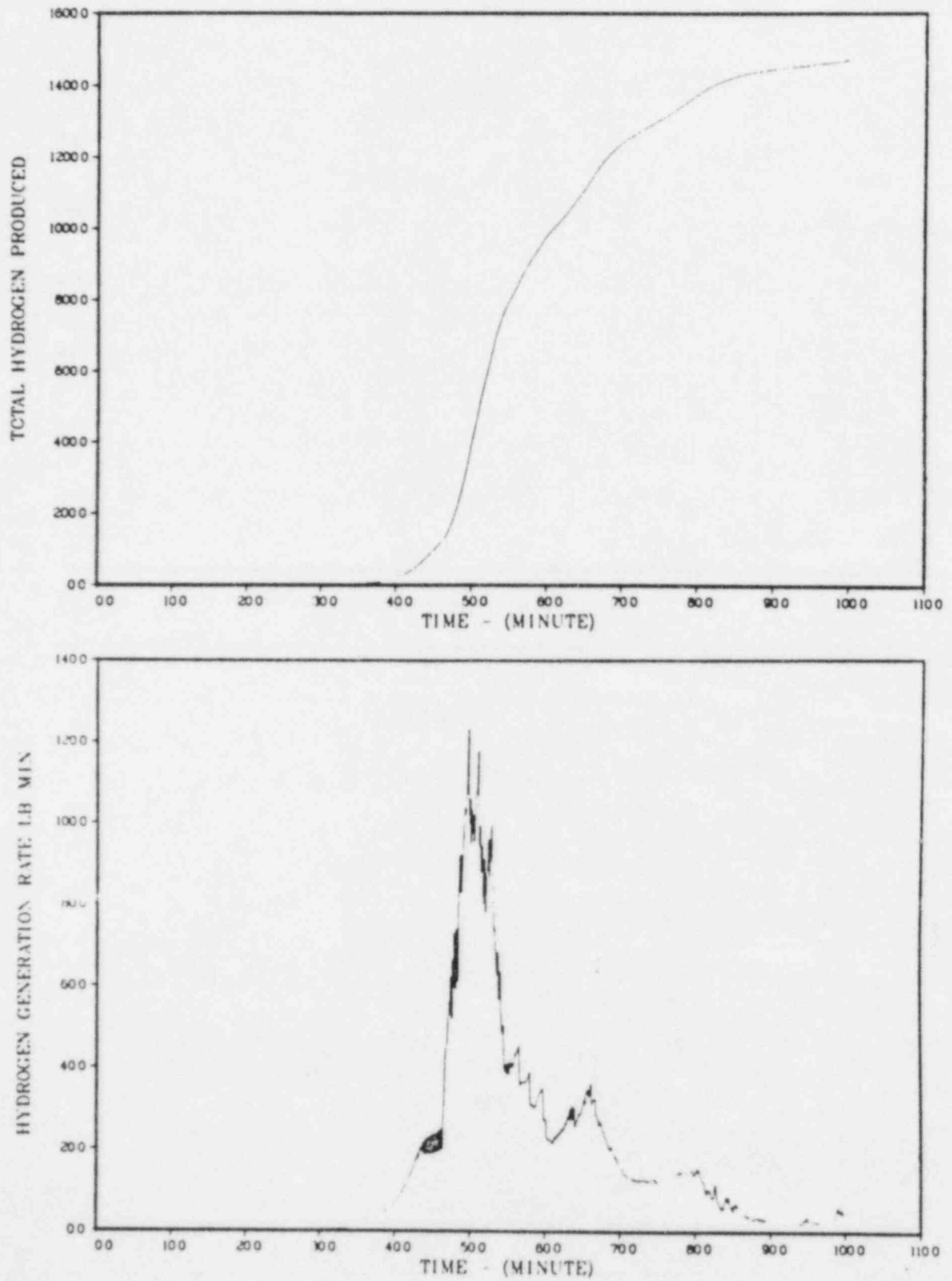
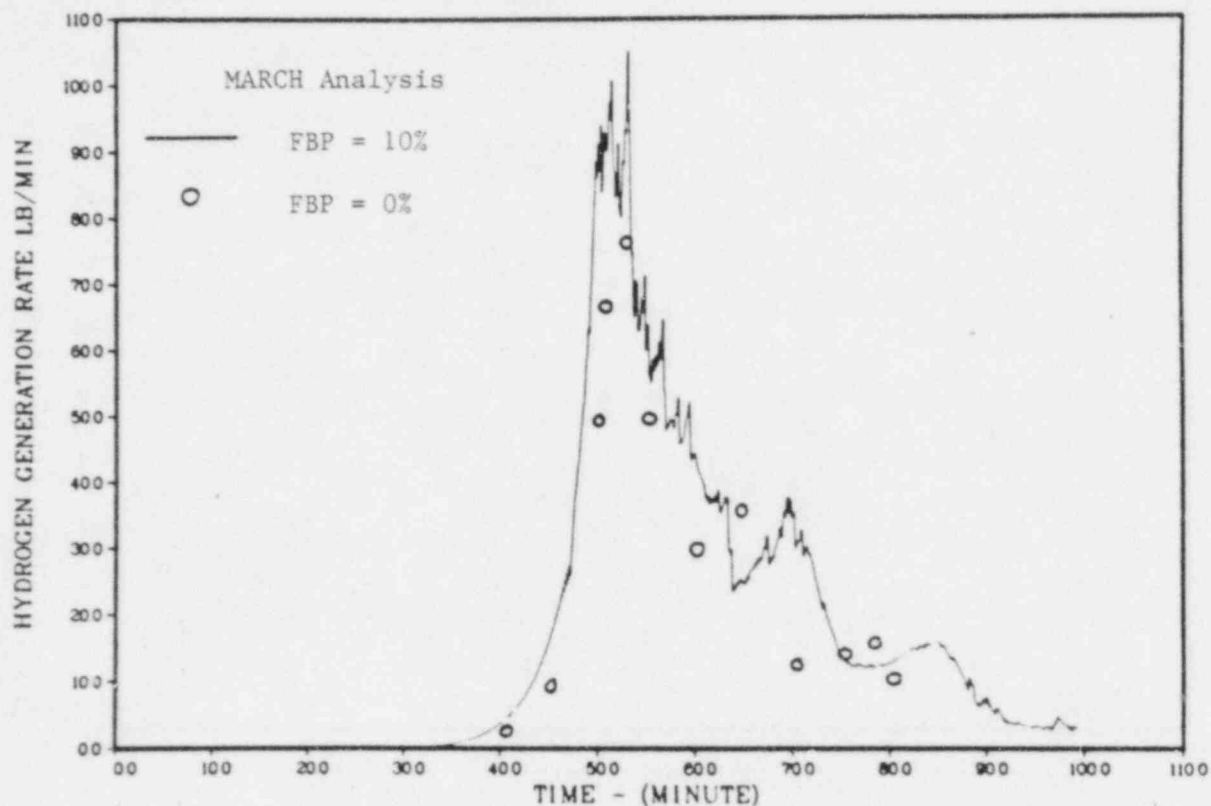


Figure 5.12 Hydrogen generation for case 5.4.



300GPM AT 42 GG POWER 10 NODES ADS(8) AT 5



300GPM AT 42 GG POWER 10 NODES ADS(8) AT 5 FBP=0

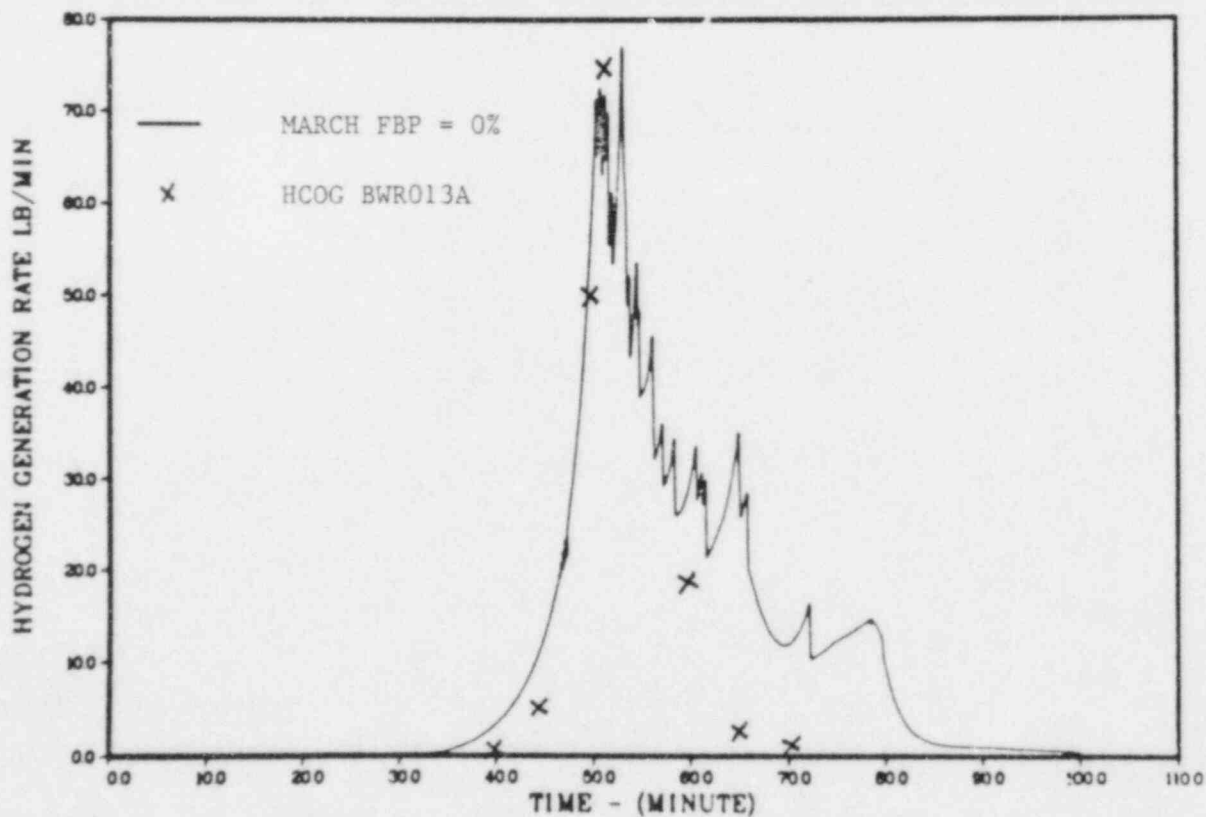
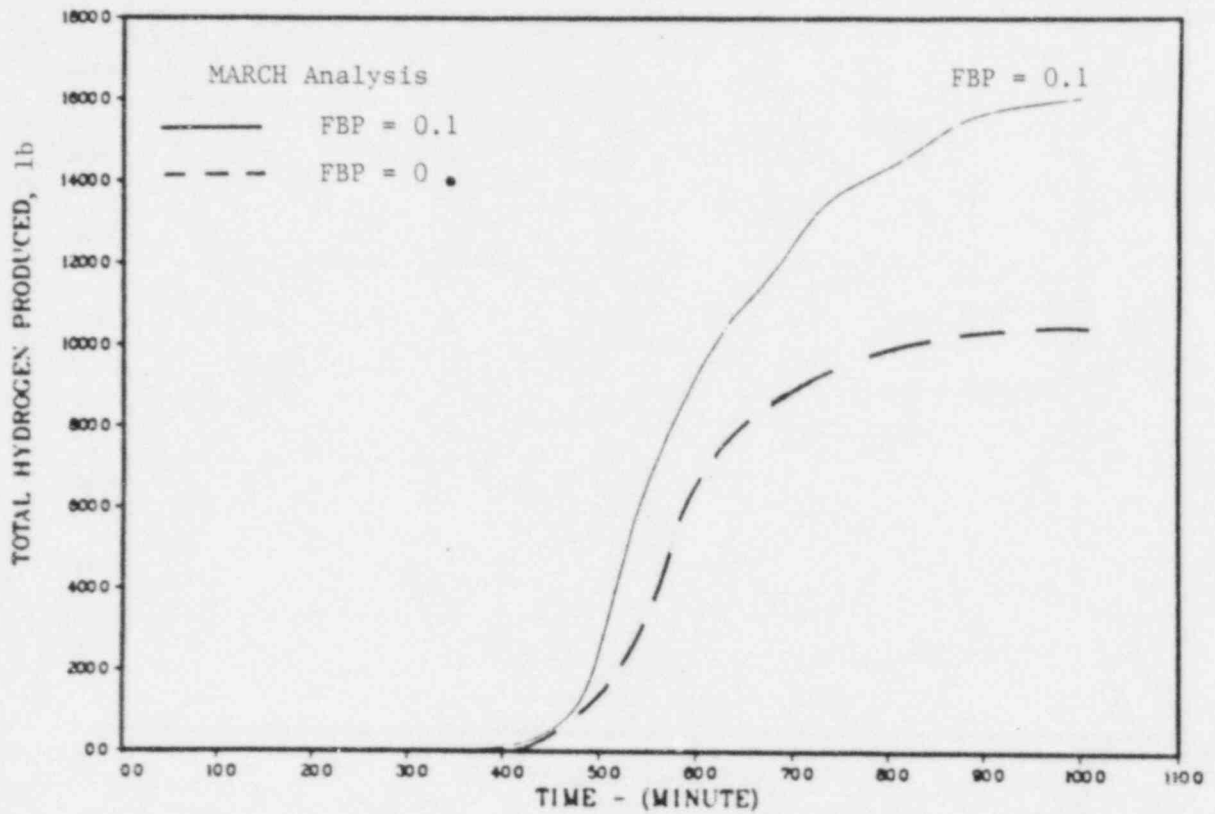


Figure 5.13 Comparison of hydrogen generation rate for cases 5.5, 4.2 and BWR013A.

300GPM AT 42 GG POWER 10 NODES ADS(8) AT 5



300GPM AT 42 GG POWER 10 NODES ADS(8) AT 5 FBP=0

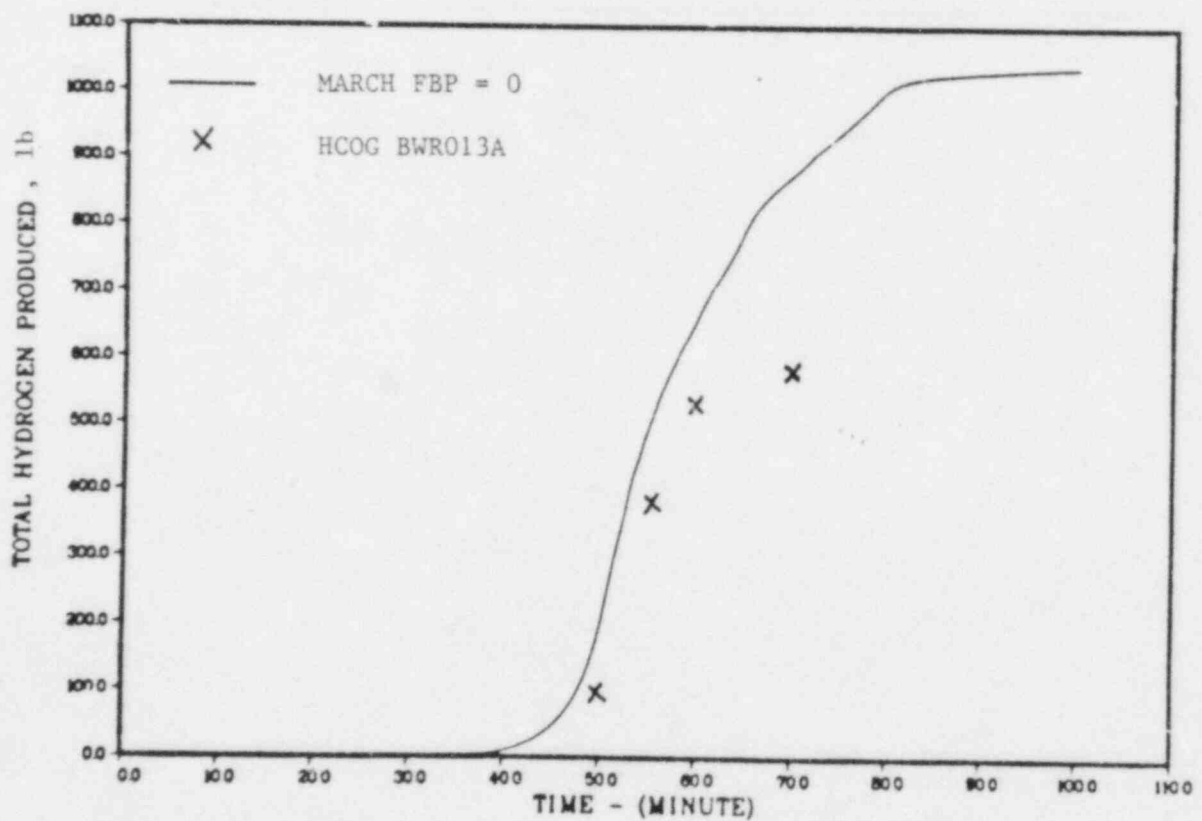
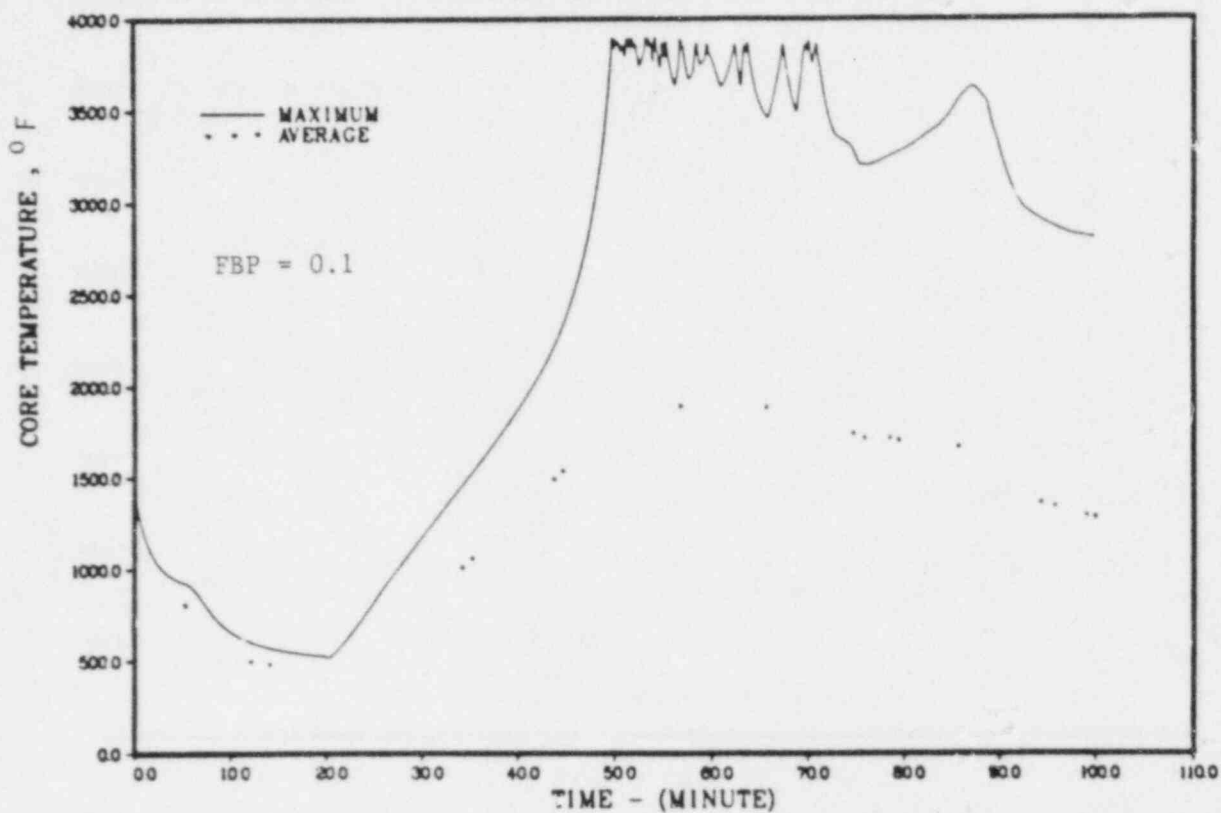


Figure 5.14 Comparison of total hydrogen production for cases 5.5, 4.2 and BWR013A.

300GPM AT 42 GG POWER 10 NODES ADS(8) AT 5



300GPM AT 42 GG POWER 10 NODES ADS(8) AT 5 FBP=0

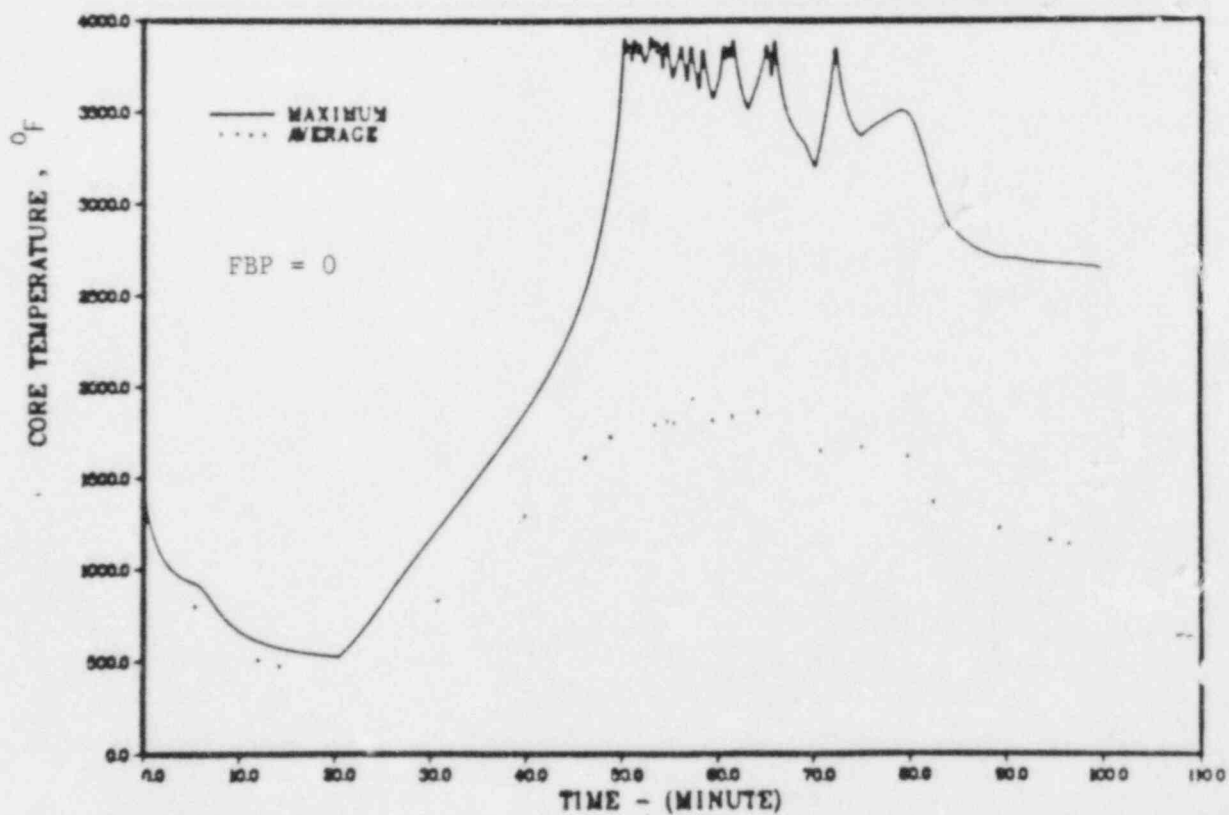
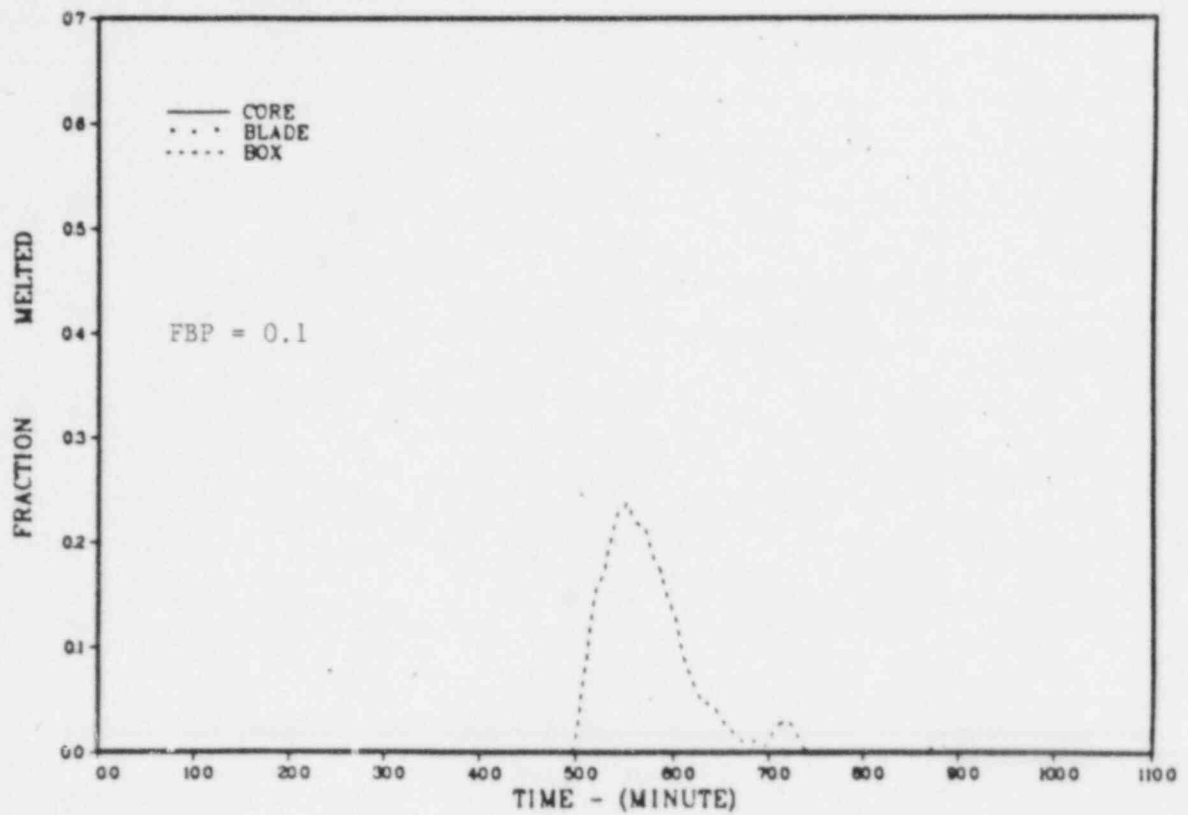


Figure 5.15 Comparison of core temperature for cases 5.5 and 4.2.

300GPM AT 42 GG POWER 10 NODES ADS(8) AT 5



300GPM AT 42 GG POWER 10 NODES ADS(8) AT 5 FBP=0

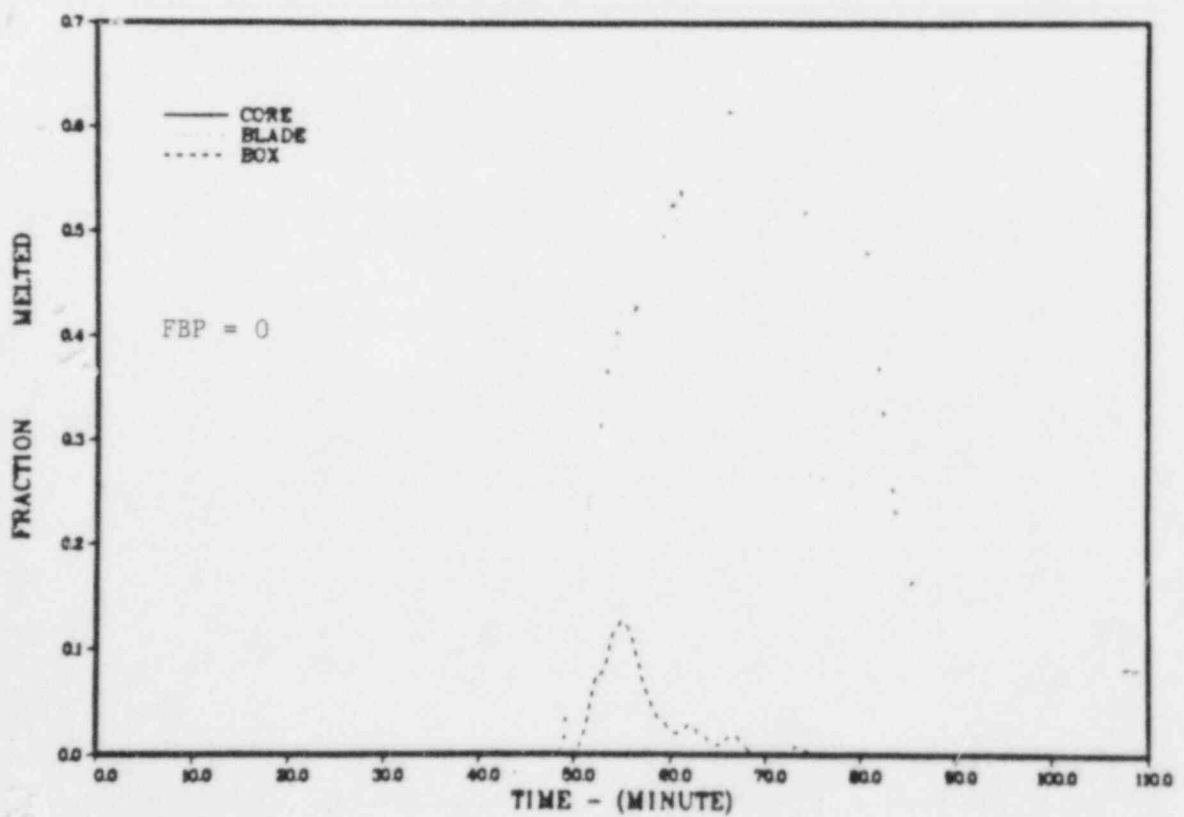
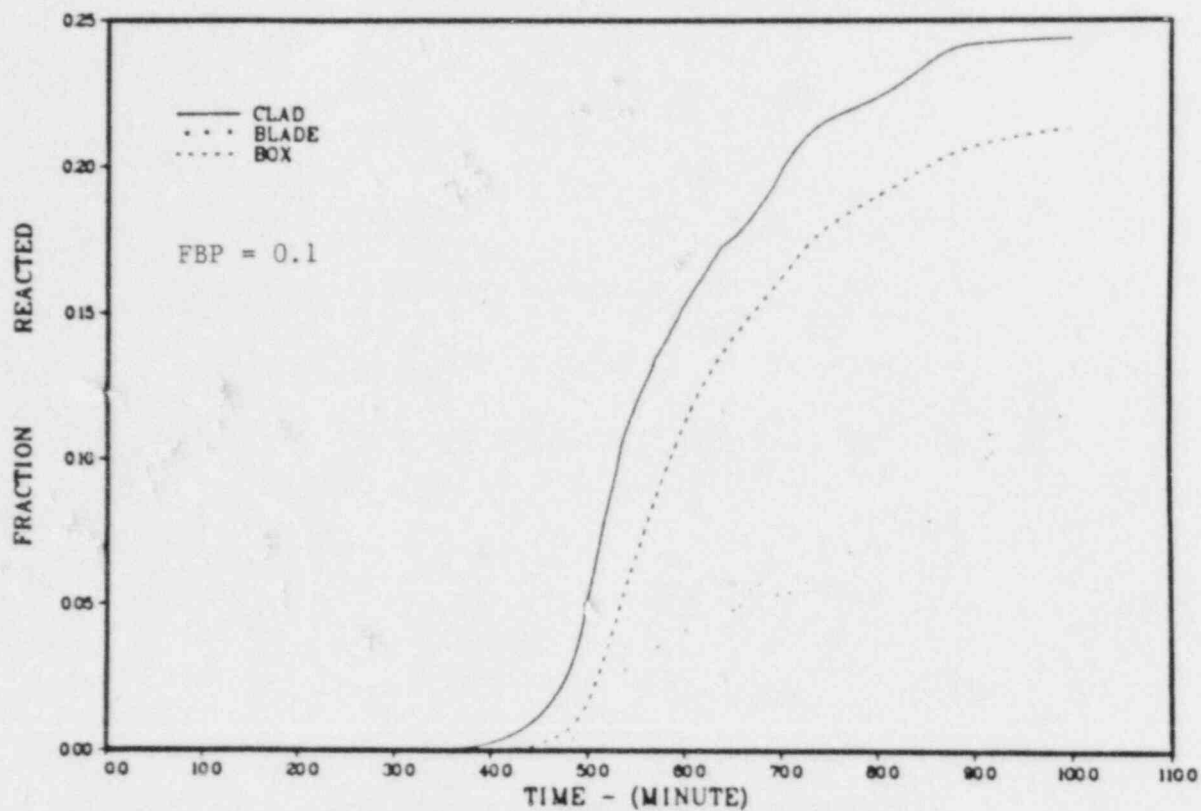


Figure 5.16 Comparison of melt fraction for cases 5.5 and 4.2.

300GPM AT 42 GG POWER 10 NODES ADS(8) AT 5



300GPM AT 42 GG POWER 10 NODES ADS(8) AT 5 FBP=0

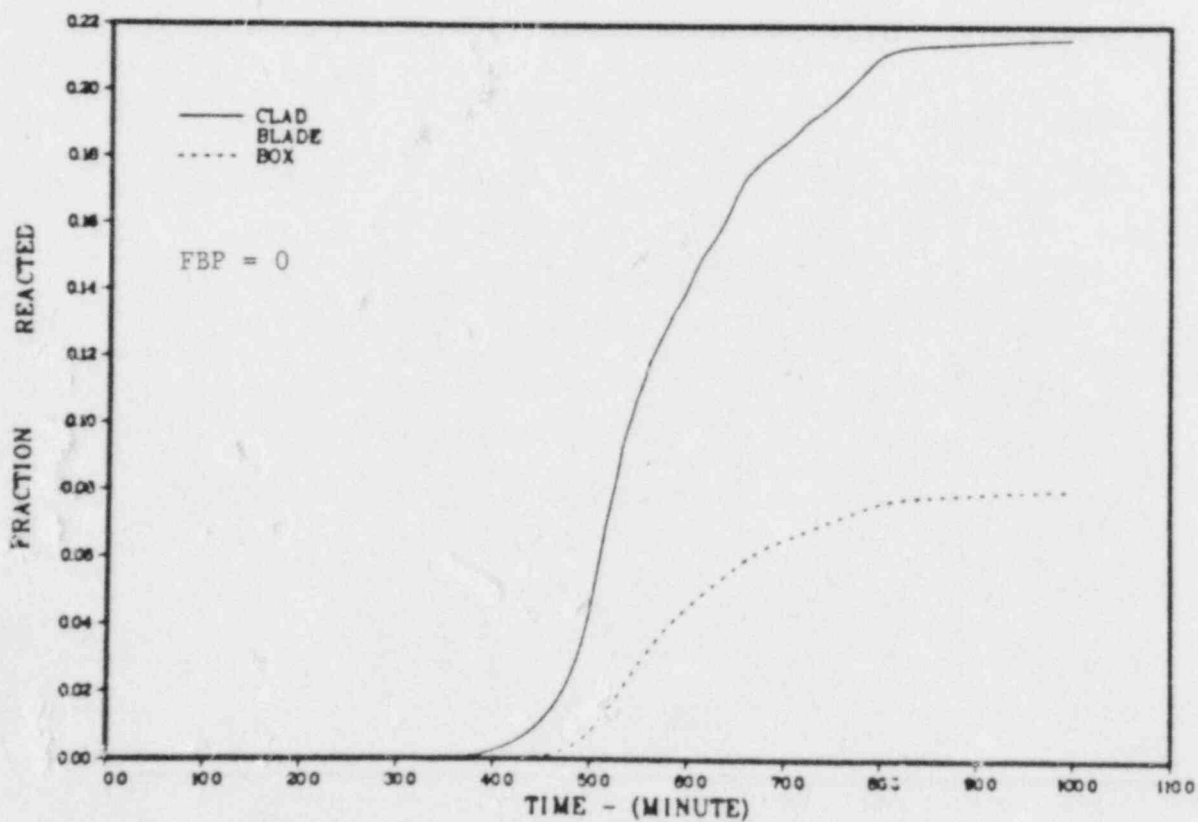


Figure 5.17 Comparison of oxidation for cases 5.5 and 4.2.

300GPM AT 42 ADS(8) AT 5 TMW OFF=6000

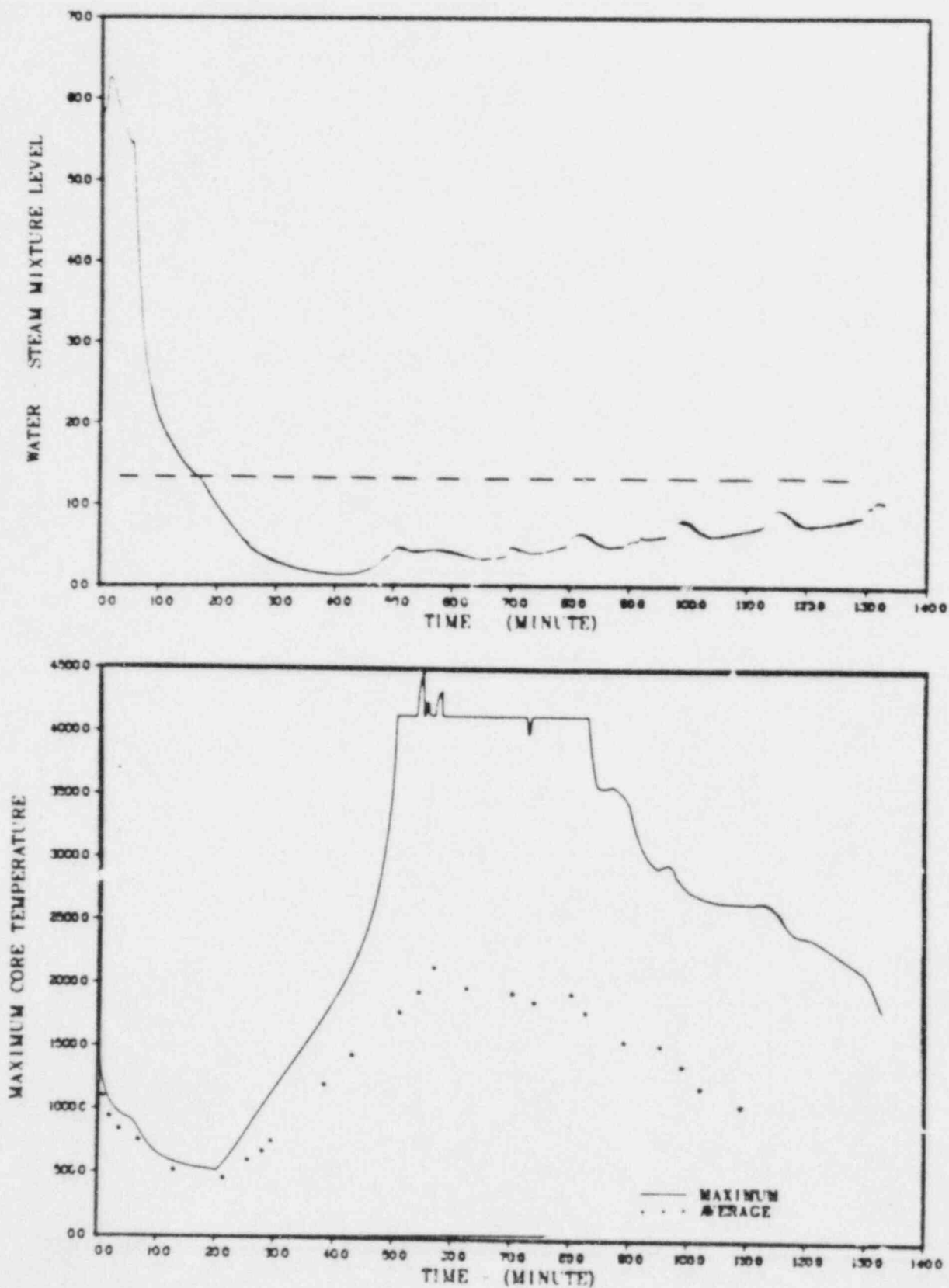


Figure 5.18 Reactor vessel water level and core temperature for case 5.6.

300GPM AT 42 ADS(8) AT 5 TMWOF=6000

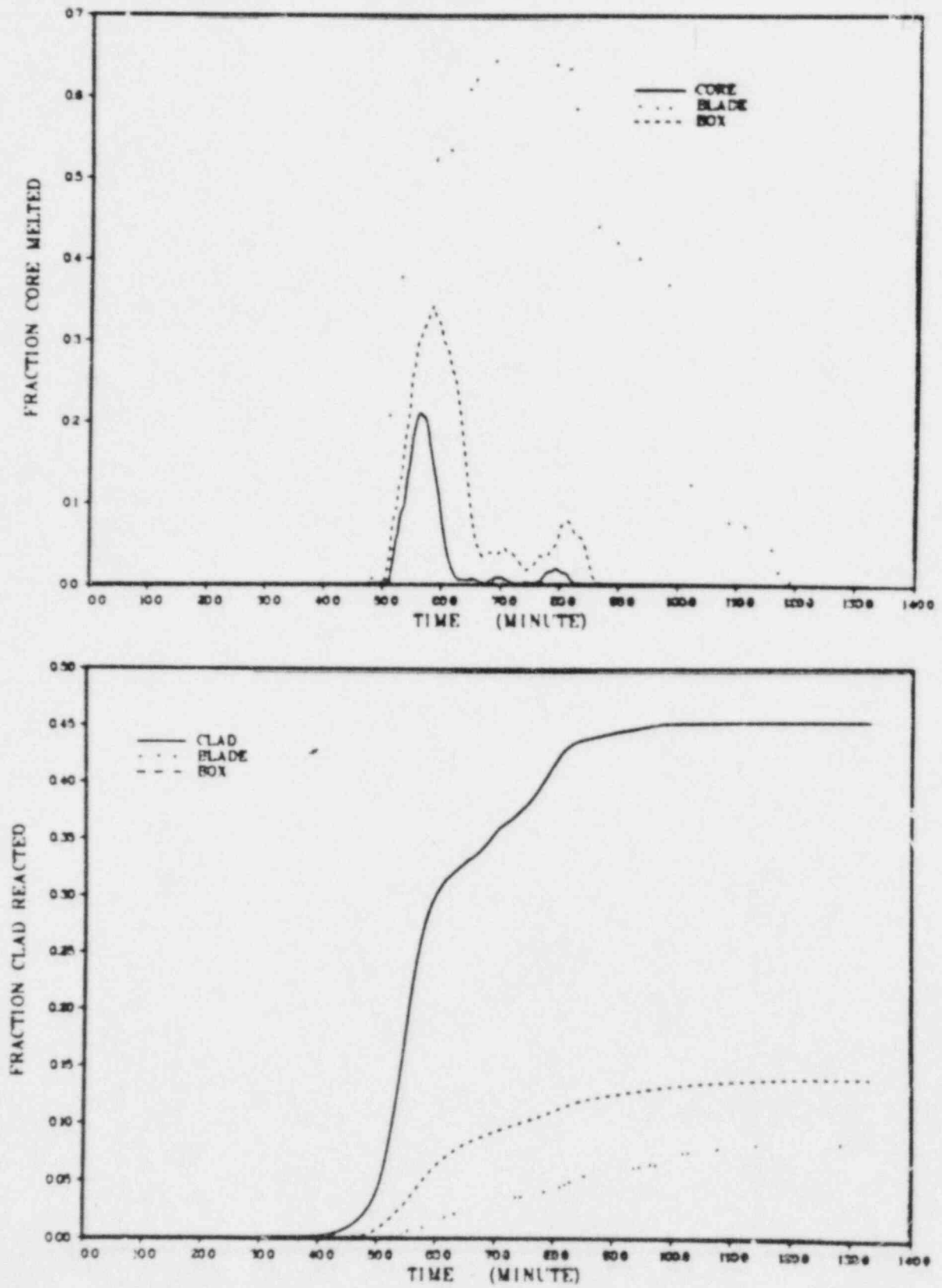


Figure 5.19 Melt fraction and oxidation fraction for case 5.6.



300GPM AT 42 ADS(8) AT 5 TMWOFF=6000

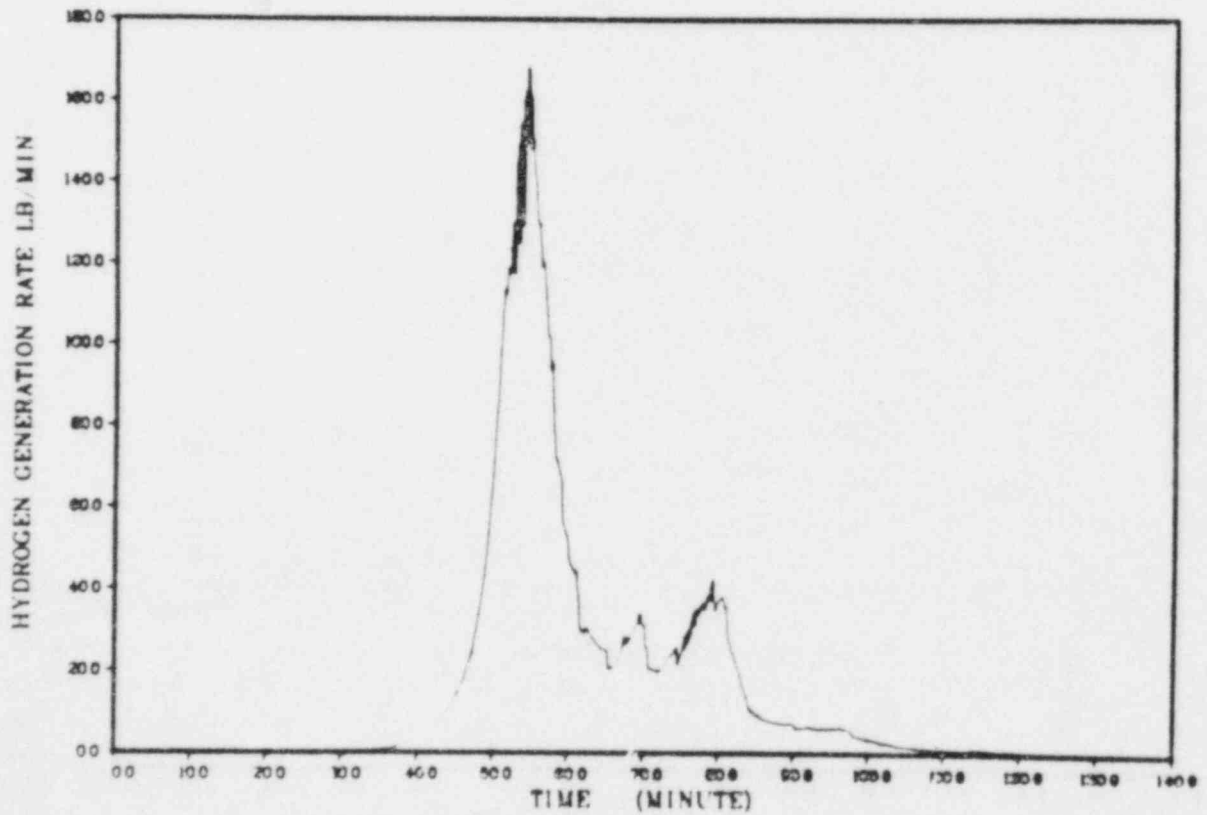
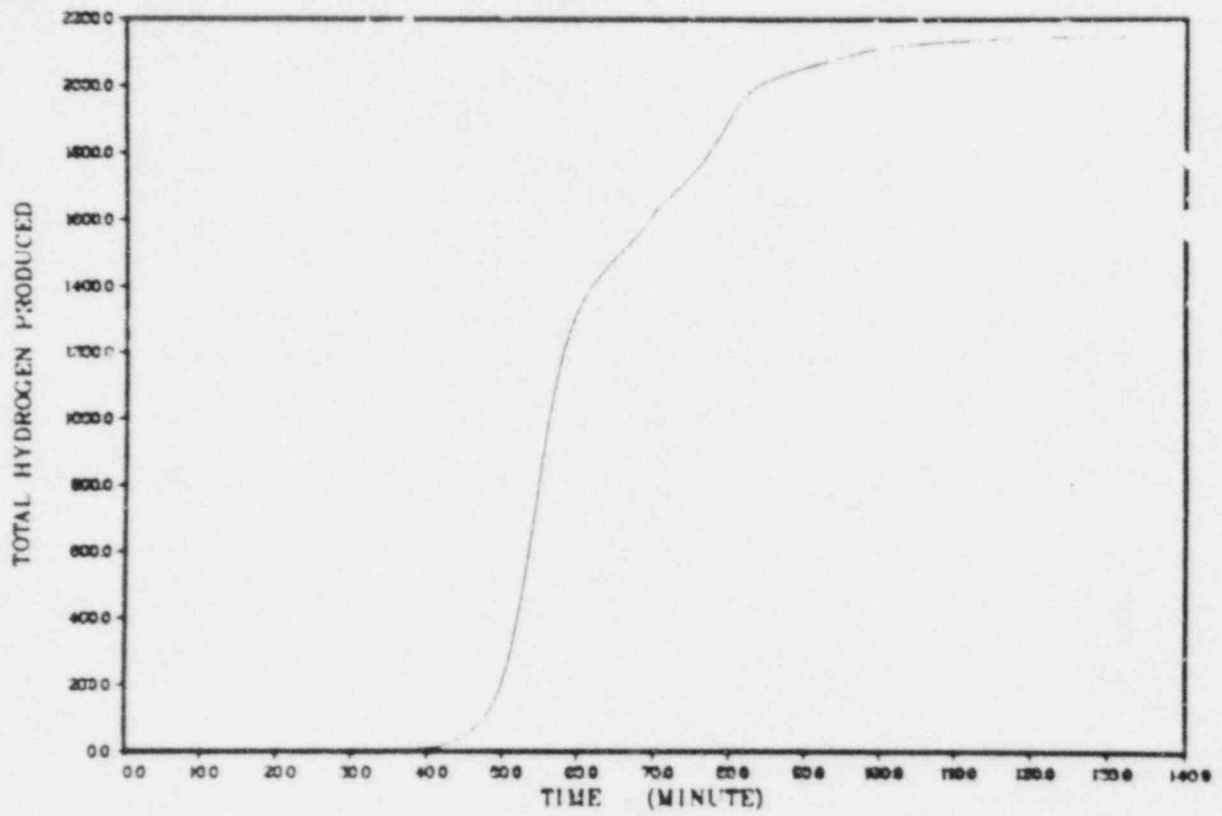


Figure 5.20 Hydrogen generation for case 5.6.

## 6. MARCH ANALYSIS USING EMERGENCY PROCEDURE GUIDELINES

All of the previous analyses of hydrogen production presented in Sections 4 and 5 were based on the initial conditions proposed by the Hydrogen Control Owners Group (HCOG). These initial conditions do not specifically follow the BWR reactor emergency procedures. At the suggestions of NRC staff, the hydrogen calculations were reanalyzed for a heatup transient in which the Emergency Procedure Guidelines (EPG)<sup>4</sup> were assumed to be followed. According to the Contingency No. 3 (steam cooling) of the EPG,<sup>4</sup> it is required to open one Steam Relief Valve (SRV) when the reactor pressure vessel (RPV) water drops to 9 ft below the top of the core and open all Automatic Depressurization System (ADS) valves when the RPV pressure drops below 700 psig.

The above Emergency Procedure Guidelines were applied to the three events, namely, (1) no core reflood, (2) core reflooded by 300 gpm of Control Rod Drive Hydraulic System (CRDHS) flow, and (3) core reflooded by 5000 gpm of Low Pressure Core Injection (LPCI) flow. In performing the analysis, it is assumed that the fraction of steam flow in the box-blade bypass region is reduced to 1% (FBP=0.01). The previous assumption of 10% steam flow in the bypass region overestimates the flow in this region as discussed in Section 5.5.

The results of this analysis are compared with the previous analysis using the HCOG's initial condition and are summarized in Table 6.1. In general, there is no major difference on total hydrogen production and on fractions of oxidation. The peak hydrogen generation rates based on the Emergency Procedure Guidelines are noticeably higher for cases of core reflood, particularly for the injection of 300 gpm CRDHS flow. However, the time duration of hydrogen generation is shorter if the EPG is followed. The time period during which the hydrogen generation rate is greater than 30 lb/min is compared in Table 6.1. The rate 30 lb/min is selected as reference for the purpose of comparison. Following the Emergency Procedure Guidelines also leads to higher core damage as shown in Table 6.1. The procedure was developed to maximize the time available to prevent core degradation and hence recovery time; not to minimize ultimate core damage in an unrecoverable scenario or hydrogen generation.

### Discussion

#### Case 6.1 - No Reflood

For the accident sequence considered in this study, the MARCH code predicts that the core uncover starts at 42.7 minutes. The swollen water level drops to 9 ft below the top of the core at 57 minutes, at which time one SRV was opened as required by the Emergency Procedure Guidelines. The vessel pressure rapidly decreases from 1200 psia to 722 psia at about 58.35 minutes, at which time all the 8 ADS valves were opened to allow a complete depressurization of the reactor system as shown in Figure 6.1. The corresponding decrease of water saturation temperature given in Figure 6.1 causes a large water boil-off (flashing) and the vessel water level is reduced to about 4 ft below the bottom of core at 64 minutes (Figure 6.2). Figure 6.3 shows that the core temperature rises rapidly as the core is uncovered. The core maximum temperature reaches 1700°F at about 70 minutes, from which time the oxidation of zircaloy and generation of hydrogen become significant. The hydrogen generation rate and the total hydrogen production are shown in Figure 6.4. The

first peak hydrogen generation rate is 12 lb/min at 84 minutes and is limited by steam availability in the reactor vessel. At this stage of the transient, the vessel water is entirely in the lower plenum and the vessel pressure is relatively stable. Hence, the decay heat and flashing do not contribute to steam generation. It appears that the thermal radiation becomes the major heat source for steam generation. The downward thermal radiation from core to water in the lower plenum is mainly emitted from the first bottom node of the fuel. The temperature of the first node in the central radial zone is illustrated in Figure 6.5. It is seen that the fuel temperature increased rapidly at 90 minutes and would emit a large amount of thermal radiation to water. The water boil-off by thermal radiation causes the second peak hydrogen generation at about 115 minutes shown in Figure 6.4. At the end of 150 minutes transient time, the core damage is about 33%, 89% and 99% for the fuel rods, channel boxes and control blades, respectively. The fractions of oxidation are 16%, 3% and 0% for cladding, channel boxes and control blades, respectively. The core damage and oxidation are shown in Figure 6.6.

Finally, comparisons with the previous analysis of Section 4 based on the HCOG initial conditions show similar results on core damage and oxidation as summarized in Table 6.1. Only the first peak hydrogen generation rate is reduced by about 50% due to the severe limitation of steam when the Emergency Procedure Guidelines are applied as shown in Figure 6.7.

#### Case 6.2 - 300 gpm of CRDHS Flow

For the case in which the CRDHS flow is available, it is assumed that 300 gpm is injected at 58.5 minutes immediately after the 8 ADS valves are actuated at 58.35 minutes. The time of injection is selected to minimize the core damage so that the accident could be terminated as a degraded core event. According to the BWR system design,<sup>8</sup> the control rod drive mechanisms use water from the condensate storage tank as operating fluid. Thus, the injected coolant was assumed to have the saturation temperature in the MARCH calculation. A similar assumption is used in the HCOG analyses.

The MARCH code predicts that the water level is about 6 inches below the bottom of core at the time of coolant injection. The injection of saturated water does not recover the core immediately, as the water is continuously evaporated due to depressurization (flashing) shown in Figure 6.8 and due to the downward thermal radiation from the core. The water drops to its lowest level of 3 ft below the bottom of the core at 61 minutes and then starts to increase. The water level is above the bottom of the core at about 75 minutes as illustrated in Figure 6.9. Small oscillations of vessel pressure, water temperature and water level were predicted as shown in Figures 6.8 and 6.9. At 93 minutes, the water level reached 2.8 ft in the core region and quenched about 1/4 of the core. A peak hydrogen generation is predicted at this time. Figure 6.10 shows that the hydrogen generation rate reached as high as 300 lb/min but over a very short time duration. The termination of the hydrogen generation is caused by core reflood which produces a large amount of steam and provides sufficient cooling of the core region. Figure 6.11 shows the decrease of core temperature after 100 minutes.

The oxidation and core damage are given in Figure 6.12. The fractions of oxidation are 30%, 19% and 4% for cladding, channel boxes and control blades, respectively. The assumption of 1% steam flow in the bypass region (FBP=0.01)

reduces oxidation on channel boxes and control blades. The core damage is about 0%, 66%, and 90% for fuel rods, channel boxes and control blades, respectively. It is noted that the core damage is represented by the fraction of material melted. A eutectic melting temperature (4130°F) is used for cladding and fuel in the MARCH analysis. The eutectic melting temperature is higher than the melting temperature of zircaloy (3365°F) assumed in the code. The 0% fuel damage predicted by the MARCH code implies no fuel melt based on the eutectic melting temperature. However, a maximum of 49% of cladding is at or above 3400°F (zircaloy melting temperature) at 97 minutes according to the MARCH analysis. It is assumed that this degree of core damage would not cause core slump leading to a complete core meltdown in this analysis. The event could be terminated as a degraded core accident. (The core damage could be reduced if the injection of CRDHS flow is started at or prior to the actuation of the 8 ADS valves.)

Comparisons with previous analysis based on the HCOG's initial conditions indicate that following the Emergency Procedure Guidelines would lead to a much higher peak hydrogen rate with a much shorter time duration as shown in Figure 6.13. The total hydrogen production is comparable for the two cases as summarized in Table 6.1.

#### Case 6.3 - 5000 gpm of LPCI flow

In this case, the low pressure coolant injection (LPCI) flow is used to terminate the accident so that a coolable core could be maintained. The LPCI system is designed to restore and maintain the reactor coolant inventory after ADS actuation. The LPCI pumps take suction from the suppression pool. The RHR heat exchanger may be used. Hence, the LPCI flow temperature is assumed to be 100°F for the entire transient period in the MARCH analysis. The injection time is delayed to 100 minutes, about 41 minutes after the ADS actuation, to maximize the hydrogen production for a degraded core event.

The MARCH analysis shows that at the time of coolant injection (100 minutes), the system pressure has decreased to 21 psia and water level is 4.4 ft below the bottom of the core (Figures 6.14 and 6.15). With the addition of 5000 gpm into the vessel, the core is rapidly reflooded. The top of the core is recovered at 103 minutes and the accident is terminated (Figure 6.16). Consequently, only 75 lbs of hydrogen are produced during the 3-minute period of reflood as indicated in Figure 6.17. The peak hydrogen generate rate is about 191 lb/min. The MARCH analysis predicts practically no damage to the fuel rods and channel boxes but 66% melting of the control blades as shown in Figure 18. The fractions of oxidation are about 8.4%, 1.4% and 1% for cladding, channel boxes and control blades, respectively. Since the core damage and oxidation are much less than that of Cases 6.1 and 6.2, it is believed that the injection of LPCI flow could be further delayed by another 20 to 30 minutes, the core would still be coolable and more hydrogen would be produced.

The comparison of hydrogen generation rate with previous analysis based on the HCOG's initial condition is shown in Figure 6.19. The results are similar between the two analyses.

Table 6.1 Summary of Results Based on Emergency Procedure Guidelines

Reflood	No	No	CRDHS		LPCI	
gpm	—	—	300	300	5000	5000
min	-	-	58.5	42	100	56.7
Emergency Procedures Guidelines	Yes	No	Yes	No	Yes	No
Steam Flow in Bypass Region, %	1	10	1	10	1	10
Oxidation, %						
Clad	16	17	30	24	8.4	8.5
Channel Box	3	5	19	21	1.4	2.9
Control Blade	0	1	4	12	1	3.1
Melt, %						
Core	33	29	0	0	0	0
Channel Box	89	86	66	24	0.3	0
Control Blade	99	93	90	70	66	39
H <sub>2</sub> Production, lb	690	764	1700	1600	359	412
Peak Rate, lb/min	18	28	300	100	191	151
Time, min	15	50	93	52	103	58
Duration for rate greater than 30 lb/min, min	0	0	9.8	23.5	0.5	1

NO ECC GG POWER 10 NODEN ADS(1,8) AT 57.58

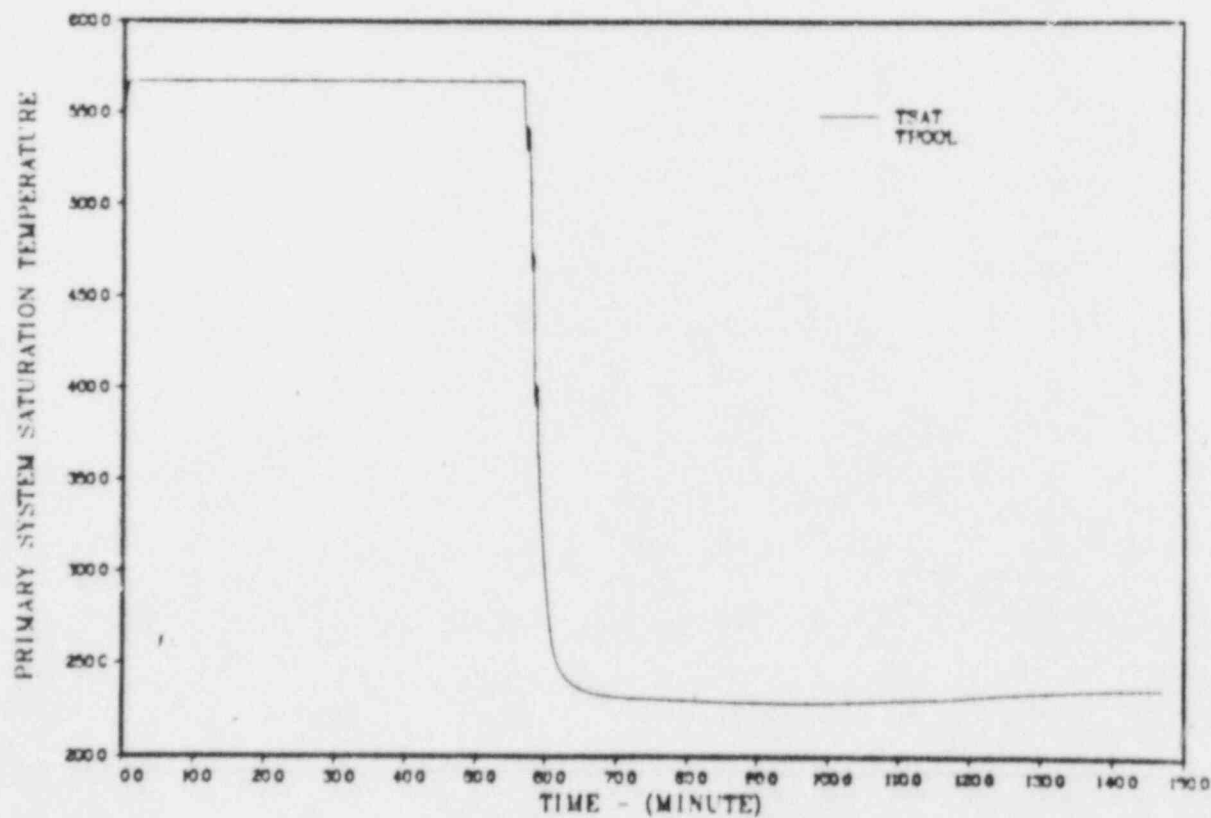
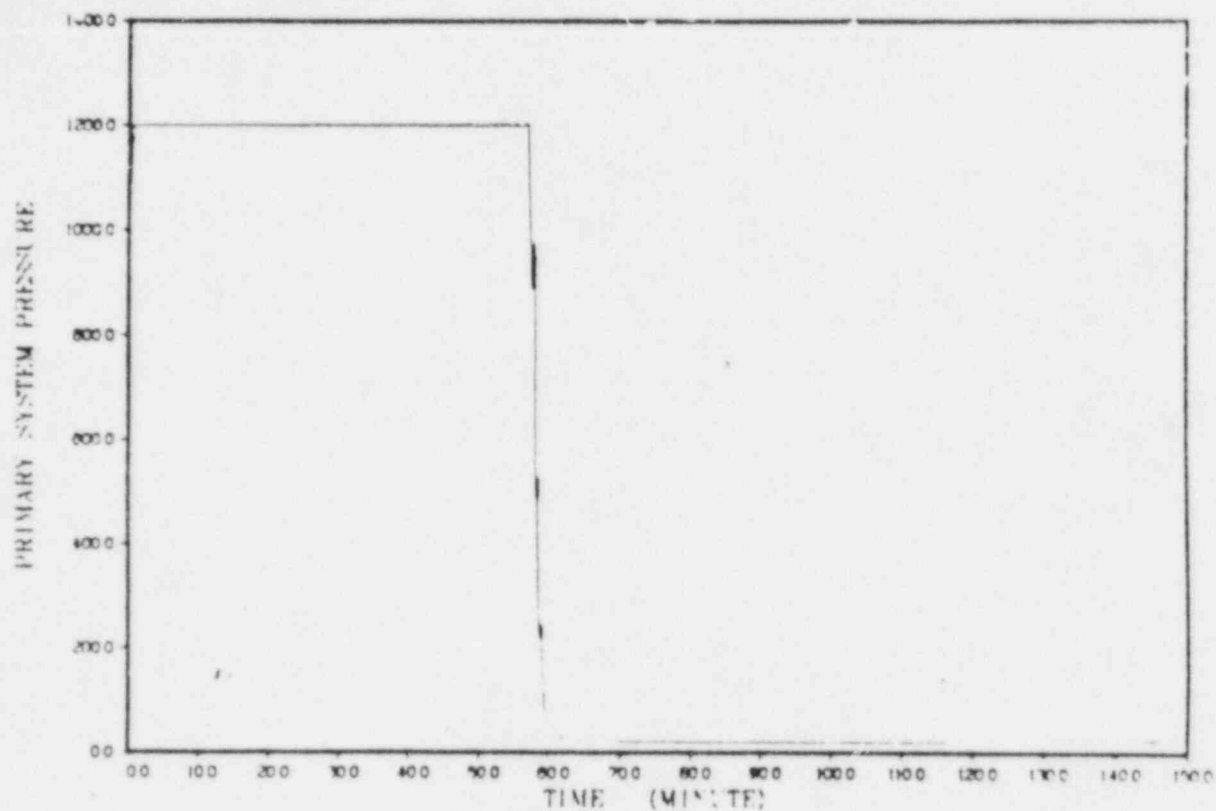


Figure 6.1 System pressure and temperature for case 6.1.



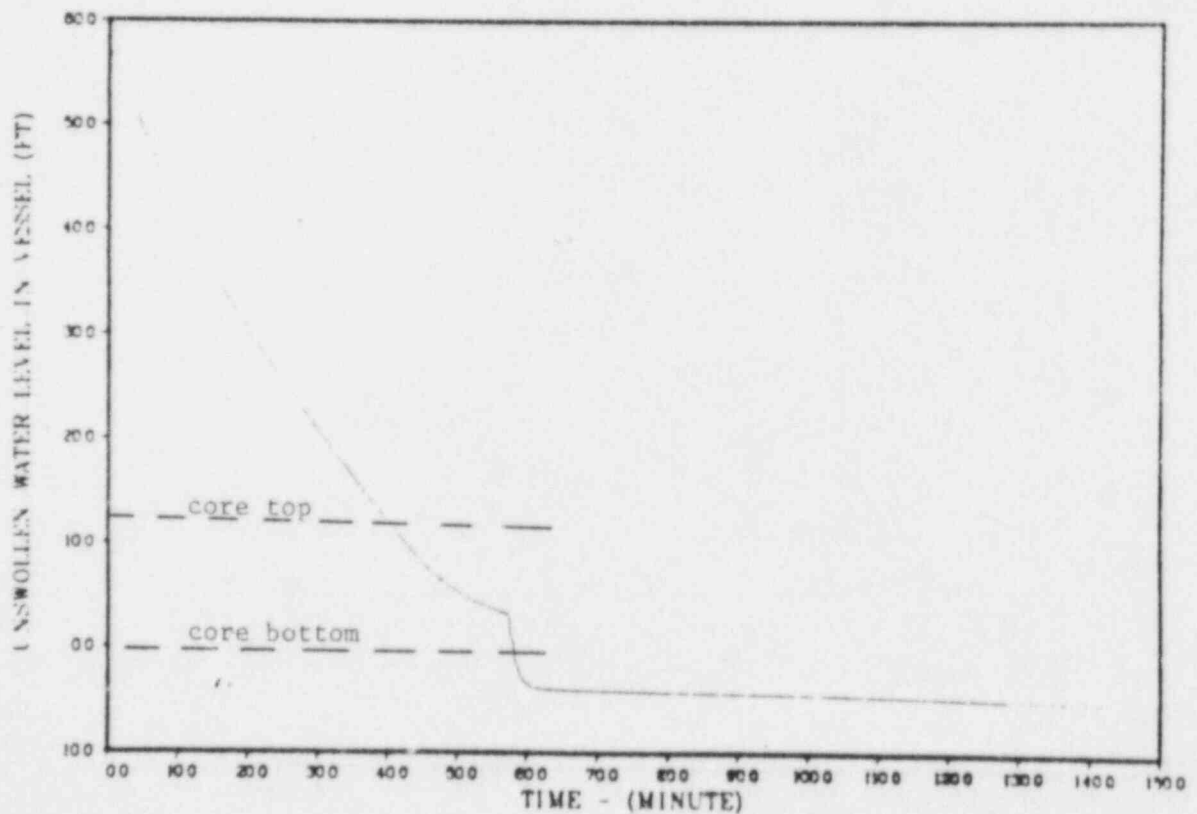
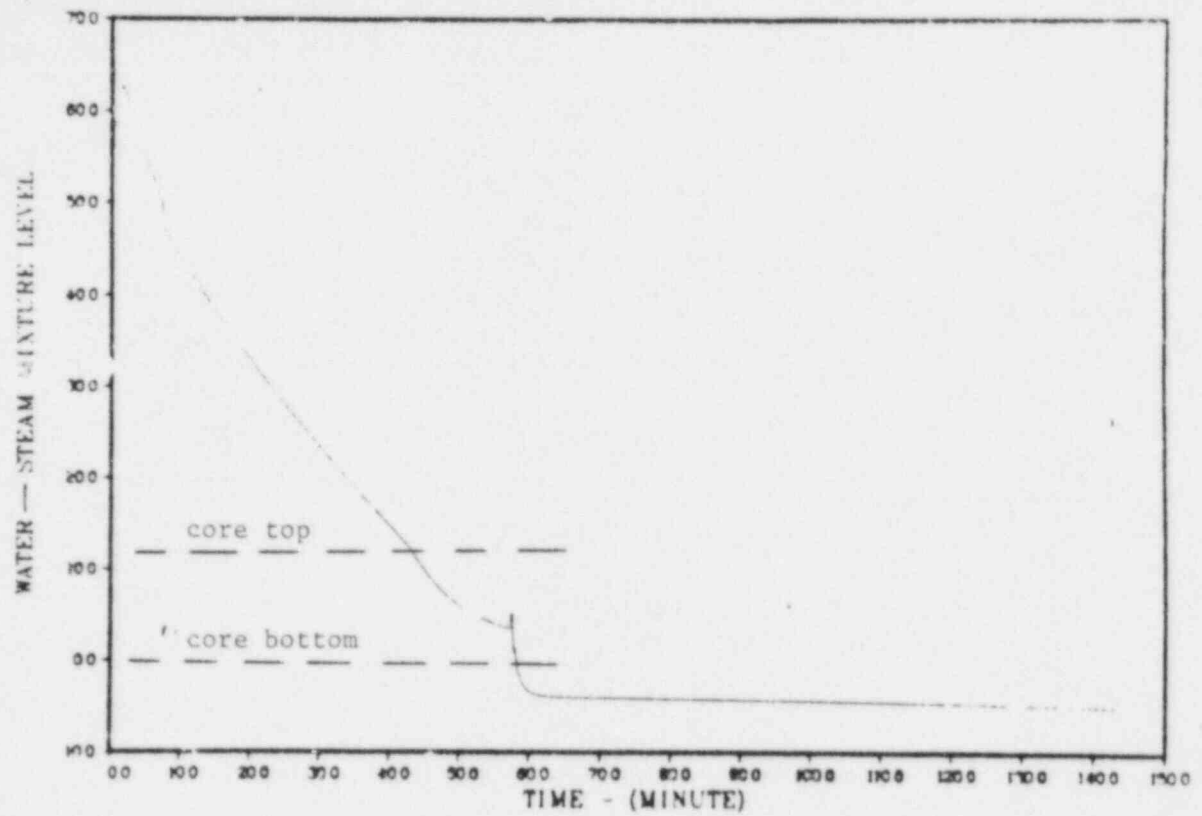


Figure 6.2 Reactor vessel water level for case 6.1.



NO EXC GG POWER 10 NODEN AD(18) AT 57.58

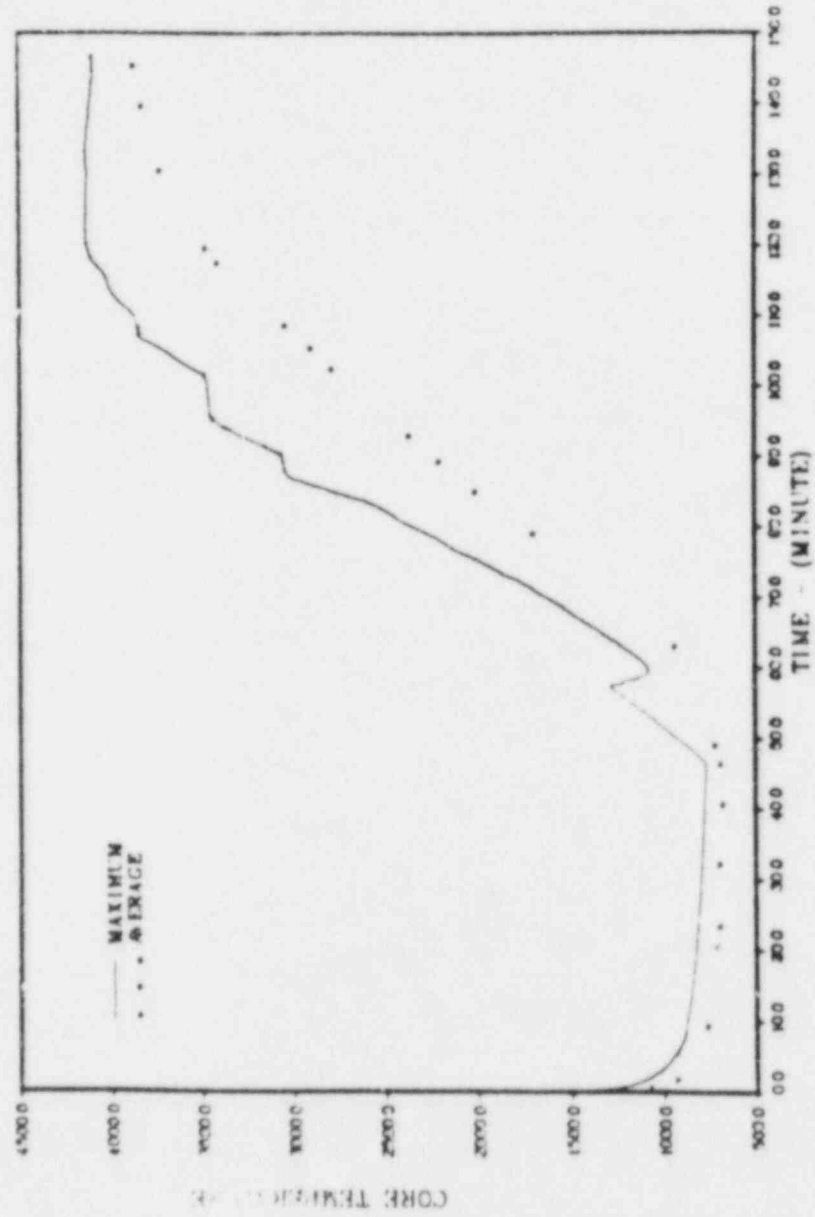


Figure 6.3 Core temperature for case 6.1.

NO ECC GG POWER 10 NODES ADS(1.8) AT 57.58

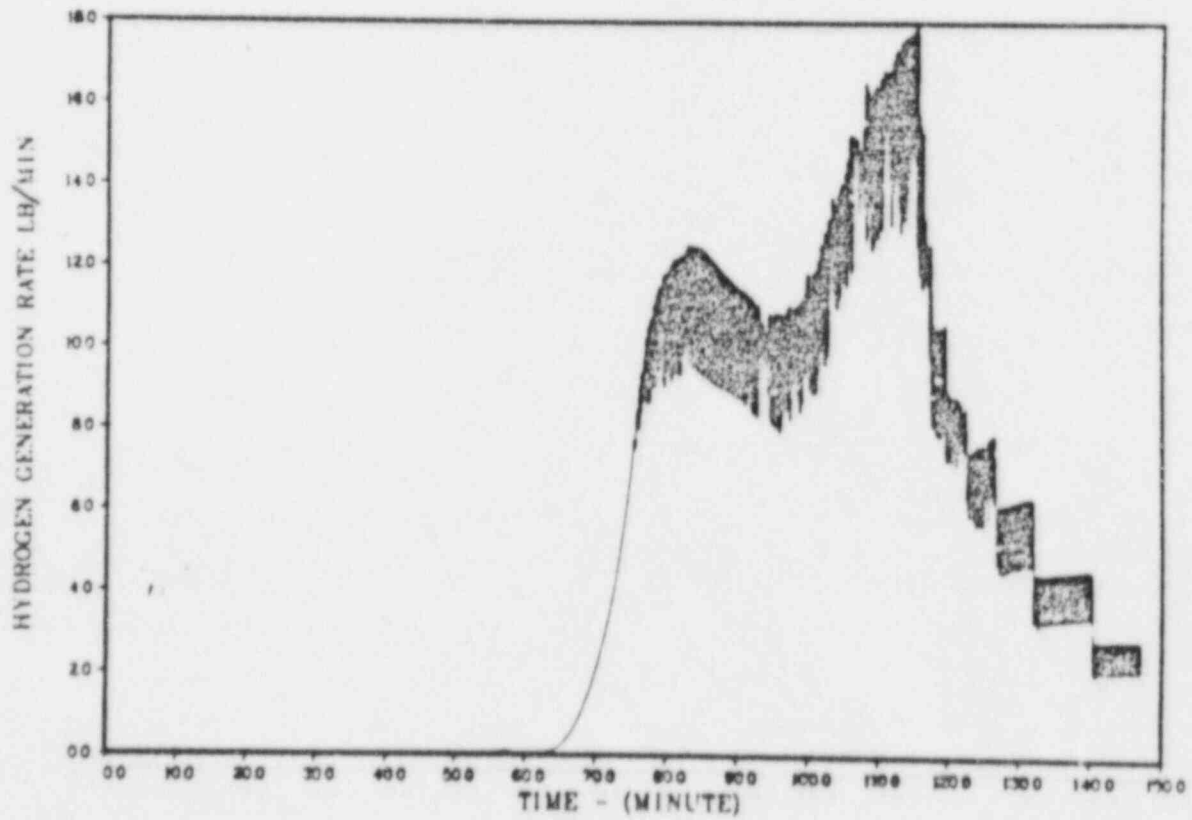
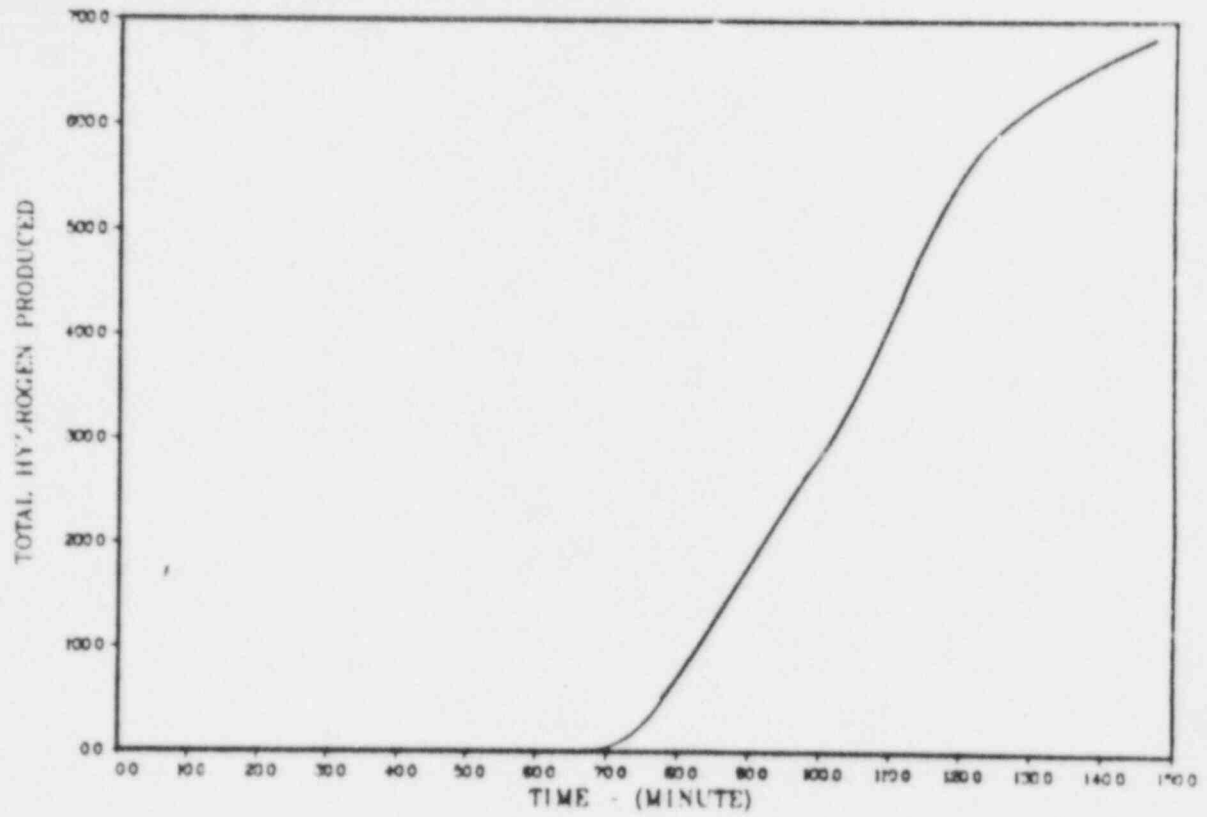


Figure 6.4 Hydrogen generation for case 6.1.

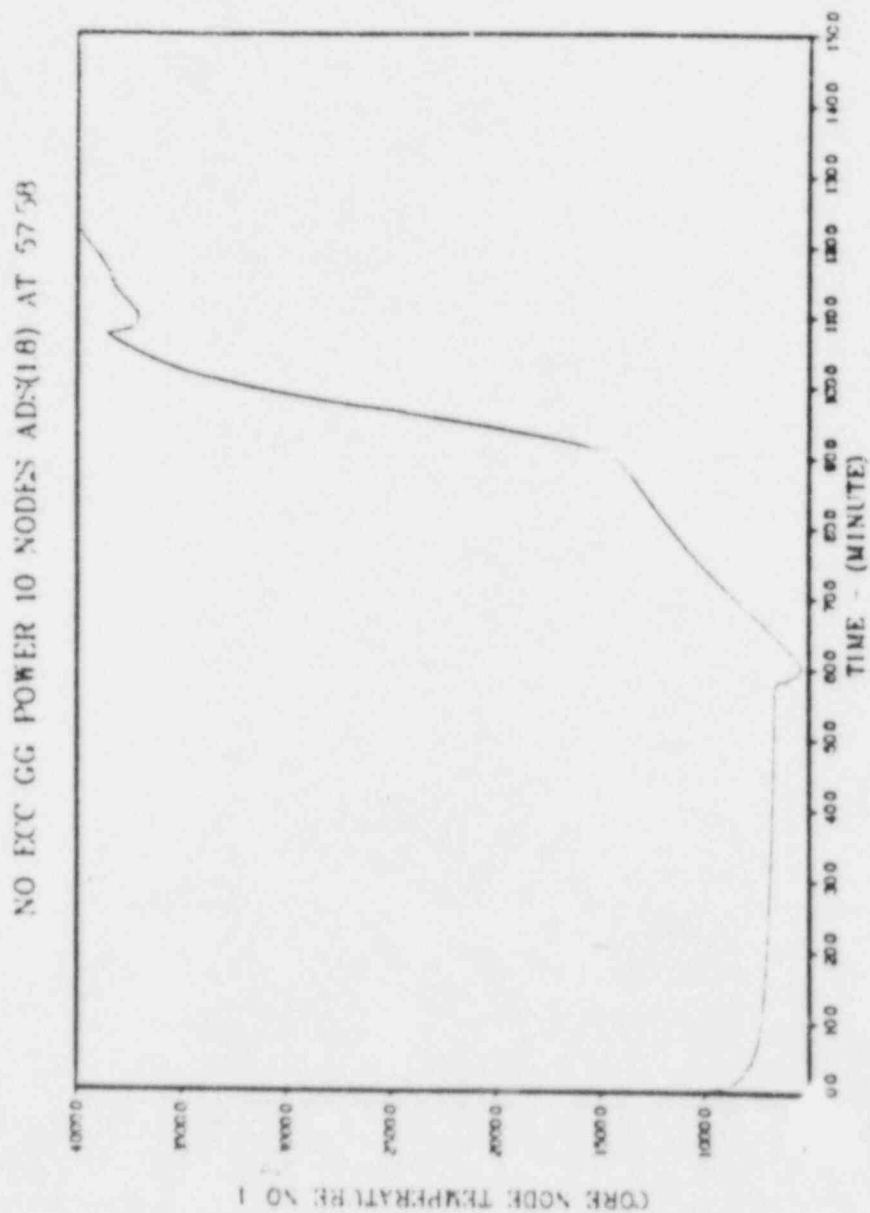


Figure 6.5 Core temperature above water level for case 6.1.

NO ECC GG POWER 10 NODES ADS(18) AT 57.58

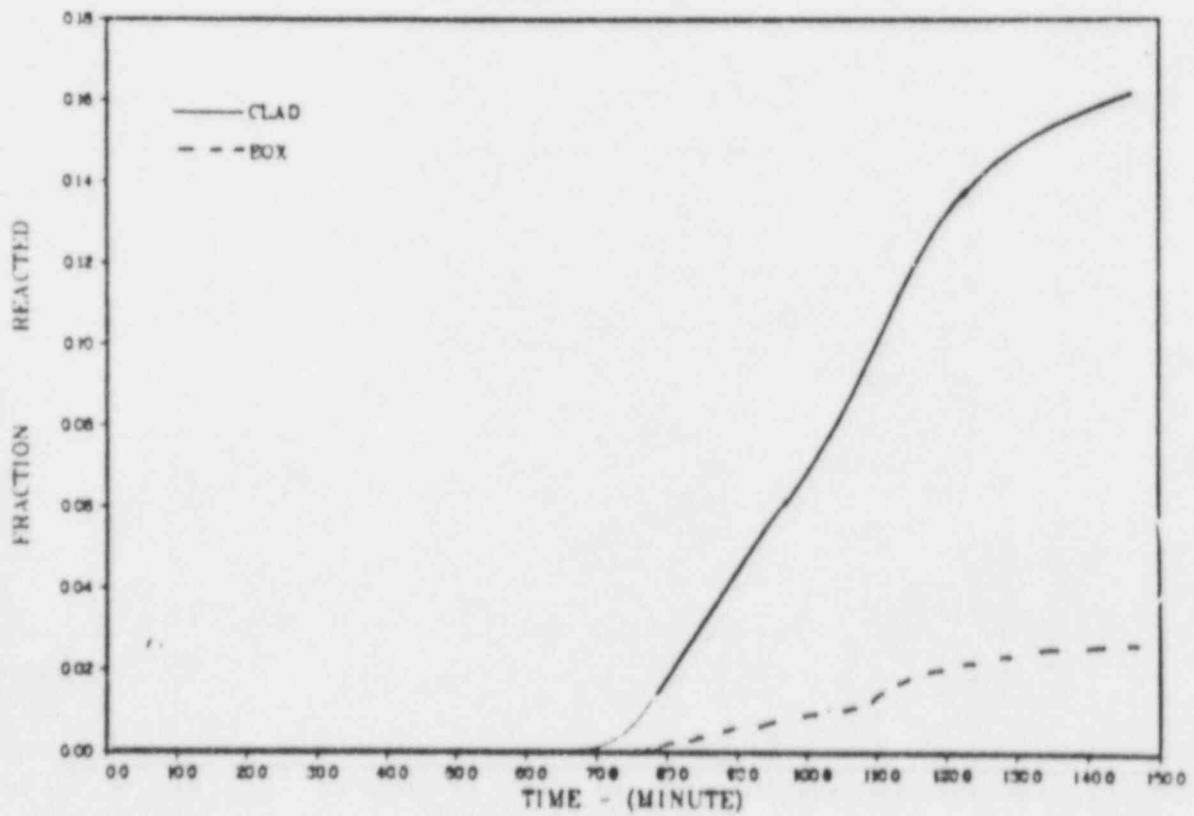
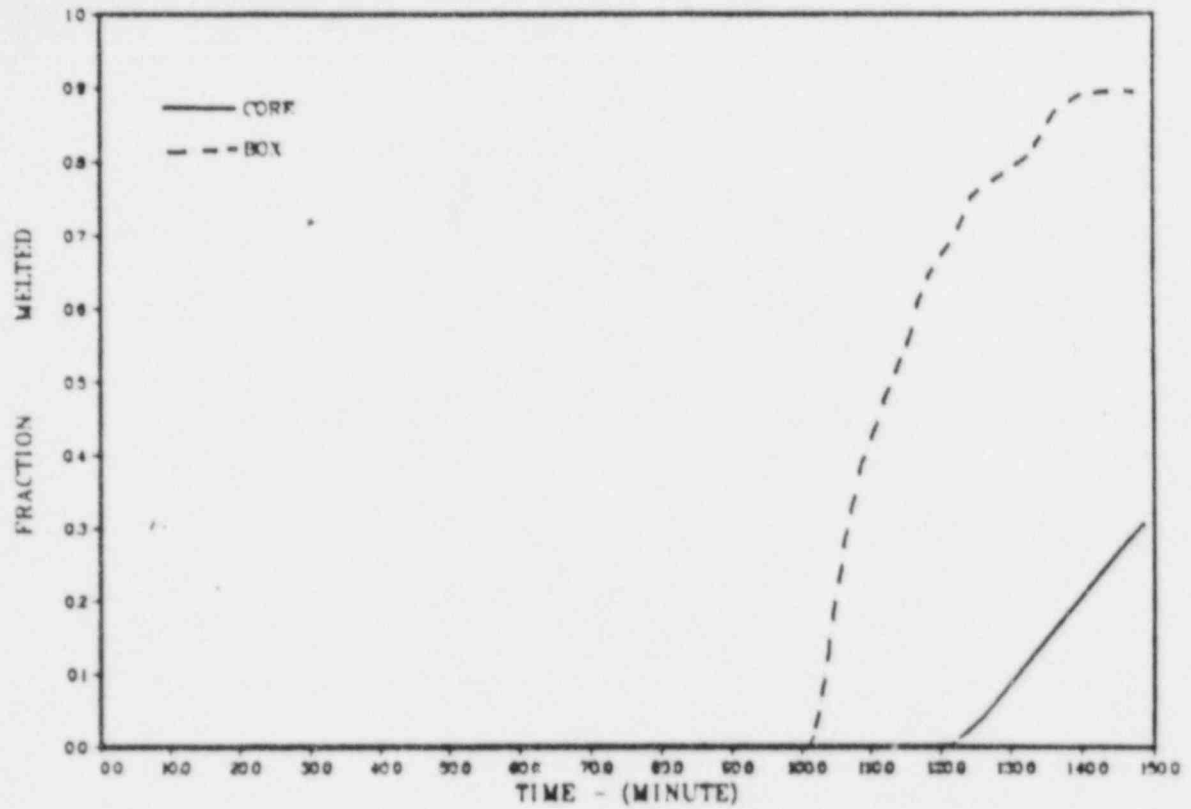
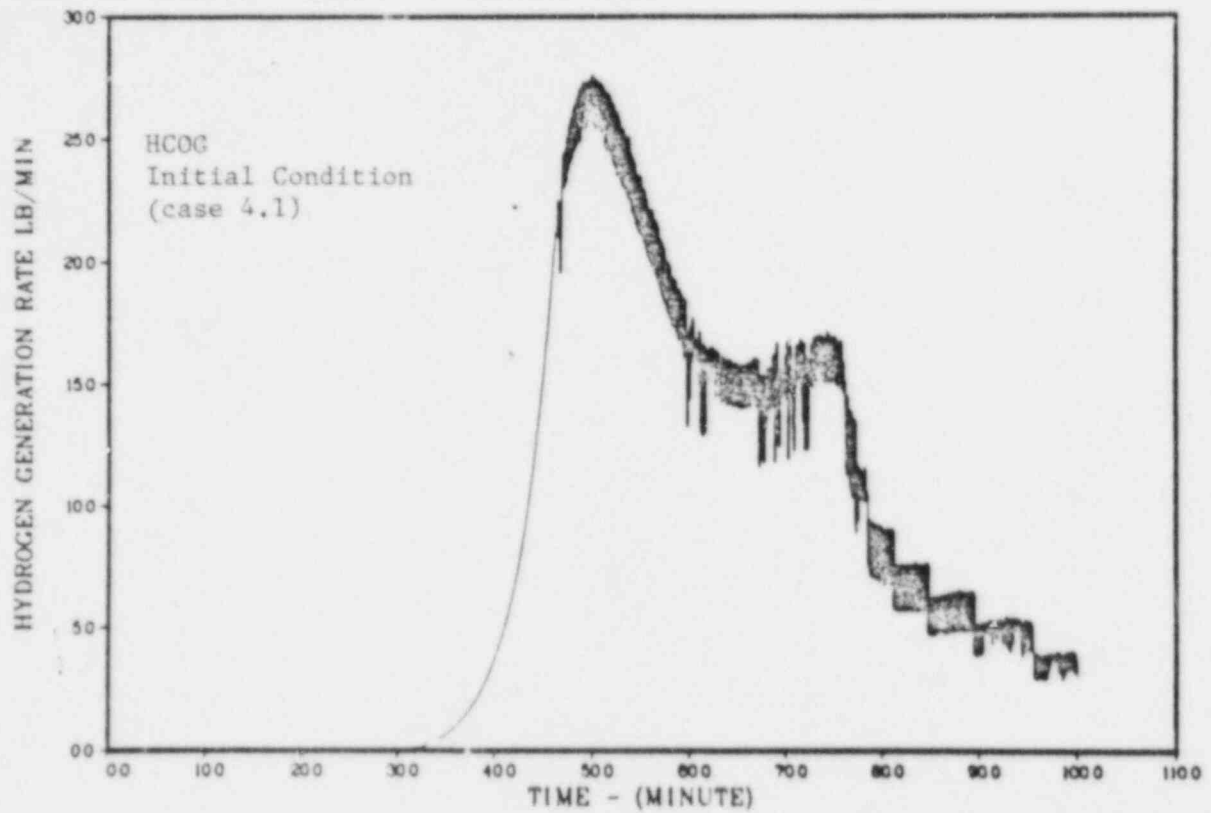


Figure 6.6 Melt fraction and oxidation fraction for case 6.1.

NO ECC GG POWER 10 NODES ADS(8) AT 5



NO ECC GG POWER 10 NODES ADS(18) AT 57.58

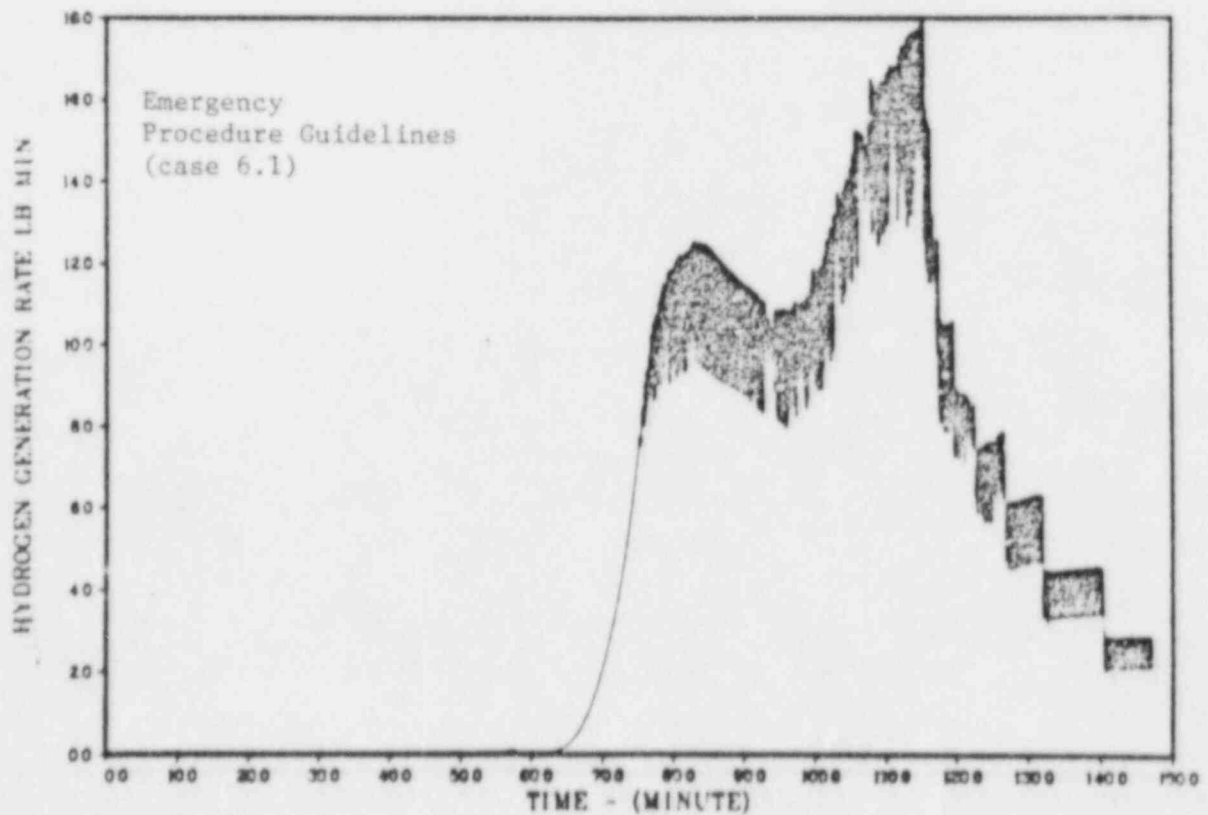


Figure 6.7 Comparison of H<sub>2</sub> generation rate for case 6.1 and 4.1.

300 GPM AT 58.5 ADS(1.8) AT 57.58.35

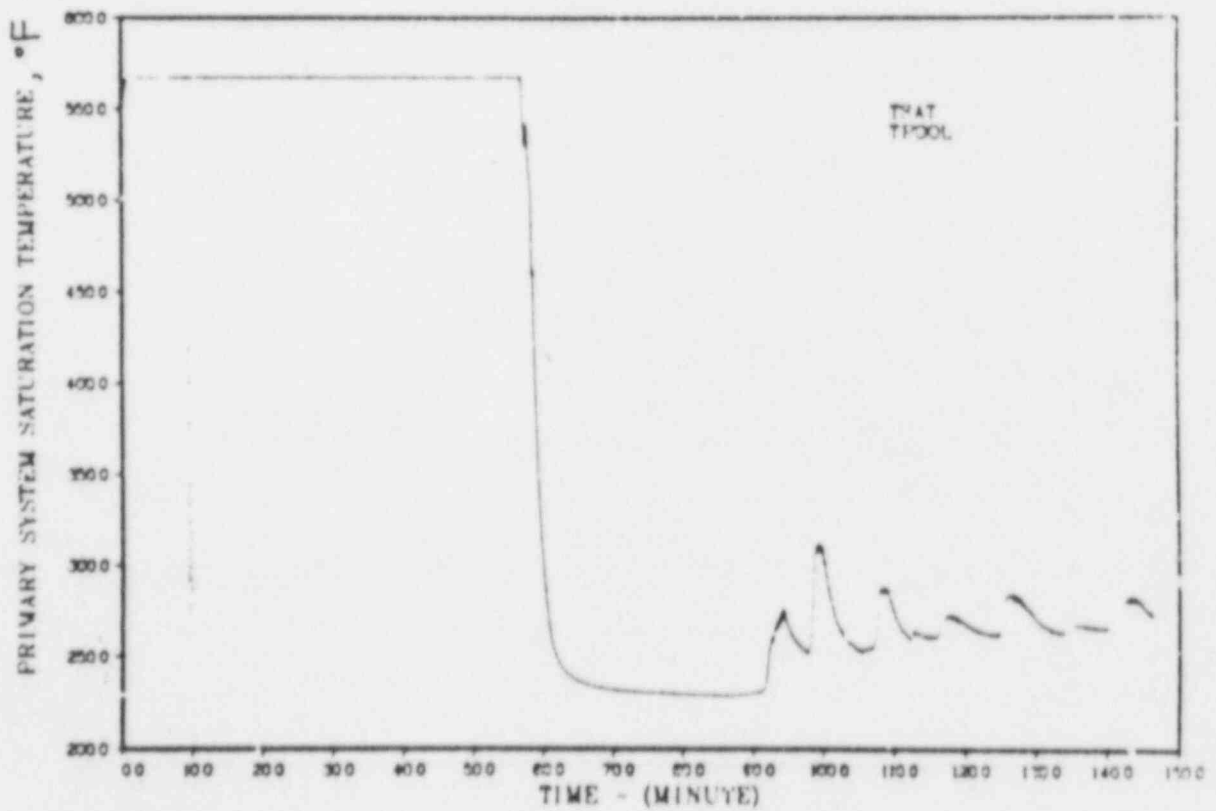
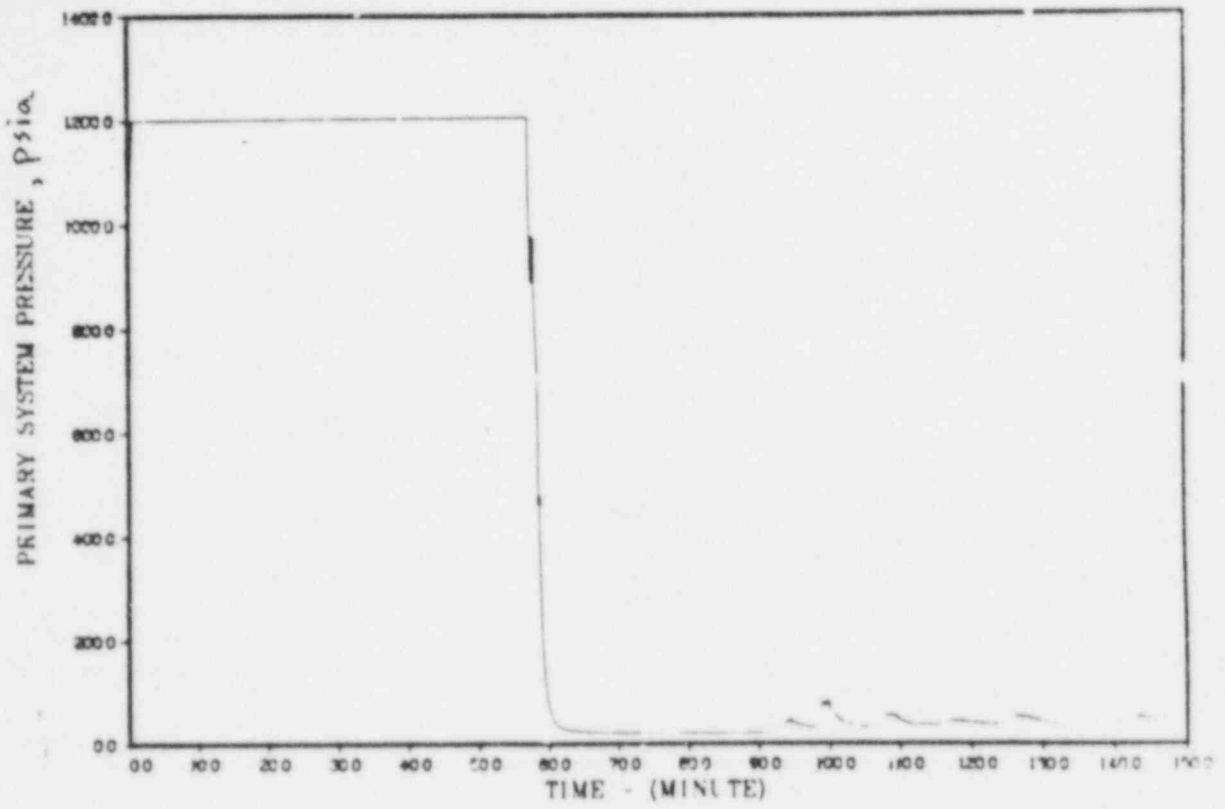


Figure 6.8 System pressure and temperature for case 6.2.

300 GPM AT 58.5 ADS(1.8) AT 57.58.35

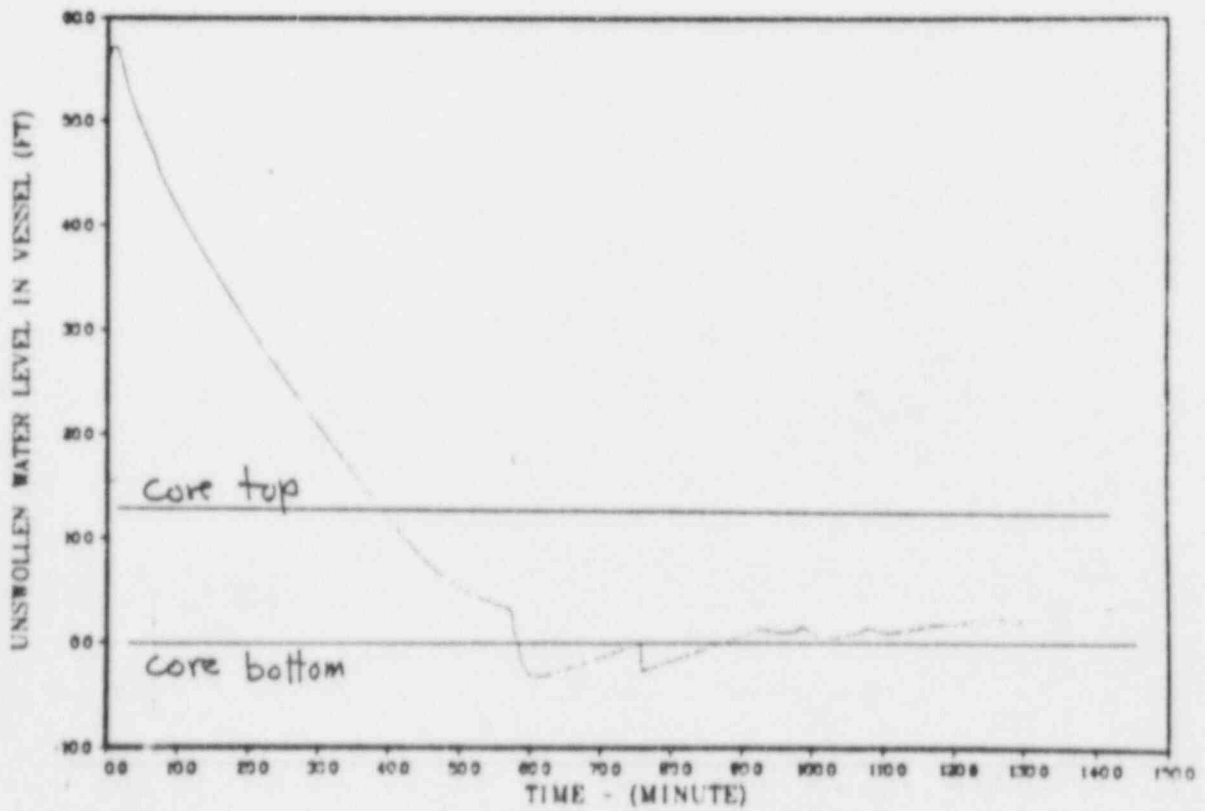
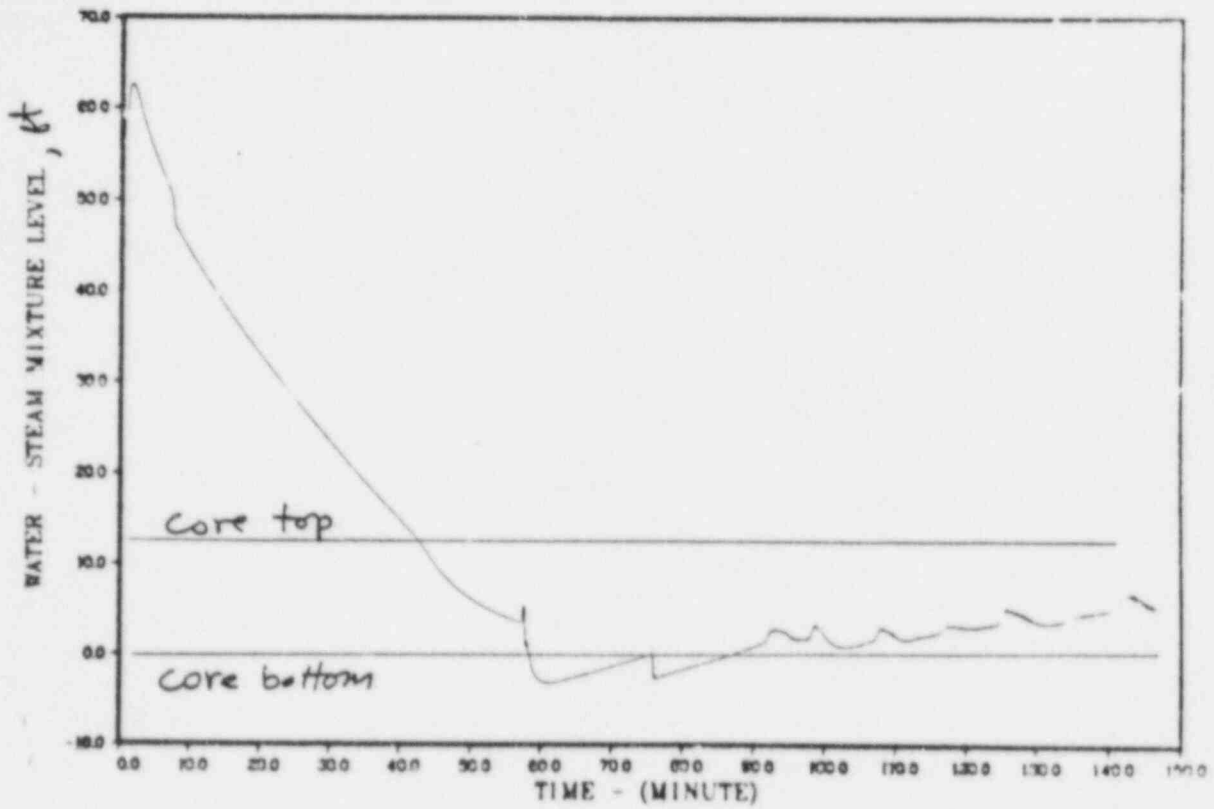


Figure 6.9 Reactor vessel water level for case 6.2.



300 GPM AT 58.5 ADS(1.8) AT 57.58.35

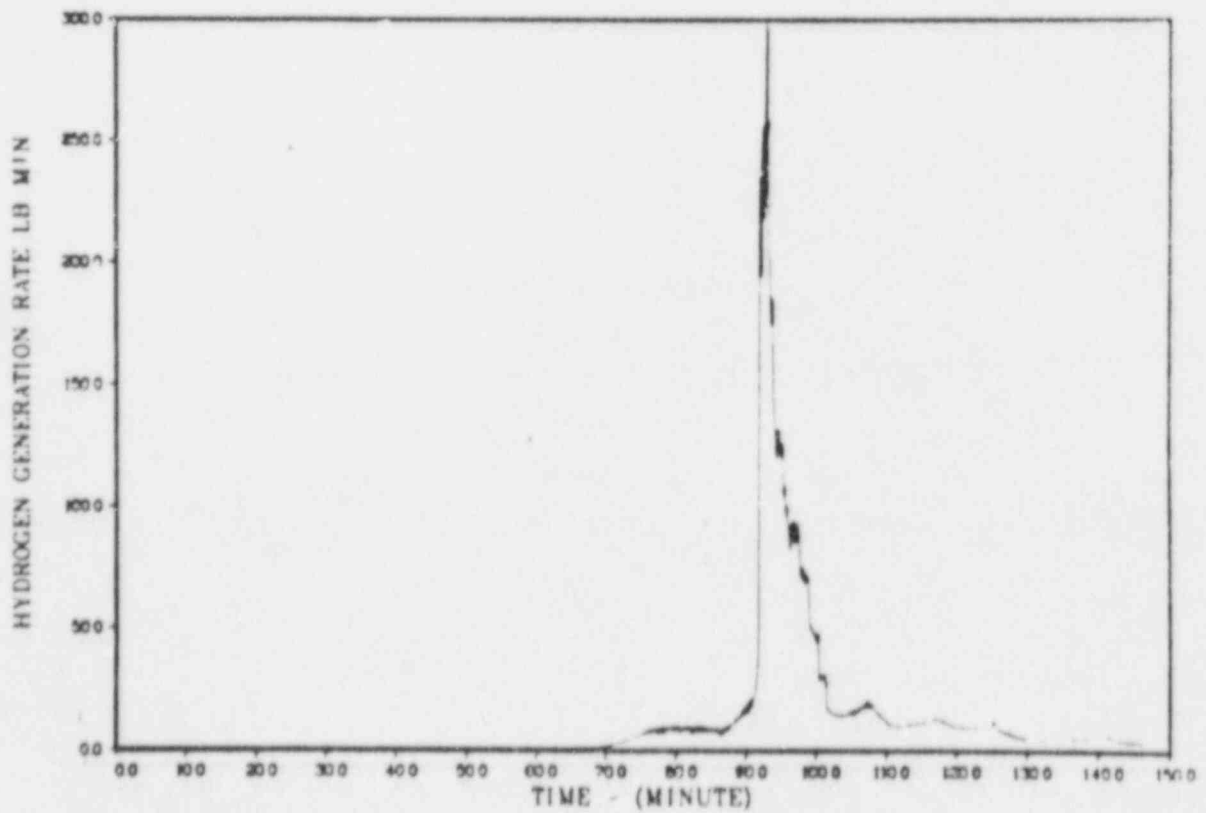
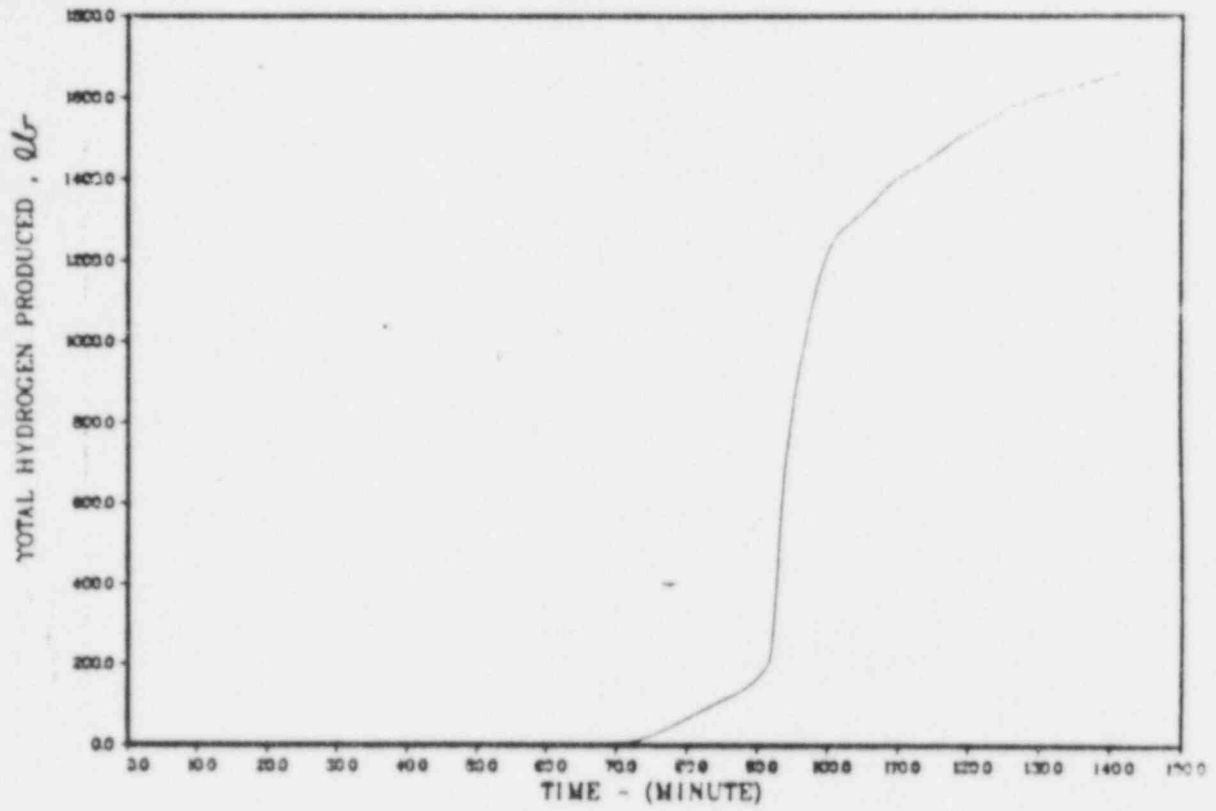


Figure 6.10 Hydrogen generation for case 6.2.

300 GPM AT 58.5 ADS(1.8) AT 57.58.35

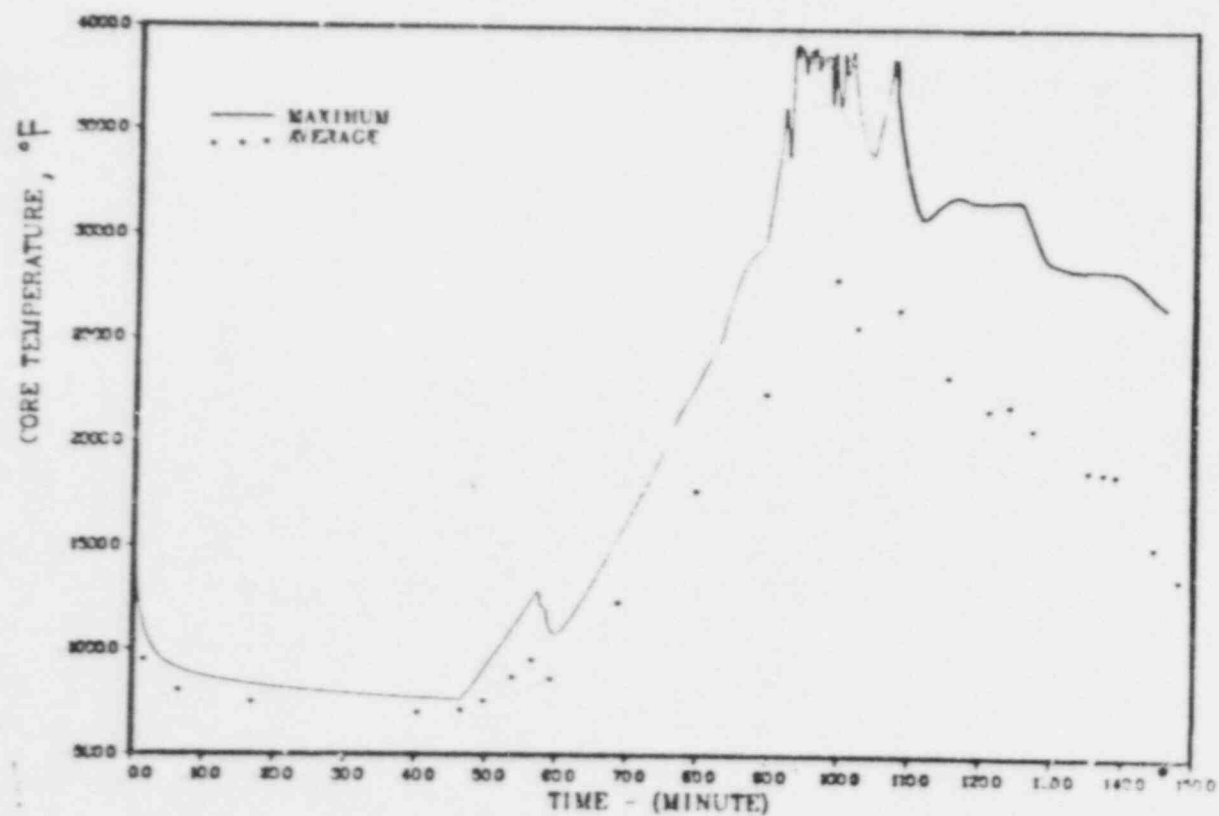


Figure 6.11 Core temperature for case 6.2.

300 GPM AT 58.5 ADS(1.8) AT 57.58.35

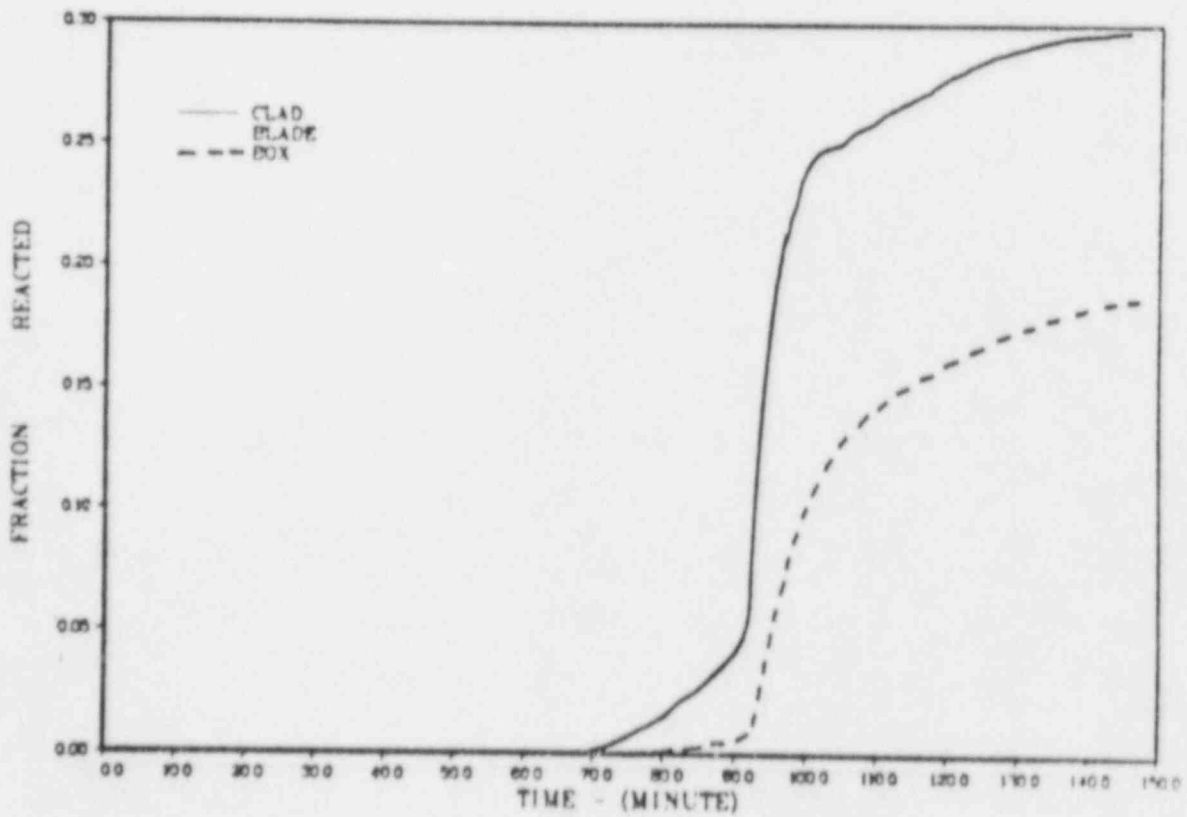
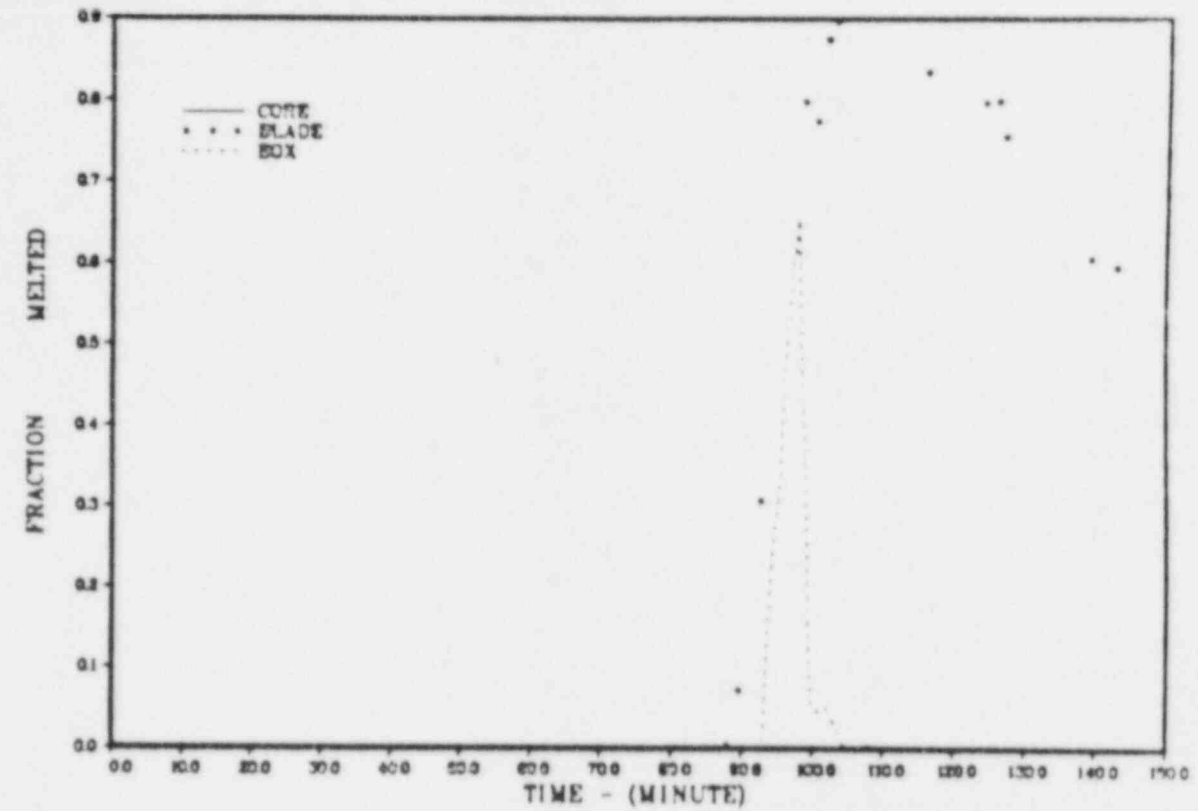
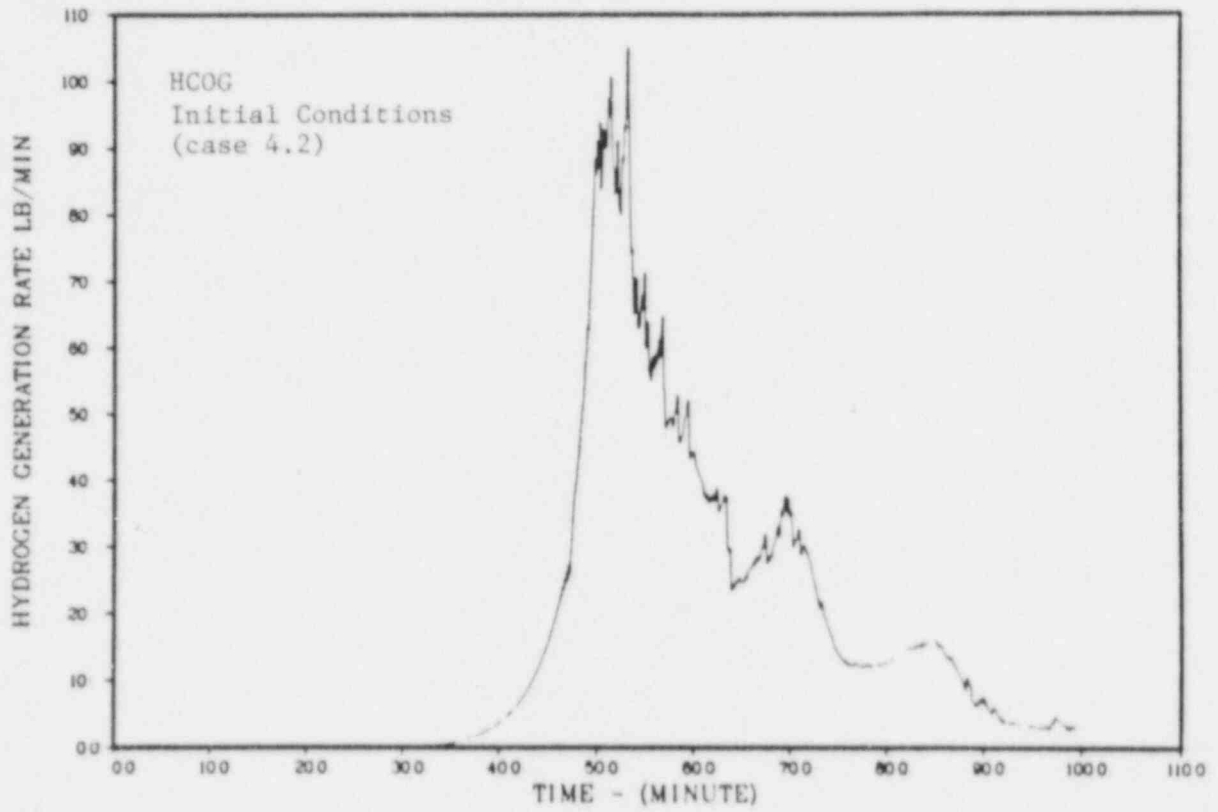


Figure 6.12 Melt fraction and oxidation fraction for case 6.2.

300GPM AT 42 GG POWER 10 NODES ADS(8) AT 5



300 GPM AT 58.5 ADS(1.8) AT 57 58.35

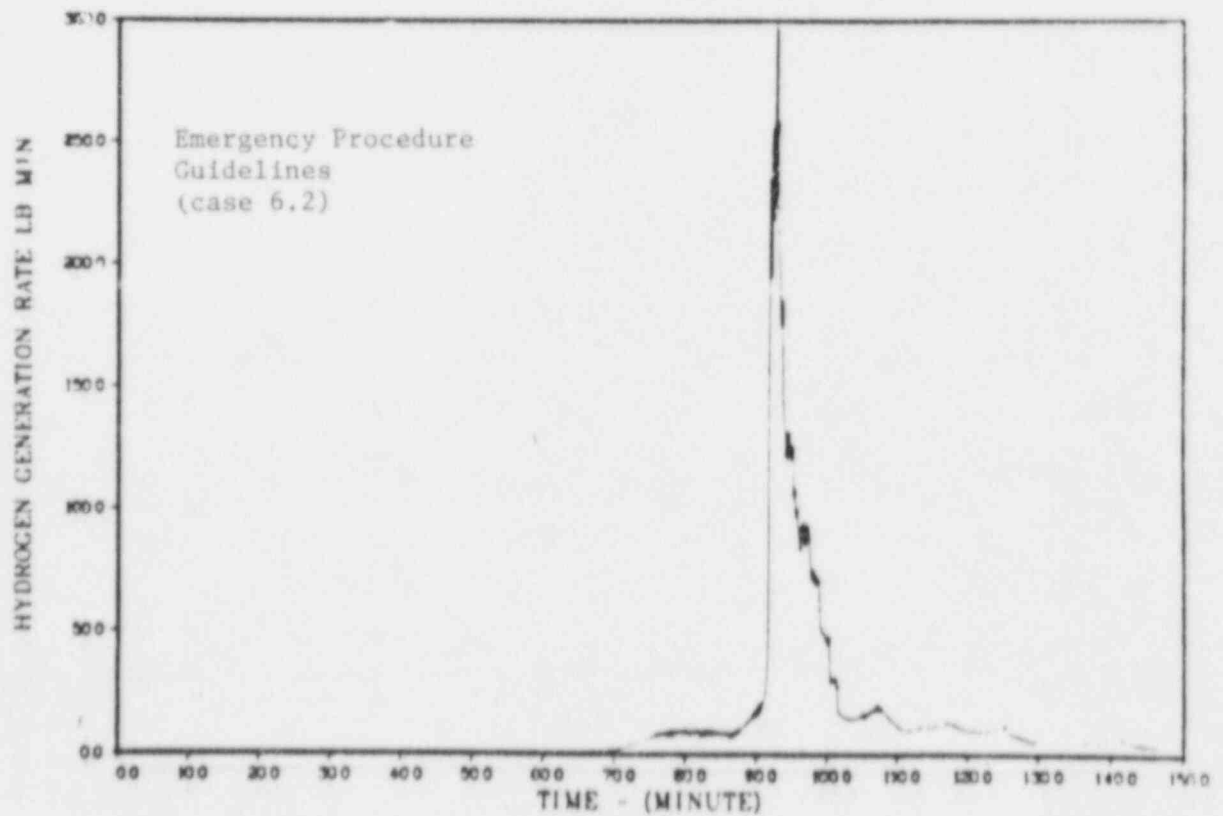


Figure 6.13 Comparison of hydrogen generation rate for case 6.2.

5000GPM AT 100 ADS(18) AT 57.58.35

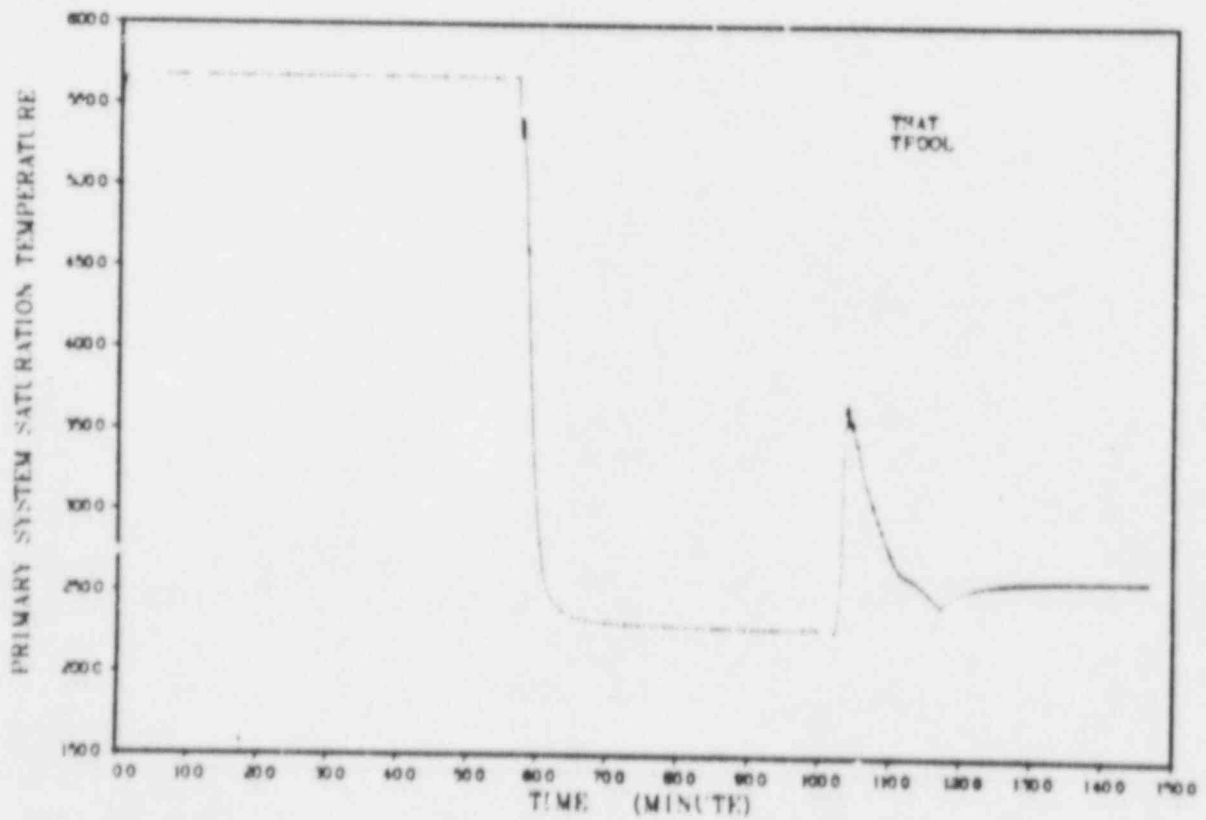
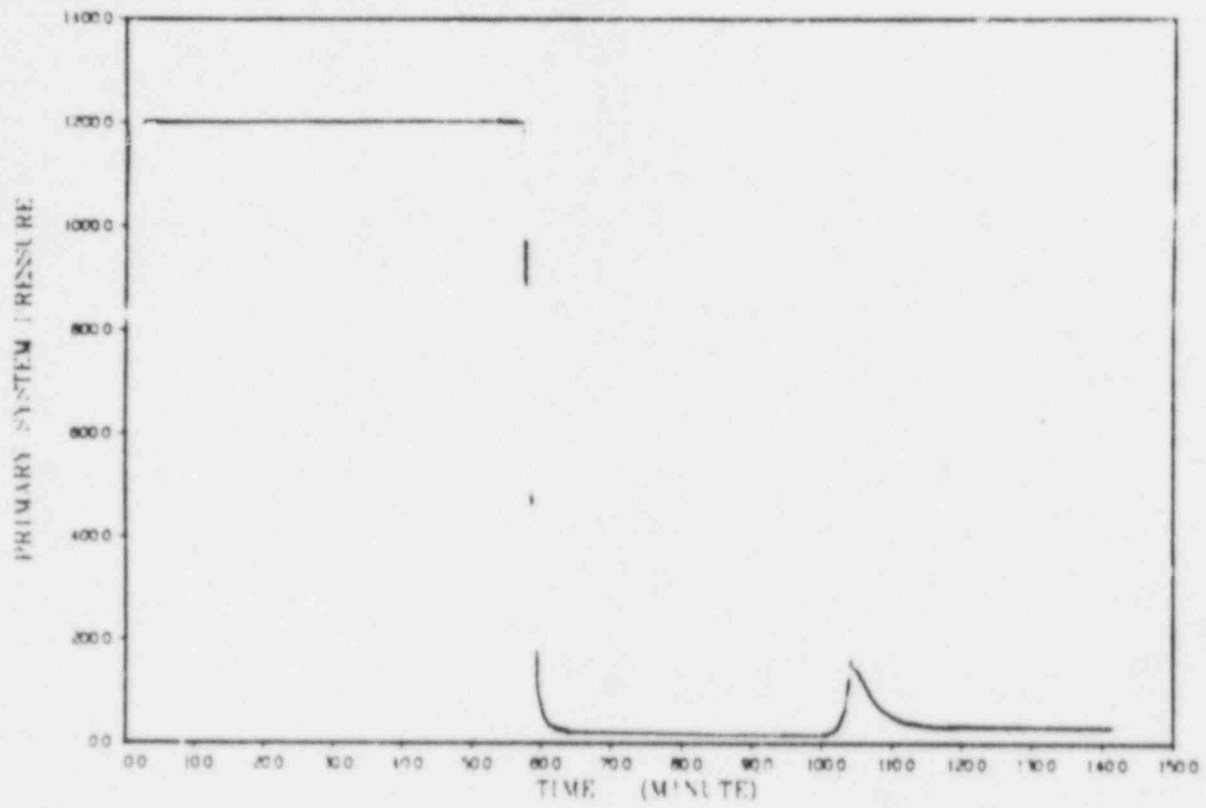


Figure 6.14 System pressure and temperature for case 6.3.

5000GPM AT 100 ADS(1.8) AT 57. 58.35

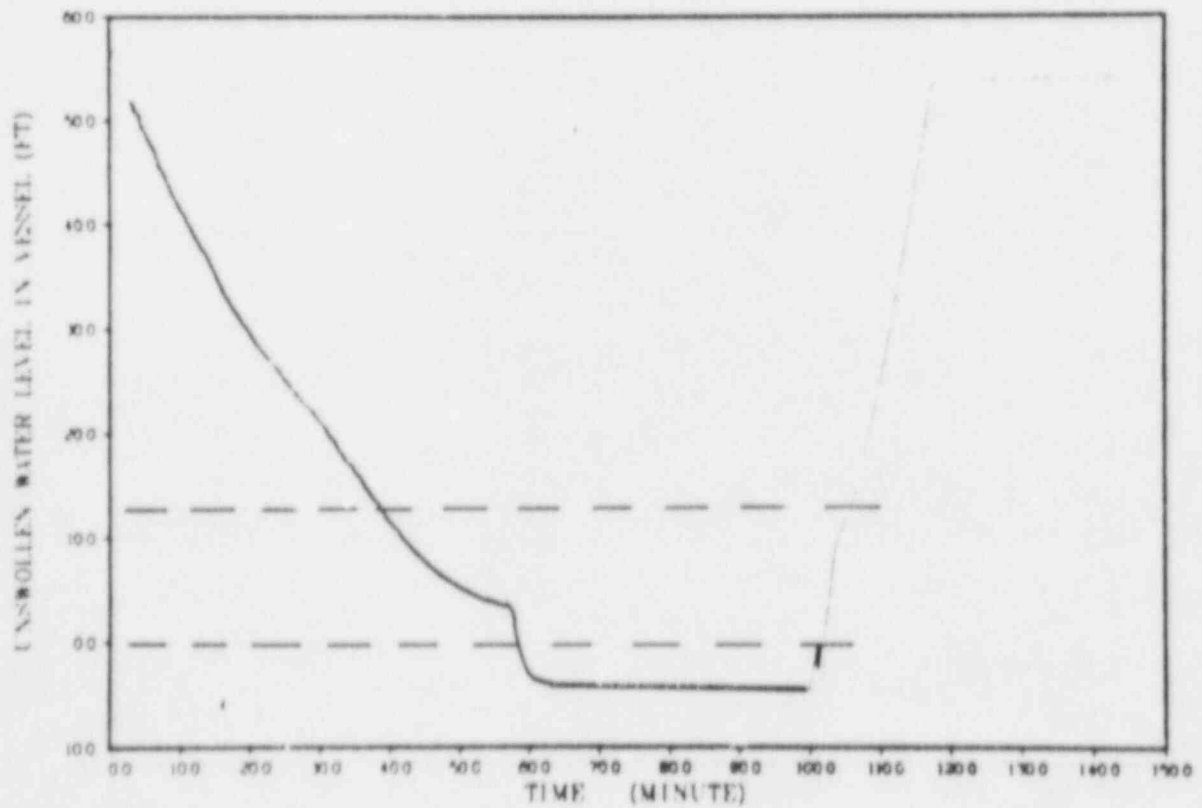
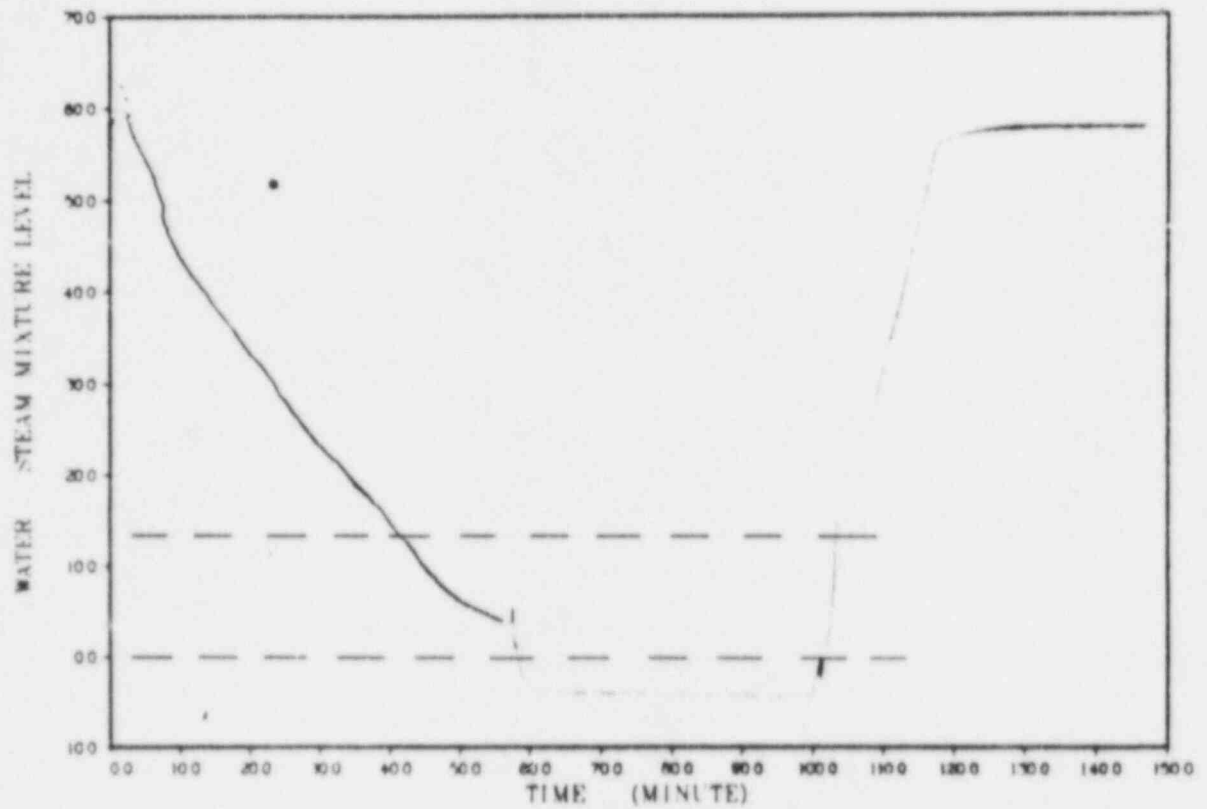


Figure 6.15 Reactor vessel water level for case 6.3.

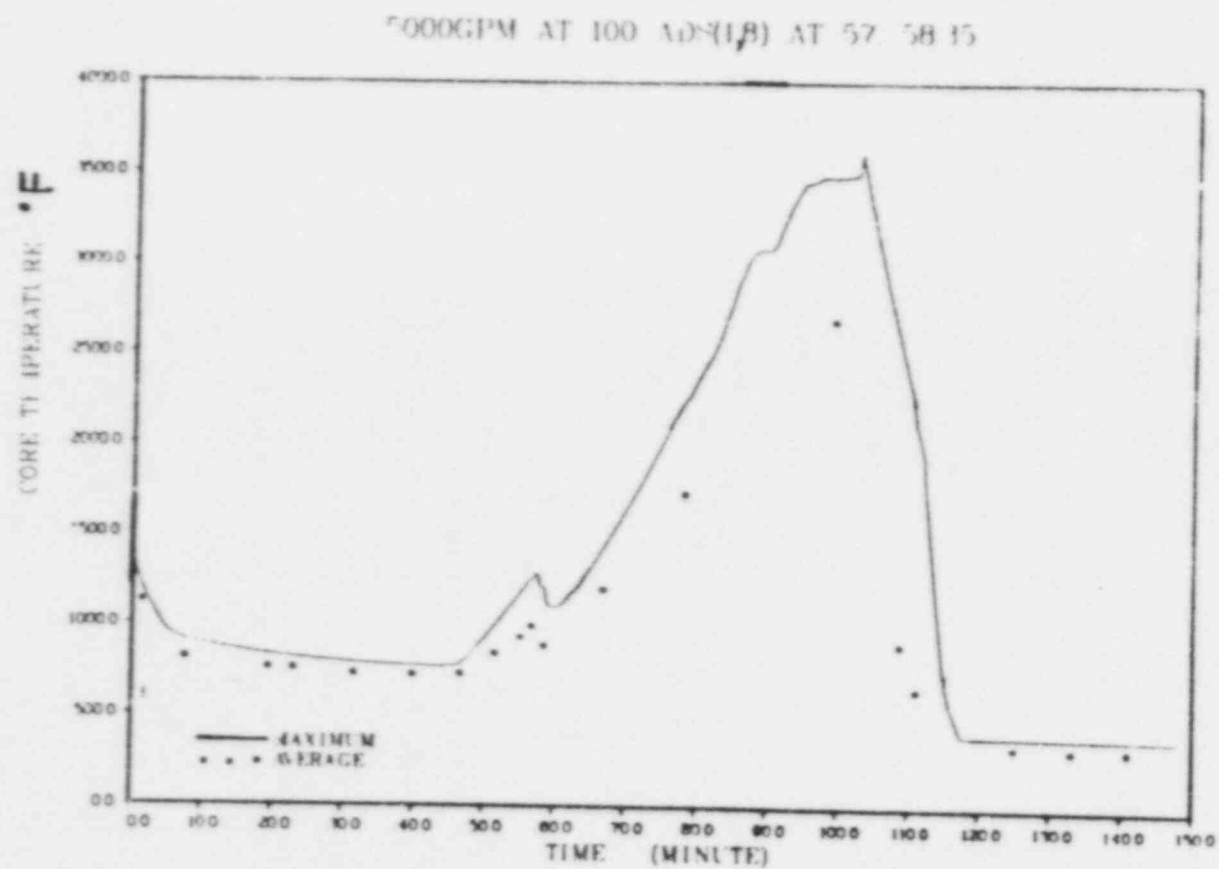


Figure 6.16 Core temperature for case 6.3.



5000GPM AT 100 ADS(1.8) AT 57. 58.35

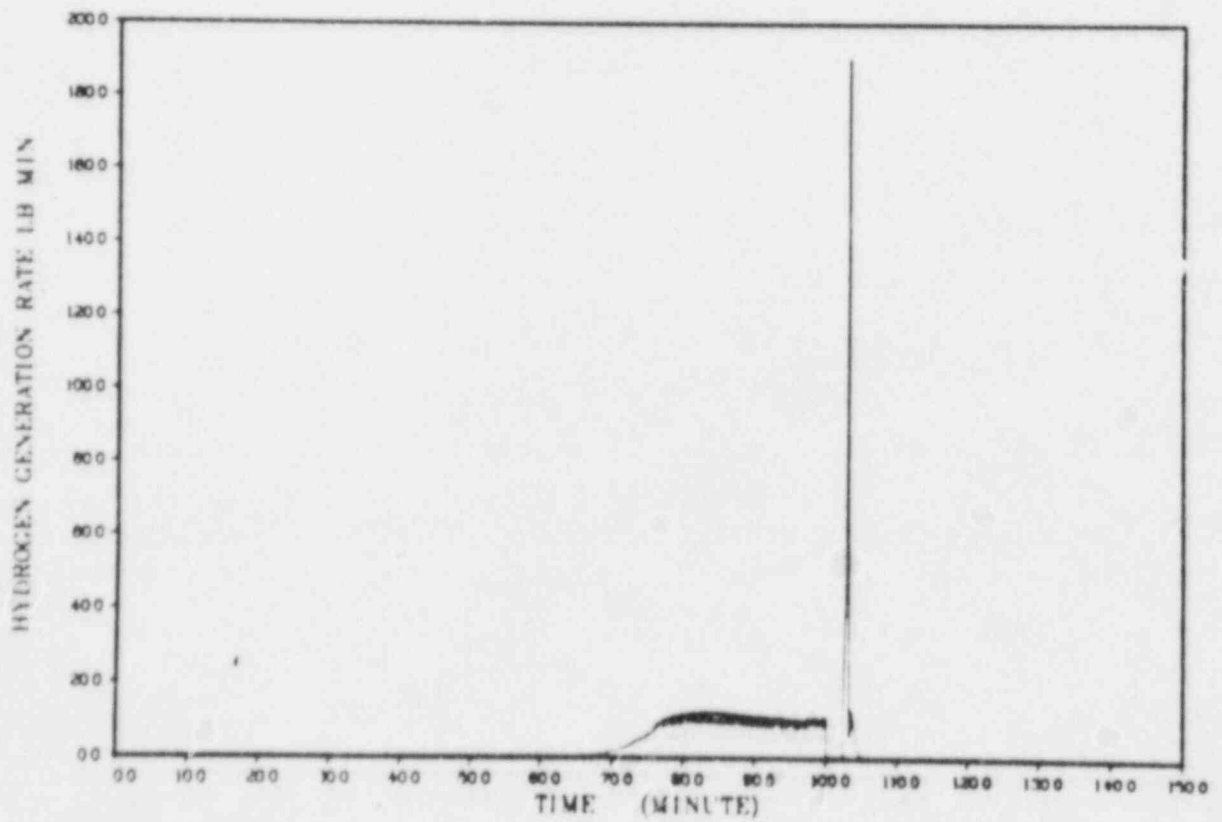
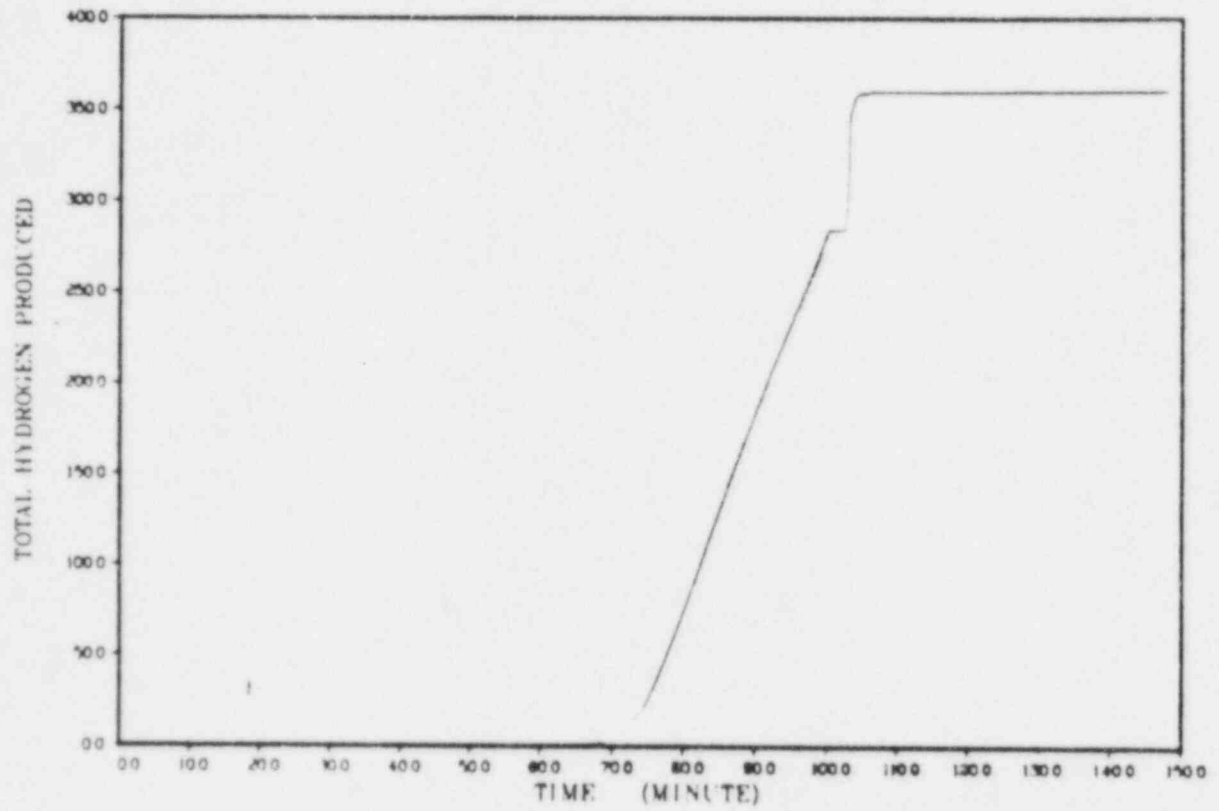


Figure 6.17 Hydrogen generation for case 6.3.

5000GPM AT 100 ADS(18) AT 57.58.35

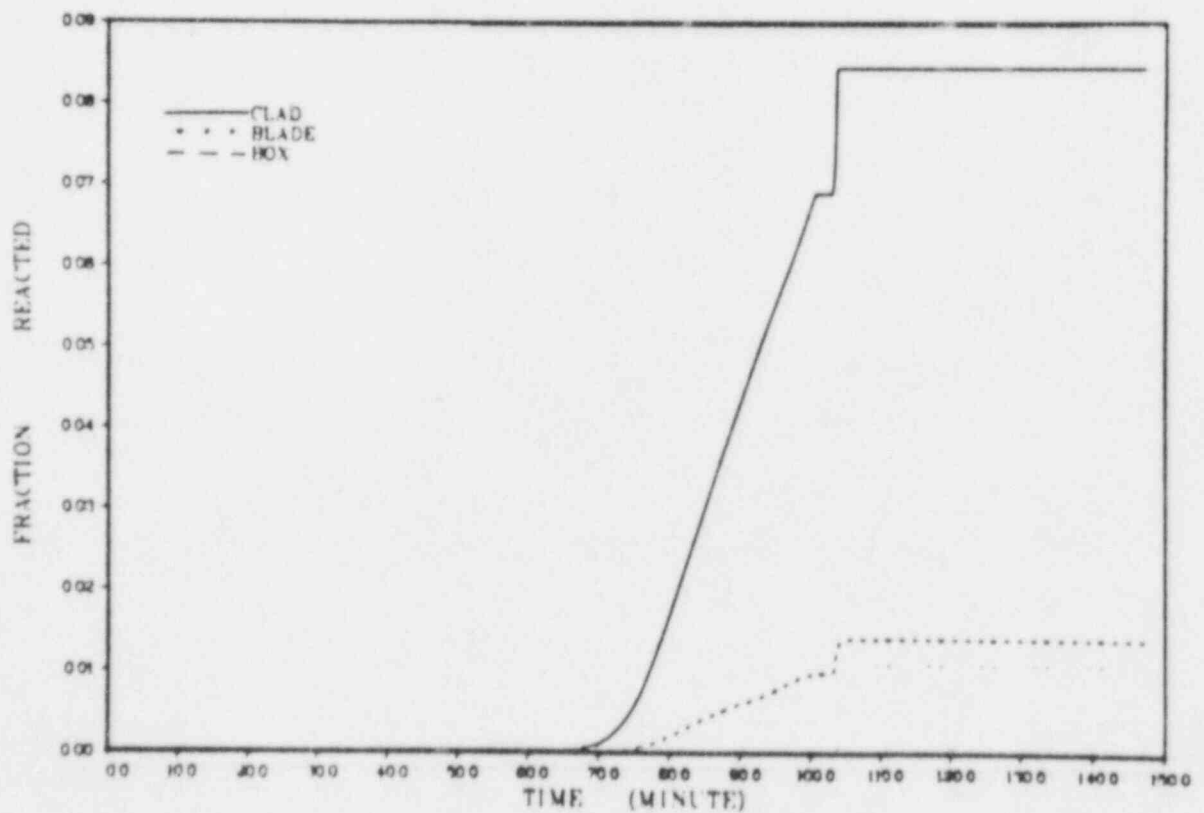
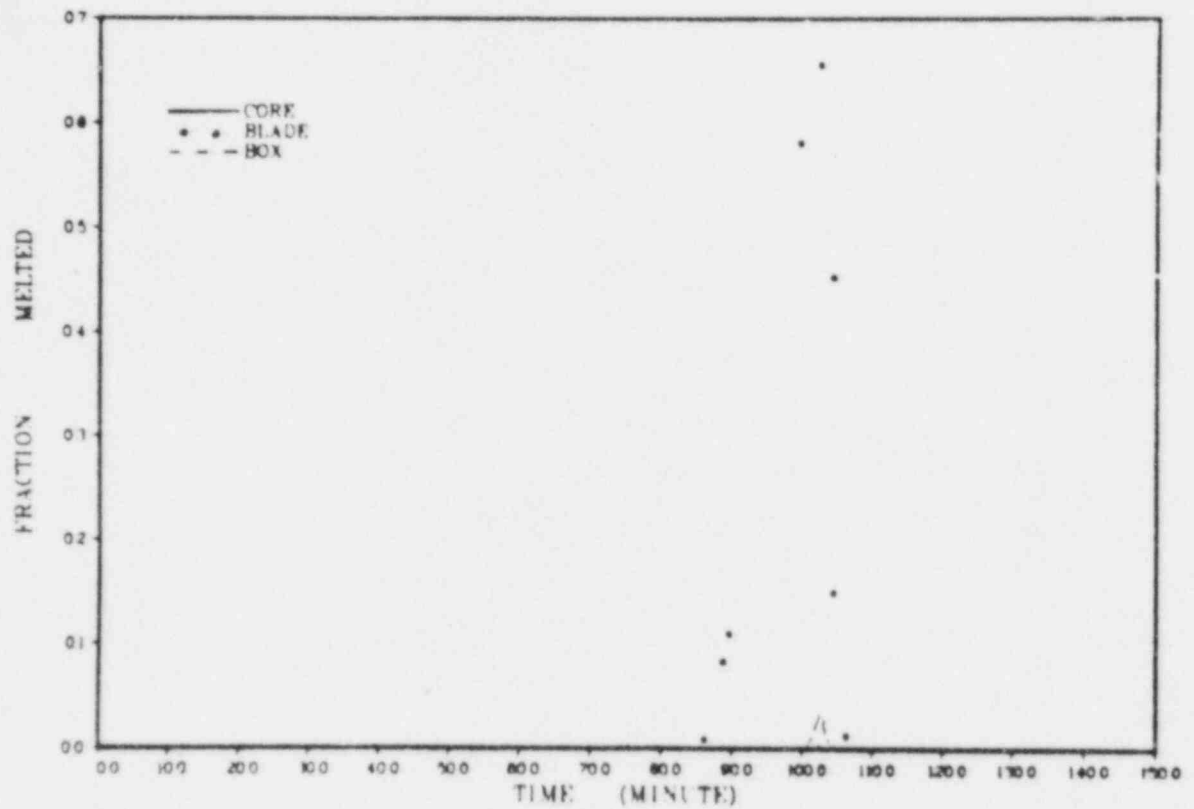
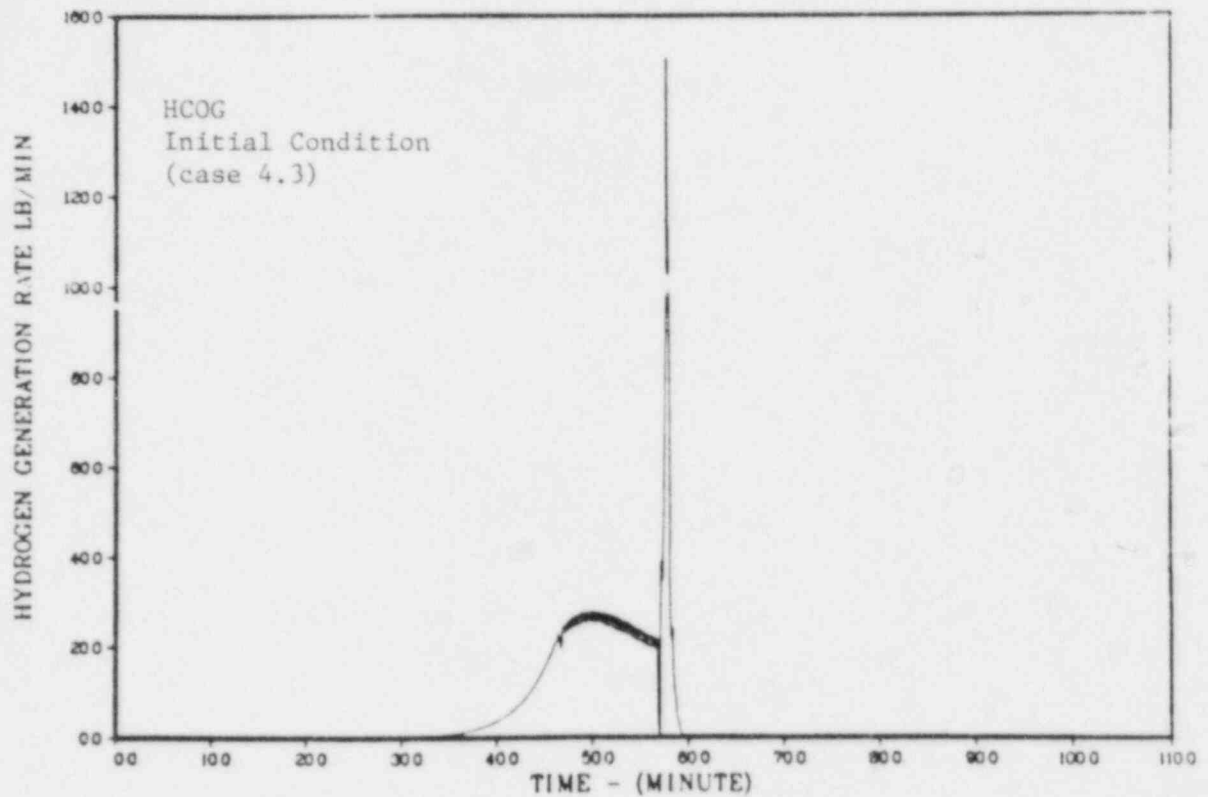


Figure 6.18 Melt fraction and oxidation fraction for case 6.3.

5000GPM AT 56.7 GG POWER 10 NODES ADS(8) AT 5



5000GPM AT 100 ADS(18) AT 57.58.35

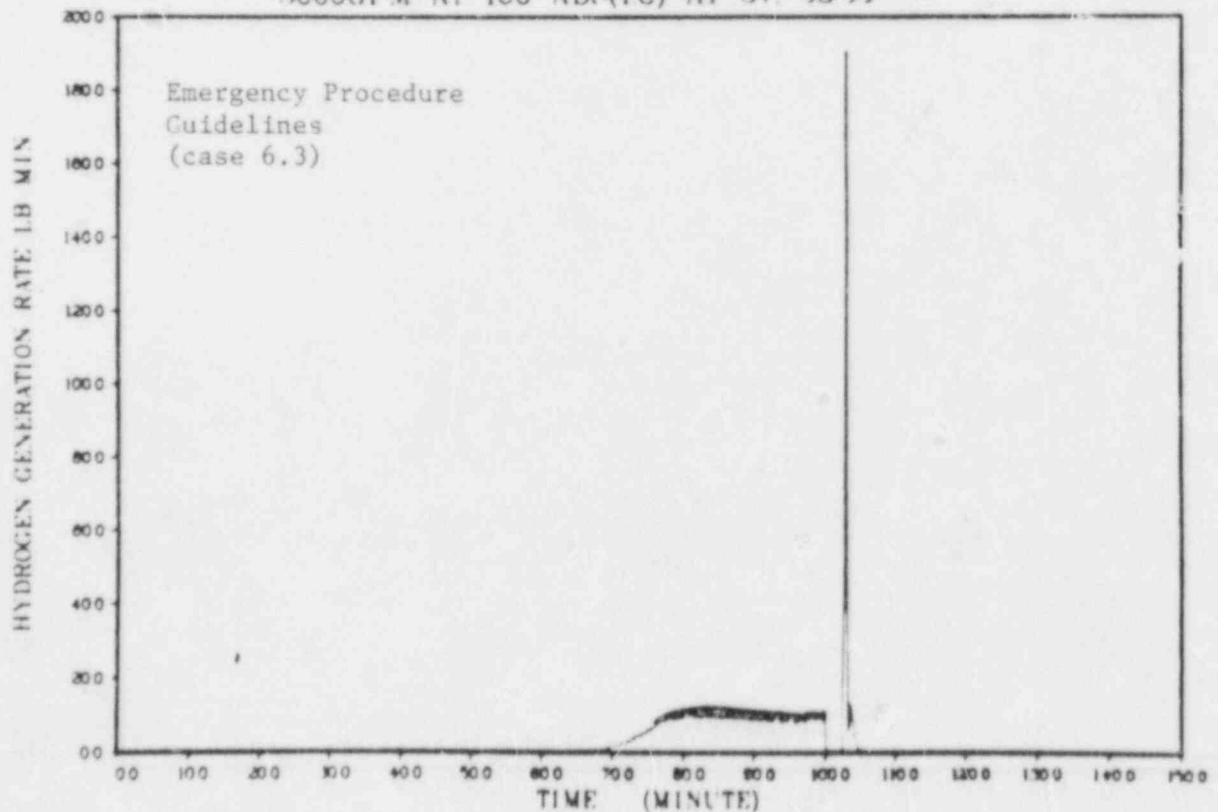


Figure 6.19 Comparison of hydrogen generation rate for case 6.3.

## 7. SCDAP/MARCH2 COMPARISON

A MARCH analysis was performed to compare the SCDAP predictions of hydrogen production during a reactor core heatup transient from 2000 seconds to 8000 seconds. A BWR 8x8 fuel bundle was considered. The initial and boundary conditions imposed on MARCH analysis are these used in a SCDAP analysis performed independently by L. Seifken of EG&G (refer to Appendix C).

### 7.1 Initial and Boundary Conditions

The initial and boundary conditions used in the SCDAP analysis are given in Appendix C, which includes the characteristics of the BWR 8x8 fuel bundle, axial and radial power distribution, bundle power history, bundle inlet mass flow rate history, and the initial axial temperature distribution, etc. An attempt was made to use these conditions in the MARCH analysis. However, due to differences in the modeling and construction of the two codes, not all the boundary and initial conditions in the SCDAP analysis were exactly matched in the MARCH analysis. The specifications of the fuel bundle and the axial power distribution described in Appendix C were used as input parameters for the MARCH code. The SCDAP code divides the 62 fuel pins in the 8x8 bundle into three radial components as shown below:

Component	No. of Pins	Radial Power Factor	Deviation from Average Power
1	14	0.9869	-1.3%
2	20	0.9937	-0.6%
3	28	1.0111	+1.1%

Since the MARCH code does not provide for a radial power variation within a fuel assembly, the above radial power distribution could not be modeled in the MARCH analysis. A radial power factor of 1.0 was therefore assumed for the 62 pins in the MARCH analysis.

The SCDAP analysis used a time-dependent inlet mass flow rate. The mass flow rate was approximated in MARCH by two liner equations as shown in Figure 7.1. The MARCH code was updated to include these equations as a time-dependent boundary condition. The fuel bundle power history was also closely approximated as illustrated in Figure 7.2. In the SCDAP analysis, the coolant pressure had a constant value of 7.56 MPa (1096 psi) during the entire transient. In the MARCH calculation, the coolant pressure varies from 1092 psia to 1097 psia depending on the transient steam mass within the reactor vessel. The initial two-phase level is 3.2 ft (0.98 in) in the SCDAP analysis and 3.4 ft in the MARCH analysis. Differences between the above boundary and initial conditions for the two codes are small and did not cause any significant impact on the predicted overall hydrogen production.

In Appendix C, an initial axial temperature distribution is specified for the SCDAP analysis. The bottom three nodes in the water covered region are assumed to be at the saturation temperature (564°K or 555°F) corresponding to 1096 psia. In the MARCH code, no cladding surface temperature is provided. The cladding and pellet are lumped together and a volume average fuel temperature is computed by the MARCH code. The initial axial temperature distribution predicted by the MARCH code is compared with the input temperatures of the SCDAP code in Table 7.1. The MARCH predicted channel box temperature and gas temperature are also included in Table 7.1 for reference.

## 7.2 MARCH Analysis

In the SCDAP analysis, only a single 8x8 fuel bundle enclosed in a canister is modeled. The initial mass of water in the bundle is 7.28 Kg. The same approach, namely, a single fuel bundle, was attempted in our MARCH analysis. However, it was found that the MARCH code exhibits an instability problem. The MARCH code is not able to analyze a single bundle containing only 7.28 Kg of water. The MARCH code was developed to include the entire primary system which contains several hundred fuel assemblies, reactor vessel internals, the steam generator and other structures in the primary system. It therefore performs an overall energy and mass balance in the primary system involving a large amount of structural material and water. In our attempt to perform the MARCH analysis, we have tried to reduce the primary system by a factor of 800 so that a single fuel bundle in the core region could be modeled. The original Grand Gulf input data is based on 800 fuel assemblies. Apparently, the reduced primary system with a single fuel assembly in the core region could not satisfy the overall energy and mass balance. Using different time-steps and other options in the code did not improve the stability of the results. Thus, this approach was not used in this study.

The second approach used the basic primary system data but made all of the 800 fuel assemblies identical to the single assembly used in the SCDAP analysis. Since the 800 fuel assemblies are identical to each other, there is no inter-assembly heat and mass transfer. Each assembly is therefore representative of the assembly analyzed in the SCDAP study. No instability was encountered using this approach and hence a complete MARCH analysis was performed.

In the SCDAP analysis, the control blade is not modeled. Only half the thickness of the canister wall is considered. The oxidation of the inner surface is counted twice to include the effect of oxidation on the outer surface of the canister wall. In the MARCH code, the control blade is coupled with the canister through radiation and convection heat transfer. The control blade is an integral part of the BWR fuel assembly heat balance and cannot be separated from the code. However, two steps were taken to reduce the impact of the presence of the control blade on total hydrogen production. First, the radiation view factor between the canister and control blade is taken as  $10^{-6}$  (FBXCB = 1.0E-6). This step practically eliminates the direct heat exchange between the canister wall and the control blade. The presence of the control blade will have no direct effect on temperature of the canister wall. Second, the option of steel/steam reaction is not used (IMWCB = 0). Thus, the control blade does not contribute to the total hydrogen production and does not consume any steam available in the interstitial region. It is believed

that the two steps are sufficient to eliminate the influence of the control blade on canister hydrogen production.

### 7.3 Results

The MARCH predicted primary system pressure, water-steam mixture level and the coolant injection rate are shown in Figures 7.3 to 7.5. Results are comparable to the SCDAP analysis. The core temperature is given in Figure 7.6. Due to the use of the cut-off temperature (3860 F) and the early injection of cooling water, the maximum core temperature is maintained below the melting temperature (4130°F) and no core melting is predicted. Figure 7.6 reveals a slower temperature rise between 70 minutes and 110 minutes during the transient. Inspection of MARCH computed results indicates that this is caused by an increase of heat removal from fuel rod to gases by convection during this period. Figures 7.7 and 7.8 show the fraction of Zr reacted and the fraction of channel box melted. Note that during the period of 70 to 110 minutes, the oxidation rate is considerably slower. The MARCH predicted hydrogen generation based on 800 fuel bundles are shown in Figures 7.9 to 7.10. The amount of hydrogen produced per bundle is comparable with that of SCDAP analysis. The results indicate that the MARCH predictions are comparable to that of SCDAP. However, the comparison is limited by the single case provided through private communication with L. Seifken of EG&G on February 1st and 14th of 1985. It is suggested to perform more comparisons with various initial and boundary conditions. The comparisons are summarized below:

	<u>MARCH</u>	<u>SCDAP</u>
Fraction of clad reacted	28%	29%
Fraction of canister reacted	15%	9%
Total hydrogen production, Kg	0.83	0.75
First peak of hydrogen production rate, Kg/s	0.0013	0.0012
at time, second	3600	3000

Table 7.1 SCDAP and MARCH Initial Axial Temperature Distributions  
(Time = 2000 seconds)

Axial <sup>1</sup> Node	SCDAP Cladding <sup>2</sup> (°F)	MARCH		
		Fuel <sup>3</sup> (°F)	Water/Steam (°F)	Channel Box (°F)
1	555	680	555	555
2	555	728	555	555
3	555	734	555	555
4	656	836	674	591
5	798	955	824	659
6	915	1032	943	744
7	978	1087	1022	823
8	1129	1114	1064	881
9	1212	1101	1066	906
10	1221	1009	1004	878

<sup>1</sup>Axial nodes 1, 2, and 3 are in water covered region.

<sup>2</sup>Surface temperature.

<sup>3</sup>Fuel volume average temperature.

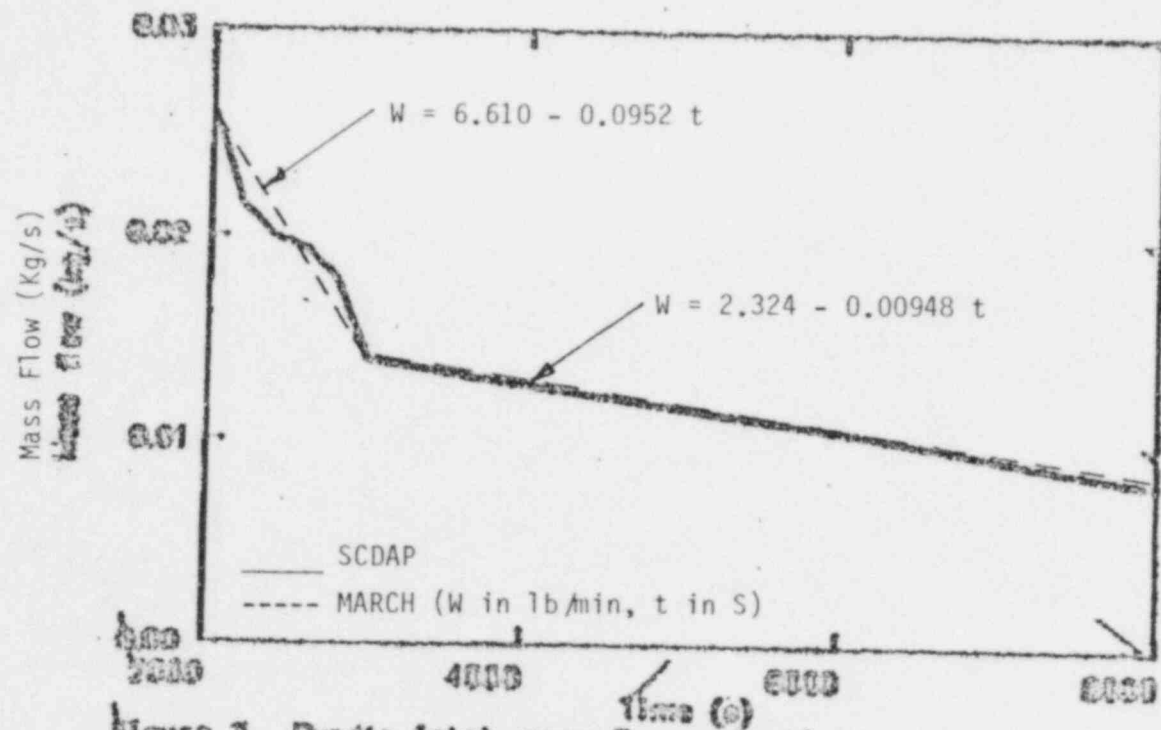


Figure 3. Bundle inlet mass flow rate history.

Figure 7.1 SCDAP bundle inlet mass flow rate.



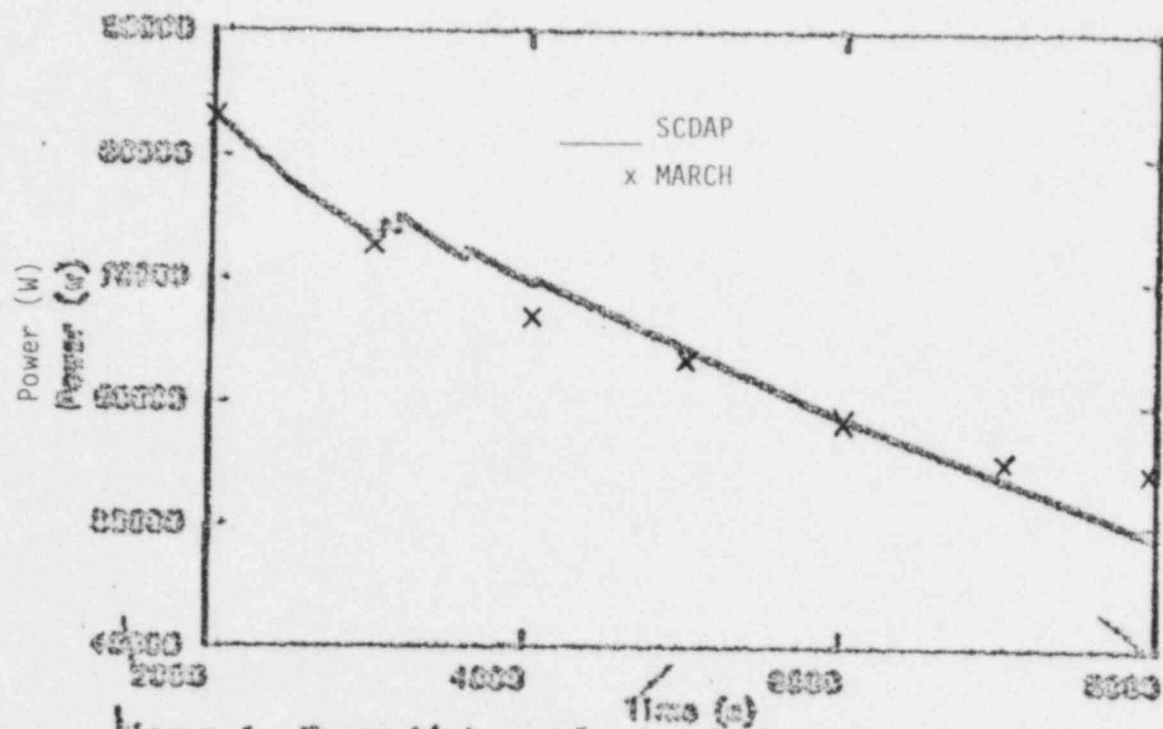


Figure 4. Power history of a hot fuel bundle.

Figure 7.2 SCDAP power history of a fuel bundle.

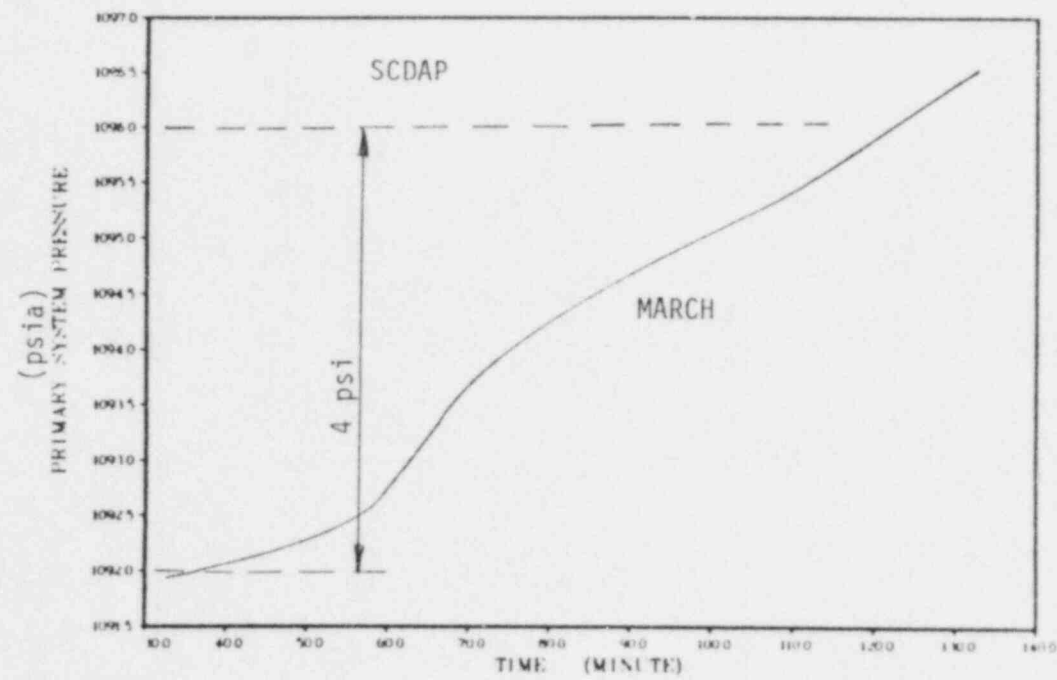


Figure 7.3 SCDAP/MARCH2 comparison: primary system pressure.

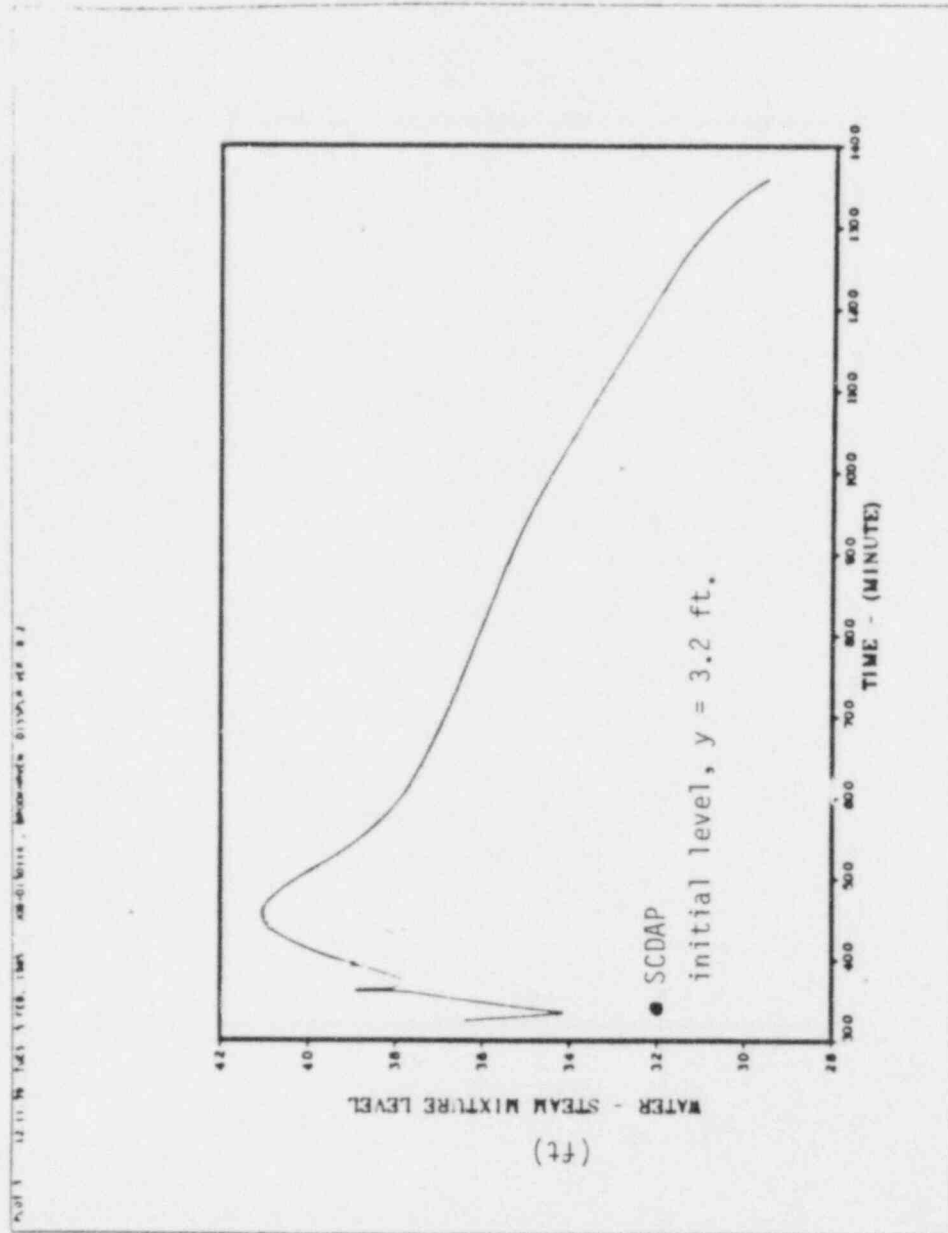


Figure 7.4 SCDAP/MARCH2 comparison: steam-water mixture level.

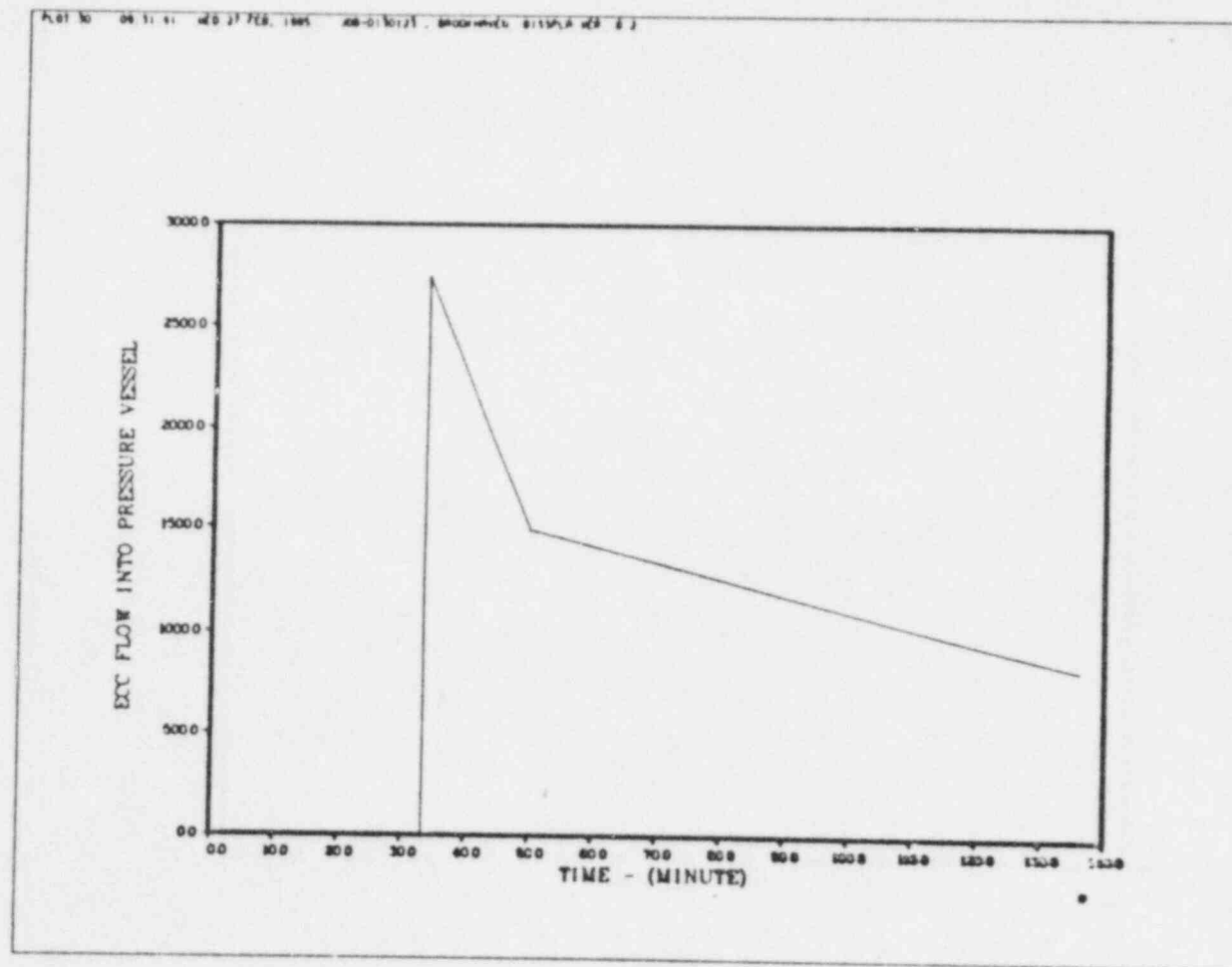
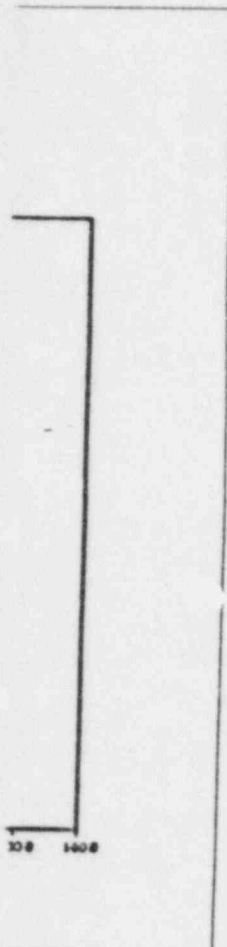


Figure 7.5 MARCH2 prediction: coolant injection rate for 800 bundles.

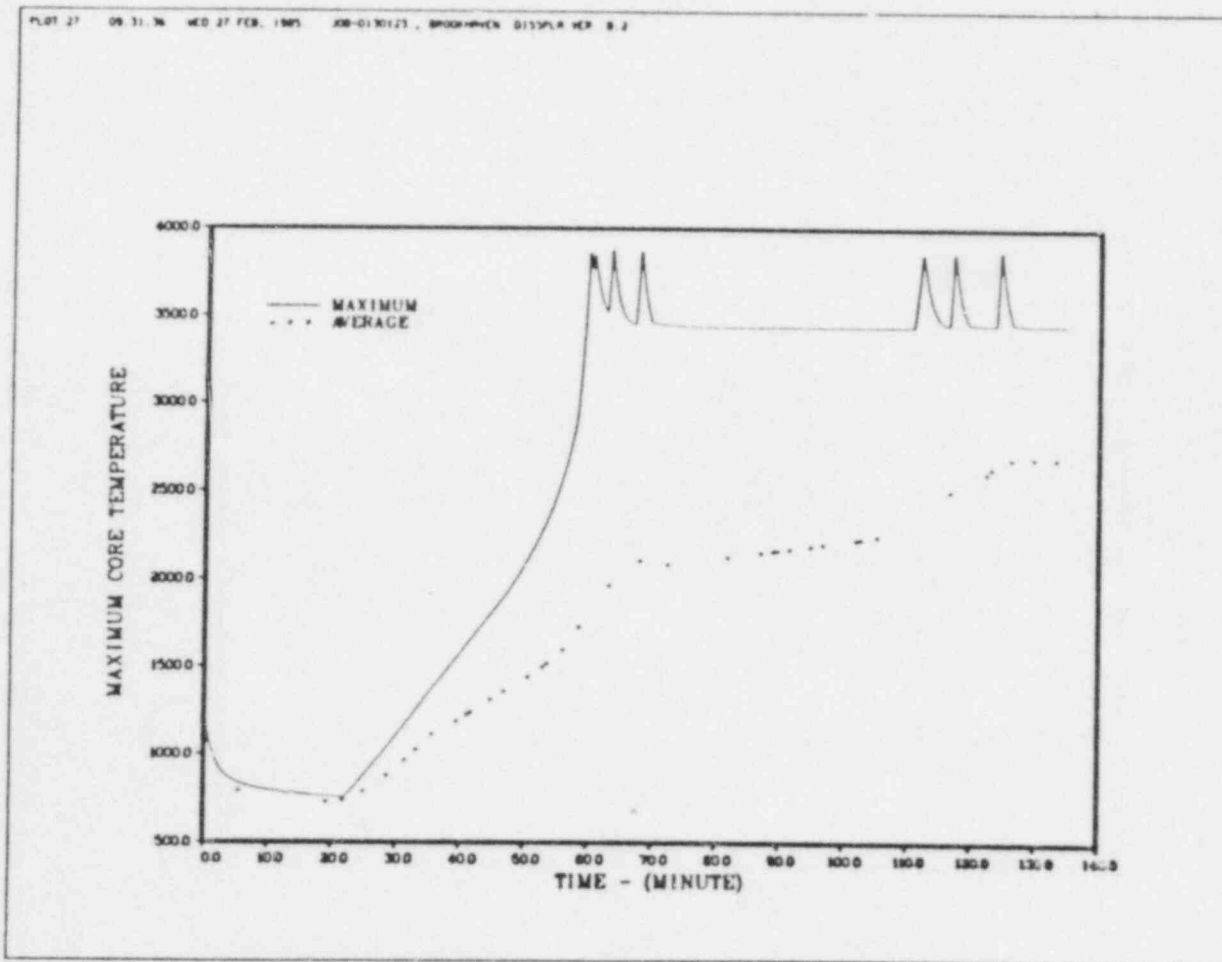


Figure 7.6 MARCH2 prediction: fuel temperature.

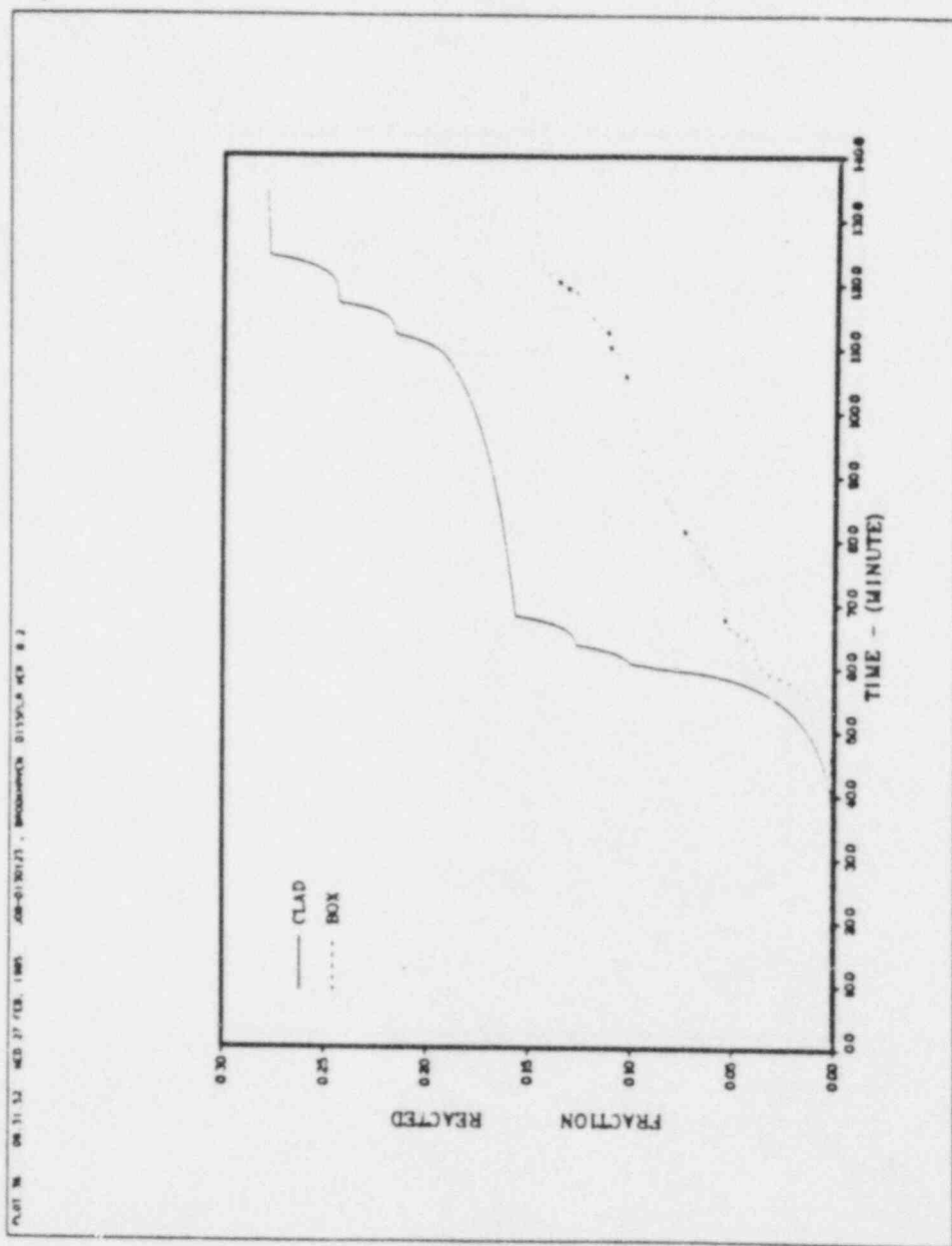


Figure 7.7 MARCH2 prediction: fraction of Zr reacted.

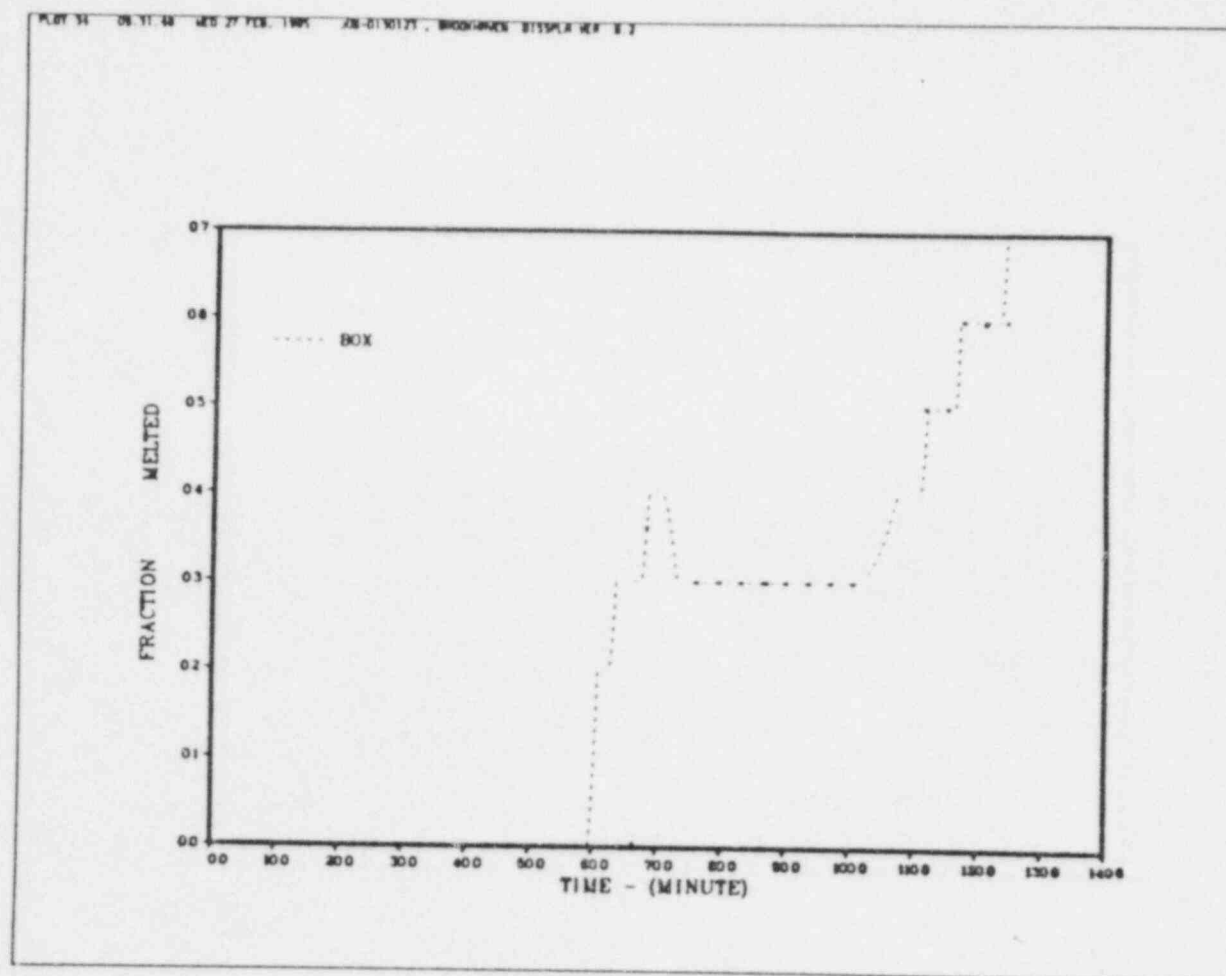


Figure 7.8 MARCH2 prediction: fraction of channel box melted.

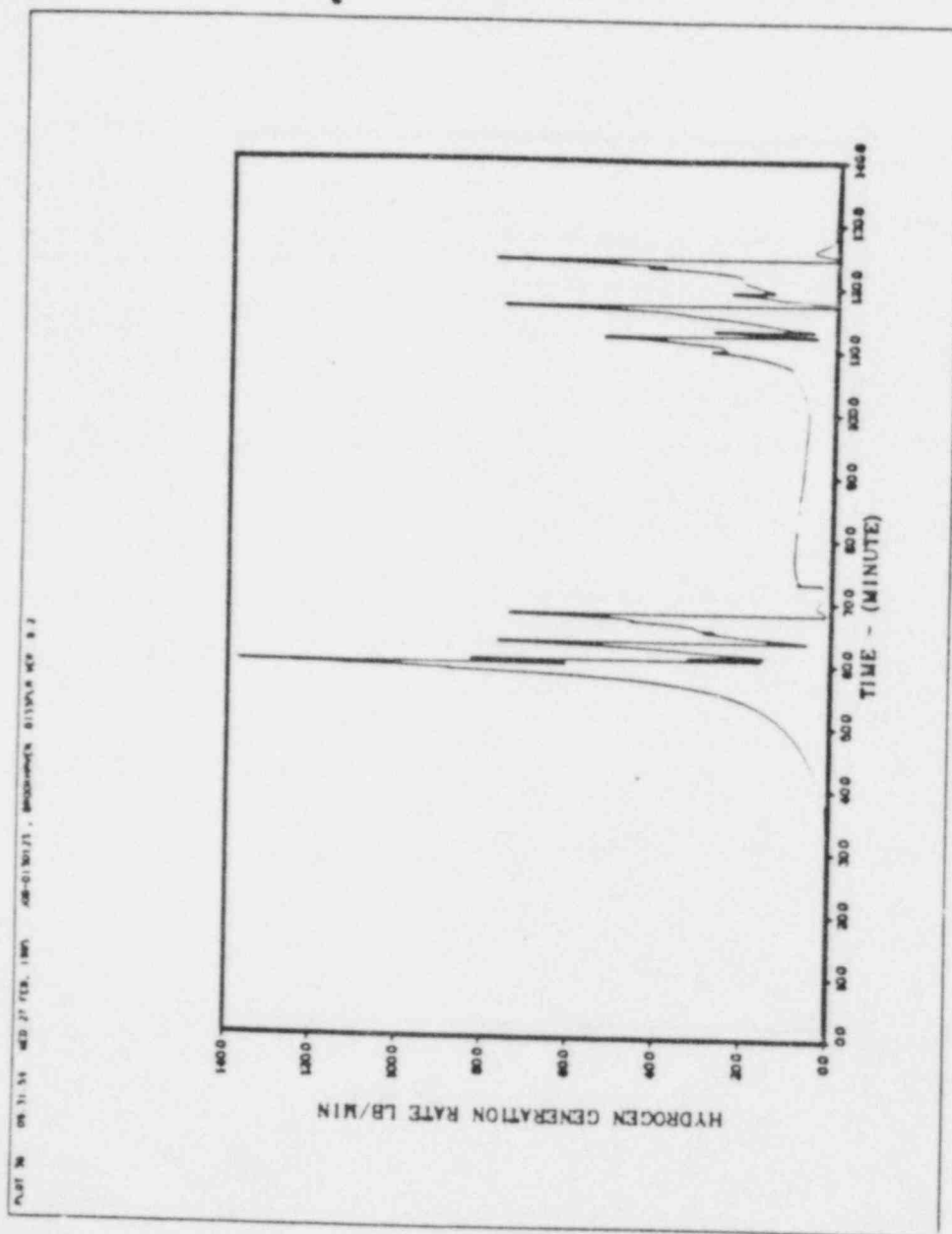
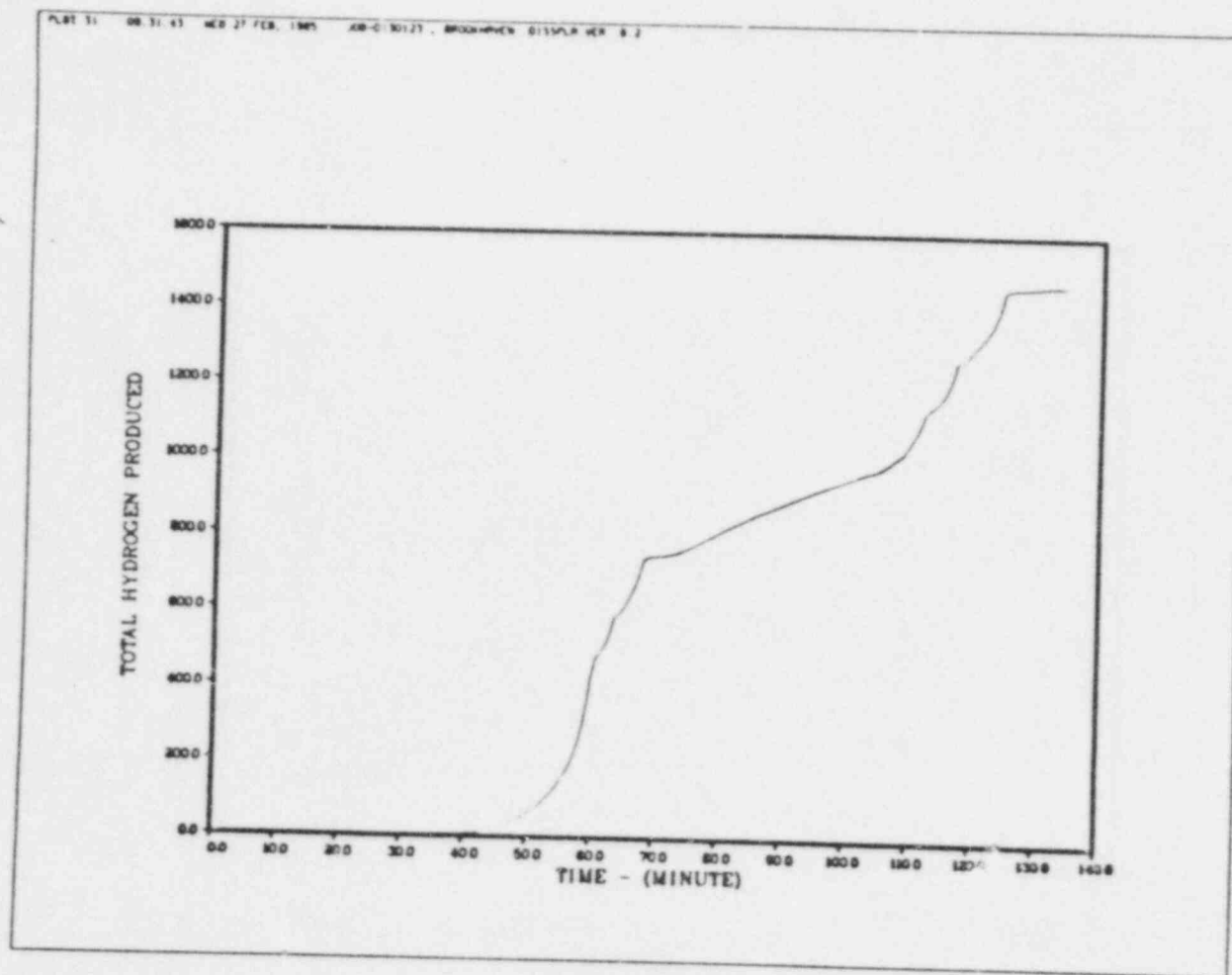


Figure 7.9 MARCH2 prediction: hydrogen generation rate for 800 bundles.





7-10  
Figure 7.10 MARCH2 prediction: total hydrogen production from 800 bundles.

## 8. ORNL MARCH-BWR/MARCH 2 COMPARISON

During the recent years, development of BWR models has been made at the Oak Ridge National Laboratory (ORNL) to support their SASA program. These models have been incorporated into the ORNL version of the MARCH1.1 code. The most important models related to the BWR hydrogen generation are the improvement in the depressurization algorithm, the separation of fuel and cladding, and the separation of the reactor vessel water inventory into a core region, lower plenum region, and a downcomer region. These models are not available in the current MARCH2 (Version 151) code used for the present analysis.

At the request of NRC staff, S. A. Hodge and L. J. Ott of ORNL analyzed two cases using the ORNL MARCH-BWR code. Similar analyses were also performed using the MARCH2 (Version 151) code for comparison purpose. In the first case, the 300 gpm CRDHS hydraulic system injection started at 62 minutes, and in the second case 43.3 minutes. The temperature of the injected coolant was assumed at 210°F for the entire transient. In both cases, ADS was initiated at 10 minutes to yield the similar initial conditions of the core heatup period. The ORNL MARCH-BWR code predicted initial conditions are:

Time, min	21.6	24.9
Reactor pressure, psia	43	30
Water/steam mixture level, ft	2.8	1.9
Average core temperature, °F	566	741

Comparison with the initial conditions predicted by the MARCH2 (Version 151) code (Table 4.1) shows a slower depressurization predicted by the ORNL code. The vessel pressure is reduced to 43 psia at 21.6 minutes which about five minutes later than that predicted by the MARCH2 code. It is noted that after depressurization to 30 psia, the water/steam mixture level is about 1.9 ft above the bottom of the core as predicted by the ORNL code and is 0.5 ft below the core region by the MARCH2 code. The ORNL models which are based on the MARCH1.1 code do not permit the reactor vessel water level drop beneath the lowest axial node as the heat transfer from a partially uncovered node into the surrounding water is neglected. The difference on the treatment of water level by the two codes has certain effect on core reflood which will be discussed later.

For the first case in which the coolant injection started at 62 minutes, the ORNL analysis terminated the transient at 78 minutes. The predicted results during this period are shown in Figures 8.1 to 8.6. It is noted in Figure 8.2 that the ORNL code does not yield the large oscillation of water level and vessel pressure as predicted by the MARCH2 code. This is probably related to the treatment of water level and the safety/relief valve actuation effects. The oxidation of cladding, channel box and control blade are illustrated in Figures 8.3 to 8.4. Detailed comparisons with the MARCH analysis are shown in Table 8.1. It is interesting to recognize the good agreement between the oxidation of cladding predicted by the two codes. There is also a good agreement on the oxidation of channel box prior to 78 minutes. At 78 minutes, the MARCH2 predicted oxidation of channel box is about three times higher than that by the ORNL code. This is caused by the refreezing of channel box when the core is reflooded according to the options used in the MARCH analysis. Table 8.1 indicates that the MARCH2 predicted fraction of channel box melted is reduced from 56% at 74 minutes to 0.06% at 78 minutes (Figure

6.8). The refreezing of channel box causes the re-start of the metal/steam reaction. Consequently, an additional 210 pounds of hydrogen is produced from the channel box at the end of 78 minutes as shown in Table 8.1. For the ORNL analysis, 75% of the channel box and 24% of cladding are melted at 78 minutes. The water level is about 2.6 ft in the core region at that time. In the event of continued reflooding, the refreezing of these large fractions of molten channel box and cladding would produce a large amount of hydrogen. However, the ORNL computation was not carried beyond 78 minutes to the completion of core recovery.

The second case analyzed at ORNL is similar to the first case, but with an early injection of coolant at 43.3 minutes. It is expected to have an early core recovery and less core damage in this case. The ORNL predicted results are shown in Figures 8.7 to 8.12. Detailed comparison of oxidation and melting are shown in Table 8.2. Again, there is a good agreement of the cladding oxidation predicted by the two codes as shown in Table 8.2. However, the MARCH2 predicted oxidation of channel box is much higher than that predicted by the ORNL code. This is caused by the predictions of core melt. In the ORNL analysis, a total of 52% of channel box is melted at the end of 88 minutes and is not available for oxidation. The ORNL code computes a rapid heating of the channel box during the transient. In the MARCH2 analysis, only 3.1% of channel box is melted between 52 minutes and 58 minutes. The early injection of coolant assumed in this case apparently reduces the melting of cladding and channel box significantly. The MARCH2 calculation indicates that the channel box temperature lies approximately between 2000°F to 3360°F (except the few molten nodes). The availability of hot surface area enhances the oxidation reaction and generates 954 pounds of hydrogen from the channel box alone (Table 8.2). On the contrary, only 135 pounds of hydrogen from the channel box is predicted by the ORNL code, as a large portion of channel box is melted and is not available for oxidation.

Based on the studies of the two cases discussed in this section, it is suggested that:

- (1) The assumption of termination of oxidation at melting and re-start of oxidation at refreezing should be critically examined;
- (2) the MARCH computation of channel box temperature should be reviewed;
- (3) the MARCH treatment of water level, refreezing of molten nodes, etc. should be reviewed.
- (4) ORNL modifications based on the MARCH2 (Version 151) be developed.

Table 8.1 Comparison of ORNL Case 1 with MARCH2 Prediction

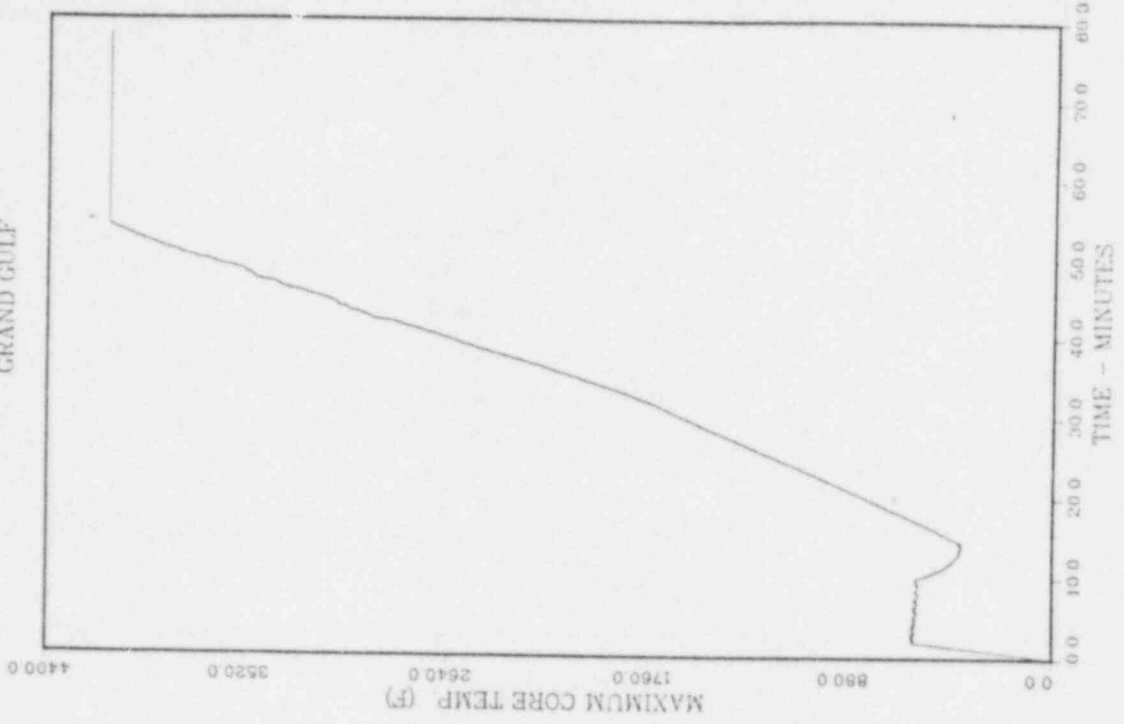
Time (min)	ORNL MARCH-BWR			MARCH2 (Version 151)		
	Clad	Channel Box	Control Blade	Clad	Channel Box	Control Blade
	% of Melt					
50	0	12	33	0	0	55
60	6	46	62	0	36	75
70	27	72	74	4	63	86
74	27	75	76	5	56	80
78	24	74	75	0	0.06	100
	% of oxidation					
50	6	1.7	0.03	7	2.0	0.6
60	11	2.8	0.09	9	2.8	0.7
70	17	3.8	0.2	12	3.4	0.9
74	18	4.0	0.2	14	4.0	1
78	20	4.0	0.2	20	11.0	2
H <sub>2</sub> , lb	736	120	1	736	330	11

Table 8.2 Comparison of ORNL Case 2 with MARCH2 Prediction

Time (min)	ORNL MARCH-BWR			MARCH2 (Version 151)		
	Clad	Channel Box	Control Blade	Clad	Channel Box	Control Blade
	% of Melt					
50	0	27	33	0	0	54
60	6.4	49	52	0	0*	87
70	4.8	52	56	0	0	95
80	1.2	52	55	0	0	96
88	0.2	52	55	0	0	100
	% of oxidation					
50	8.9	2.6	0.1	6.4	2	0.6
60	15	4.0	0.4	22	11	2.5
70	19	4.4	0.5	25	23	3.1
80	23	4.5	0.6	28	29	3.3
88	27	4.5	0.6	30	32	3.3
H <sub>2</sub> , lb	983	13 <sup>b</sup>	3	1119	954	18

\*MARCH2 (Version 151) predicted a maximum of 3.1% of channel box melt between 52 minutes and 58 minutes.

TQUV  
WITH 300 GPM INJECTION  
GRAND GULF



TQUV  
WITH 300 GPM INJECTION  
GRAND GULF

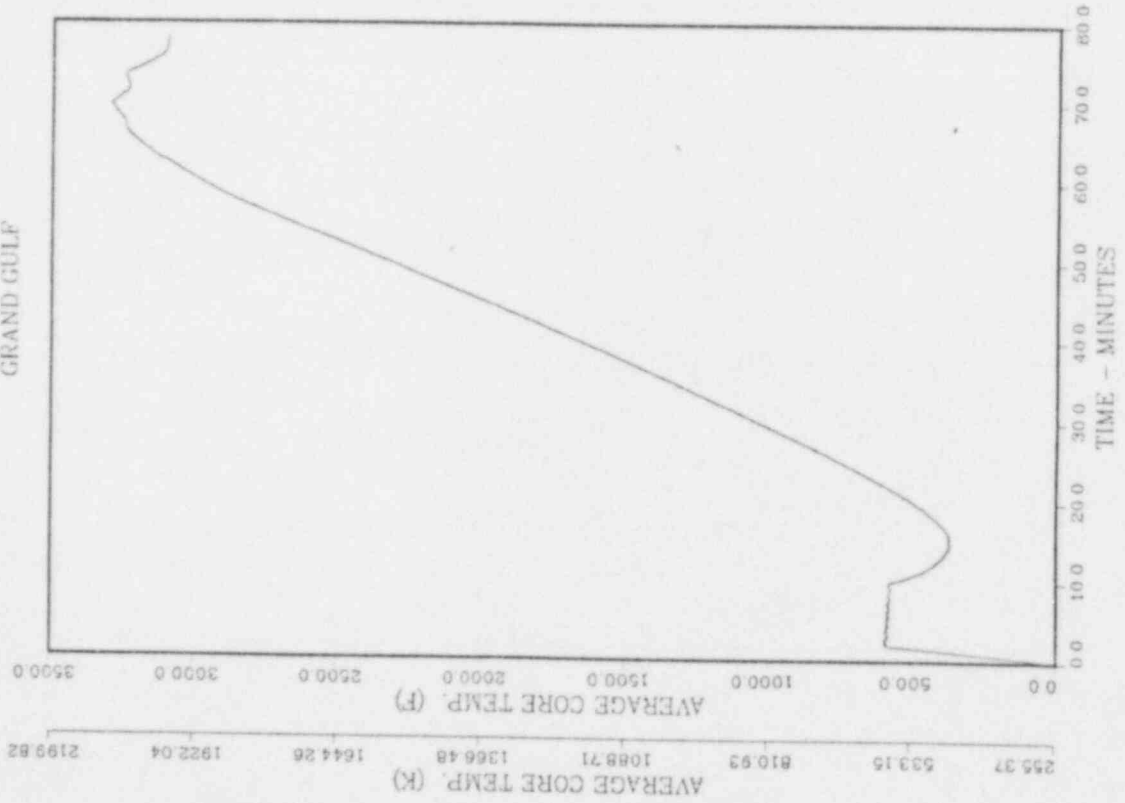
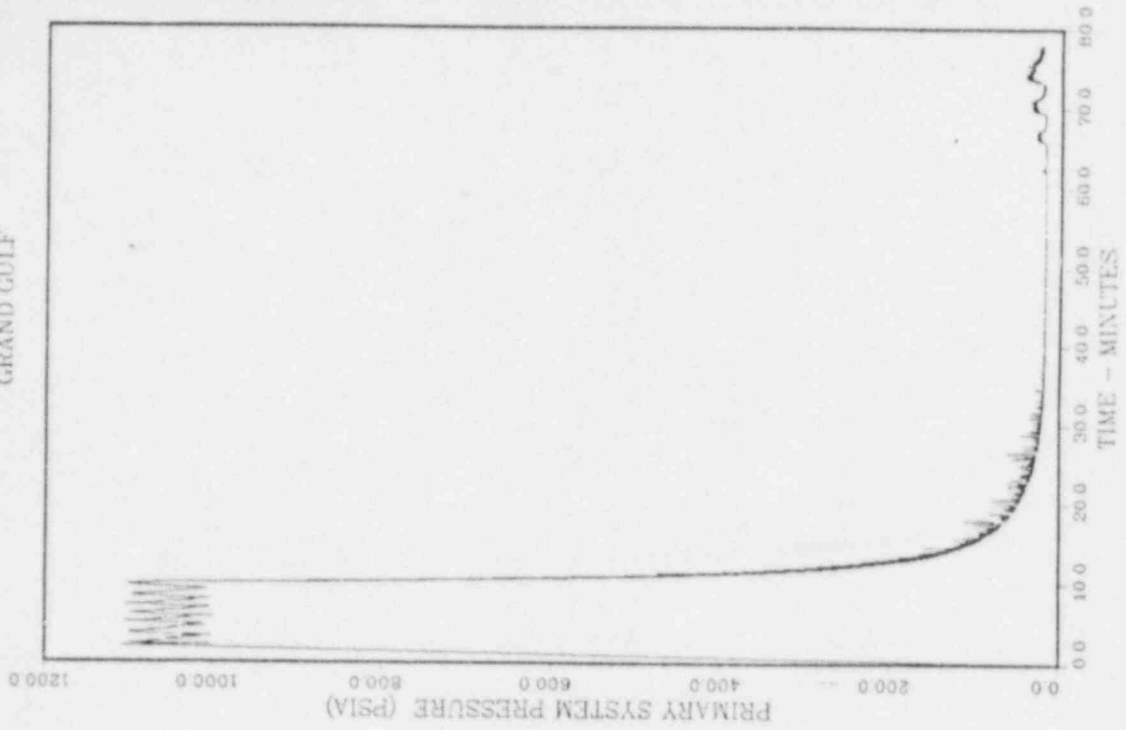


Figure 8.1 ORNL Case 1: core temperature.

TQUV  
WITH 300 GPM INJECTION  
GRAND GULF



TQUV  
WITH 300 GPM INJECTION  
GRAND GULF

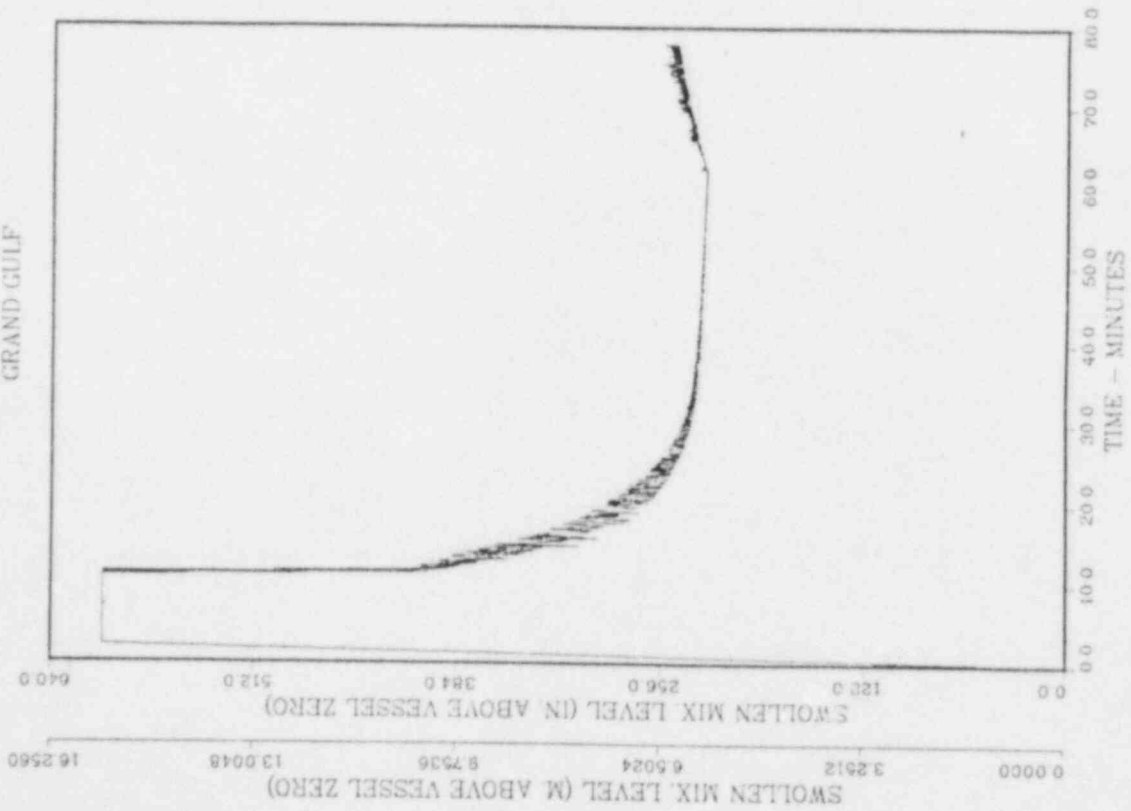


Figure 8.2 ORNL Case 1: swollen mixture level and primary system pressure.

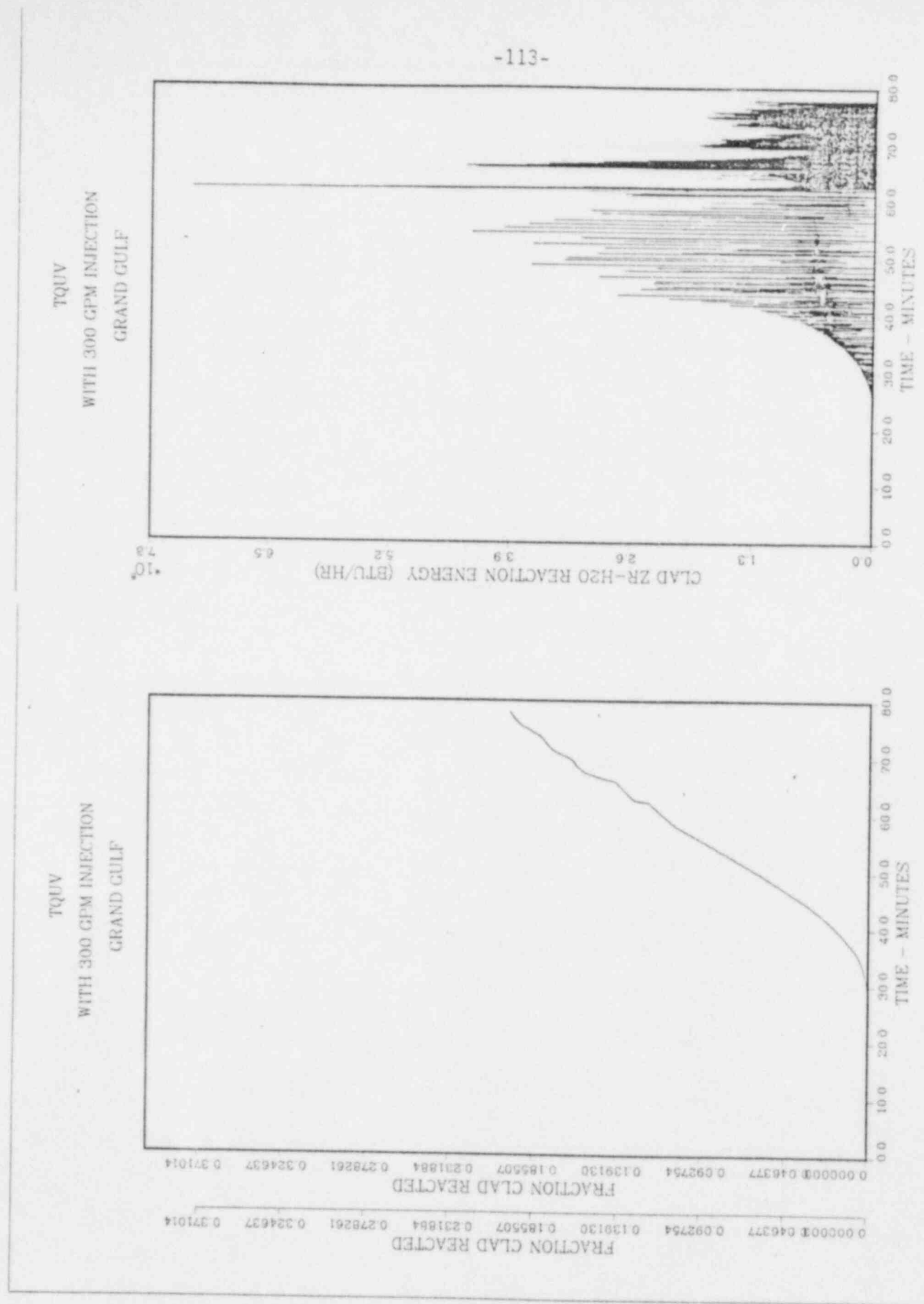
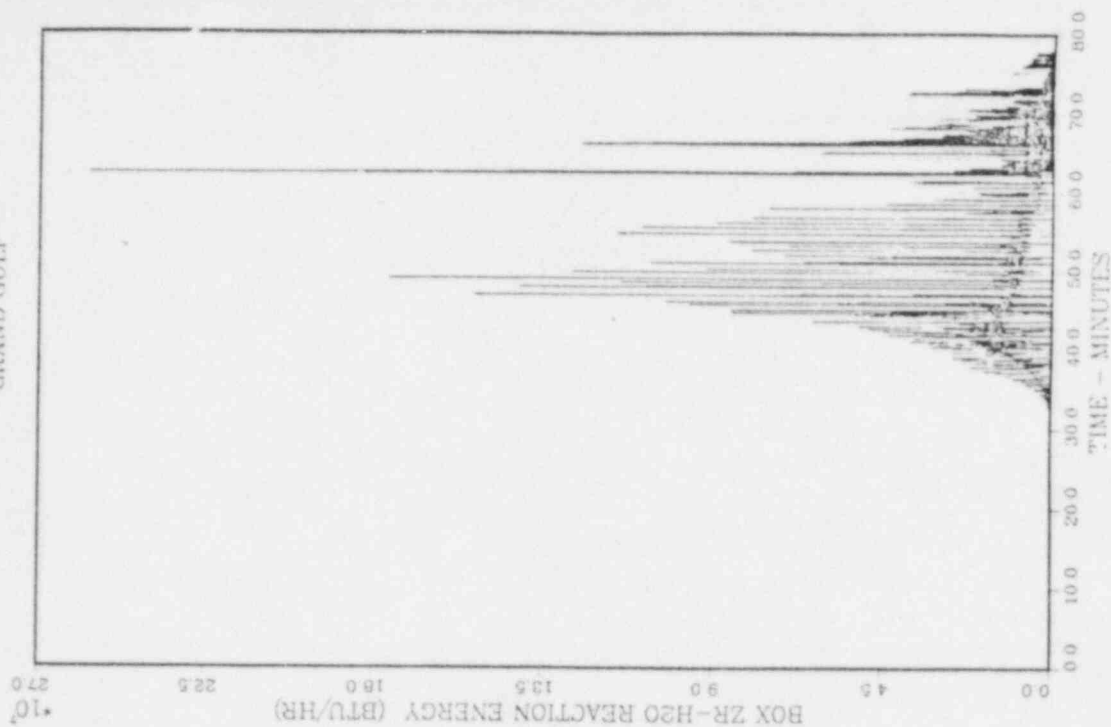


Figure 8.3 ORNL Case 1: clad oxidation.



TQUV  
WITH 300 GPM INJECTION  
GRAND GULF



TQUV  
WITH 300 GPM INJECTION  
GRAND GULF

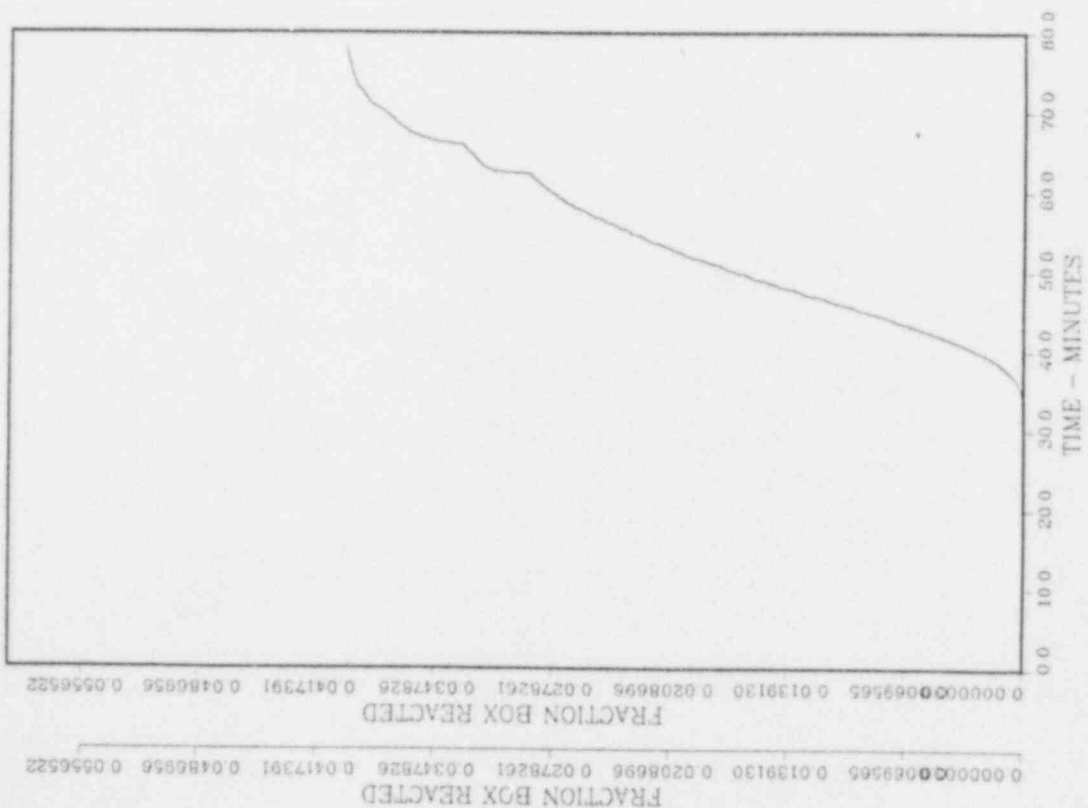


Figure 8.4 ORNL Case 1: Channel box oxidation.

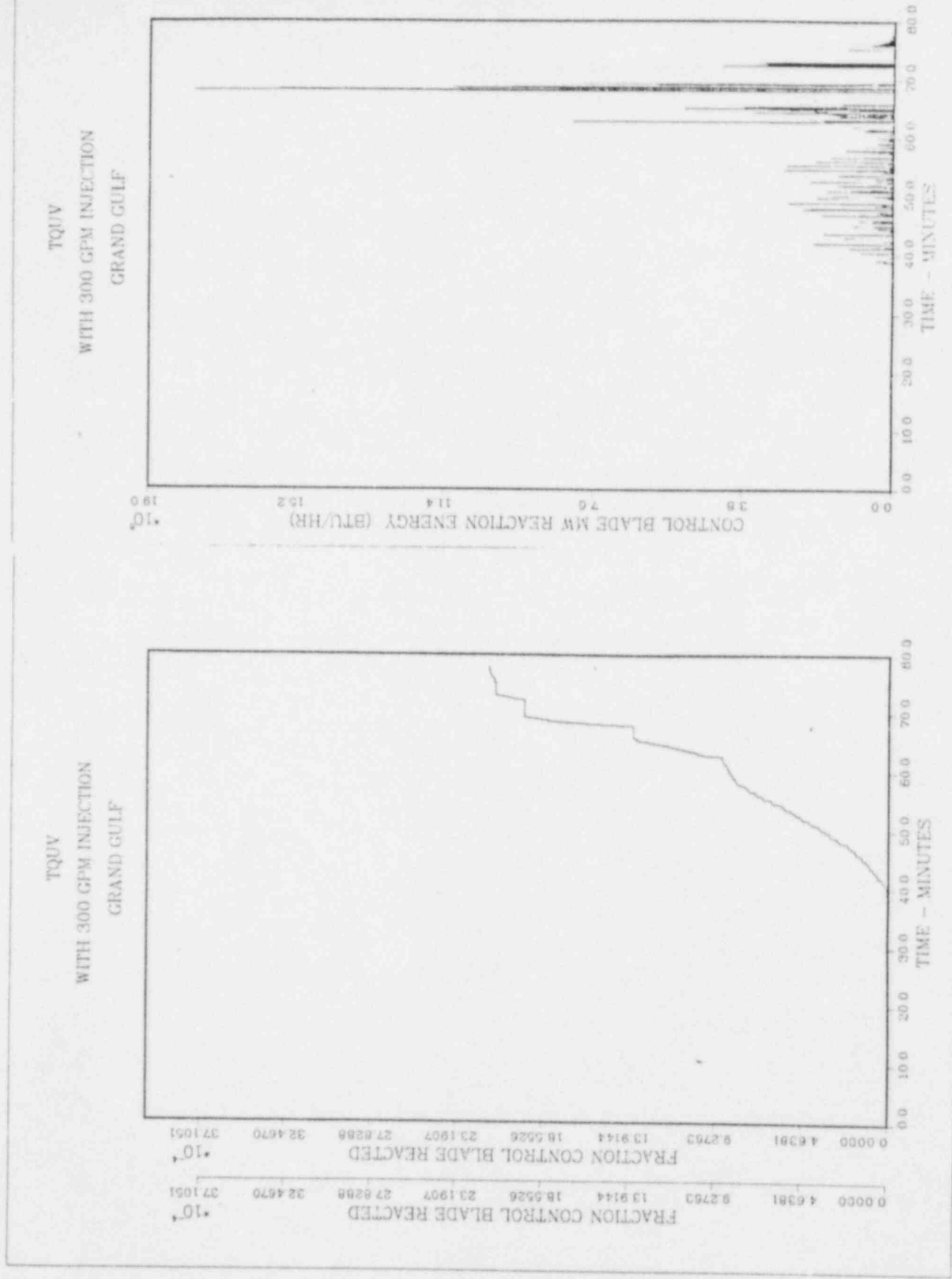
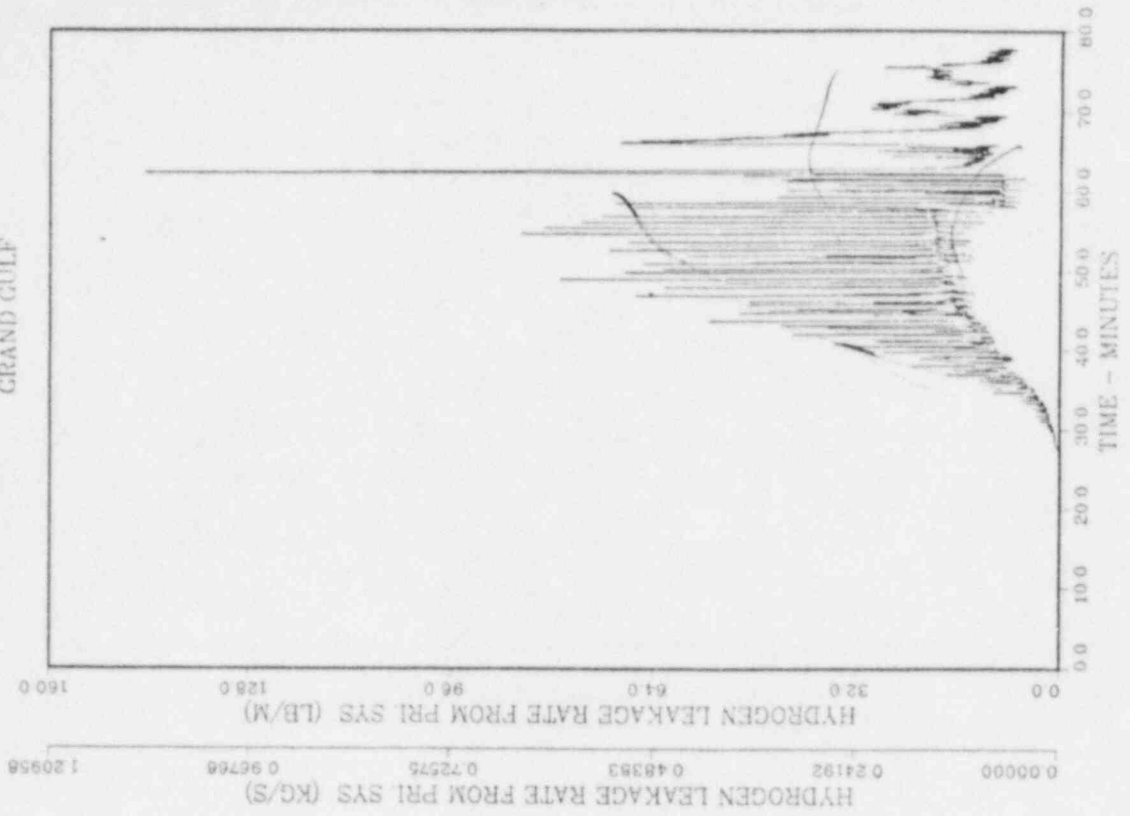


Figure 8.5 ORNL Case 1: control blade oxidation.

TQUV  
WITH 300 GPM INJECTION  
GRAND GULF



TQUV  
WITH 300 GPM INJECTION  
GRAND GULF

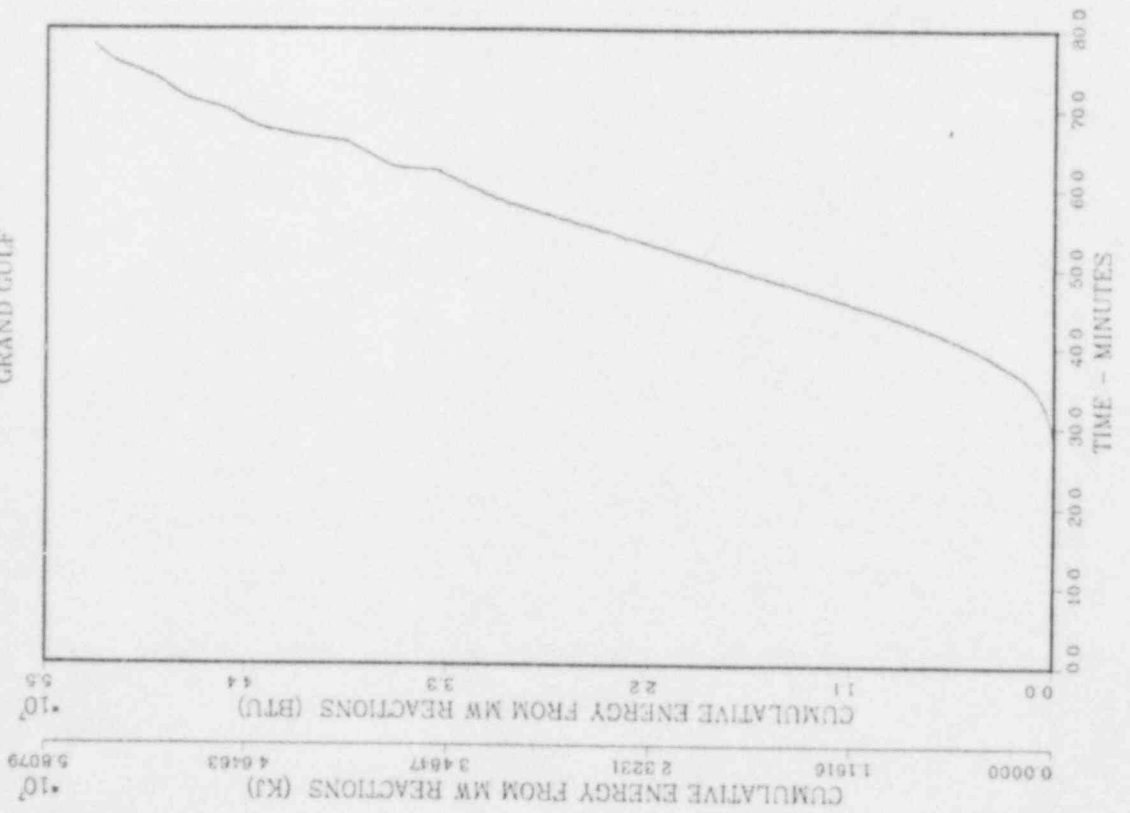


Figure 8.6 ORNL Case 1: hydrogen generation.

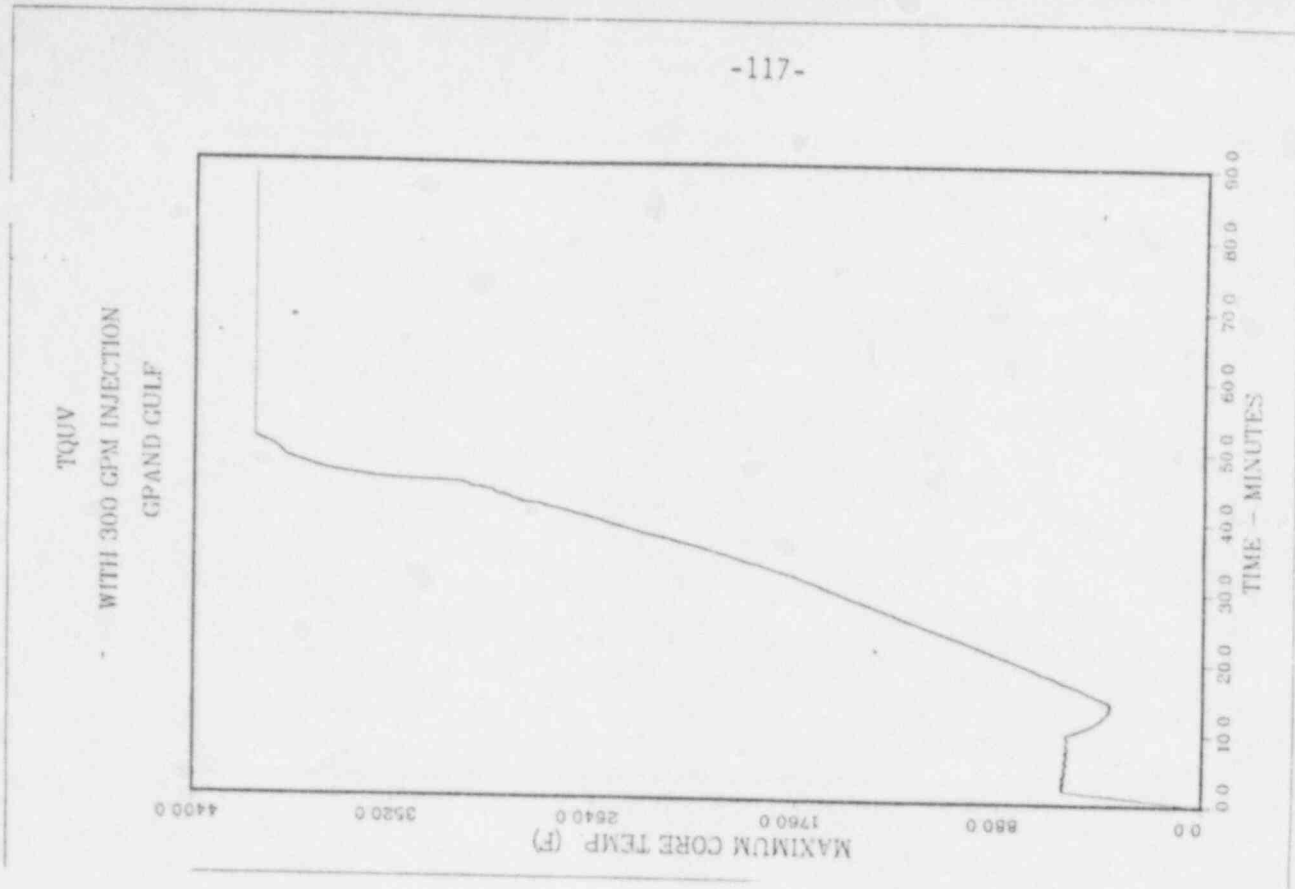
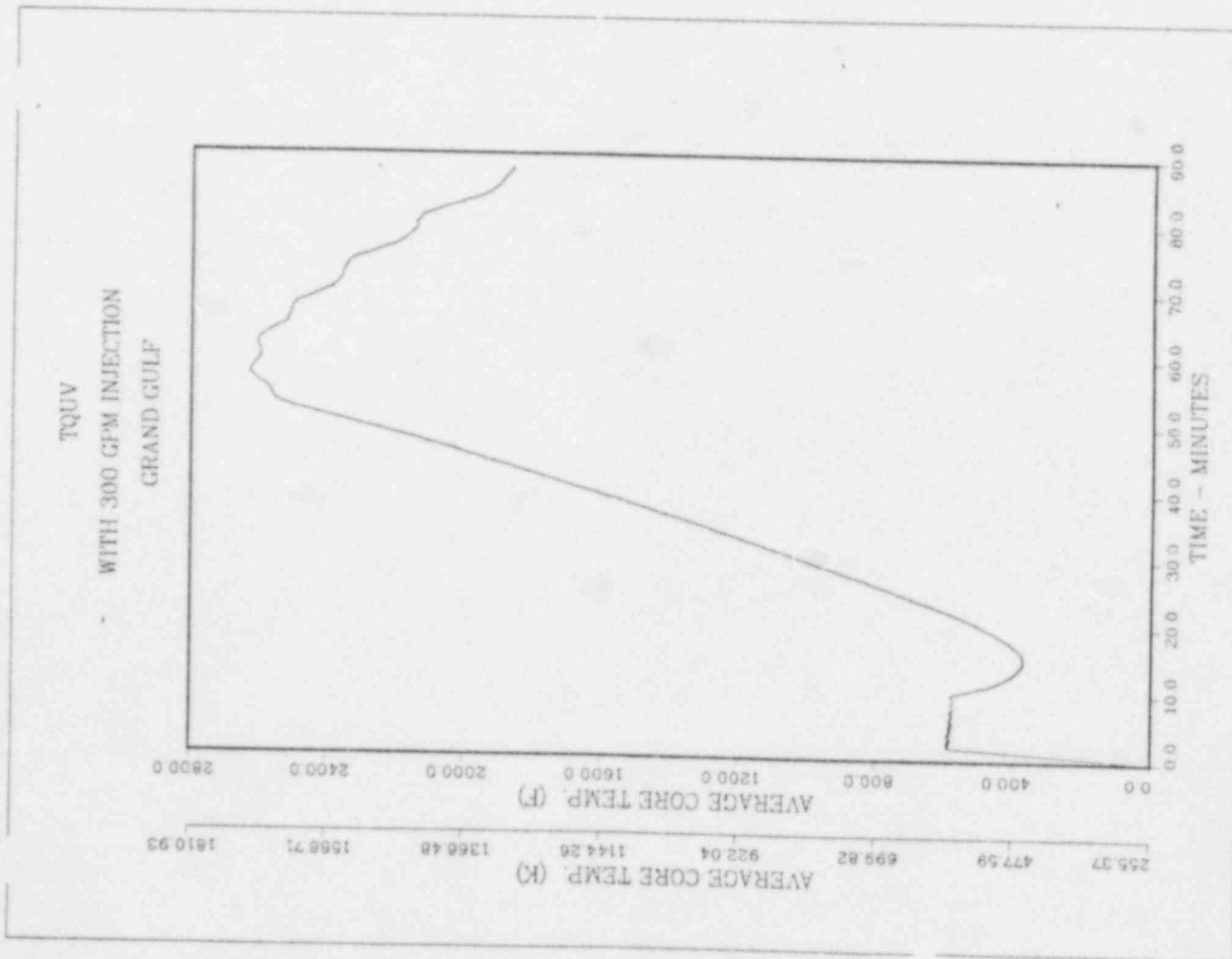


Figure 8.7 ORNL Case 2: core temperature.

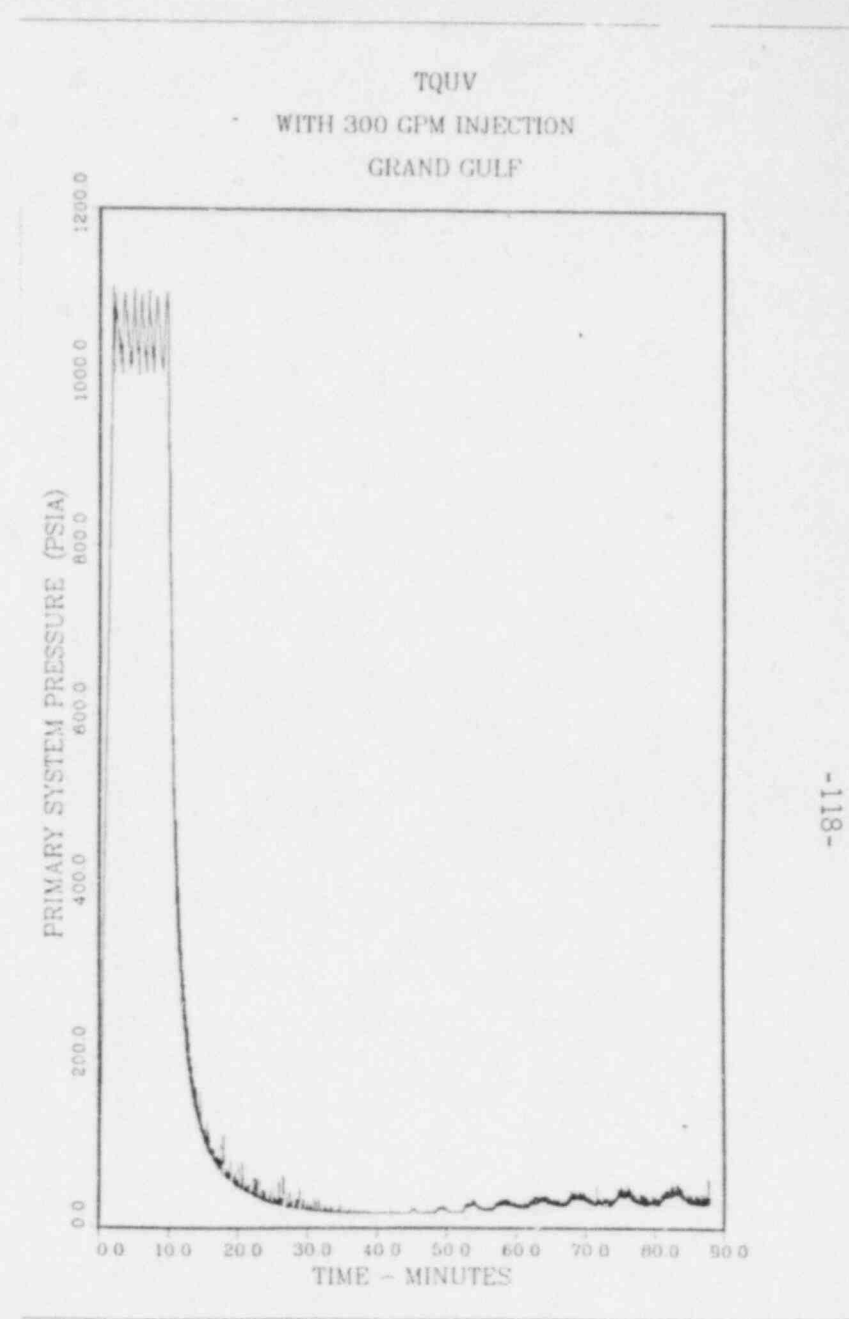
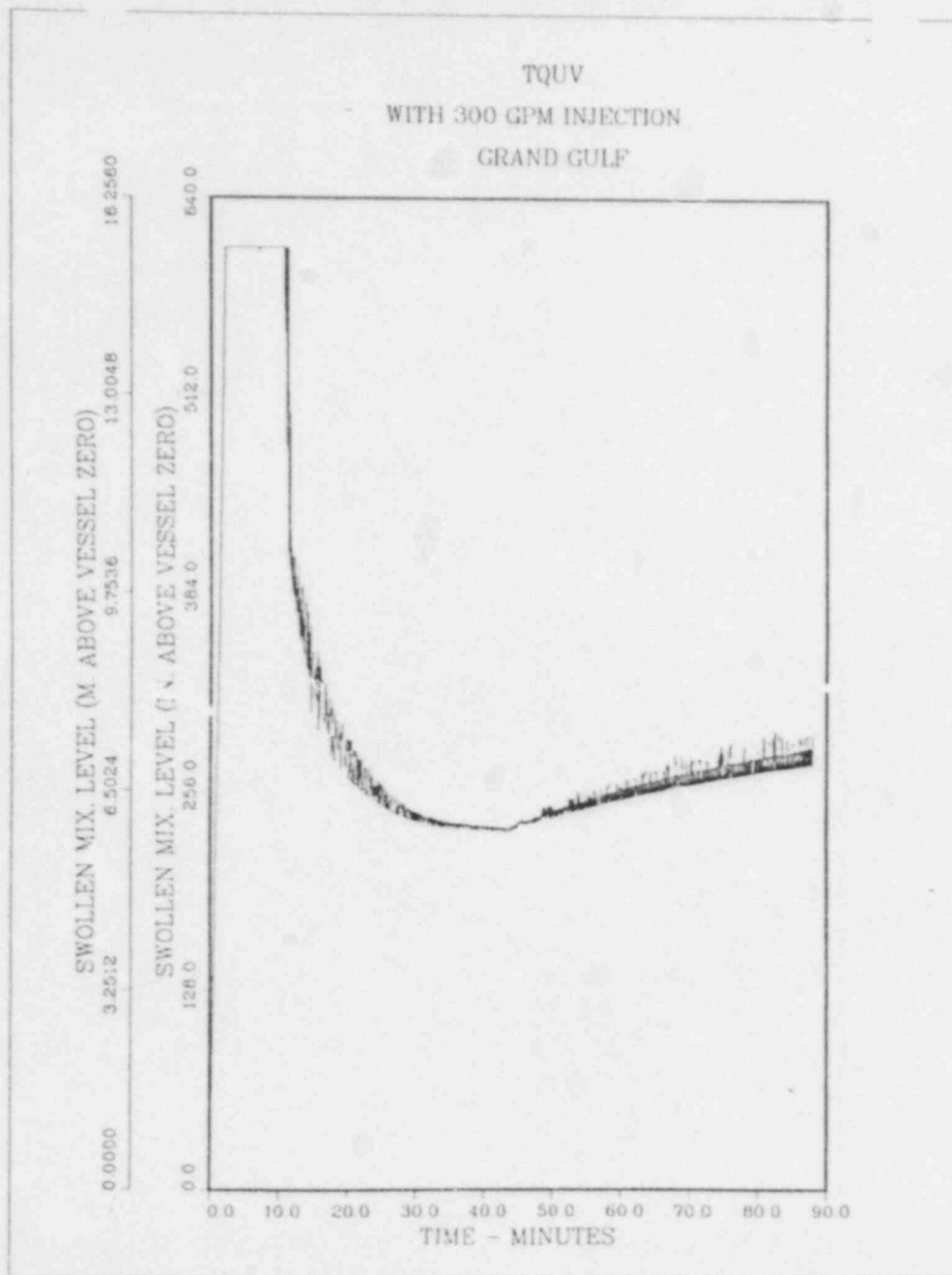
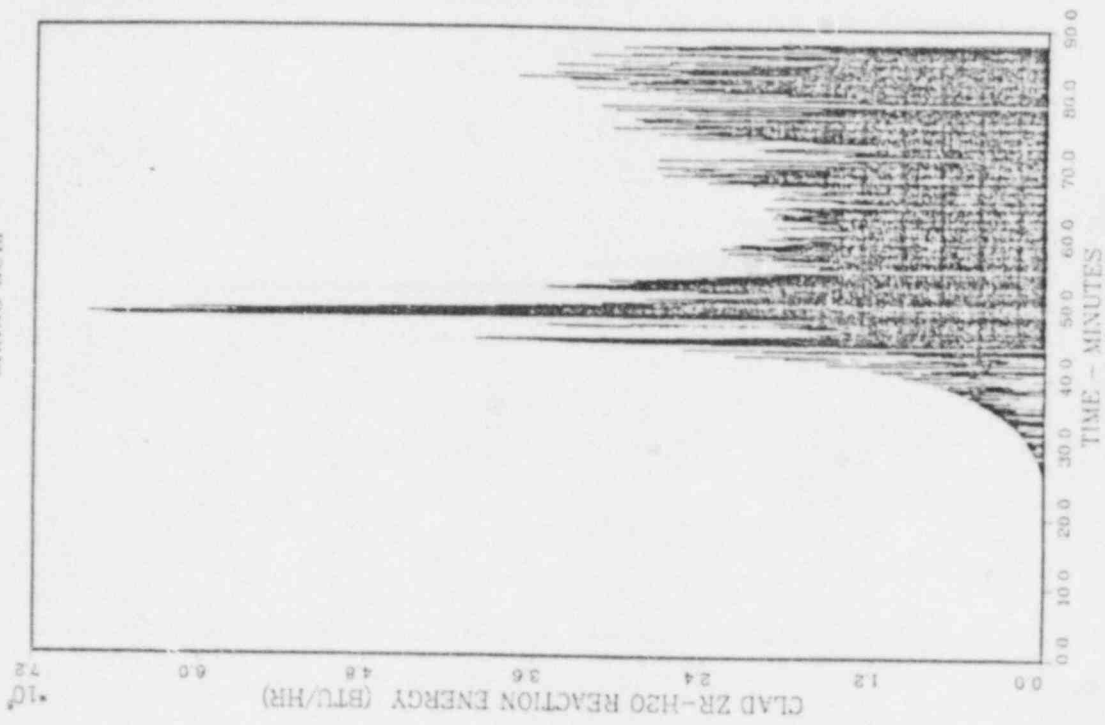


Figure 8.8 ORNL Case 2: swollen mixture level and primary system pressure.

TQUV  
WITH 300 GPM INJECTION  
GRAND GULF



TQUV  
WITH 300 GPM INJECTION  
GRAND GULF

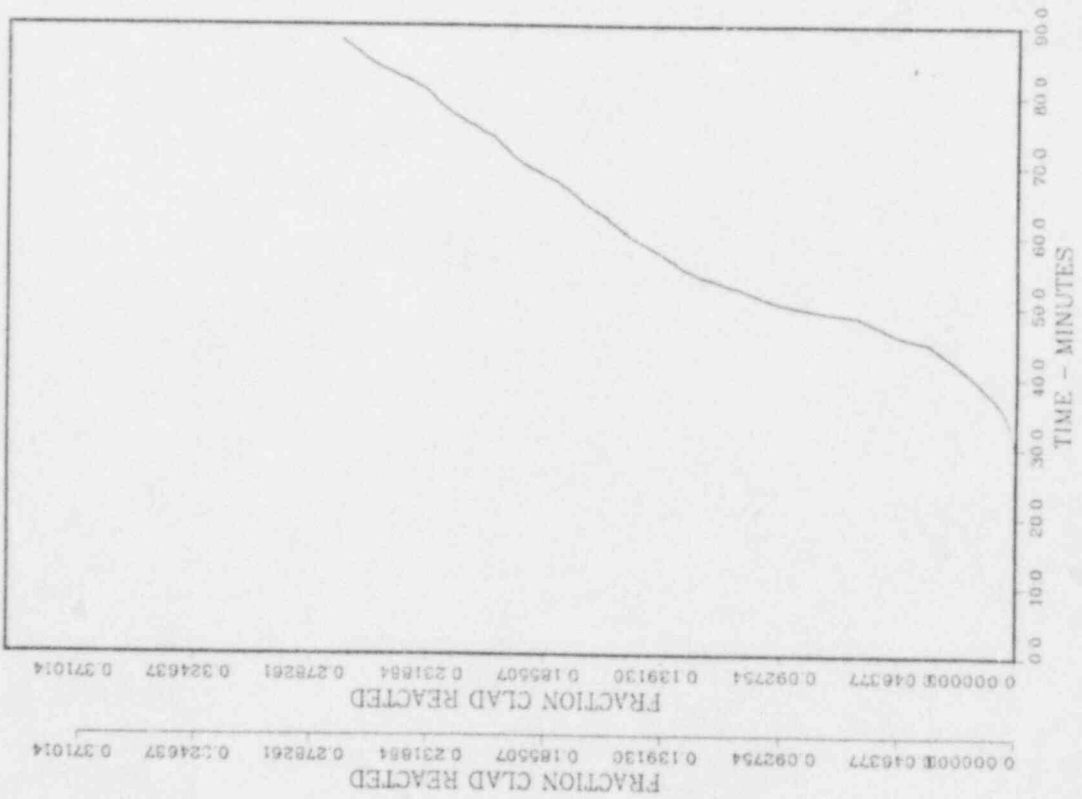
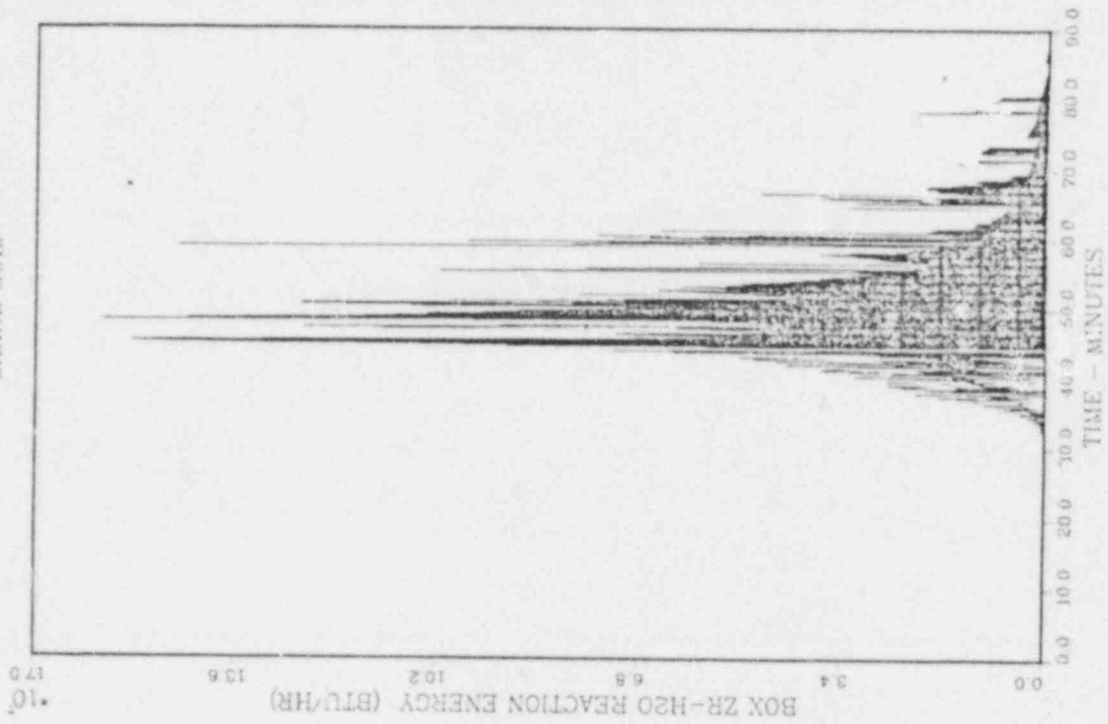


Figure 8.9 ORNL Case 2: clad oxidation.

TQUV  
WITH 300 GPM INJECTION  
GRAND GULF



TQUV  
WITH 300 GPM INJECTION  
GRAND GULF

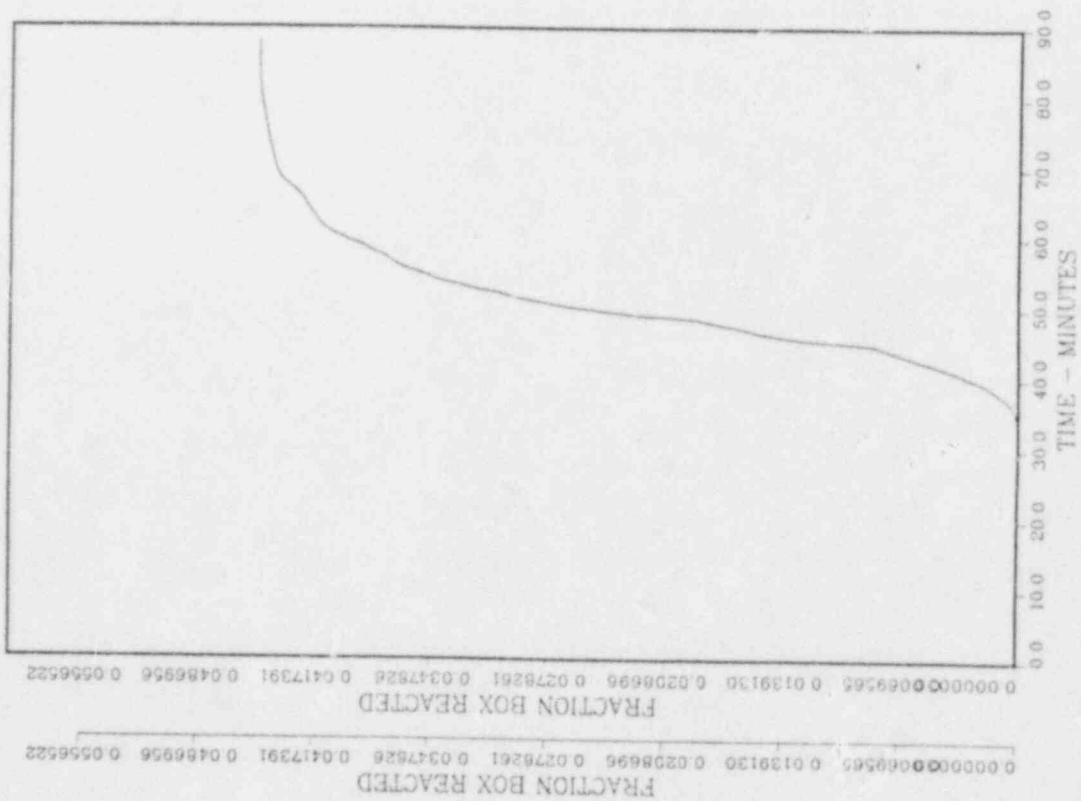
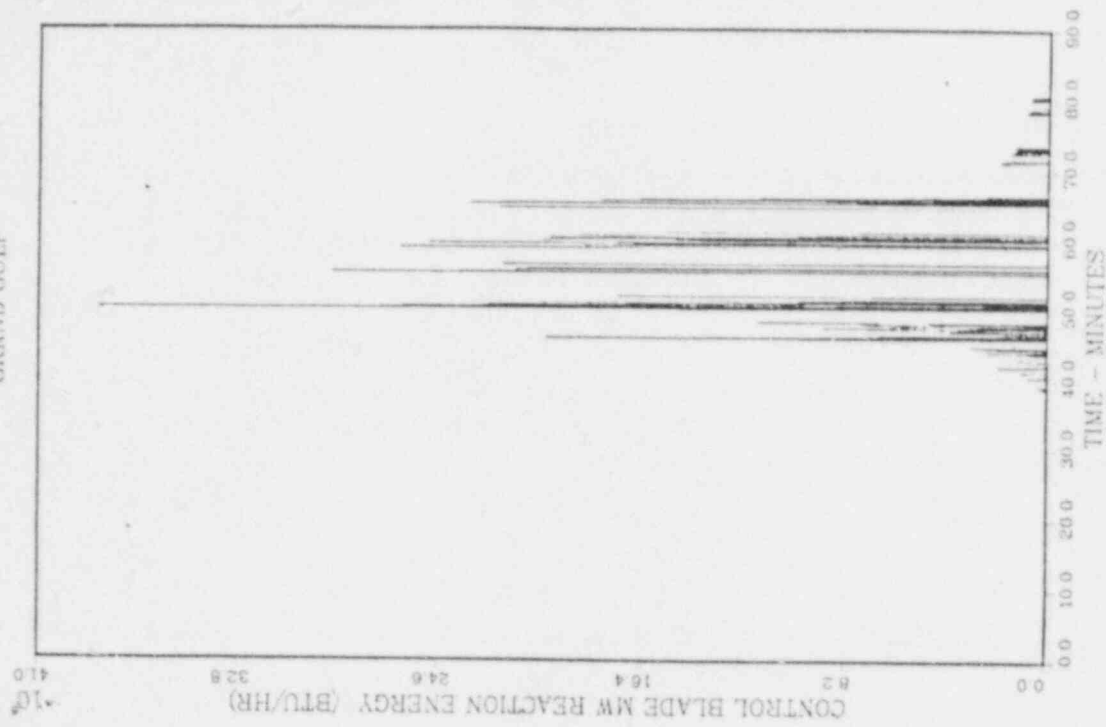


Figure 8.10 ORNL Case 2: channel box oxidation.

TQUV  
WITH 300 GPM INJECTION  
GRAND GULF



TQUV  
WITH 300 GPM INJECTION  
GRAND GULF

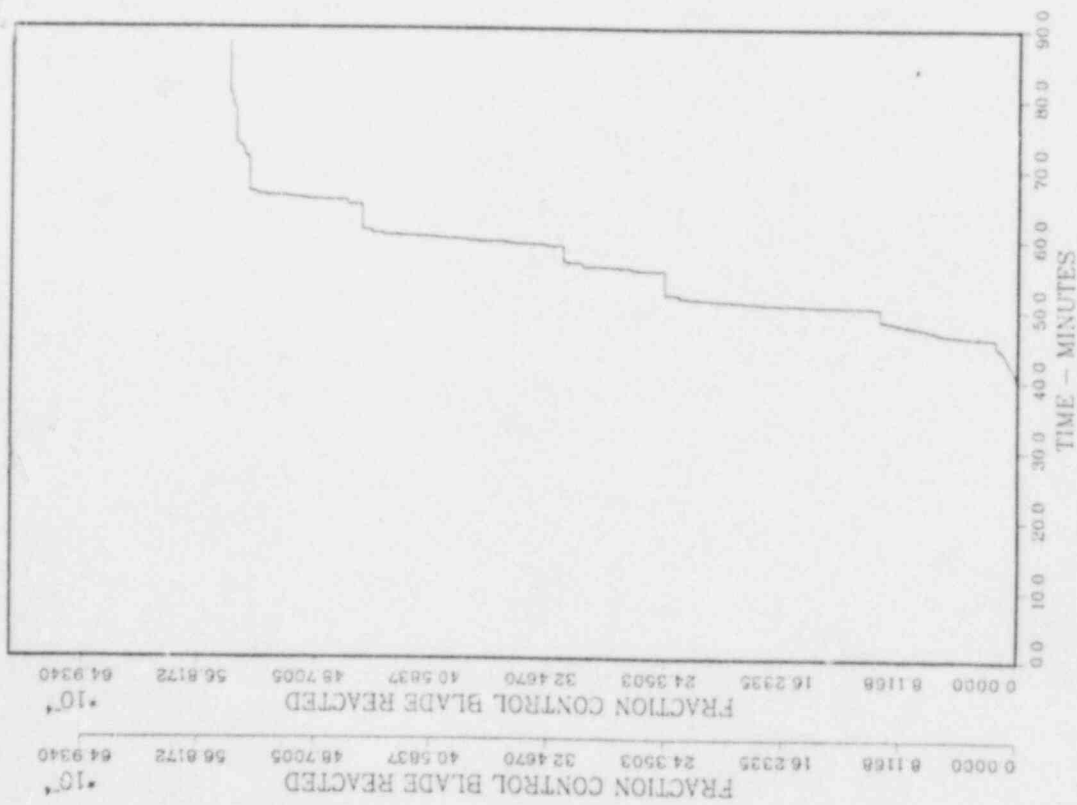


Figure 8.11 ORNL Case 2: control blade oxidation.



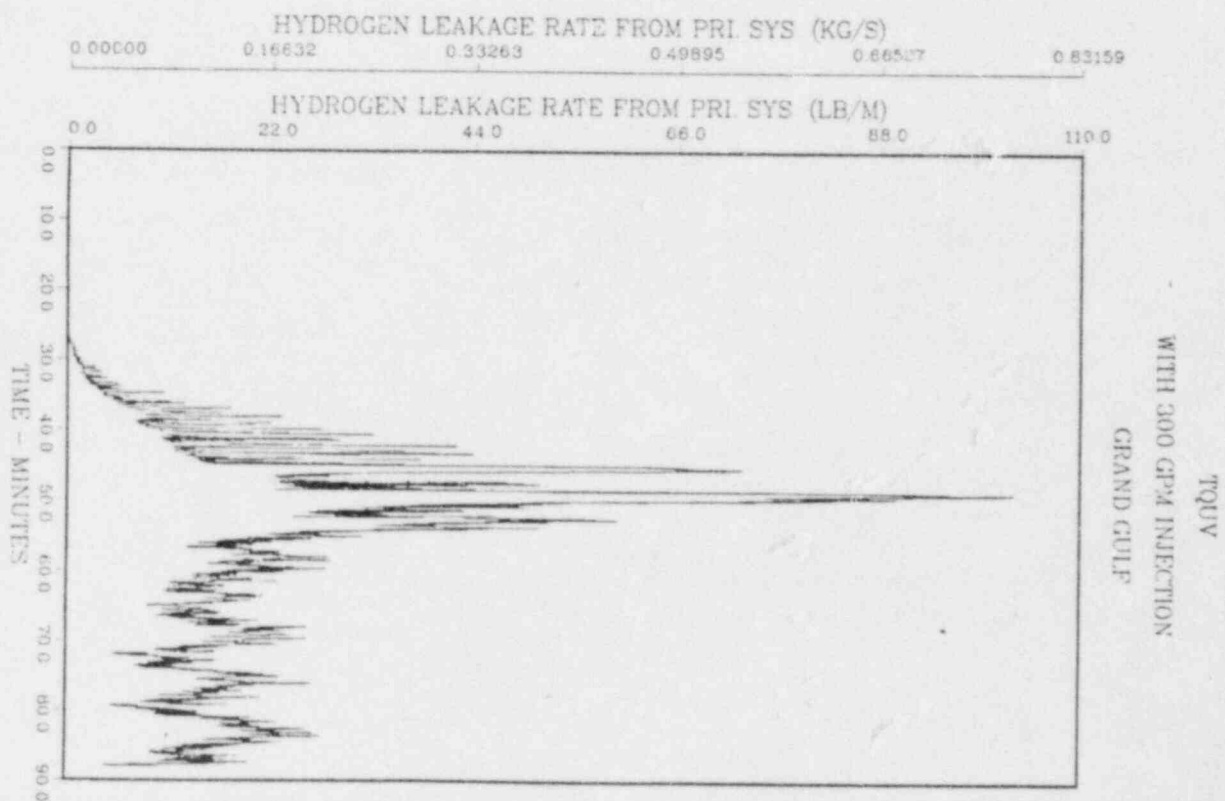
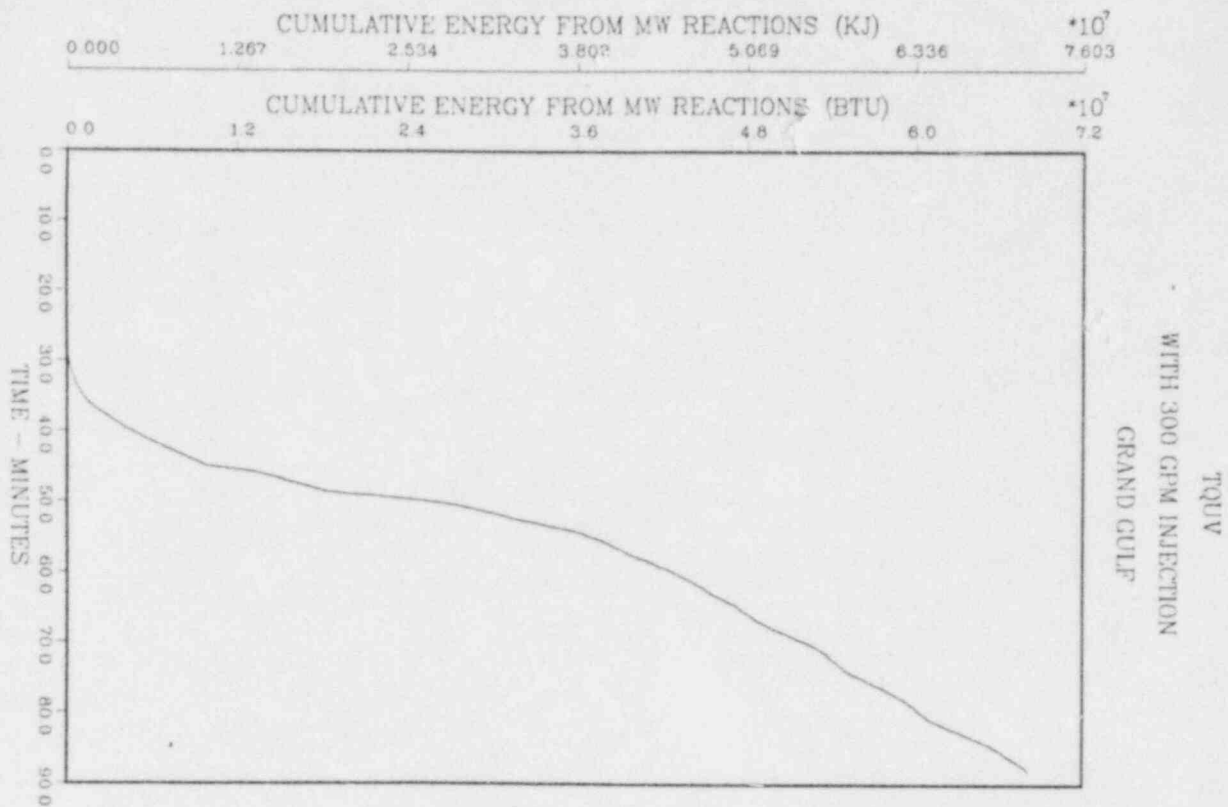


Figure 8.12 ORNL Case 2: hydrogen generation.

9. APPLICATIONS TO GRAND GULF, CLINTON, PERRY, AND RIVER BEND POWER PLANTS

All the MARCH analyses presented in this report are based on the design data of Grand Gulf which is of the BWR6/Mark III type. The Clinton, Perry, and River Bend plants are similar to the Grand Gulf plant. The FSAR for the River Bend plant contains comparisons of design parameters between these four plants and are given in Appendix E. The rated power of the River Bend plant (2894 MWt), Clinton plant (2894 MWt) and the Perry plant (3579 MWt) are 75.5%, 75.5%, and 93.4% of the rated power of the Grand Gulf plant (3833 MWt). The designed steam flow rate, number of fuel assemblies (i.e., mass of  $\text{UO}_2$  and zircaloy), number of control blades (i.e., mass of stainless steel) and other related design parameters of the River Bend, Clinton, and Perry plants are, respectively, 75%, 75%, and 93% of the corresponding parameters of the Grand Gulf plant. All the four plants have the similar Emergency Core Cooling Systems (ECCS). The ECCS capacities of the Perry plant are about 86% to 95% of that of the Grand Gulf plant. Both plants have eight relief valves for the Automatic Depressurization System (ADS). The ECCS capacities of the River Bend and Clinton plants are about 68% to 85% of that of the Grand Gulf plant. There are seven ADS relief valves for the River Bend and Clinton plants. Because of the similarities between these four plants, it is expected to have similar behavior for the production and release of hydrogen from these four plants, in the event of a degraded core accident. The estimated hydrogen production and hydrogen generation rate for the River Bend, Clinton, and Perry plants should be lower than that presented in this report for the Grand Gulf plant. The reduction of hydrogen production is expected to be proportional to the rated power of each plant.

## 10. SUMMARY

An extensive study was performed by using the MARCH2 (Version 151) code to assess the hydrogen generation rate and total hydrogen production during a BWR6 core heatup transient. The oxidations of cladding, channel boxes and control blades are modeled in the MARCH code. The study includes using the initial conditions imposed by the HCOG analysis and conditions determined by following the Emergency Procedure Guidelines. Separate effects, such as time and flowrate of coolant injection, fuel axial node and power profile, and Zr/steam oxidation cut-off temperature were investigated. Comparisons with the HCOG code, SCDAP code and the ORNL MARCH-BWR code were made. Conclusions and summary of results were given in detail in each section of this report.

The MARCH analysis clearly indicates that the hydrogen production is closely related to steam generation in the core. An accurate evaluation of core heat transfer and hydraulics are essential for the assessment of hydrogen production. The MARCH code, in general, is a efficient tool to provide a first approximation of hydrogen production under various conditions of a core heatup transient. However, there are two major deficiencies of the MARCH code. First, the lump of fuel and cladding into one material could mis-estimate the cladding temperature, at which the zircaloy oxidation rate is computed. Second, the lack of core relocation model forces the MARCH code to use the cut-off temperature to terminate the zircaloy oxidation process with a large uncertainty. In view of the approximations of the MARCH code, it is recommended to perform some analyses using the SCDAP code for the three basic cases represented in this report. The SCDAP code contains the methodology needed to perform phenomenological analysis of the degraded core accidents. The SCDAP/MOD1 code is currently available at the Brookhaven National Laboratory.

## 11. REFERENCES

1. J. C. Gillis, et al., "User's Manual and Details of Modeling for the BWR Core Heatup Code," SLI-8414, Rev. 1, GRT/QA84-5, Rev. 1, (July 1984).
2. G. R. Thomas and J. C. Gillis, "Hydrogen Generation in Recoverable BWR Degraded Core Accidents," presentation to the U.S. Nuclear Regulatory Commission, San Jose, California, (October 3-4, 1984).
3. R. O. Wootton, P. Cybulskis, and S. F. Quayle, "MARCH2 Code Description and User's Manual," Final Report, Battelle Columbus Laboratories, NUREG/CR-3988, BMI-2115, (August 1984).
4. Emergency Procedure Guidelines, Pre-publication Draft, Revision 3, (December 8, 1982).
5. American National Standard for Decay Heat Power in Light Water Reactors, ANSI/ANS-5.1-1979, American Nuclear Society.
6. R. Jaung, private communication.
7. Grand Gulf Nuclear Station: Final Safety Analysis Report, Mississippi Power and Light Company.
8. S. R. Greene, "Realistic Simulation of Severe Accidents in BWRs - Computer Modeling Requirements," NUREG/CR-2940, ORNL/TM-8517, Oak Ridge National Laboratory, (April 1984).
9. General Electric Company Analytical Model for Loss-of-Coolant Analysis in Accordance with 10CFR50 Appendix K, Amendment No. 5, Backflow Leakage from the Bypass Region for ECCS Calculations, by B. S. Shiralkar and J. R. Ireland, NEDE-20566-5-P, Class III, (June 1978).
10. H. Komariya and P. B. Abramson, "Existence of a Temperature Cut-Off for Zircaloy Oxidation: Experimental Bases and Analytical Models," ITS/LWR/BNL85-1, International Technical Services, Inc.

APPENDIX A

HCOG Core Heatup Code Input Data

(provided by G. Thomas)

# APPENDIX A

## BWR Dimensions

The following dimensions are used for 7x7\* and 8x8 fuel:

<u>Measurement</u>	<u>7x7</u>	<u>8x8</u>	<u>Dimensions</u>	<u>Materials</u>
Fuel Diameter	0.01237	0.01019	M	UO <sub>2</sub>
Cladding Diameter	0.01430	0.01008	M	Zircaloy
Cladding Thickness	0.00081	0.00813	M	
Water Rod Diameter	-	0.01501	M	
Water Rod Wall Thickness	-	0.00076	M	
Rod Pitch	0.01875	0.01615	M	
Active Fuel Length	3.658	3.810	M	
Gas Plenum Length	-	0.30	M	
Channel Width (inside)	0.1382	0.1325	M	Zircaloy
Channel Thickness	0.00203	0.003048	M <sup>2</sup>	
Flow Area	0.01010	0.009865	M <sup>2</sup>	
Bypass Area (per bundle)	0.00463			
Control Blade Arm Length	0.1105	0.1105	M	Boron Carbide
Blade Thickness	0.00832	0.00832	M	
No. of Fuel Rods per Assembly	49	62		
No. Assemblies	764	800		
Rated Thermal Power	3.579x10 <sup>9</sup>	3.833x10 <sup>9</sup>	Watts	
Area of Jet Pumps	1.33	1.33	M <sup>2</sup>	
Shroud Inner Diameter	5.258	5.258	M	
RPV Inner Diameter	6.376	6.376	M	
Upper Plenum Mass	63192	63192	kg	
Upper Plenum Area	2117	2117	M <sup>2</sup>	

\* None of the BWR/6s will use 7x7 fuel. The option for 7x7 fuel has been included in the BWR Core Heatup Model to represent earlier generations of BWRs.

A-1

A-1

# APPENDIX

## Core Power Peaking Factors

The following are the peaking factors built into the BWR Core Heatup Code, representing a 800-Bundle Core.

<u>Radial Peaking Factors</u>			<u>Quarter Core Bundle Groupings and Relative Powers</u>			
<u>Cells</u>	<u>Peaking for 8 4-Bundle Cells</u>	<u>No. Cells Represented By Computed Cell</u>	<u>Peaking for 4 4-Bundle Cells</u>	<u>No. Cells Represented By Computed Cell</u>	<u>Peaking for 2 4-Bundle Cells</u>	<u>No. Cells Represented By Computed Cell</u>
1	1.240	25	1.208	50	1.144	100
2	1.176	25	1.080	50	0.856	100
3	1.104	25	0.942	50		
4	1.056	25	0.770	50		
5	1.004	25				
6	0.880	25				
7	0.852	25				
8	0.688	25				

A-2

## Bundled Peaking Factors (within one 4-bundle cell)

<u>Bundle</u>	<u>Peaking Factor</u>
High Power (1 each)	1.35
Average Power (2 each)	1.00
Low Power (1 each)	0.65

## Rod Group Peaking Factors

<u>Rod Group</u>	<u>Peaking for 4-Rod Groups</u>	<u>Peaking for 2-Rod Groups</u>
Water Rods	0.0	0.0
Center Rods	0.90	1.0
Side Rods	1.1083	
Corner Rods	1.20	

Axial Peaking power--User Input - Section 2.2



=====

BWR530 3/4 UNCOVERED CORE AT 2 ATM--IRAD=0 + 4 NODE OPT. BOILDOWN TO 2800 SEC

=====

SIMULATION START TIME	TIME =	2000.0 (SECS)
SIMULATION STOP TIME	TEND =	2800.0 (SECS)
INITIAL TIME STEP	DTIME =	1.0 (SECS)
TIME INTERVAL BETWEEN START TIME AND REACTOR SCRAM	TSCRAM =	0. (SECS)
FULL-POWER DAYS OF OPERATION PRIOR TO REACTOR SCRAM	TPOW =	730.0 (DAYS)
PRINT INTERVAL OF SUMMARIZED RESULTS	TSUM =	5.0 (SECS)
PRINT INTERVAL OF DETAILED RESULTS	TDET =	100.0 (SECS)
NUMBER OF AXIAL NODES (2 THROUGH 20)	NAX =	10 (NODES)
NUMBER OF UNIT CELLS OR BUNDLE GROUPS (1, 2, 4, OR 8)	NBGPS =	4 (NODES)
NUMBER OF ROD GROUPS (2 OR 4)	NRGPS =	4 (NODES)
NUMBER OF CHANNEL NODES (1 OR 4)	NCHN =	4 (NODES)
NUMBER OF CONTROL BLADE NODES (1 OR 4)	NCON =	4 (NODES)
FUEL ROD BUNDLE GEOMETRY (7 X 7 OR 8 X 8)	IFUEL =	8 (TYPE)
MELTING TEMPERATURE OF UO2 FUEL	TRMELT =	3125.0 (DEG.K)
MELTING TEMPERATURE OF ZIRCALLOY FUEL CLADDING AND CHANNEL	TCMELT =	2175.0 (DEG.K)
MELTING TEMPERATURE OF STAINLESS-STEEL CONTROL BLADE SHEATH	TBMELT =	1825.0 (DEG.K)
TEMPERATURE WHEN CHANNEL MELTS AND BECOMES BLOCKED	TBLOCK =	5000.0 (DEG.K)
TEMPERATURE WHEN ZIRCALLOY OXIDATION IS CUT OFF	TOXOFF =	2375.0 (DEG.K)
UNIT CELL TO UNIT CELL RADIATION (0-INCLUDED 1-NOT INCLUDED)	IRAD =	0 (NONE)
(0-ANS 1-INPUT) DECAY HEAT CURVE USED	IDCAV =	1 (NONE)
OUTPUT (0-NOT WRITTEN 1-WRITTEN) TO FISSION PRODUCT FILE	IFIS =	0 (NONE)
INITIAL WATER LEVEL AT (0-TOP OF BUNDLE 1- .95300 METERS)	ILEV =	1 (NONE)
1-NO RESTART; 2-WRITE ONLY 3-READ AND WRITE 4-READ ONLY	IRES =	2 (NONE)



```

=====
BOUNDARY CONDITIONS
=====
STEP
=====
NO.  TIME  VALUE
-----
1    2000.  203000.
2    6000.  203000.
3
4
5
6
7
8
9
10
11
12
13
14
15
16
17

=====
PRESSURE
=====
TIME  VALUE
-----
2000.  203000.
6000.  203000.
=====
FEEDWATER FLOW
=====
TIME  VALUE
-----
2000.  0.
6000.  0.
7000.  18.9
=====
FEEDWATER TEMP
=====
TIME  VALUE
-----
0.  0.
0.  0.
0.  0.
0.  0.
=====
SPRAY FLOW
=====
TIME  VALUE
-----
0.  0.
0.  0.
=====
SPRAY TEMP
=====
TIME  VALUE
-----
0.  0.
=====
DECAY HEAT
=====
TIME  VALUE
-----
2000.  *01681
2200.  *01632
2400.  *01586
2600.  *01546
2800.  *01508
3000.  *01476
3250.  *01431
3500.  *01404
3750.  *01373
4000.  *01344
4500.  *01295
5000.  *01253
5500.  *01217
6000.  *01186
7000.  *01133
8000.  *01091
9000.  *01056
=====

```

```

=====
AXIAL POWER SHAPE SPECIFICATION
=====
HEIGHT  PLATING FACTOR
-----
0.  *296
*635
1.270  *858
1.248  1.248
1.905  1.387
2.540  1.248
3.175  *858
3.810  *296
=====

```

## APPENDIX B

Representative MARCH2 (Version (151) Code Input Data

(Case 4.2)

```

MARCH 2 151 IAE) MARCH2-GRAND GULF DATA ADS USED
* * * INPUT FOR NAMELIST NAMEAR * * *

COMPUTATION EXIT CONTROLS
ICHECK= 0 CPSTP = 9.999E+03 IS = 10 PRST = 1.000E+03 TRST = 100

MARCH FLAGS
IBLD1 = 0 IBLOP = 2 IBRK = 1 ICE = 0 ICSV =
IECCK = 2 IFPSR = 2 IFDIL = 7 ISPH = 0 ITRAN =
IU = 0 IAPL = 0 MINIRL = 12 NPAIRL = 0

TIME DATA
ATIME = 1.000E-02 DTINTL = 2.500E-02 TAP = 1.051E+06

INPUT WAS IN AMERICAN ENGINEERING UNITS
PRINTED OUTPUT IS IN AMERICAN ENGINEERING UNITS
CORRAL OUTPUT IS IN AMERICAN ENGINEERING UNITS

UNIT NUMBERS OF INPUT/OUTPUT FILES
INPUT FILE (LINE) 5 OUTPUT FILE (OUTPUT) 8
DEFAULT INPUT FILE (DEFAULT) 2 SUMMARY TABLE OUTPUT (SUMRY) 12
BLOOMMAN INPUT FILE (BLOOM) 3 Error Output (ERRORS) *****
ERROR TEXT FILE (ERRMSG) 4

RG = PLOT FILE (BOILPT) 9 MAKE PLOT FILE (MAKEPT) 11
CORRAL OUTPUT (CORRAL) 0 CORSOR OUTPUT (CORSOR) 0
MASS FLOW OUTPUT (FLOWSI) 0 MERGE OUTPUT (MERGE) 0

* * * NAMELIST NAMEINTL * * *

```

MARCH 2 VISI 1AE1

NUMBER OF MATERIALS 2

[illegible]

DENSITY	407	157
---------	-----	-----

HEAT CAPACITY	.113	.238
---------------	------	------

<p>             THERMAL CONDUCTIVITY 25.0              800           </p>
---

SILAB PROPERTIES

NAME	IVL	IVR	NR01	NR02	MAT1	MAT2	AREA	HIF	OTDX
DAYHELL1	1	1	9	0	2	2	1.950E+04	0.	0.
DAYHELL2	2	2	9	0	2	2	1.950E+04	0	0.
CONCSHELL	2	2	3	9	1	2	7.324E+04	100	0.
MISCSTEEL	2	2	2	0	1	1	1.953E+05	0.	1.00
MISC CONC	2	2	10	0	2	2	1.172E+04	0	0.

NODE COORDINATES MEASURED FROM LEFT BOUNDARY OF EACH SLAB

[illegible]

ORIGINAL: TELETYPE

[illegible]

NUMBER OF YEARS OF MARCH	10	19	31	34 ARE SAVED
1	10	19	31	34 ARE SAVED
2	10	19	31	34 ARE SAVED
3	10	19	31	34 ARE SAVED
4	10	19	31	34 ARE SAVED
5	10	19	31	34 ARE SAVED
6	10	19	31	34 ARE SAVED
7	10	19	31	34 ARE SAVED
8	10	19	31	34 ARE SAVED
9	10	19	31	34 ARE SAVED
10	10	19	31	34 ARE SAVED
11	10	19	31	34 ARE SAVED
12	10	19	31	34 ARE SAVED
13	10	19	31	34 ARE SAVED
14	10	19	31	34 ARE SAVED
15	10	19	31	34 ARE SAVED
16	10	19	31	34 ARE SAVED
17	10	19	31	34 ARE SAVED
18	10	19	31	34 ARE SAVED
19	10	19	31	34 ARE SAVED
20	10	19	31	34 ARE SAVED
21	10	19	31	34 ARE SAVED
22	10	19	31	34 ARE SAVED
23	10	19	31	34 ARE SAVED
24	10	19	31	34 ARE SAVED
25	10	19	31	34 ARE SAVED
26	10	19	31	34 ARE SAVED
27	10	19	31	34 ARE SAVED
28	10	19	31	34 ARE SAVED
29	10	19	31	34 ARE SAVED
30	10	19	31	34 ARE SAVED
31	10	19	31	34 ARE SAVED
32	10	19	31	34 ARE SAVED
33	10	19	31	34 ARE SAVED
34	10	19	31	34 ARE SAVED
35	10	19	31	34 ARE SAVED
36	10	19	31	34 ARE SAVED
37	10	19	31	34 ARE SAVED
38	10	19	31	34 ARE SAVED
39	10	19	31	34 ARE SAVED
40	10	19	31	34 ARE SAVED
41	10	19	31	34 ARE SAVED
42	10	19	31	34 ARE SAVED
43	10	19	31	34 ARE SAVED
44	10	19	31	34 ARE SAVED
45	10	19	31	34 ARE SAVED
46	10	19	31	34 ARE SAVED
47	10	19	31	34 ARE SAVED
48	10	19	31	34 ARE SAVED
49	10	19	31	34 ARE SAVED
50	10	19	31	34 ARE SAVED
51	10	19	31	34 ARE SAVED
52	10	19	31	34 ARE SAVED
53	10	19	31	34 ARE SAVED
54	10	19	31	34 ARE SAVED
55	10	19	31	34 ARE SAVED
56	10	19	31	34 ARE SAVED
57	10	19	31	34 ARE SAVED
58	10	19	31	34 ARE SAVED
59	10	19	31	34 ARE SAVED
60	10	19	31	34 ARE SAVED
61	10	19	31	34 ARE SAVED
62	10	19	31	34 ARE SAVED
63	10	19	31	34 ARE SAVED
64	10	19	31	34 ARE SAVED
65	10	19	31	34 ARE SAVED
66	10	19	31	34 ARE SAVED
67	10	19	31	34 ARE SAVED
68	10	19	31	34 ARE SAVED
69	10	19	31	34 ARE SAVED
70	10	19	31	34 ARE SAVED
71	10	19	31	34 ARE SAVED
72	10	19	31	34 ARE SAVED
73	10	19	31	34 ARE SAVED
74	10	19	31	34 ARE SAVED
75	10	19	31	34 ARE SAVED
76	10	19	31	34 ARE SAVED
77	10	19	31	34 ARE SAVED
78	10	19	31	34 ARE SAVED
79	10	19	31	34 ARE SAVED
80	10	19	31	34 ARE SAVED
81	10	19	31	

CPU 3 1.4.2

MARCH 2 1951 (AE) MARCH2-GRAND GULF DATA ADS USED

\* \* \* INPUT FOR NAMELIST NLECC \* \* \*

	UPPER HEAD INJECTION TANK	ACCUMULATOR	BORATED WATER STORAGE TANK
INITIAL PRESSURE	0.	0.	- - - -
INITIAL MASS OF WATER	0.	0.	2.490E+06
INITIAL WATER TEMP.	100.	100.	100.

FRACTIONAL VALUE OF RWSTM TO START ECC RECIRCULATION \* -0.30

FRACTIONAL VALUE OF RWSTM TO STOP INJECTION AND START SPRAY RECIRCULATION \* 2.00

MINIMUM SUBCOOLING TO PREVENT RECIRCULATION PUMP CAVITATION \* 10.0

MINIMUM SLUMP MASS TO AVOID RECIRCULATION PUMP CAVITATION \* -100.

ECC PUMP DATA

NPUMP = 1

PUMP	HIGH PRESSURE SHUTOFF (P)	LOW PRESSURE SHUTOFF (P/LO)	START TIME (STR)	STOP TIME (STR)	FLOW RATE (M/CL)
1	1.800E+03	0.	56.7	1.000E+10	648

CPU 3 0.00

MARCH 2 11:51 1AE1 MARCH2-GRAND GOLF DATA ADS USED

\* \* \* INPUT FOR NAMELIST NLHX \* \* \*

HEAT EXCHANGER INPUT DATA AT RATED CONDITIONS

ECC HX	CAPACITY	PRIMARY	SECONDARY	PRIMARY	SECONDARY
CS HX	0.	FLOW	FLOW	INLET	INLET
	0.	RATE	RATE	TEMP.	TEMP.
		0.	0.	0.	0.
		0.	0.	185.	50.0

\* \* \* INPUT FOR NAMELIST NLCOOL \* \* \*

CONTAINMENT BUILDING COOLER DATA

THE COOLER IS IN VOLUME NO. 0  
 THE COOLER STARTS AT TIME = 0.  
 AT RATED CONDITIONS

0. = 0.  
 MP = 0.  
 WS = 0.  
 TP = 0.  
 TS = 0.  
 CVAP = 0.693

THERE IS NO ADDITIONAL FAN COOLER

MARCH 2 1951 (A.E.)

\* \* \* INPUT FOR NAMELIST IN PLACE \* \* \*

## CONTAINMENT FLAGS

0	IBERN =	0	ICECLUB=	-1	TDRV	=	1	IVENT =	-	0	IUEI =
-2	JRPV3 =	1	NPLAV =	12	NCUB	=	2	NRPV1 =	-	1	NRPV2 =
-2	KCNP =	2									

## CONTAINING: MODELS AND TIME DATA

Variable	Mean	Standard Deviation	Minimum	Maximum	Number of Missing Values
DIC	5.000E+02	10.0	0.5	5.000E+03	0
MAXX	280.	14.7	191.1	0.	0
PO			1.000E+06		0
CV6000			5.000E+04		0
FALL			0		0
YFLR			0		0

## PAGE SLIDE SUPPLEMENT DATA

DEF = 100. DEFICE = 100. TICE = 20.0. TPOOL = 100. TSTM = 105. TWTR = 190.  
WTR2 = 130. WICE = 0. WPOOL = 9.670E+06

## SAFF GUJAROS CONTROL

```

FSPPRA = 0.      STPECC = 1.00DE+06  STPSPP = 1.00DE+06  WPMAX = 6.80DE+05

```

COMPANY FLAGS

1	2	3	4	5	6	7	8	9	10	11	12	13	14	15	16	17	18	19	20	21	22	23	24	25	26	27	28	29	30	31	32	33	34	35	36	37	38	39	40	41	42	43	44	45	46	47	48	49	50	51	52	53	54	55	56	57	58	59	60	61	62	63	64	65	66	67	68	69	70	71	72	73	74	75	76	77	78	79	80	81	82	83	84	85	86	87	88	89	90	91	92	93	94	95	96	97	98	99	100
1	2	3	4	5	6	7	8	9	10	11	12	13	14	15	16	17	18	19	20	21	22	23	24	25	26	27	28	29	30	31	32	33	34	35	36	37	38	39	40	41	42	43	44	45	46	47	48	49	50	51	52	53	54	55	56	57	58	59	60	61	62	63	64	65	66	67	68	69	70	71	72	73	74	75	76	77	78	79	80	81	82	83	84	85	86	87	88	89	90	91	92	93	94	95	96	97	98	99	100

### RESULTS DATA

[illegible]

## COMPARING INITIAL CONDITIONS

NUMBER	FLOOR	VOLUME	AREA	HUMIDITY	TEMP	WATER		
						W-D	W-T	W-T-W
1	2	2.7016+03	4.000E+03	500	135	-3.320E-04	0	0
2	1	1.400E+06	1.200E+04	900	80.0	-3.320E-04	0	0

## NOT A LAME HALF EVENTS

Variable	Value	Unit
$C_1$	1.000E+03	
$C_2$	1.00E-03	
$C_3$	0.00	

[illegible]

$\lambda$	KT (1,1)	EM (1,1)	prob SS
1	NO TRANSFER		
2		0	
3		0	
4	NO TRANSFER		







```

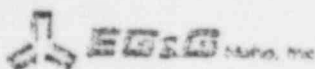
NAME = 2 1151 1411 MATCH2 GRAND GOLF DATA ADS USED
* * * INPUT FOR NAMELIST NHEAD * * *
CONO = 6.00 DBH = 20.9
SLOF = 5.00E+04 THICK = .522
WAOXXX = 8.66E+05 WZROXX = 1.74E+05
* * * INPUT FOR NAMELIST NHEAD * * *
HOTDRP FLAGS
IDRLO = 103 IDOT = 100 IDIR = 1 NSTOP = 200
DEBRIS PARAMETERS
ACAV = 3N2 CON = 2.00
TMS = 2.00E+03 IPOOLH = 100
* * * INPUT FOR NAMELIST NINTR * * *
INTEC FLAGS
IGAS = 1 IAPC = 1 IZMEO = 0 NEPS = 2
MODEL PARAMETERS
CATXXX = 1.30E-02 CPCXXX = 900
FC2XXX = 150 FC3XXX = 1.00E-02
M1J = 1.00E-02 ROXXX = 323
TDC = 1.37E+03 TF = 3.60E+04
NEPS 1 0. EPSILON
2 3.60E+07 500
500

```

## APPENDIX C

Initial and Boundary Conditions Used for the SCDAP Analysis

(provided by L. Seifken)



FORM 3 (Rev. 1-77)  
(Page 1 of 2)

C-1

TELECOPIER TRANSMITTAL REQUEST

TO ORGANIZATION Brockhous National Lab  
ADDRESS Watson, New York  
ATTENTION J. W. Young  
TYPE OF TELECOPIER \_\_\_\_\_  
TELECOPIER TELEPHONE NO. 666-2394  
VERIFICATION TELEPHONE NO. 666-2547

FROM L. A. Siskin TELEPHONE NO. 6-9319  
COMPANY EC & C Labs

TYPE OF TELECOPIER \_\_\_\_\_

TELECOPIER TELEPHONE NO. \_\_\_\_\_

VERIFICATION TELEPHONE NO. \_\_\_\_\_

TOTAL PAGES (excluding transmittal sheet) 10 DATE 1-24-85

RETURN ORIGINAL YES X NO \_\_\_\_\_

NAME Sandy Burr EXT 6-9854

## Introduction:

Enclosed is information to provide you with the initial conditions and boundary conditions for a MARCH code analysis of the response of a hot fuel bundle in a 8 x 8 BWR-4 nuclear power plant during an anticipated transient without scram. The start time of the conditions is 2000s, which is the time at which oxidation in the fuel bundle begins. The end time is 8000s. The outside surface of the bundle canister was assumed to have a heat transfer coefficient of zero in the SCDAP analysis.

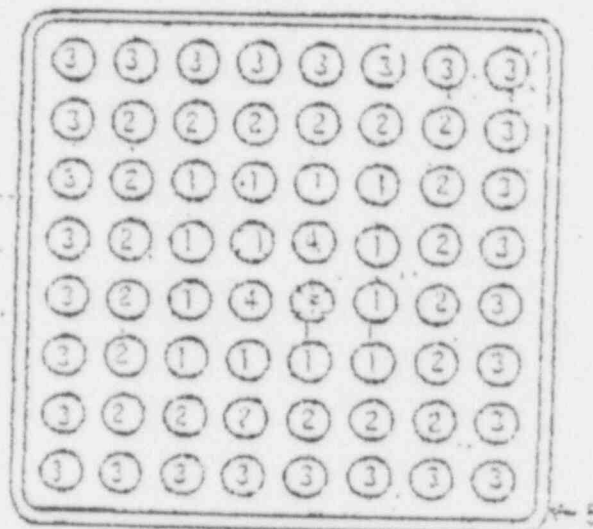
The following information is enclosed:

1. Grouping of bundle rods for SCDAP analysis.
2. Characteristics of fuel bundle.
3. Locations of axial zones in upper vessel region.
4. Geometric characteristics and masses of axial zones in upper plenum.
5. Bundle axial power distribution.
6. Bundle radial power distribution.
7. Bundle inlet mass flow rate history.
8. Bundle power history.
9. Initial axial temperature distribution.

The initial mass of water in the bundle was 7.28 kg and the initial elevation of the top of the two-phase coolant mixture was 0.98m.

If any further information is required, please call Larry Stefken, FIS 583-9319.

*Coolant pressure had constant value of 7.56 MPa during the entire transient. Enthalpy of inlet flow had a constant value of 1.24 E+6 J/kg.*



- 1 - component 1 fuel rods
- 2 - component 2 fuel rods
- 3 - component 3 fuel rods
- 4 - water rods
- 5 - canister

Figure 2 <sup>2</sup> Grouping of bundle rods for SEDAP analysis  
~~SEDAP bundle components~~

A 12/11/84 TSB Doc 7802J Disk 1034J Job 37247 Proof 4 \_ \_ \_ BLT

TABLE <sup>3</sup><sub>2</sub>. CHARACTERISTICS OF FUEL BUNDLE

Characteristic	Units	Value
Active fuel length	m	3.91
Fuel pellet radius	m	0.005207
Cladding outside radius	m	0.005134
Cladding inside radius	m	0.005321
Plenum void volume	m <sup>3</sup>	$1.84 \times 10^{-5}$
Amount of Helium fill gas	kg	$4.8 \times 10^{-5}$
Pitch	m	0.0163
Coolant pressure (2000 s),	N/m <sup>2</sup>	$7.169 \times 10^5$
Bundle cross-sectional area (including rods)	m <sup>2</sup>	$1.86598 \times 10^{-2}$
Bundle flow area	m <sup>2</sup>	$1.29086 \times 10^{-2}$
Inner circumference of bundle canister	m	0.52
Thickness of canister wall	m	$1.524 \times 10^{-3}$
Number of grid spacers	--	7
Average fuel burnup	MW.s/kg	$8.05 \times 10^5$

A 12/11/84 TS8 Doc 7802J Disk 1034J Job 37247 Proof 4 - - 9LT

TABLE 6. BUNDLE AXIAL POWER DISTRIBUTION

<u>Elevation (m)</u>	<u>Axial Node</u>	<u>Ratio of Local Power Density to Axially Averaged Power Density</u>
0.7905	1	0.876
0.5715	2	1.127
0.9525	3	1.166
1.3335	4	1.176
1.7145	5	1.156
2.0955	6	1.132
2.4765	7	1.079
2.8575	8	0.986
3.2385	9	0.826
3.6195	10	0.525



A 12/11/84 TSB Doc 78023 Disk 10343 Job 37247 Proof 4 \_ \_ BLT

TABLE 7. BUNDLE RADIAL POWER DISTRIBUTION

<u>Rod Group Number</u>	<u>Ratio of rod group power density to average power density of bundle fuel rods</u>
1	0.9859
2	0.9937
3	1.0111

A 12/11/84 TSB Dec 7802J Disk 1034J Job 37247 Proof 4 \_ \_ \_ BLT

TABLE 4. LOCATIONS OF AXIAL ZONES IN UPPER PLENUM OF VESSELS

---

<u>Zone Number</u>	<u>Type of component in Zone</u>
1	Upper plenum of fuel rods
2	Upper core support plate and top of canisters
3	Core shroud head
4	Standpipe
5	Separator
6	Dryer
7	Steam dome

---

A 12/11/84 TSS Doc 7802J Disk 10343 Job 37247 Proof 4 \_ \_ \_ BLT

TABLE 5. GEOMETRIC CHARACTERISTICS AND MASSES OF AXIAL ZONES IN VESSEL UPPER PLENUM

<u>Axial Zone Number</u>	<u>Height of Zone (m)</u>	<u>Surface Area Facing Steam (m<sup>2</sup>)</u>	<u>Cross-sectional Area for Steam Flow (m<sup>2</sup>)</u>	<u>Mass of Material (kg)</u>	<u>Composition of Material</u>
1	0.2408	0.923	0.01133	2.70	Zr
2	0.2530	0.597	0.01860	22.80	Zr
3	0.9205	0.078	0.00510	7.33	SS
4	1.860	0.250	0.00510	13.57	SS
5	2.300	1.140	0.00510	27.96	SS
6	2.260	9.36	0.01420	46.28	SS
7	5.510	0.100	0.04170	14.46	SS

## INITIAL AXIAL TEMPERATURE DISTRIBUTION

<u>Axial Node Number</u>	<u>Elevation (m)</u>	<u>Temperature (K)</u>
1	0.1905	564
2	0.5715	564
3	0.9525	564
4	1.3335	620
5	1.7145	699
6	2.0955	764
7	2.4765	799
8	2.8575	883
9	3.2385	929
10	3.6195	934

22-142 30 SHEETS  
22-143 100 SHEETS  
22-144 200 SHEETS



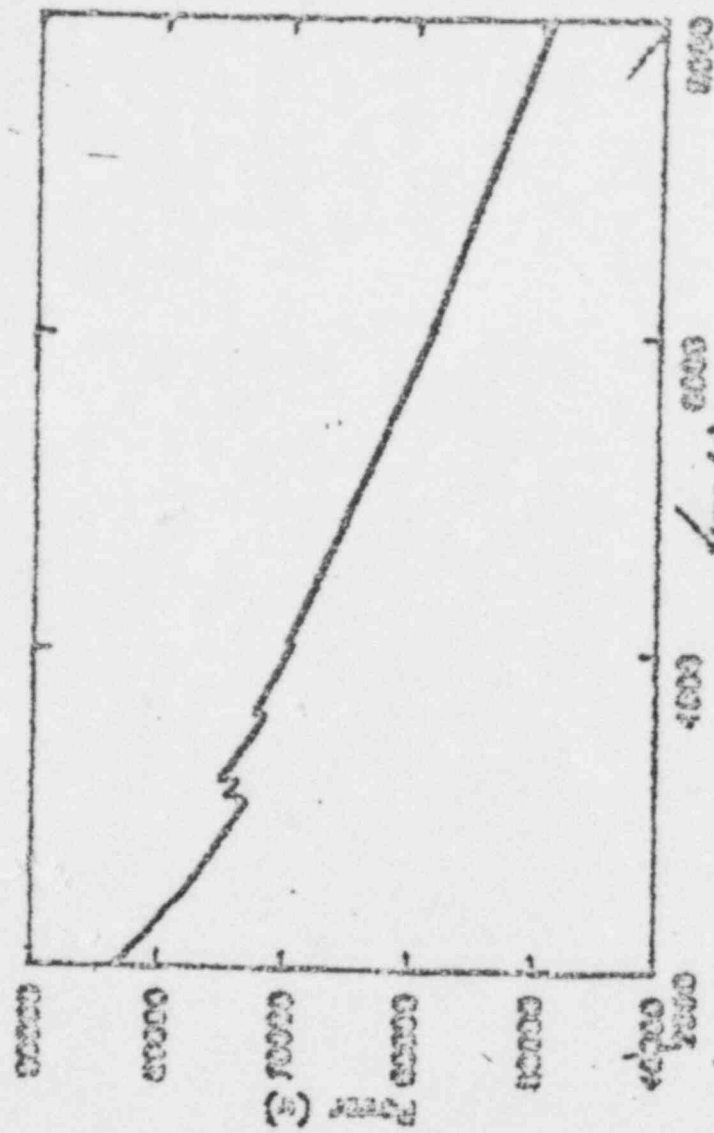


Figure 4. Power History of a Hot Fuel Element.

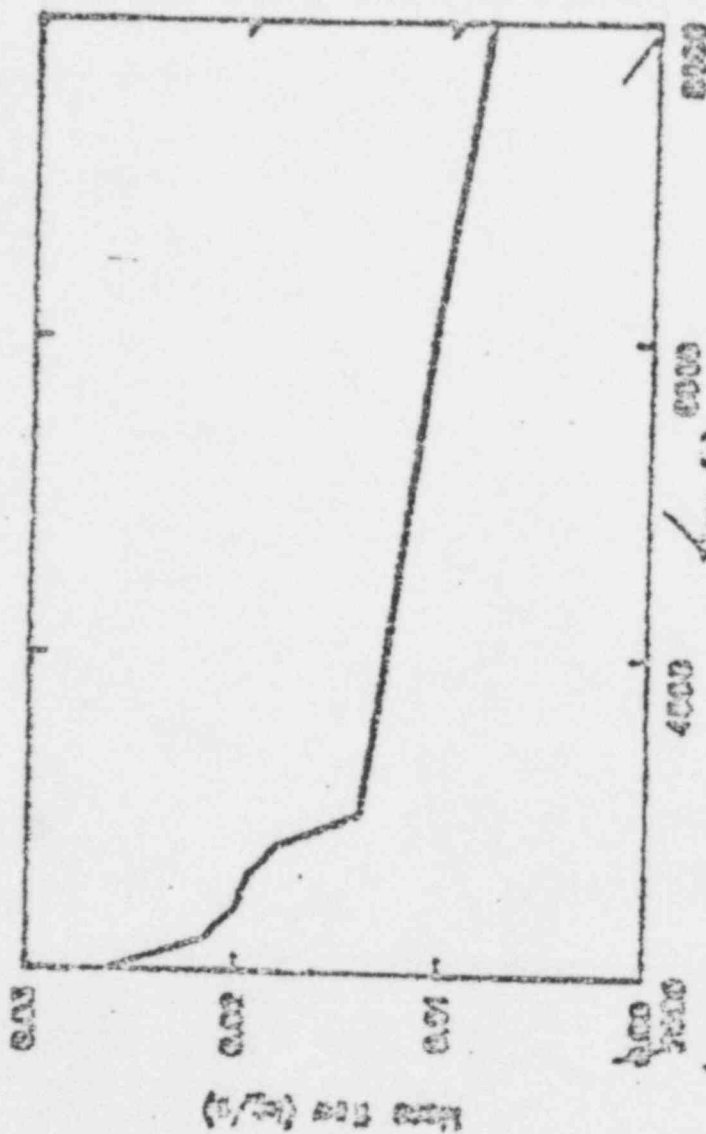


Figure 3. Radio Inlet mass flow rate history.

APPENDIX D

ORNL MARCH-BWR Code Input Data

(provided by S. Hodge)

CLUBS (C) 1987 BY THE BOARD OF DIRECTORS

[illegible]

GRAND GULL DWR 6/MARK III TURV WITH 300 GIM

◆ ◆ ◆ PLATE II PLATE-LAY ◆ ◆ ◆

TRAN	1	2	3	4	5	6	7	8	9	10	11	12	13	14	15	16	17	18	19	20	21	22	23	24	25	26	27	28	29	30	31	32	33	34	35	36	37	38	39	40	41	42	43	44	45	46	47	48	49	50	51	52	53	54	55	56	57	58	59	60	61	62	63	64	65	66	67	68	69	70	71	72	73	74	75	76	77	78	79	80	81	82	83	84	85	86	87	88	89	90	91	92	93	94	95	96	97	98	99	100
TRAN	1	2	3	4	5	6	7	8	9	10	11	12	13	14	15	16	17	18	19	20	21	22	23	24	25	26	27	28	29	30	31	32	33	34	35	36	37	38	39	40	41	42	43	44	45	46	47	48	49	50	51	52	53	54	55	56	57	58	59	60	61	62	63	64	65	66	67	68	69	70	71	72	73	74	75	76	77	78	79	80	81	82	83	84	85	86	87	88	89	90	91	92	93	94	95	96	97	98	99	100
TRAN	1	2	3	4	5	6	7	8	9	10	11	12	13	14	15	16	17	18	19	20	21	22	23	24	25	26	27	28	29	30	31	32	33	34	35	36	37	38	39	40	41	42	43	44	45	46	47	48	49	50	51	52	53	54	55	56	57	58	59	60	61	62	63	64	65	66	67	68	69	70	71	72	73	74	75	76	77	78	79	80	81	82	83	84	85	86	87	88	89	90	91	92	93	94	95	96	97	98	99	100
TRAN	1	2	3	4	5	6	7	8	9	10	11	12	13	14	15	16	17	18	19	20	21	22	23	24	25	26	27	28	29	30	31	32	33	34	35	36	37	38	39	40	41	42	43	44	45	46	47	48	49	50	51	52	53	54	55	56	57	58	59	60	61	62	63	64	65	66	67	68	69	70	71	72	73	74	75	76	77	78	79	80	81	82	83	84	85	86	87	88	89	90	91	92	93	94	95	96	97	98	99	100
TRAN	1	2	3	4	5	6	7	8	9	10	11	12	13	14	15	16	17	18	19	20	21	22	23	24	25	26	27	28	29	30	31	32	33	34	35	36	37	38	39	40	41	42	43	44	45	46	47	48	49	50	51	52	53	54	55	56	57	58	59	60	61	62	63	64	65	66	67	68	69	70	71	72	73	74	75	76	77	78	79	80	81	82	83	84	85	86	87	88	89	90	91	92	93	94	95	96	97	98	99	100
TRAN	1	2	3	4	5	6																																																																																														

THERE IS NO CURRENTLY LISTED INPUT



\* \* \* CARBONITE SLAB THICK \* \* \*

## NUMBER OF SLABS C NUMBER OF MATERIALS 2

MATERIAL PROPERTIES  
 SPECIFIC GRAVITY 151.0  
 HEAT CAPACITY 0.252  
 THERMAL CONDUCTIVITY 25.0  
 0.100

## SLAB PROPERTIES

SLAB	IVL	IVL	THICK	THICK	MAT1	MAT2	AREA	THICK	DFIX
DOWNLDR	1	1	10	10	2	2	3.4021	0.3	0.0
UPDR	2	2	10	10	1	1	5.9001	0.3	0.0
DOWNDR	1	1	11	11	2	2	4.6031	0.3	0.0
UPDR	2	2	11	11	1	1	3.1501	0.3	0.0
DOWNDR	1	1	12	12	2	2	6.0421	0.4	0.0
UPDR	2	2	12	12	1	1	7.3521	0.4	0.0
DOWNDR	1	1	17	17	2	2	6.3121	0.3	1.00
UPDR	2	2	17	17	1	1	1.6021	0.4	1.00

## DOWN COORDINATES REACHED FROM LEFT BOUNDARY OF EACH SLAB

DOWNLDR	0.0	1.0001-0.2	2.0001-0.2	4.0001-0.2	8.0001-0.2	0.100	0.220	0.640	1.00	2.00
UPDR	4.00	0.00	0.00	12.0	16.0	0.0	24.0	26.0	1.20	2.50
DOWNDR	0.0	1.0001-0.2	2.0001-0.2	4.0001-0.2	8.0001-0.2	0.100	0.320	0.640	1.20	2.00
UPDR	4.00	0.00	0.00	12.0	16.0	0.0	24.0	26.0	1.20	2.00
DOWNDR	0.0	1.0001-0.2	2.0001-0.2	4.0001-0.2	8.0001-0.2	0.100	0.320	0.640	1.00	2.00
UPDR	4.00	0.00	0.00	12.0	16.0	0.0	24.0	26.0	1.20	2.00
DOWNDR	0.0	1.0001-0.2	2.0001-0.2	4.0001-0.2	8.0001-0.2	0.100	0.320	0.640	1.00	2.00
UPDR	4.00	0.00	0.00	12.0	16.0	0.0	24.0	26.0	1.20	2.00
DOWNDR	0.0	1.0001-0.2	2.0001-0.2	4.0001-0.2	8.0001-0.2	0.100	0.320	0.640	1.00	2.00
UPDR	4.00	0.00	0.00	12.0	16.0	0.0	24.0	26.0	1.20	2.00
DOWNDR	0.0	1.0001-0.2	2.0001-0.2	4.0001-0.2	8.0001-0.2	0.100	0.320	0.640	1.00	2.00
UPDR	4.00	0.00	0.00	12.0	16.0	0.0	24.0	26.0	1.20	2.00

## INITIAL TEMPERATURES

DOWNLDR	1.50	1.50	1.50	1.50	1.50	1.50	1.50	1.50	1.50	1.50
UPDR	1.50	1.50	1.50	1.50	1.50	1.50	1.50	1.50	1.50	1.50
DOWNDR	1.50	1.50	1.50	1.50	1.50	1.50	1.50	1.50	1.50	1.50
UPDR	1.50	1.50	1.50	1.50	1.50	1.50	1.50	1.50	1.50	1.50
DOWNDR	1.50	1.50	1.50	1.50	1.50	1.50	1.50	1.50	1.50	1.50
UPDR	1.50	1.50	1.50	1.50	1.50	1.50	1.50	1.50	1.50	1.50
DOWNDR	1.50	1.50	1.50	1.50	1.50	1.50	1.50	1.50	1.50	1.50
UPDR	1.50	1.50	1.50	1.50	1.50	1.50	1.50	1.50	1.50	1.50
DOWNDR	1.50	1.50	1.50	1.50	1.50	1.50	1.50	1.50	1.50	1.50
UPDR	1.50	1.50	1.50	1.50	1.50	1.50	1.50	1.50	1.50	1.50
DOWNDR	1.50	1.50	1.50	1.50	1.50	1.50	1.50	1.50	1.50	1.50
UPDR	1.50	1.50	1.50	1.50	1.50	1.50	1.50	1.50	1.50	1.50

TEMPERATURES OF MATERIALS 1 2 3 4 5 6 7 8 9 10 11 12 13 14 15 16 17 18 19 20 21 22 23 24 25 26 27 28 29 30 31 32 33 34 35 36 37 38 39 40 41 42 43 44 45 46 47 48 49 50 51 52 53 54 55 56 57 58 59 60 61 62 63 64 65 66 67 68 69 70 71 72 73 74 75 76 77 78 79 80 81 82 83 84 85 86 87 88 89 90 91 92 93 94 95 96 97 98 99 100

\*\*\* EMERGENCY CORE COOLING SYSTEM INPUT DATA \*\*\*

	UPPER HEAD INJECTION TANK	ACCUMULATOR	BORATED WATER STORAGE TANK
INITIAL PRESSURE	0.0	0.0	- - - -
INITIAL MASS OF WATER	0.0	0.0	3.100E 06
INITIAL WATER TEMP.	0.0	0.0	90.0

	HIGH HEAD	SAFETY INJECTION	LOW HEAD
TIME TO START PUMP (MIN)	0.100E 09	0.100E 09	0.100E 09
PRESSURE SET POINT	0.100E 07	0.0	0.100E 07
FLOW RATE	0.500E 04	0.0	0.0
TIME TO STOP PUMP (MIN)	0.100E 09	0.100E 09	0.100E 09
LOW PRESSURE TRIP POINT	100.	0.0	50.0

FRACTIONAL VALUE OF PWSM TO START ECC RECIRCULATION = 0.100E-01

FRACTIONAL VALUE OF PWSM TO STOP INJECTION AND START SPRAY RECIRCULATION = 0.0

MINIMUM SUBCOOLING TO PREVENT RECIRCULATION PUMP CAVITATION = -100.

MINIMUM CUMP MASS TO AVOID RECIRCULATION PUMP CAVITATION = 1.00

STOP TIME FOR ALL ECC PUMPS = 0.100E 09

\*\*\*\*\* VARIABLE SPEED PUMP DATA \*\*\*\*\*

NUMBER OF PUMPS = 3

	1	2	3
NP	1	2	3
TM	0.0	0.0	0.0
STP	0.0	0.0	0.0
P	295.0	219.0	1300.0
PEC	41429.0	16246.0	300.0
PLD	0.1	0.1	-0.1
NPSTP	2	2	1
NPSEC	2	2	1
TMPLCC	90.0	90.0	210.0
TMCHG	100000.0	100000.0	100000.0
TMPCNG	90.0	90.0	90.0
IVULC	2	3	2
DISECC	LPCT	CS	GRD
PUMP	1 ** PUMP PERFORMANCE CURVE **		
PUMP	2 ** PUMP PERFORMANCE CURVE **		
PUMP	3 ** CONSTANT INJECTION **		

coolant Injection time for ORNL Case 1.  
TM=62.0 for ORNL Case 2.

\*\*\* EMERGENCY COOLING AND CONTAINMENT SPRAY \*\*\*

HEAT EXCHANGER TUBES DATA AT RATED CONDITIONS

ECC HX C- HX	CAPACITY 0.0 1.147E 03	PRIMARY		SECONDARY		PRIMARY		SECONDARY	
		FLOW RATE	0.0 6.109E 04	FLOW RATE	0.0 6.503E 04	INLET TEMP.	0.0 105.	INLET TEMP.	0.0 90.0

CONTAINMENT BUILDING COOLING DATA

THE COOLER IS IN VOLUME HD 0  
 THE COOLER STARTS AT TIME = 0.0 MIN  
 AT INLET CONCENTRATION

0 = 0.0  
 X1 = 0.0  
 X2 = 0.0  
 X3 = 0.0  
 X4 = 0.0

COOLER IS USED TO CONTROL PRESSURE IN VOLUME D

COOLER CAPACITY = 0.0

AT INLET = 0.0

OF PRESSURE = 0.0







[illegible]

## OWN CONTROL PLATE POSITION INFORMATION

AXIAL ROW	1	2	3	4	5	6	7	8	9	10
1	1	1	1	1	1	1	1	1	1	1
2	1	1	1	1	1	1	1	1	1	1
3	1	1	1	1	1	1	1	1	1	1
4	1	1	1	1	1	1	1	1	1	1
5	1	1	1	1	1	1	1	1	1	1
6	1	1	1	1	1	1	1	1	1	1
7	1	1	1	1	1	1	1	1	1	1
8	1	1	1	1	1	1	1	1	1	1
9	1	1	1	1	1	1	1	1	1	1
10	1	1	1	1	1	1	1	1	1	1
11	1	1	1	1	1	1	1	1	1	1
12	1	1	1	1	1	1	1	1	1	1
13	1	1	1	1	1	1	1	1	1	1
14	1	1	1	1	1	1	1	1	1	1
15	1	1	1	1	1	1	1	1	1	1
16	1	1	1	1	1	1	1	1	1	1
17	1	1	1	1	1	1	1	1	1	1
18	1	1	1	1	1	1	1	1	1	1
19	1	1	1	1	1	1	1	1	1	1
20	1	1	1	1	1	1	1	1	1	1
21	1	1	1	1	1	1	1	1	1	1
22	1	1	1	1	1	1	1	1	1	1
23	1	1	1	1	1	1	1	1	1	1
24	1	1	1	1	1	1	1	1	1	1

WHAT 1 INDICATES IN AND 0 INDICATES OUT.

## OWN CONTROL PLATE BALANCE POINT

1023 = 207.400 H3S = 30.000 DJP = 10.100 AJP = 20.000  
 104500 (1) = 530.0  
 104500 (2) = 530.0  
 104500 (3) = 530.0  
 104500 (4) = 530.0  
 104500 (5) = 530.0  
 104500 (6) = 530.0



\*\*\* SUBROUTINE READ INPUT \*\*\*

WTRC = 1.747E 05 VFCC = 3.045E 04 WJ32 = 3.664E 05 WGRD = 1.229E 05 WHEAD = 2.076E 05 TMLT = 4.130E 03  
 TVCL = 5.00 DDP = 20.9 THICK = 0.565 LI = 0.0 I2 = 0.0 FOPEN = 1.000E -01  
 COND = 5.00

\*\*\* SUBROUTINE ROTDRP INPUT \*\*\*

THOT = 100. THOT = 100. HPR = 1 DP = 0.125 CON = 5.00 FLRMC = 3.397E 03 WTR = 100.  
 TPODRP = 100. NSTOP = 1000

\*\*\* SUBROUTINE INTER INPUT \*\*\*

CAYC = 1.355E -02 CPC = 0.096 DENS = 2.52 TIC = 293. FC1 = 0.800 FC2 = 0.150  
 IC3 = 1.040E -02 IC4 = 3.000E -02 HPR = 0.135 RO = 320. R = 6.000E 03 DI = 3.60  
 IF = 3.601E 04 TPRIN = 1.000E 03 DPRIN = 1.800E 03 HIM = 1.000E -02 HIQ = 1.000E -02 FIDPRN = 0.500  
 IWRC = 1 IC5 = 1 ZI = 1000. WALL = 9.000E 03 TADL = 0.500 TAUS = 5.00

WJTS TIME EPSILON

1 0.0 0.500  
 2 0.360E 08 0.500

## APPENDIX E

Design Parameters of Grand Gulf, Clinton, Perry, and River Bend Plants  
(from River Bend Station FSAR)

## RBS FSAR

TABLE 1.3-1

## COMPARISON OF NUCLEAR STEAM SUPPLY SYSTEM DESIGN AND OPERATING CHARACTERISTICS

	River Bend BWR 6 <u>219-624</u>	Grand Gulf BWR 6 <u>251-800</u>	Clinton BWR 6 <u>218-624</u>	Perry BWR 6 <u>238-748</u>	Zimmer BWR 5 <u>218-560</u>
THERMAL AND HYDRAULIC DESIGN (Section 4.4)					
Rated power (MWt)	2,894	3,833	2,894	3,579	2,436
Design power (MWt) (ECCS design basis)	3,015	4,025	3,039	3,758	2,550
Steam flow rate (x 10 <sup>6</sup> lb/hr)	12.453	16.491	12.453	15.4	10.477
Core coolant flow rate (x 10 <sup>6</sup> lb/hr)	84.5	112.5	84.5	104.0	78.5
Feedwater flow rate (x 10 <sup>6</sup> lb/hr)	12.428	16.455	12.428	15.367	10.447
System pressure, nominal in steam dome (psia)	1,040	1,040	1,040	1,040	1,020
Average power density (kW/l)	52.4	54.1	52.4	54.1	50.51
Maximum thermal output (kW/ft)	13.4	13.4	13.4	13.4	13.4
Average thermal output (kW/ft)	5.74	5.92	6.04	5.90	5.40
Maximum heat flux (Btu/hr-ft <sup>2</sup> )	361,600	362,000	361,600	361,600	354,255
Maximum UC <sub>2</sub> temperature (°F)	3,435	3,430	3,435	3,435	3,325
Average volumetric fuel temperature (°F)	2,164	1,100	-	2,185	2,130
Average cladding surface temperature (°F)	566	558	-	565	566

## RBS FSAR

TABLE 1.3-1 (Cont)

	River Bend EWR 6 <u>218-624</u>	Grand Gulf BWR 6 <u>211-800</u>	Clinton BWR 6 <u>218-624</u>	Perry BWR 6 <u>238-748</u>	Zimmer BWR 5 <u>218-560</u>
Minimum critical power ratio (MCPR)	1.18	1.13	1.20	1.20	1.24
Coolant enthalpy at core inlet (Btu/lb)	527.8	527.9	527.8	527.7	527.4
Core maximum exit voids within assemblies	76	76	76	79	75
Core average exit quality, (% steam)	14.6	14.7	14.6	14.7	13.2
Feedwater temperature (°F)	420	420	420	420	420
<u>Design Power Peaking Factor</u> (Section 4.3.2.2)					
Local peaking factor	1.13	1.13	1.132	1.13	1.24
Total peaking factor	2.33	2.26	2.33	2.21	2.43
NUCLEAR DESIGN (FIRST COPE) (Section 4.3)					
Water/UO <sub>2</sub> volume ratio (cold)	2.70	2.70	2.70	2.70	2.55
Reactivity with strongest control rod out (keff)	<0.99	<0.99	<0.99	<0.99	<0.99
Initial average U-235 enrichment (wt.%)	1.71	1.70	1.70	1.90	1.90
CORE MECHANICAL DESIGN					
<u>Fuel Assembly</u> (Section 4.2.2.2)					
Number of fuel assemblies	624	800	624	748	560
Fuel rod array	8 x 8	8 x 8	8 x 8	8 x 8	8 x 8
Overall length (in)	176	176	176	176	176

E-2

## RBS FSAR

TABLE 1.3-1 (Cont)

	River Bend EWR 6 <u>218-624</u>	Grand Gulf BWR 6 <u>251-800</u>	Clinton BWR 6 <u>218-624</u>	Perry BWR 6 <u>238-748</u>	Zimmer Bwr 5 <u>218-560</u>
Weight of $\text{UO}_2$ per assembly lb (pellet type)	457	458	457	456	466
<u>Fuel Rods</u> (Section 4.2.2.3)					
Number per fuel assembly	62	62	62	62	63
Outside diameter (in)	0.483	0.483	0.483	0.483	0.493
Cladding thickness (in)	0.032	0.032	0.032	0.032	0.034
Diametral gap, pellet to cladding (in)	0.009	0.009	0.009	0.009	0.009
Cladding material <sup>(*)</sup>	Zircaloy-2	Zircaloy-2	Zircaloy-2	Zircaloy-2	Zircaloy-2
<u>Fuel Pellets</u> (Section 4.2.2.3)					
Material	$\text{UO}_2$	$\text{UO}_2$	$\text{UO}_2$	$\text{UO}_2$	$\text{UO}_2$
Density (% of theoretical)	95	95	95	95	95
Diameter (in)	0.410	0.410	0.410	0.410	0.416
Length (in)	0.410	0.410	0.410	0.410	0.420
<u>Fuel Channel</u> (Section 4.2.2.3)					
Thickness (in)	0.120	0.120	0.120	0.120	0.100
Material	Zircaloy-4	Zircaloy-4	Zircaloy-4	Zircaloy-4	Zircaloy-4
<u>Core Assembly</u> (Section 4.2.2.3)					
Fuel weight as $\text{UO}_2$ (lb)	285,180	366,400	285,181	341,640	260,551
Core diameter, equivalent (in)	169.1	191.5	169.1	185.2	160.2
<u>Reactor Control System</u> (Section 4.2.2.4)					
Method of variation of reactor power	Movable control rods; variable forced coolant flow				
Number of movable control rods	145	193	145	177	137

m  
t  
w

RBS FSAR

TABLE 1.3-1 (Cont)

	River Bend BWR 6 <u>218-624</u>	Grand Gulf BWR 6 <u>251-800</u>	Clinton BWR 6 <u>218-624</u>	Perry BWR 6 <u>238-748</u>	Zimmer Bwr 5 <u>218-560</u>
Shapes of movable control rods	Cruciform	Cruciform	Cruciform	Cruciform	Cruciform
Pitch of movable control rods	12.0	12.0	12.0	12.0	12.0
Control material in movable rods	←————— B <sub>4</sub> C granules compacted in SS tubes —————→				
Type of control rod drives	←————— Bottom entry locking piston —————→				
Type of temporary reactivity control for initial core	←————— Burnable poison; gadolinia uranium fuel rods —————→				

Incore Neutron Instrumentation (Section 7.6.1.3)

Total number of LPRM detectors	132	176	132	164	124
Number incore LPRM penetrations	33	44	33	41	31
Number of LPRM detectors per penetrations	4	4	4	4	4
Number of SRM penetrations	4	6	4	4	4
Number of IRM penetrations	8	8	8	8	8
Total nuclear instrument penetrations	45	58	45	53	43
Source range monitor, range	←————— Shutdown through criticality —————→				
Intermediate range monitor, range	←————— Prior to criticality to low power —————→				
Power range monitors, range	←————— Approximately 1% to 125% power —————→				

## RBS FSAR

TABLE 1.3-1 (Cont)

	River Bend EWR 6 <u>218-624</u>	Grand Gulf BWR 6 <u>251-800</u>	Clinton BWR 6 <u>218-624</u>	Perry BWR 6 <u>238-748</u>	Zimmer Bwr 5 <u>218-560</u>
Local power range monitors	132	176	132	164	124
Average power range monitors	8	8	6	8	6
Number and type of incore neutron sources	5Sb-Be	7Sb-Be	5Sb-Be	7Sb-Be	5Sb-Be
REACTOR VESSEL DESIGN (Section 5.3)					
Material	Low alloy steel/ stainless clad	Low alloy steel/ stainless clad	Low alloy steel/ partially clad	Low alloy steel/ stainless clad	Carbon steel/ stainless clad
Design pressure (psig)	1,250	1,250	1,250	1,250	1,250
Design Temperature (°F)	575	575	575	575	575
Inside diameter (ft-in)	18-2	20-11	18-2	19-10	18-2
Inside height (ft-in)	69-4	73-0	69-4	70-5	69-4
Minimum base metal thickness (cylindrical section (in)	5.4	6.14	5.20	6.0	5.375
Minimum cladding thickness (in)	1/8	1/8	1/8	1/8	1/8
REACTOR COOLANT RECIRCULATION DESIGN (Section 5.4.1)					
Number of recirculation loops	2	2	2	2	2

## RBS FSAR

TABLE 1.3-1 (Cont)

	River Bend BWR 6 <u>218-624</u>	Grand Gulf BWR 6 <u>251-800</u>	Clinton BWR 6 <u>218-624</u>	Perry BWR f <u>238-748</u>	Zimmer Bwr 5 <u>218-560</u>
Design pressure:					
Inlet leg (psig)	1,250	1,250	1,250	1,250	1,250
Outlet leg (psig)	1,650 <sup>(2)</sup>	1,625 <sup>(2)</sup>	1,650 <sup>(2)</sup>	1,650 <sup>(2)</sup>	1,675 <sup>(2)</sup>
	1,550 <sup>(3)</sup>	1,525 <sup>(3)</sup>	1,550 <sup>(3)</sup>	1,550 <sup>(3)</sup>	1,575 <sup>(3)</sup>
Design temperature (°F)	575	575	575	575	575
Pipe diameter (in)	20	24	20	24	20
Pipe material (ANSI)	304/316	304/316	304/316	304/316	304/316
Recirculation pump flow rate (gpm)	32,500	44,900	32,500	42,000	32,500
Number of jet pumps in reactor	20	24	20	20	20
MAIN STEAM LINES					
Number of steam lines	4	4	4	4	4
Design pressure (psig)	1,250	1,250	1,250	1,250	1,250
Design temperature (°F)	575	575	575	575	575
Pipe diameter (in)	24	28	24	26	24
Pipe material	← carbon steel →				

(1) Freestanding loaded tubes.

(2) Pump and discharge piping to and including the discharge block valve.

(3) Discharge piping from the discharge block valve to vessel.



## RES FSAR

TABLE 1.3-2

## COMPARISON OF POWER CONVERSION SYSTEM DESIGN CHARACTERISTICS

	River Bend BWR 6 <u>218-624</u>	Grand Gulf BWR 6 <u>251-800</u>	Clinton BWR 6 <u>218-624</u>	Perry BWR 6 <u>238-748</u>	Zimmer BWR 5 <u>218-560</u>
<u>Turbine-Generator (Section 10.2)</u>					
Rated Power (MWe) (Gross)	991	1,306	985	1,252	883
Generator Speed (rpm)	1,800	1,800	1,800	1,800	1,800
Rated Steam Flow (lb/hr)	$12.435 \times 10^6$	$15.542 \times 10^6$	$11.340 \times 10^6$	$14.68 \times 10^6$	$11.001 \times 10^6$
Turbine Inlet Pressure (psig)	965	965	965	965	950
<u>Steam Bypass System (Section 10.4.4)</u>					
Capacity (Percent of Design Steam Flow)	10	35	35	35	25
<u>Main Condenser (Section 10.4.1)</u>					
Heat Removal Capacity (Btu/hr)	$6,860 \times 10^6$	$8,506 \times 10^6$	$6,453 \times 10^6$	$8,100 \times 10^6$	$7,053 \times 10^6$
<u>Circulating Water System (Section 10.4.5)</u>					
Number of pumps	4	2	3	3	3
Flow Rate (gpm/pump)	127,890	285,500	189,600	185,000	150,000
<u>Condensate and Feedwater Systems (Section 10.4.7)</u>					
Design Flow Rate of Feedwater to Reactor (lb/hr)	$12.428 \times 10^6$	$15.542 \times 10^6$	$12.428 \times 10^6$	$14.68 \times 10^6$	$10.971 \times 10^6$
Number of Condensate Pumps	3	3	4	3	3
Number of Condensate Booster Pumps	0	3	4	3	3
Number of Feedwater Pumps	3	2	3	3	2
Number of Feedwater Booster Pumps	none	none	none	none	none
Condensate Pump Drive	AC power	AC power	AC power	AC power	AC power
Condensate Booster Pump Drive	NA	AC power	AC power	AC power	AC power
Feedwater Pump Drive	AC power	Turbine	Turbine-2 AC-1	Turbine	Turbine

E-7

## RES FSAR

TABLE 1.3-3

## COMPARISON OF ENGINEERED SAFETY FEATURES DESIGN CHARACTERISTICS

	River Bend BWR 6 <u>218-624</u>	Grand Gulf BWR 6 <u>251-800</u>	Clinton BWR 6 <u>218-624</u>	Perry BWR 6 <u>238-748</u>	Zimmer BWR 5 <u>218-560</u>
EMERGENCY CORE COOLING SYSTEMS (Systems sized on design power) (Section 6.3)					
<u>Low-Pressure Core Spray System</u>					
Number of loops	1	1	1	1	1
Flow rate (gpm)	5,010 at 119 psid	7,115 at 128 psid	5,010 at 119 psid	6,110 at 128 psid	4,725 at 119 psid
<u>High-Pressure Core Spray System</u>					
Number of loops	1	1	1	1	1
Flow rate (gpm)	1,400 at 1,147 psid	1,650 at 1,147 psid	1,400 at 1,147 psid	1,550 at 1,147 psid	1,330 at 1,110 psid
	5,010 at 200 psid	7,115 at 200 psid	5,010 at 200 psid	6,000 at 200 psid	4,725 at 200 psid
<u>Automatic Depressurization System</u>					
Number of relief valves	7	8	7	8	6
<u>Low-Pressure Coolant Injection<sup>(1)</sup></u>					
Number of loops	3	3	3	3	3
Number of pumps	3	3	3	3	3
Flow rate (gpm/pump)	5,050 at 20 psid	7,450 at 24 psid	5,050 at 20 psid	7,000 at 20 psid	5,050 at 20 psid

m  
1  
∞

RBS FSAR

TABLE 1.3-3 (Cont)

	River Bend BWR 6 <u>218-624</u>	Grand Gulf BWR 6 <u>251-800</u>	Clinton BWR 6 <u>218-624</u>	Perry BWR 6 <u>238-748</u>	Zimmer BWR 5 <u>218-560</u>
<u>AUXILIARY SYSTEMS</u>					
<u>Residual Heat Removal System (Section 5.4.7)</u>					
Reactor Shutdown Cooling Mode:					
Number of pumps	2	2	2	2	2
Flow rate (gpm/pump) <sup>(2)</sup>	5,050	7,450	5,050	7,100	5,050
Duty (millions Btu/hr/heat exchanger) <sup>(3)</sup>	37.8	50.0	37.8	46.9	30.8
Number of heat exchangers	2	2	2	2	2
Suppression pool cooling mode:					
Flow rate (gpm) <sup>(4)</sup>	5,050	7,450	5,050	7,100	5,050
<u>Standby Service Water System (Section 9.2.7)</u>					
Flow rate (gpm/heat exchanger)	7,000	25,300 total	33,100 total	12,800 total	5,000
Number of pumps	4/unit	3/unit (2 at 12,000) (1 at 1,300)	2 at 16,000 1 at 1,100	2/unit (1 at 11,900) (1 at 900)	4
<u>Reactor Core Isolation Cooling System (Section 5.4.6)</u>					
Flow rate (gpm)	600 at 1,177 psid	800 at 1,120 psid	600 at 1,177 psid	700 at 1,177 psid	400 at 1,120 psid
<u>Fuel Pool Cooling and Cleaning System (Section 9.1.3)</u>					
Capacity (millions Btu/hr)	9.8	12.5	19.7	20	6.6

<sup>(1)</sup>A mode of the FHR system.

<sup>(2)</sup>Capacity during reactor flooding mode with more than one pump running.

<sup>(3)</sup>Heat exchanger duty at 20 hr following reactor shutdown.

<sup>(4)</sup>Flow per heat exchanger.

RES FSAR

TABLE 1.3-4

COMPARISON OF CONTAINMENT CHARACTERISTICS

	River Bend EWR 6 218-624	Grand Gulf BWR 6 251-800	Clinton BWR 6 218-624	Perry BWR 6 238-748	Zimmer BWR 5 218-560
<u>Containment</u> (Section 3.8.2)					
Type	Mark III; freestanding steel; horizontal pressure suppression	Mark III; reinforced concrete containment, but with pressure suppression; containment encloses drywell and suppression pool	Mark III; reinforced concrete as for PWR plants, but with pressure suppression; containment encloses drywell and suppression pool	Mark III; steel containment with pressure suppression, enclosed by reinforced concrete reactor building. Containment encloses drywell and suppression pool	Mark II; over-and-under primary containment, enclosing drywell and suppression pool; enclosed by reactor building
Leakage rate (%/day)	0.26	0.35	0.65	0.20	0.635
Construction	Freestanding steel	Reinforced concrete cylindrical structure (not prestressed) with hemispherical head; steel lined	Reinforced concrete cylindrical structure (not prestressed) with hemispherical dome; steel lined	Steel shell enclosed by reinforced concrete cylindrical structure (not prestressed) with hemispherical head	Prestressed concrete cylinder plus truncated cone above cylinder; steel lined
Internal design temperature (°F)	185	185	185	185	Not applicable
Design pressure (psig)	15	15	15	+15,-0.8	Not applicable
Free (air) volume (cu ft)	1.192x10 <sup>6</sup>	1.67x10 <sup>6</sup>	1.4575x10 <sup>6</sup>	1.2x10 <sup>6</sup>	Not applicable
<u>Drywell</u> (Section 3.8.3)					
Construction	Reinforced concrete cylinder; flat concrete roof with a steel refueling head	Reinforced concrete; basically cylindrical; flat concrete roof with a steel refueling head	Reinforced concrete cylinder; steel concrete form plate; steel access head	Reinforced concrete; basically cylindrical; flat concrete roof with a steel refueling head	Prestressed concrete; drywell is frustrum of a cone; steel lined

E-10

## RBS FSAR

TABLE 1.3-4 (Cont)

	River Bend BWR 6 218-624	Grand Gulf BWR 6 251-800	Clinton BWR 6 218-624	Perry BWR 6 238-748	Zimmer BWR 5 218-560
Internal design temperature (°F)	330	330	330	330	340
Design pressure (psig)	25	30	30	+30, -21	+45, -2
Free (air) volume, total (cu ft)	251,000	270,000	246,500	278,000	287,000
<u>Suppression Pool</u> (Section 3.8.3)					
Construction	Concrete; steel	Reinforced concrete; steel lined; basically cylindrical	Steel lined concrete cylinder	Reinforced concrete; steel lined; basically cylindrical	Prestressed concrete; pool is cylindrical; steel lined
Design pressure (psig)	20	15	15	1	+45, -2
Internal design temperature (°F)	185	185	185	185	340
Water volume (cu ft)	127,930	136,000	135,700	120,000	106,000

E-11